THE UNIVERSITY
of EDINBURGH

Interactions between *Pax6, Barhl2* and *Shh* in the early patterning of the mammalian diencephalon

Elisa Parish

PhD

The University of Edinburgh

2015

Abstract

Diencephalic development requires the transcription factors *Pax6* and *Barhl2* in order to proceed correctly. Both genes are necessary for the normal development of the organizer region known as the *zona limitans intrathalamica* (ZLI). The ZLI goes on to pattern the diencephalon via its secretion of the morphogen *Shh*, which inhibits the expression of *Pax6*. These findings suggest that interactions between *Pax6*, *Barhl2* and *Shh* may be involved in the control of diencephalic development. This project aims to characterise these interactions and investigate their roles.

The expression domains of *Pax6* and *Barhl2* were mapped during the early development of the mouse diencephalon. Qualitative approaches were employed to confirm the high complementarity of their expression domains and obtain evidence of a mutually repressive relationship existing between the two genes. The findings from a quantitative analysis suggested that this inhibition is incomplete within the thalamus. Investigations using the *Pax6*-null mutant mouse confirmed that in the absence of *Pax6* the thalamic *Barhl2* expression domain expands beyond the ventricular zone, the site of thalamic neurogenesis.

The influence of *Shh* signalling on the expression of *Pax6* and *Barhl2* was investigated via a gain-of-function approach utilising *in utero* electroporation to activate the *Shh* pathway. This led to a downregulation of both *Pax6* and *Barhl2* within the thalamus.

In *Shh* loss-of-function experiments drug treatment with the *Shh* antagonist vismodegib led to an upregulation of *Barhl2* and the loss of the GABAergic pTh-R in the *Pax6*-null mutant thalamus, but not in the wild type thalamus, suggesting that *Pax6* and *Shh* may be required to inhibit *Barhl2* in order for GABAergic neurogenesis to proceed. *Barhl2* expression was detected in the *Shh*-null mutant mouse confirming that, in contrast with their homologues in Drosophila, *Shh* may be expressed downstream of *Barhl2*.

Together these findings have been used to develop a novel model of thalamic development in which *Barhl2* induces ZLI development, inhibition of *Barhl2* by *Pax6* restricts its expansion, and secretion of *Shh* by the ZLI then goes on to inhibit *Pax6* and *Barhl2* in the pTh-R while mutual repression between *Pax6* and *Barhl2* modulates neurogenesis in the more caudal regions of the thalamic neuroepithelium.

Lay summary

Early in embryonic development the forebrain is formed into two distinct regions- the telencephalon, which gives rise to structures including the cerebral cortex, and the diencephalon, from which the thalamus develops. The thalamus serves to receive input from sensory neurons and then relay it to the appropriate region of the cerebral cortex. During development cells are induced to differentiate into different types of neuron. This process is controlled by transcription factors- proteins which act within individual cells to initiate or suppress gene expression. The genes encoding these proteins can also be controlled in this manner and can be involved in complex interactions with each other. Development is also influenced by another class of proteins known as the morphogens, which are secreted by specialised regions of tissue known as organizer regions. Morphogens direct the differentiation of cells in the surrounding tissue via effects they exert on the expression of transcription factors. Within the mammalian diencephalon an organizer region known as the *zona limitans intrathalamica* (ZLI) secretes the morphogen *Sonic hedgehog* (*Shh*). The transcription factors *Pax6* and *Barhl2* are both strongly expressed within the developing diencephalon and appear to suppress each other's expression in addition to interacting with *Shh*. For this project changes in the expression of *Pax6* and *Barhl2* were observed throughout the development of the mouse diencephalon in order to characterise the relationships between them. *Pax6*-null and *Shh*-null mutant mice were used to investigate the effects of gene deletion, and drug treatment with the *Shh*-blocking drug vismodegib was utilised to examine the influence of *Shh* on expression of *Pax6* and *Barhl2*. The technique of *in utero* electroporation was used to increase levels of *Shh* in cells of the embryonic diencephalon and observe the resulting changes in gene expression. Results suggested that interactions between *Pax6* and *Barhl2* are required to allow the ZLI to develop correctly and that *Shh* from the ZLI then goes on to suppress the expression of both genes, allowing the most ventral region of the thalamus to develop, while in other regions neurogenesis continues to be modulated by mutual repression between *Pax6* and *Barhl2*.

Declaration

I (Elisa Parish) composed this thesis. The work presented here is my own. I performed all of the experiments described within unless otherwise clearly stated in the text. No part of this work has been submitted for any other qualification.

Signed _____ Date _____

Acknowledgements

This project was funded by a Medical Research Council Capacity Building Studentship with additional funding provided by RIKEN via the International Programme Associate scheme. An additional grant to cover travel expenses was provided by Edinburgh Neuroscience via the Edinburgh Neuroresearchers Fund.

First and foremost I would like to thank my supervisors, David Price and John Mason- for having given me a great opportunity to join a remarkable group of scientists, for their faith in me when I was plagued with doubt, and for four years of positivity and encouragement which have inspired me to keep trying to be as a good a scientist as I can be.

I would also like to thank the members of DBUG for their guidance and support, in particular Martine Manuel, Nikky Huang, Mi Da, Elena Dora, Hannah Parkin, Cass Li, Idoia Quintana-Urzainqui, Tom Pratt and Thomas Theil. Mike Molinek is deserving of a special mention for his invaluable advice and great patience.

Additional thanks are due to the Biological Research Resources staff at the Hugh Robson Building for making all of my experiments possible, along with Trudi Gillespie and Anisha Kubasik-Thayil of IMPACT for their training and assistance with confocal microscopy, and Professor Robert Hill of the MRC Human Genetics Unit for the kind gift of the *Shh*-null mutant embryos.

I would like to thank Tomomi Shimogori as my host and *sensei* at the Lab for Molecular Mechanisms of Thalamus Development at the RIKEN Brain Science Institute, and for the kind gift of the *cShh* pXeX plasmid. I am grateful to Asuka Matsui, Tim Young, Yurie Maeda, Aya Yoshida, Miyako Hirabayashi, Hiromi Mashiko and Ayumi Abe for the scientific training, for giving me new perspectives, and for helping me to adjust to a new life halfway around the world. A special thank you goes out to Asuka Suzuki-Hirano for providing me with the *Barhl2* plasmid and for her work on the paper which inspired this project.

Finally I would like to thank Chris Lawless- this project brought us together, and his love and support eventually got me through it.

Abbreviations

AC	amacrine cell
AP	alar plate
Ascl1	*Achaete-scute complex homolog 1*
ato	*atonal*
BarH1 /2	*Bar homeobox 1/2*
Barhl1/2	*Bar homeobox-like 1/2*
BCIP	5-Bromo-4-chloro-3-indolyl phosphate
bHLH	basic Helix-Loop-Helix
BMP	bone morphogenetic protein
BP	basal plate
cShh	chick (*Gallus gallus*) *Sonic hedgehog*
Cb	cerebellum
CH	cortical hem
CNS	central nervous system
CP	choroid plexus
Ctx	cortex
DAPI	4',6-diamidino-2-phenylindole
Dbx1/2	*Developing brain homeobox 1/2*
Di	diencephalon
DIG	digoxigenin
Dlx1/2	*Distal-less homeobox 1/2*
DNA	deoxyribonucleic acid
DNP	2,4-dinitrophenyl
dNTP	Deoxynucleotide triphosphate
E0.5-E18.5	embryonic day 0.5-18.5
Ebf1	*Early B cell factor 1*
ECM	Extracellular matrix
E. coli	*Escherichia coli*
EDTA	Ethylenediamine-tetraacetic acid
ET	eminentia thalami
ey	*eyeless*
FezF1	*Fez family zinc finger 1*
FGF	fibroblast growth factor
FL	fluorescein

FP	floorplate
GABA	γ-aminobutyric acid
Gbx2	*Gastrulation brain homeobox 2*
GFP	green fluorescent protein
Gli1/2/3	*GLI-Kruppel family member 1/2/3*
Gli2/3A	*GLI-Kruppel family member 2/3* activator form
Gli2/3R	*GLI-Kruppel family member 1/2/3* repressor form
Hes1	*Hairy and enhancer of split 1*
Hh	*hedgehog*
Hyp	hypothalamus
Irx1b/3	*Iroquois related homeobox 1b/3*
Islet1	*ISL LIM homeobox 1*
LGE	lateral ganglionic eminence
LB	Luria Bertani
Lef1	*Lymphoid enhancing binding factor 1*
Mes	mesencephalon
MGE	medial ganglionic eminence
mRNA	messenger ribonucleic acid
NBT	nitro blue tetrazolium
Ngn1/2	*Neurogenin 1/2*
Nkx2-2	*NK2 homeobox 2*
OCT	optimal cutting temperature
Olig2/3	*Oligodendrocyte transcription factor 2/3*
Otx1l/2	*Orthodenticle homolog 2*
Pal	pallium
Pax6	*Paired box gene 6*
PBS	phosphate-buffered saline
PCR	polymerase chain reaction
P0- onwards	Postnatal day 0
PFA	paraformaldehyde
PSB	pallial-subpallial boundary

PT	pretectum
Ptch1	*patched homolog 1*
pTh	prethalamus
qPCR	quantitative polymerase chain reaction
R1-8	*Drosophila* photoreceptor subtype 1-8
Rh	rhombencephalon
Robo/3	*Roundabout/3*
RT	room temperature
Sey	*small-eye*
Shh	*Sonic hedgehog*
Six3	*Sine oculis-related homeobox 3*
Smo	*Smoothened homologue*
SOC	super optimal condition
SubPal	subpallium
Sox2	*SRY (sex determining region Y)-box 2*
Tel	telencephalon
Th	thalamus
VZ	ventricular zone
WT	wild-type
ZLI	*zona limitans intrathalamica*

Contents

8. Discussion

1. Introduction

1.1 Early development of the mammalian forebrain

During the early development of the vertebrate embryo the process of gastrulation causes the cells to segregate into three germ layers. The innermost of these is the endoderm, the outermost is the ectoderm, and the third layer, the mesoderm, lies between them. The ectoderm is the germ layer which is fated to give rise to the skin and also to the central nervous system via the process of neurulation (Tam and Behringer 1997, Vieira *et al* 2010).

In the embryo of the house mouse (*Mus musculus*) neurulation begins at around the seventh day of gestation (Theiler 1989). A dorsal region of ectoderm, known as the neural plate, is fated to become neurectoderm (Rubenstein *et al* 1998, Patthey and Gunhaga 2011). The neural plate develops a furrow, known as the neural fold, and begins to fold inwards. The two edges of the neural plate move towards each other and eventually fuse, forming a closed tube of neuroepithelium which then detaches from the surface epithelium. This structure is the neural tube and it is fated to develop into the central nervous system- the brain, spinal cord and neural retinae- while the surface ectoderm develops into the skin and ectodermal appendages (Weinstein and Hemmati-Brivanlou 1999, Colas and Schoenwolf 2001, Copp *et al* 2003) (Fig 1.1).

As the neural tube closes it begins to undergo further changes in gross morphology as the structures of the central nervous system develop and become distinct from one another. The neural tube develops constrictions along its rostrocaudal axis, dividing it into regions which correspond with the positions of the prosencephalon, mesencephalon, rhombencephalon and spinal cord (Fig. 1.2A). Later in development the prosencephalon develops a constriction which divides it into the more rostral telencephalon and the more caudal diencephalon (Fig. 1.2B). The diencephalon itself later becomes regionalized into three molecularly distinct areas of neuroepithelium known as the prethalamus, thalamus and pretectum (Keynes and Lumsden 1990, Altmann and Brivanlou 2001, Puelles and Rubinstein 2003, Lim and Golden 2007, Puelles *et al* 2013) (Fig. 1.2C). Of these structures, the thalamus plays particularly

important roles in the adult brain, and is perhaps most commonly described as the structure which serves to relay sensory input, bar olfaction (Shepherd 2005), to the appropriate region of the cerebral cortex (Jones 2002, Sherman and Guillery 2002).

As the telencephalon grows in size it begins to envelop the diencephalon (Price *et al* 2011) (Fig. 1.2D) and in coronal sections cut from embryonic brain tissue it can be distinguished as two telencephalic vesicles lateral to the ventricle of the diencephalon, while the pretectum, thalamus and prethalamus respectively can be seen running from dorsal to ventral (Paxinos and Franklin 2001) (Fig. 1.3).

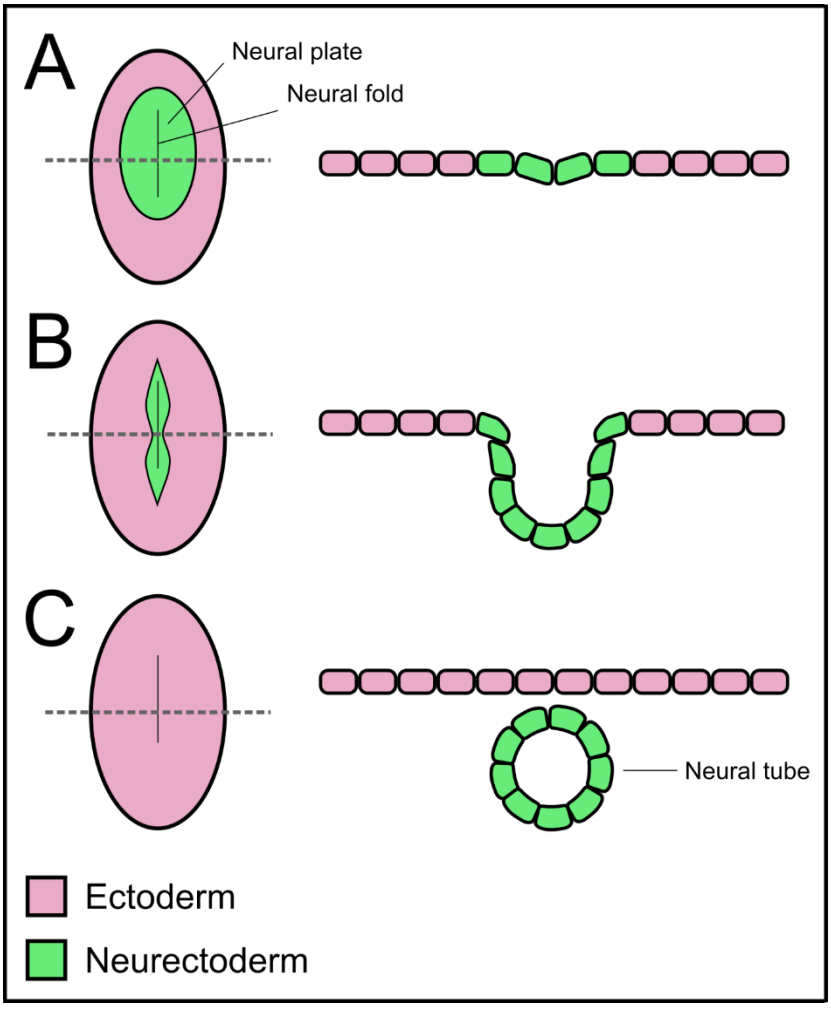

Fig. 1.1: Schematic illustrating the process of neurulation. A. The neural plate is a region of ectoderm fated to become the central nervous system. Neurulation begins with the development of the neural fold. B. The neural plate becomes furrowed and its edges move towards each other. C. The edges of the neural plate become fused, forming the neural tube which then detaches from the surface ectoderm.

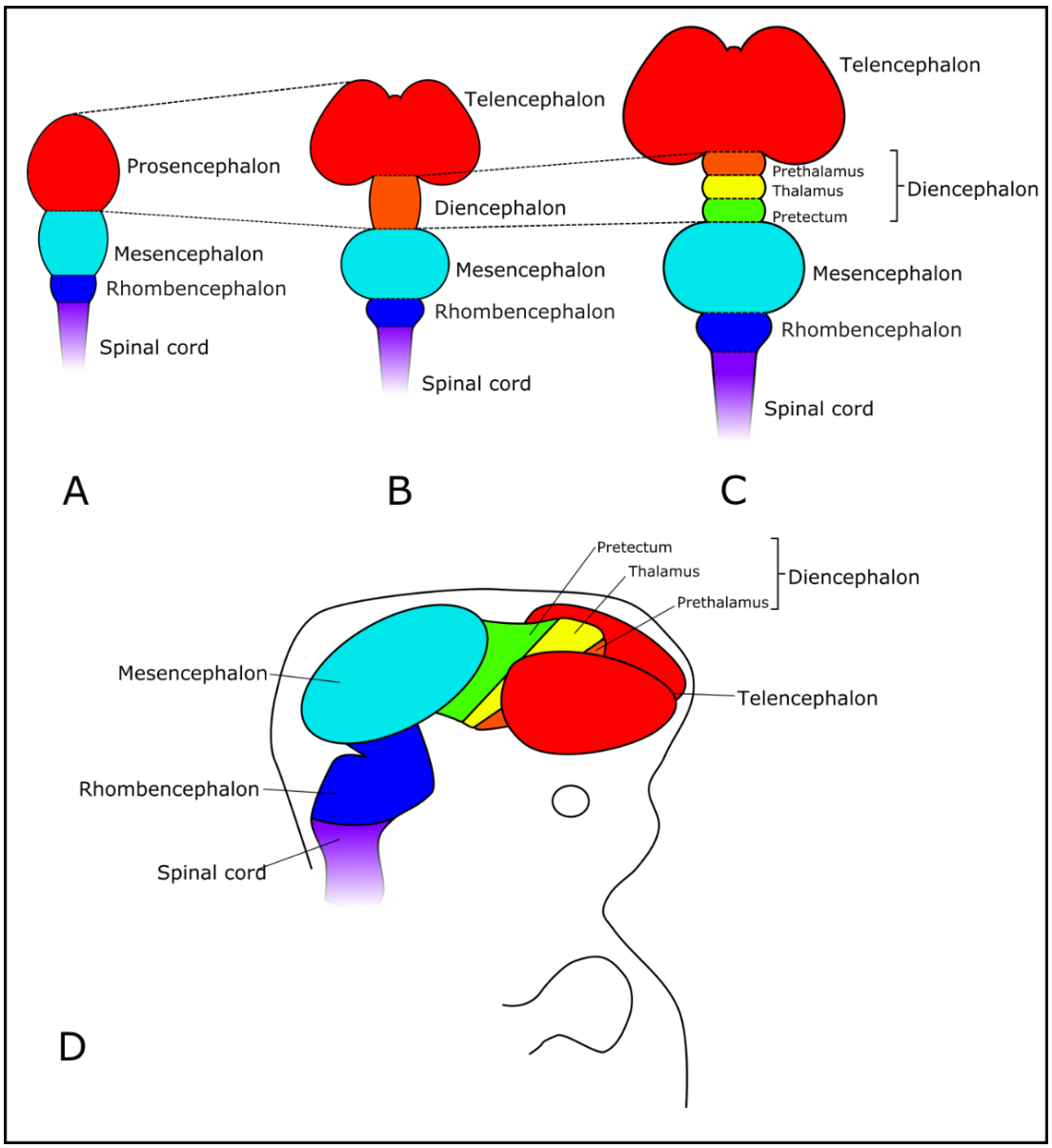

Fig. 1.2: Schematic illustrating the early regionalisation of the neural tube following closure. A. The neural tube begins to develop constrictions along its rostrocaudal axis. Initially three constrictions develop, and these correspond with the caudal extent of the prosencephalon, mesencephalon and rhombencephalon respectively. B. Later in development the prosencephalon differentiates into the more rostral telencephalon and the more caudal diencephalon and an addition constriction develops at the boundary between these two regions. C. Later still the diencephalon differentiates into the pretectum, thalamus and prethalamus and further constrictions form between these regions. D. Schematic to illustrate the positions these brain regions occupy in relation to each other within the mouse embryo following the development of the head fold.

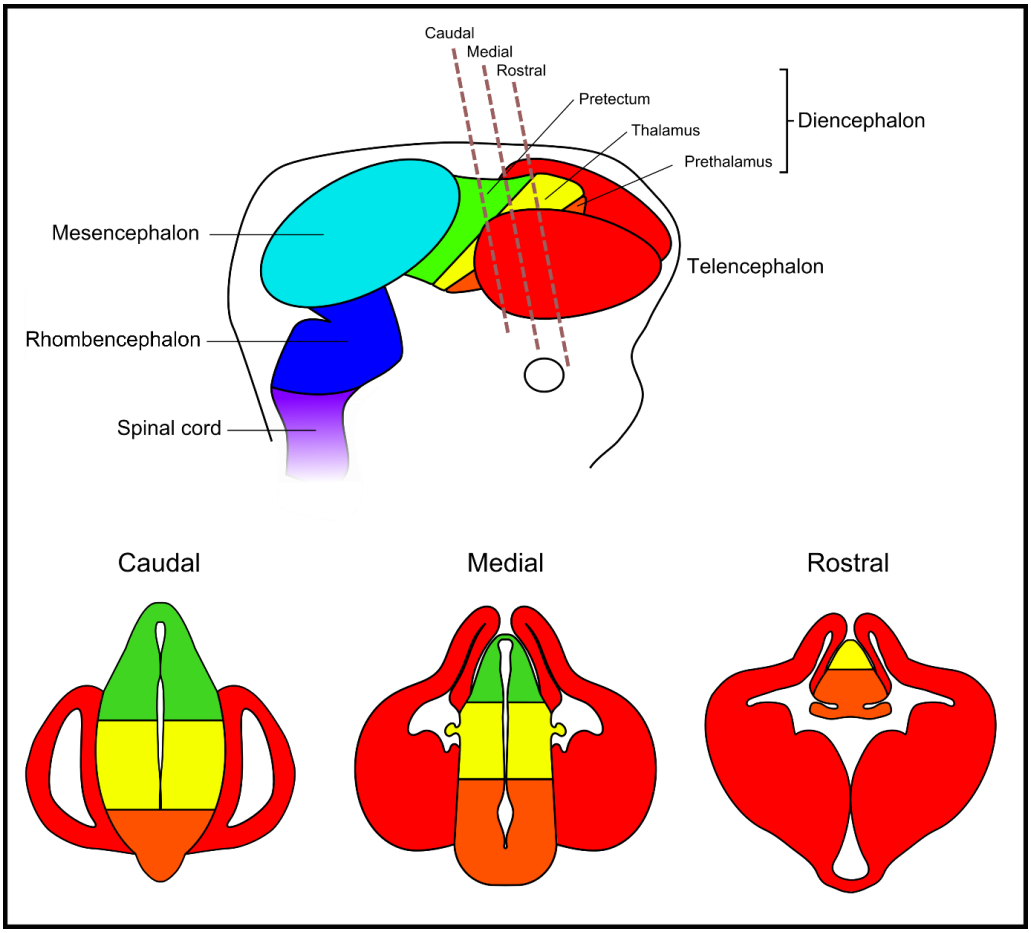

Fig. 1.3: Schematic illustrating the arealisation of the diencephalon into three molecularly and morphologically distinct regions- the pretectum, thalamus and prethalamus- and how these regions appear in relation to each other in coronal sections.

1.2 Organizers: the *zona limitans intrathalamica*

The arealisation of embryonic tissues is controlled in part by the action of organizers- specialised regions of tissue which direct the development of surrounding tissues via the actions of signalling molecules which they secrete. Known as morphogens, these signalling molecules diffuse into the surrounding tissue and direct its differentiation by inducing changes in gene expression (Shimamura *et al* 1995, Rhinn *et al* 2006, Wilson and Houart 2009, Scholpp and Lumsden 2010).

The vertebrate forebrain is known to contain several organizers. The roofplate, which runs along the dorsal midline of the neural tube at the region where its edges fuse during neurulation, secretes Wnts and bone morphogenetic proteins (BMPs) (Chizhikov and Millen 2005). Fibroblast growth factors (FGFs) are secreted from the anterior neural ridge, an organizer region situated at the rostral extent of the prosencephalon (Wilson and Houart 2009). The floor plate, running along the ventral midline of the neural tube, secretes *Sonic hedgehog* (*Shh*) (Kiecker and Lumsden 2004). For a brief period during the early development of the embryo a narrow wedge-shaped region of *Shh*-secreting cells extends from the floor plate into the diencephalon. This is an additional organizer region known as the *zona limitans intrathalamica* (ZLI) (Vieira *et al* 2010, Kiecker and Lumsden 2012, Robertshaw and Kiecker 2012) (Fig. 1.4).

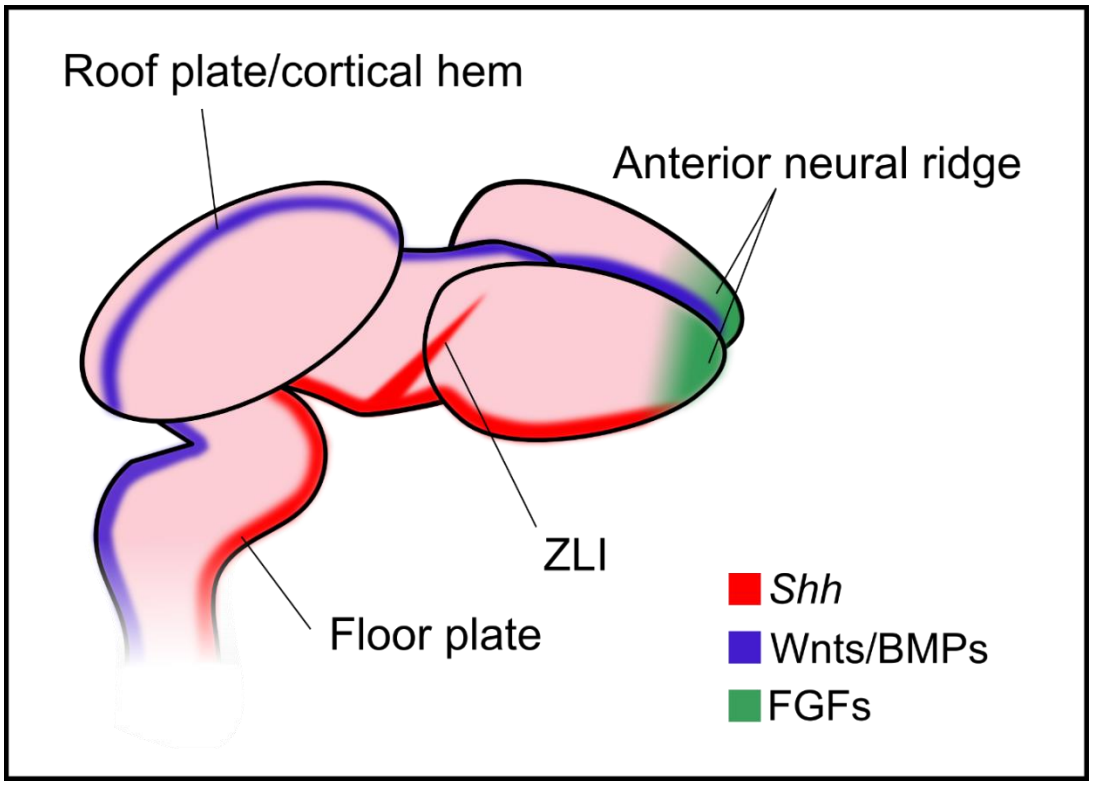

Fig. 1.4: Schematic illustrating the position of organizers within the developing vertebrate brain and examples of the morphogens they are known to secrete.

The ZLI develops from progenitor cells in the alar plate (Staudt and Houart 2007) and begins to form at the point where the prechordal plate, situated ventral the notochord (Rubenstein *et al* 1998), meets the epichordal region of the neural plate,

dorsal to the notochord (Larsen *et al* 2001). The formation of the ZLI may be induced by interactions between the transcription factors *Sine oculis-related homeobox 3* (*Six3*) in the prechordal plate and *Iroquois homeobox 3* (*Irx3*) in the epichordal plate, and mutual inhibition between the two transcription factors may also act to establish a boundary between their domains and serve to correctly position the ZLI (Kobayashi *et al* 2002). The possibility of interactions between prechordal and epichordal tissues playing a role in ZLI induction is supported by experiments in which the grafting of a region of prechordal tissue into the epichordal plate leads to the induction of ectopic ZLI-like structures at the borders of the graft (Vieira *et al* 2005).

One model for ZLI development, based on observations in zebrafish, implicates two transcription factors of the *Orthodentical homeobox* (*Otx*) family, *Otx1l* and *Otx2* along with an *Iroquois related homeobox* (*Irx*) transcription factor, *Irx1b*. *Otx1l* and *Otx2* are expressed within the presumptive ZLI and thalamus, conferring the neuroepithelium in this region with the competence to develop into the ZLI. *Irx1b* is expressed in the presumptive thalamus, and serves to inhibit *Shh* expression, and ZLI development, in this region of neuroepithelium. *Otx1l* and *Otx2* therefore act to induce ZLI development, while *Irx1b* serves to restrict its expansion into more caudal regions of the diencephalic neuroepithelium (Scholpp *et al* 2007).

The ZLI extends dorsally towards the roofplate but does not extend into the roofplate itself. Retinoic acid, a metabolite of retinol, acts as a signalling molecule in several developmental processes (Duester 2008). Studies in chick have shown that it is synthesised in the epithalamus during ZLI development and that it may serve to inhibit the extension of the ZLI into the most dorsal regions of the diencephalon (Guinazu *et al* 2007).

As the ZLI develops from the point at which the prechordal and epichordal plates meet, it extends along the boundary between the prethalamus and thalamus (Larsen *et al* 2001). Lineage tracing experiments in chick have been used to demonstrate that the ZLI is a lineage restriction compartment (Larsen *et al* 2001). The establishment of lineage restriction serves to stabilise the position of the ZLI in order to establish

the concentration gradients of *Shh* required for the correct patterning of the surrounding neuroepithelium (Scholpp and Lumsden 2010).

The role of the ZLI as a local organizer region acting via the secretion of *Shh* has been confirmed with *Shh* gain-of-function and loss-of-function experiments in chick (Kiecker and Lumsden 2004). In the mouse embryo the ZLI begins to form at approximately E10.5 (Shimamura *et al* 1995) and expression data for *Shh* over a series of developmental stages suggest that the ZLI is maintained until E14.5 (Visel *et al* 2004, Lim and Golden 2007).

The differentiation of the diencephalon into three morphologically distinct regions of differing molecular character is due to the fact that *Shh* signalling from the ZLI does not influence the rostrocaudal patterning of the diencephalon in a symmetrical fashion. *Shh* is known to upregulate the expression of its receptor *Ptch1* (Marigo *et al* 1996). *Ptch1* and a second *bona fide Shh* target gene, *NK2 homeobox2* (*Nkx2-2*) (Barth and Wilson 1995, Shimamura *et al* 1995) are both expressed in the neuroepithelium immediately adjacent to the ZLI, suggesting that tissues both rostral and caudal to the ZLI are competent to respond to the *Shh* signal (Kiecker and Lumsden 2004). This observation suggests that it is the differing molecular character of the regions fated to become the thalamus and prethalamus which allows the tissues to give differing responses to the *Shh* signal, and that these regions of neuroepithelium must become molecularly distinct prior to ZLI formation.

Candidates for the factors conferring differential competence have been selected from transcription factors which are expressed as the neural plate is patterned and diencephalic structures are first specified. *Fez family zinc finger 1* (*FezF1*) is known to be required for the specification of the prethalamus (Hirata *et al* 2006) while *Distal-less homeobox 1* (*Dlx1*) and *Distal-less homeobox 2* (*Dlx2),* have also been suggested as transcription factors which are required for its specification (Bulfone *et al* 1993). *Irx3* is required for the specification of the thalamus (Kiecker and Lumsden 2004, Robertshaw *et al* 2013) while *Early B cell factor 1* (Ebf1) has been suggested as a candidate for the specification of the pretectum (Garel et al 1997).

The position of the ZLI and other structures within the embryonic mouse brain are detailed in Figs. 1.5 and 1.6.

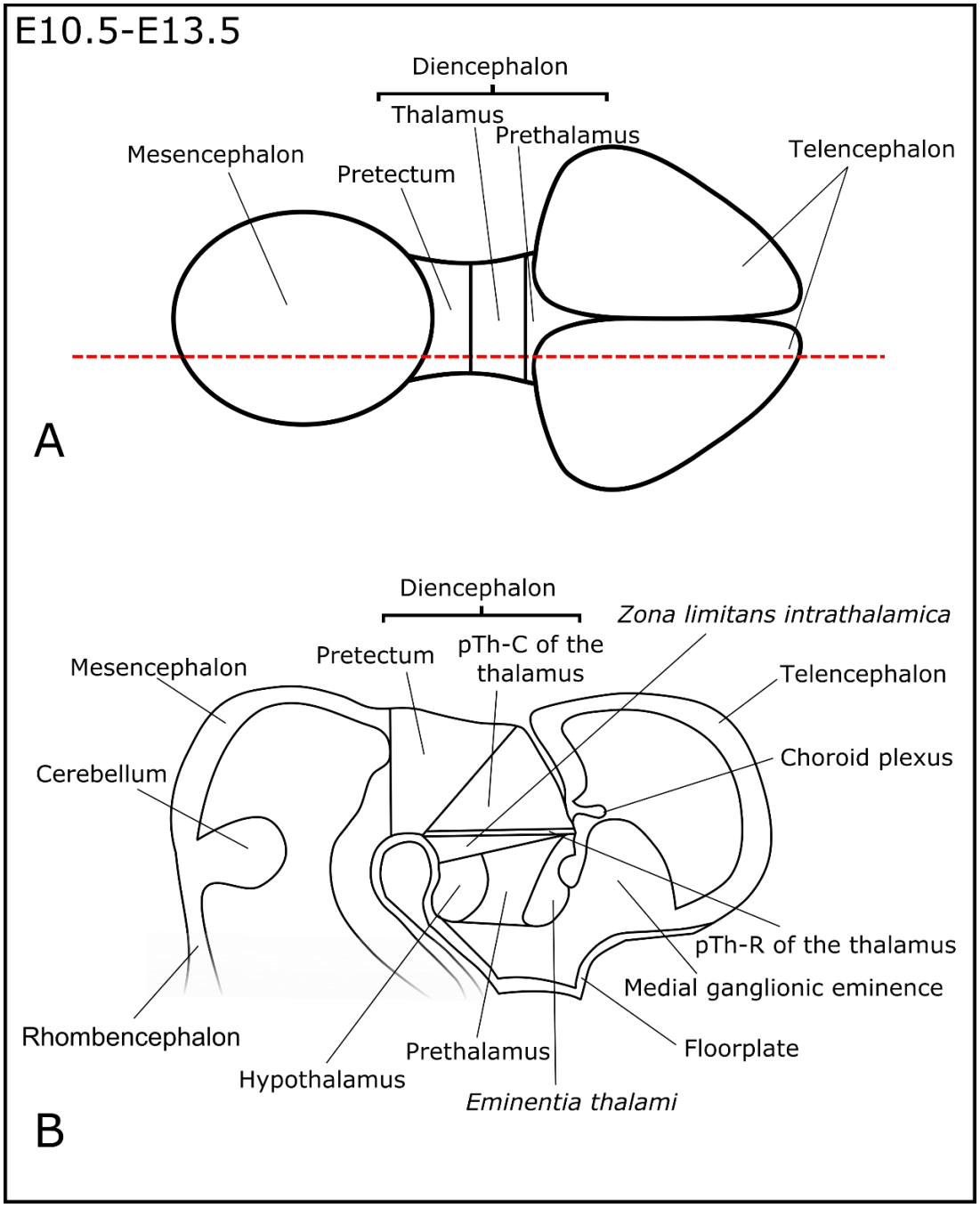

Fig. 1.5: A. Schematic of the E12.5 mouse brain, dorsal view, rostral to right, to illustrate the sagittal plane of section. B. The structures visible in a sagittal section.

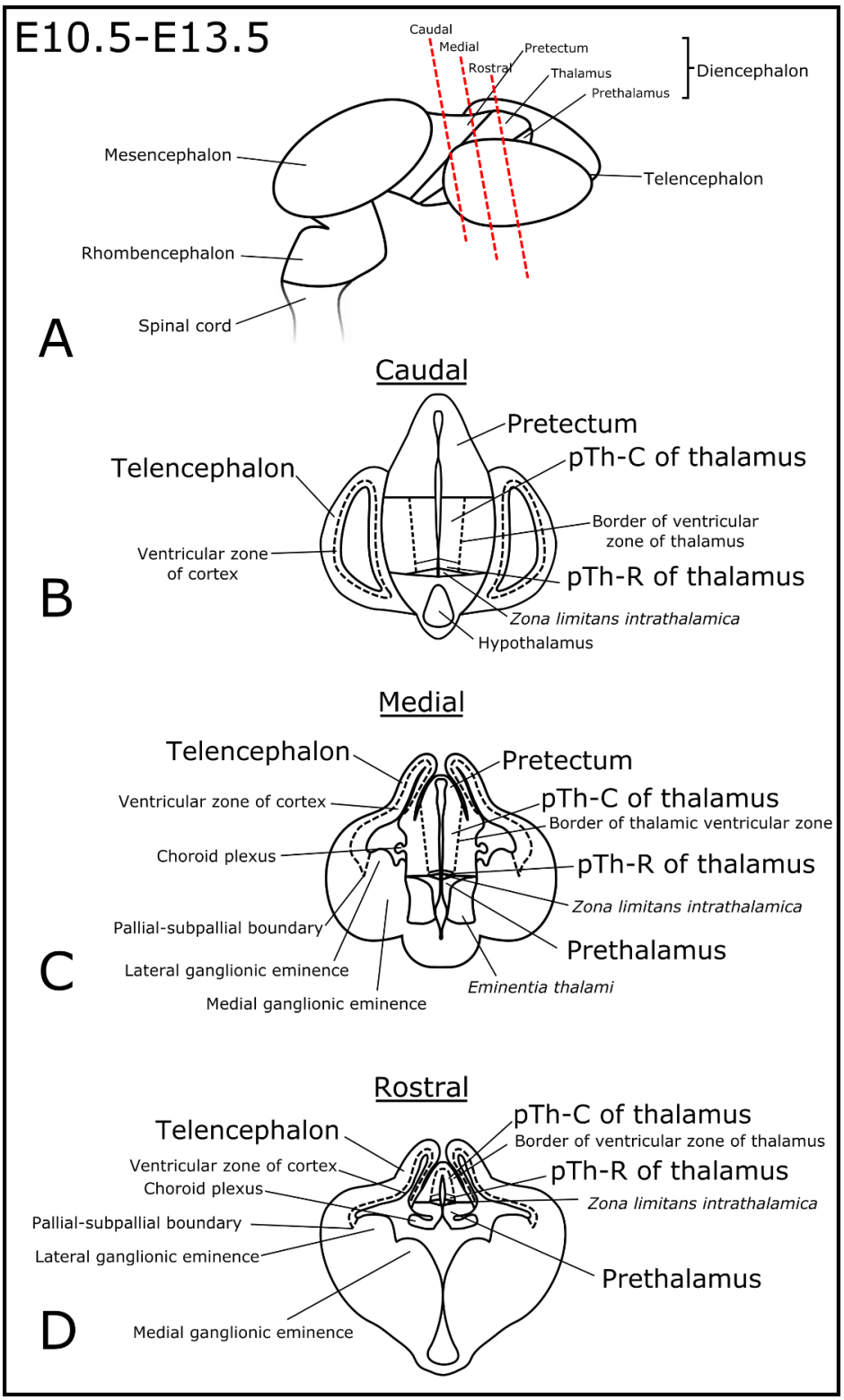

Fig. 1.6: A. Schematic of the E12.5 mouse brain as viewed from the left-hand side, rostral to right, to illustrate the coronal plane of section. B. The structures visible in a caudal coronal section. C. The structures visible in a medial coronal section. D. The structures visible in a rostral coronal section.

1.3 Morphogens: *Sonic hedgehog*

Shh is one of three mammalian homologues of the *Drosophila* morphogen *hedgehog* (*Hh*) (Echelard *et al* 1993, Chang *et al* 1994, Ingham and McMahon 2001). Loss of *Shh* leads to a very severe embryonic lethal mutant phenotype with morphological abnormalities including truncated limbs, fused digits, and cyclopia- the most severe form of holoprosencephaly (Chang *et al* 1996, Roessler *et al* 1996). *Shh* plays important roles in the development of limbs and digits (Riddle *et al* 1993, Chang *et al* 1994, Hill 2007) and is essential for the correct development of the central nervous system (CNS) (Echelard *et al* 1993, Chiang *et al* 1996). Elevated levels of *Shh* activity have also been implicated in some carcinomas (Oro *et al* 1997, Katoh and Katoh 2005, Peng and Joyner 2015) and components of the *Hedgehog* pathway have been studied as drug targets for chemotherapeutic agents (Dormoy *et al* 2012, Kieran 2014, Robinson *et al* 2015). The importance of *Shh* in a wide range of developmental processes and pathologies has led to it becoming the best studied ligand of the vertebrate *Hedgehog* pathway.

Secreted *Shh* molecules are able to bind to the transmembrane receptor proteins *Ptch1* and *Patched homologue 2* (*Ptch2*) on the surface of the target cell (Motoyama *et al* 1998, Fuse *et al* 1999). *Ptch1* is the only one of these two receptors expressed by cells of the developing CNS (Carpenter *et al* 1998). Within the developing CNS *Ptch1* acts to inhibit *Smo*, a G protein-coupled receptor (Ruiz-Gómez *et al* 2007), by controlling its location within the cell (Taipale *et al* 2002). In the absence of *Shh*, *Smo* is located on the membrane of vesicles within the cytoplasm. When *Shh* binds to *Ptch1* these vesicles translocate to the cell's primary cilium and fuse with the cell membrane, resulting in an accumulation of *Smo* at the primary cilium, the site at which *Smo* is active in the *Shh* pathway (Corbit *et al* 2005).

Active *Smo* regulates the expression of *Shh* target genes via interactions with the *GLI-Kruppel family member* (*Gli*) transcription factors, *Gli2* and *Gli3*. A third *Gli* transcription factor, *Gli1*, is also expressed in mammalian cells but does not appear to interact with *Smo* to as great an extent as *Gli2* and *Gli3*. *Gli1*-null mouse mutants are viable and resemble wild type mice while loss of *Gli2* is embryonic lethal (Park

et al 2000, Bai *et al* 2002) and loss of *Gli3* leads to perinatal lethality (Hui and Joyner 1993, Maynard *et al* 2002).

The mechanisms of the interactions between *Gli2*, *Gli3* and *Smo* are not well understood but it is known that in the absence of *Shh*, when *Smo* is inactive, *Gli2* and *Gli3* are phosphorylated. This enables the proteolytic cleavage of *Gli2* and *Gli3*, leading to the formation of their repressor forms, known as *Gli2R* and *Gli3R*, which diffuse into the nucleus and inhibit the transcription of *Shh* target genes. When *Shh* binds to *Ptch1* and *Smo* is active at the primary cilium, this phosphorylation is inhibited and *Gli2* and *Gli3* remain in their activator forms, referred to as *Gli2A* and *Gli3A*, which activate the transcription of *Shh* target genes. (Briscoe and Thérond 2013) (Fig. 1.7).

Tissues in range of secreted morphogen signal need to be competent to respond to it, and the expression of different transcription factors within those tissues mediates the response to the signal. In addition to this, cells are able to produce different responses to different concentrations of a given morphogen, with the concentration of a given morphogen being required to reach a particular threshold, with a cell being exposed to the morphogen for a minimum length of time, in order to activate or inhibit the transcription of each of the morphogen's target genes (Ashe and Briscoe 2006, Rogers and Schier 2011). This phenomenon is known as graded signalling and it is a property of *Shh* signalling which has been studied and quantified extensively in a range of experimental models and embryonic tissues (Patten and Placzek 2000, McGlinn and Tabin 2006, Briscoe 2009).

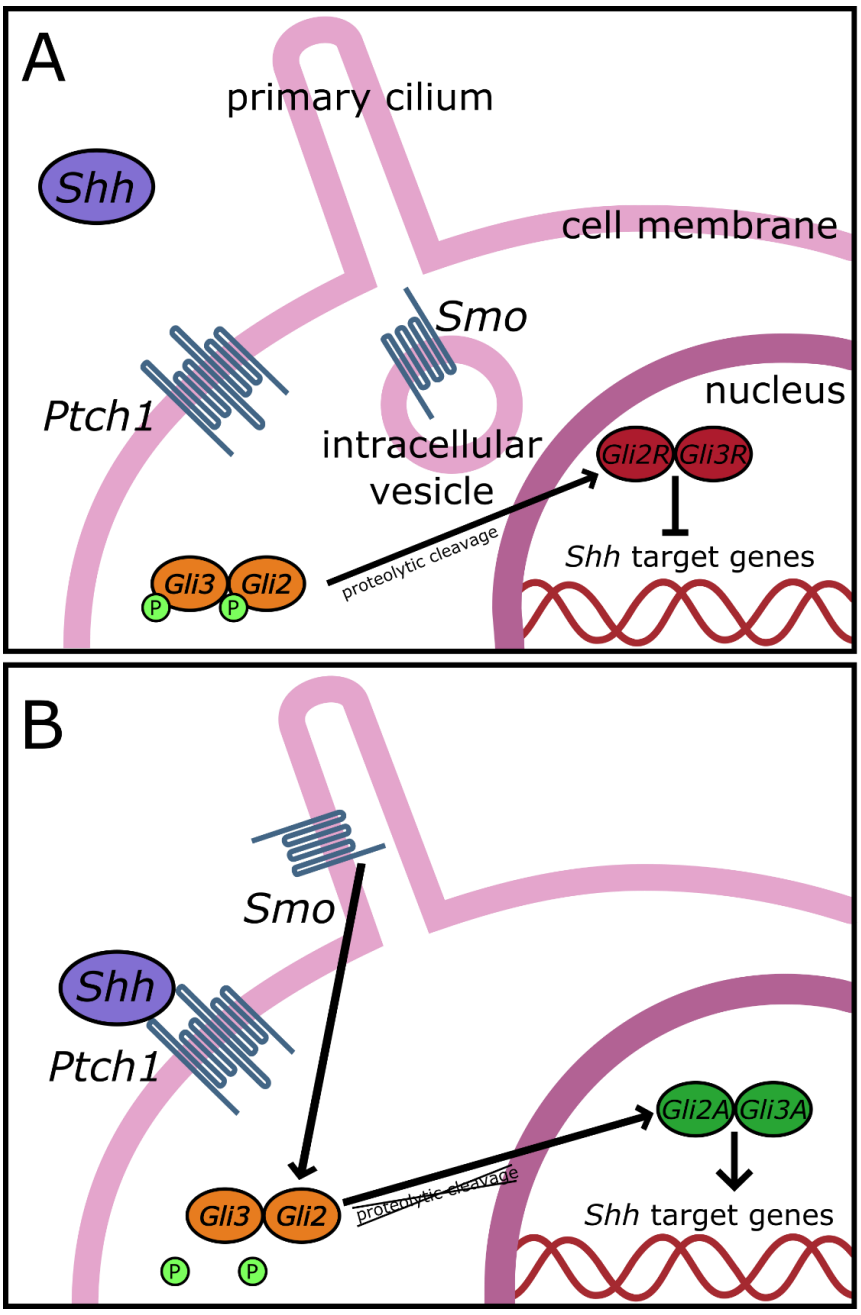

Fig. 1.7: A simplified schematic illustrating the Shh *signalling pathway. A. When* Shh *is not bound to the receptor* Ptch1, *the receptor* Smo *is largely confined to the membranes of intracellular vesicles.* Gli1 *and* Gli2 *are phosphorylated, enabling proteolytic cleavage to their repressor forms, Gli2R and Gli3R, which translocate to the nucleus and represses the transcription of Shh target genes. B. When* Shh *binds to* Ptch1 Smo *translocates to the primary cilium, the phosphorylation of* Gli2 *and* Gli3 *is inhibited and they remain in their activator forms,* Gli2A *and* Gli3A, *translocate to the nucleus and induce the transcription of* Shh *target genes.*

The effects of graded *Shh* signalling at different points along the *Shh* morphogen gradient have perhaps been studied most comprehensively in the spinal cord, where graded *Shh* signalling leads to the specification of different neuronal progenitor pools (Briscoe and Ericson 1999, Ribes and Briscoe 2009, Balaskas *et al* 2012, Cohen *et al* 2013) but graded *Shh* signalling has also been observed within the developing diencephalon, where it serves to pattern the thalamus (Vue *et al* 2009).

Graded *Shh* signalling has been shown to be required for the specification of the glutamatergic pTh-C and the GABAergic pTh-R, the latter of which is closer to the ZLI and is exposed to a higher concentration of *Shh*. Activating the *Shh* pathway in via ectopic expression of *Smo* causes an expansion of the pTh-R at the expense of the pTh-C, with GABAergic neurons being specified instead of glutamatergic neurons (Vue *et al* 2009) while loss of *Shh* leads to an absence of the pTh-R (Szabó *et al* 2009, Vue et al 2009).

1.4 Transcription factors: *Paired-box gene 6*

Paired-box gene 6 (*Pax6*) is a member of the *Paired-box* (*Pax*) family of transcription factors which are characterised by the presence of two DNA binding domains: the paired box and the homeobox (Hill *et al* 1991). *Pax6* is highly conserved between species, with the *Drosophila* homologue *eyeless* (*ey*) exhibiting 94% amino acid sequence identity with that of murine *Pax6* (Quiring *et al* 1994), and the amino acid sequence of murine *Pax6* being identical to that of human *PAX6* (Ton *et al* 1991, Gehring and Ikeo 1999). In mouse the gene encoding *Pax6* is located on chromosome 2 (Walther e*t al* 1991). The onset of *Pax6* expression in the mouse embryo is the two-cell stage (Guo *et al* 2010, Tang et al 2011), approximately E1.5 (Theiler 1989).

Loss of *Pax6* results a very severe perinatal lethal phenotype. The external morphology is greatly altered, with *Pax6*-null mouse embryos being reduced in size overall and exhibiting severe craniofacial defects including a shortened snout (Kaufman *et al* 1994, Favor *et al* 2001). These craniofacial abnormalities cause null mutant mouse pups to die shortly after birth as a result of being unable to breathe while suckling (Hill *et al* 1991). Heterozygous mouse mutants have not been studies

as extensively but in humans the loss of one copy of *PAX6* is linked to aniridia (Ton *et al* 1991) and defects of neural development (Sisodiya *et al* 2001).

Pax6-null mouse mutants also fail to develop eyes (Hill *et al* 1991). This is due to *Pax6* being required for the induction of eye development (Collinson *et al* 2000, Chow and Lang 2001), a function which is conserved across vertebrate and invertebrate species. Ectopic expression of human *PAX6* in the *Drosophila* embryo is sufficient to induce the development of ectopic compound eyes (Halder *et al* 1995).

Pax6 is widely expressed throughout the vertebrate CNS (Walther and Gruss 1991, Kawakami *et al* 1997, Duan *et al* 2013) and the loss of *Pax6* has been implicated in many defects in neural development. The gross morphology of the forebrain is greatly altered, with the forebrain being greatly reduced in size overall (Quinn *et al* 2007) and the neuroepithelium being reduced in thickness (Jones *et al* 2002, Quinn *et al* 2007). Within the diencephalon the lumen of the diencephalon expands laterally (Schmahl *et al* 1993) as a result of two diencephalic structures, the paraventricular nucleus and the caudal *zona incerta*, failing to develop correctly (Stoykova *et al* 1996).

Many other processes of neural development are disrupted as a result of loss of *Pax6*, including axon guidance (Jones *et al* 2002, Pratt *et al* 2000a, Manuel *et al* 2008, Georgala *et al* 2011) and the control of cell cycle exit (Sansom *et al* 2009, Farhy *et al* 2013, Mi *et al* 2013, Manuel *et al* 2015). *Pax6* has been shown to be essential for the correct patterning of the forebrain, with numerous roles in the control of diencephalic patterning. The loss of *Pax6* also disrupts the specification of several diencephalic structure- for example, *Pax6* is required for the formation of the boundary between the mesencephalon and pretectum (Mastick *et al* 1997, Warren and Price 1997) while the differentiation of the pTh-C is disrupted in the *Pax6*-null mutant (Pratt *et al* 2000a).

Pax6 is required for the development and shaping of the ZLI. The *Shh* promoter (Mutoh *et al* 2011) is regulated by *Pax6*, which binds to the promoter and indirectly inhibits the expression of *Shh*. In regions of neuroepithelium adjacent to the ZLI this inhibition serves to limit ZLI expansion (Caballero *et al* 2014). Loss of *Pax6* results

in the ZLI becoming greatly expanded along the rostrocaudal axis (Grindley *et al* 1997, Pratt *et al* 2000a).

The specification of the thalamus also requires the expression of *Pax6*. The thalamus develops in a region of the forebrain which expresses both *Pax6* and *Irx3*. Expression of both transcription factors is required to confer thalamic competence on the cells of the diencephalon. Ectopic expression of *Irx3* within the *Pax6*-positive telencephalon is sufficient to induce the expression of thalamic markers, while ectopic expression of *Pax6* and *Irx3* has the same effect on cells of the mesencephalon (Robertshaw *et al* 2013).

Ectopic expression of *Shh* within the thalamus has been shown to downregulate *Pax6* expression (Kiecker and Lumsden 2004, Vieira *et al* 2005). *Pax6* is expressed in pTh-C (Kiecker and Lumsden 2004) but is absent from the pTh-R (Vue *et al* 2007, Suzuki-Hirano *et al* 2011). While cells of the *Pax6*-expressing pretectum and prethalamus can differentiate into GABAergic neurons (Virolainen *et al* 2012) *Pax6* expression in the thalamus inhibits the differentiation of GABAergic neurons (Szabó et al 2009, Vue et al 2009). This inhibition must therefore be suppressed in order for the pTh-R to develop, and experiments in chick have confirmed that *Shh* serves to inhibit *Pax6* expression in the presumptive pTh-R, thereby playing a role in allowing the development of the pTh-R to proceed (Robertshaw et al 2013). In *Pax*6-null mouse mutants the pTh-R, like the ZLI, undergoes an expansion along the rostrocaudal axis, and is specified at the expense of the pTh-C, possibly as a consequence of increased levels of *Shh* protein and an increase in its inhibition of *Pax6* expression (Caballero *et al* 2014).

1.5 Transcription factors: *Bar homeobox-like 2*

The *Bar homeobox-like* transcription factors, *Bar homeobox-like 1* (*Barhl1)* and *Bar homeobox-like 2* (*Barhl2*), are the respective vertebrate homologues of the *Drosophila Bar* transcription factors, *Bar homeobox 1* (*BarH1*) and *Bar homeobox 2* (*BarH2*) (Schumacher *et al* 2011). The name *Bar* refers to the implication of the two *Drosophila* genes in the development of the "*Bar-eye*" *Drosophila* mutant phenotype

in which the eyes are reduced in size along the anteroposterior axis and exhibit a characteristic “bar” shape.

The *Bar-eye* phenotype was first described in *Drosophila* when it was observed as a consequence of a spontaneous mutation and found to be a sex-linked condition (Tice 1914). The *Bar-eye* phenotype was found to be caused by a duplication of a region of the X chromosome. The severity of the phenotype was found to increase with greater numbers of duplications, with narrower eyes observed in flies with greater numbers of duplications (Sturtevant 1925). Later studies referred to this region of the X chromosome as the *Bar* locus and considered it as the location of a hypothetical gene named *Bar*. The *Bar* locus is now known to be the region of the X chromosome within which both *BarH1* and *BarH2* are located (Kojima *et al* 1991)

Overexpression of *BarH1* and *BarH2* in *Drosophila* gives rise to the *Bar-eye* phenotype by disrupting the patterning of the retina. The *Drosophila* compound eye consists of 750-800 cone-shaped structures known as ommatidia, which develop in evenly-spaced rows across the eye field during development (Ready *et al* 1974, Reifegerste and Moses 1999, Kumar 2011, Sato *et al* 2013). Each ommatidium contains a cluster of photoreceptor cells at its basal extent. Eight *Drosophila* photoreceptor subtypes have been identified and these are termed R1-R8. In *Drosophila* the first subtype to differentiate is R8 (Jarman *et al* 1994, Hsiung and Moses 2002). The differentiation of R8 induces the induction of R1-7 in adjacent cells, leading to the development of an individual photoreceptor cluster (Hsiung and Moses 2002, Sato et al 2013). R8 photoreceptors, and in turn photoreceptor clusters, develop in rows during a wave of neurogenesis which moves across the eye field from dorsal to ventral. The modulation of this process during eye development results in the formation of a compound eye with ommatidia which are evenly spaced (Brennan and Moses 2000, Sato *et al* 2013).

The differentiation of R8 requires the proneural transcription factor *atonal* (*ato*) (White and Jarman 2000). Expression of *ato* is inhibited by *BarH1* and *BarH2*. Overexpression of the *Drosophila Bar* genes acts via transcriptional repression of *ato* to reduce the rate of neurogenesis and slow the process by which rows of ommatidia form, resulting in an eye which is reduced in size along the dorsoventral axis.

Gain-of-function experiments in *Drosophila* have shown that overexpression of *BarH1* is sufficient to induce the development of the *Bar* phenotype, with increased levels of *BarH1* leading to an increase in the transcriptional inhibition of *ato* (Higashijima *et al* 1992). Conversely, loss of *BarH1* and *BarH2* results in the *rough eye* phenotype with affected flies exhibiting ectopic ommatidia outside the eye field and a consequent alteration in the gross morphology of the eye. Ommatidia also appear crowded together rather than being evenly spaced (Lim and Choi 2003).

As with *Pax6*, homologues of the *Drosophila BarH* genes have been identified in a wide range of invertebrate and vertebrate species and found to be highly conserved (Reig *et al* 2007). *Drosophila* phenotypes caused by mutations in *BarH1* and *BarH2* are sex-linked due to both genes being located on the X chromosome. In mouse *Barhl1* is located on chromosome 2 (Bulfone *et al* 2000) while *Barhl2* is located on chromosome 5 (Mouse Genome Informatics Scientific Curators 2002) and conditions in which the two murine homologues are implicated are therefore not sex-linked. The onset of *Barhl2* expression in the mouse embryo is not currently known, with the earliest reported expression being at E9.5 (Yokoyama *et al* 2009).

In *Drosophila BarH1* and *BarH2* exhibit functional redundancy (Higashijima *et al* 1992) but loss-of-function experiments have suggested that this is not the case with murine *Barhl1* and *Barhl2*, with loss of *Barhl2* resulting in a much more severe phenotype than that caused by loss of *Barhl1*. While the *Barhl1*-null mutant mouse is viable, exhibiting progressive hearing loss but apparently phenotypically normal in all other respects studied (Li *et al* 2002), loss of *Barhl2* causes postnatal lethality at around P21, with mouse null mutants failing to thrive and exhibiting ataxia and numerous CNS defects (Ding *et al* 2012)

Barhl1 has been found to be required for the maintenance, but not the induction, of hair cells in the cochlea (Li et al 2002) and while it is expressed in the diencephalon and rhombencephalon (Gray *et al* 2004) loss of *Barhl1* does not seem to affect neural development to as great an extent as loss of *Barhl2*.

Loss of *Barhl2* disrupts neuronal subtype specification in specific regions of the vertebrate CNS. In the developing mouse spinal cord, where *Barhl2* is normally

strongly expressed (Saba *et al* 2003), it serves to specify dl1 interneuron subtype: the loss of *Barhl2* leads to an increase in the number of contralaterally-projecting interneurons with a reduction in the number that project ipsilaterally (Ding *et al* 2012). In the murine retina *Barhl2* is required for amacrine cell (AC) subtype specification: loss of *Barhl2* leads to the specification of increased numbers of cholinergic ACs at the expense of glycinergic and GABAergic ACs and *Barhl2*-null mice exhibit abnormal retinal electrophysiology (Ding *et al* 2012). The premature expression of *Barhl2* in the zebrafish retina induces the differentiation of GABAergic ACs at the expense of non-GABAergic ACs and photoreceptors (Jusuf *et al* 2012).

Barhl2 appears to play several important roles in the patterning of the forebrain. In mouse it is strongly expressed in a region corresponding with the developing ZLI at E10.5 (Suzuki-Hirano *et al* 2011) and in *Xenopus Barhl2* has been shown to be required for the initiation of the ZLI, with morpholino knockdown of *Barhl2* inhibiting its formation (Juraver-Geslin *et al* 2014). While the expression of *Barhl2* has yet to be mapped comprehensively within the vertebrate forebrain, it has been suggested as a marker of the presumptive diencephalon (Colombo *et al* 2006) and used as such in fate-mapping studies in zebrafish (Staudt and Houart 2007).

Barhl2 is also known to be strongly expressed within the murine thalamus. While its expression has not been described in full it appears to be expressed within the thalamic ventricular zone in a domain with a shape comparable to that of *Pax6*. Outside the thalamus it appears to be expressed in *Pax6*-negative regions of the forebrain such as the *eminentia thalami* and subpallium, while it is not expressed in *Pax6*-positive regions such as the prethalamus and pallium (Suzuki-Hirano *et al* 2011).

The proteins encoded by the *BarH* genes and their vertebrate homologues are characterised by the presence of a homeobox along with either one or two FIL domains- DNA-binding regions which are rich in the amino acids phenylalanine, isoleucine, and leucine, referred to by their single-letter amino acid codes as F, I and L respectively (Reig *et al* 2007). Transcription factors containing FIL domains act as transcriptional repressors (Smith and Jaynes 1996) via a mechanism involving their recruitment of homologues of the *Drosophila* co-repressor *Groucho* (Muhr et al

2001, Bae et al 2003). The resulting interactions lead to the formation of a large nucleoprotein complex, known as the *Groucho* repressosome, which serves to inhibit promoter function (Courey and Jia 2001).

In *Drosophila* the formation of the *Groucho* repressosome is likely to be the mechanism by which *BarH1* and *BarH2* inhibit the expression of *ato* (Higashijima *et al* 1992) and this is because LIM domains have the ability to bind to motifs encoding bHLH transcription factors, of which *ato* is one example.

The potential for *Barhl1* to inhibit the transcription of antiproneural bHLH transcription factors in vertebrates has been considered. Experiments in mice have shown that ectopic expression of *Barhl1* inhibits the transcription of *Achaete-scute complex homolog 1* (*Ascl1*), the mammalian homologue of *ato* (Gradwohl *et al* 1996), but that, perhaps surprisingly, *Barhl1* upregulates the expression of *Neurogenin2* (*Ngn2*) (Saito *et al* 1998).

It is not known if *Barhl2* interacts with any proneural bHLH transcription factors in the developing vertebrate CNS or if it serves any functions comparable with those of *Barhl1*, but a number of proneural bHLH transcription factors are known to be expressed within the thalamic ventricular zone in domains similar in shape and position to that of the thalamic *Barhl2* domain. While *Ascl1* is not expressed in the murine pTh-C (Osório *et al* 2010), it is expressed in the pTh-R (Caballero *et al* 2014), while *Neurogenin1* (*Ngn1*) (Vue *et al* 2007), *Ngn2* (Gradwohl *et al* 1996, Osório et al 2010, Suzuki-Hirano et al 2011) and *Oligodendrocyte transcription factor 3* (*Olig3*) (Gray et al 2004) are among the bHLH transcription factors known to be expressed in the ventricular zone of the pTh-C.

Barhl2 is also known to modulate Wnt signalling during the early development of the diencephalon. In the canonical Wnt pathway, the binding of secreted Wnt proteins to the membrane-bound receptors of the *Frizzled* class prevents the degradation of intracellular β-catenin, instead allowing it to accumulate within the nucleus. Nuclear β-catenin can then bind to transcription factors and induce or inhibit the transcription of Wnt target genes (Rao and Kühl 2010). Studies in Xenopus have shown that by acting upstream of the enzyme *Caspase3*, *Barhl2* is able to prevent the degradation

and nuclear accumulation of β-catenin, thereby inhibiting canonical Wnt pathway activity. This effect of *Barhl2* serves to modulate Caspase3-mediated apoptosis and the rate of proliferative cell division (Juraver-Geslin *et al* 2011). Wnt3a is among the morphogens known to be secreted by the ZLI in addition to *Shh* (Shimogori *et al* 2010) but it not clear what the relationship between *Barhl2* and Wnt signalling from the ZLI is, or if any interactions between the transcription factor and the signalling pathway exist in this context.

1.6 Developing a model for the control of diencephalic development

Pax6, *Barhl2* and *Shh* all play important roles in diencephalic development. Interactions between the three genes may therefore serve to modulate the developmental processes in which they are involved. By investigating these relationships it may be possible to develop a model for the control of some processes of diencephalic patterning, and to build on what is already known about the interactions between the three genes.

The correct development of the diencephalon has been shown to require signalling by *Shh* secreted from the ZLI (Kiecker and Lumsden 2004, Vieira *et al* 2005). Both *Pax6* and *Barhl2* are required for the development of the ZLI, with *Barhl2* being required to initiate its development (Juraver-Geslin *et al* 2014) and *Pax6* to inhibit its expansion (Caballero *et al* 2014). *Pax6* is also known to interact with *Shh*, indirectly inhibiting its expression via the *Shh* promoter (Caballero *et al* 2014).

The relationship between *Barhl2* and *Shh* is not as well understood. In *Drosophila Hh* is required to initiate the expression of *BarH1* and *BarH2* before each gene begins to regulate and maintain its own expression (Lim and Choi 2004). In the vertebrate CNS the nature of the interactions of *Shh* with *Barhl1* and *Barhl2* has yet to be determined and the requirement for *Barhl2* in ZLI development suggests that *Barhl2* acts upstream of *Shh* in this context (Juraver-Geslin *et al* 2014).

The potential for interactions between *Pax6* and *Barhl2* has not been investigated in depth but there is limited evidence that the two transcription factors may act to inhibit each other's expression. Target screens of murine *Pax6* and human *PAX6*

have identified thirteen different binding sites for *Barhl2*, suggesting that it may be among the genes which interact directly with *Pax6* (Coutinho *et al* 2011). In *Xenopus* embryos, inhibition of *Barhl2* activity at the neural plate stage appears to cause an expansion of the *Pax6* expression domain, suggesting that *Barhl2* may act to inhibit *Pax6* expression (Offner *et al* 2005). While *Pax6* and *Barhl2* are both expressed within the murine thalamus, there is limited evidence that they are not co-expressed within other regions of the vertebrate forebrain (Suzuki-Hirano *et al* 2010). This may suggest the possibility of a mutually repressive relationship existing between the two genes, with the potential for a different relationship existing between them in the thalamus.

While *Barhl1* is known to interact with the proneural bHLH transcription factors *Ascl1* and *Ngn2* (Saito *et al* 1998), the potential for *Barhl2* to exert a comparable influence on the expression of proneural bHLH transcription factors has yet to be investigated. Along with homeobox and LIM domains of the *Barhl2* protein exhibiting structures similar to those of the *Barhl1* protein (Reig *et al* 2007), the expression of *Barhl2* in a domain comparable to those of *Ngn1*, (Vue *et al* 2007), *Ngn2* (Gradwohl *et al* 1996, Osório et al 2010, Suzuki-Hirano et al 2011) and *Olig3* (Gray et al 2004) may suggest a role for *Barhl2* in the control of bHLH transcription factor expression during thalamic neurogenesis.

Barhl2 has only recently been considered as a candidate for the control of diencephalic patterning (Suzuki-Hirano *et al* 2011). Studies of *Barhl2* expression and function have been carried out on a diverse range of animal models, and within each model, a wide range of tissues from different CNS structures.

This project aims to investigate the potential for interactions between *Pax6* and *Barhl2* and to identify and characterise any relationships which are found to exist between the two genes, and between their expression and the activity of *Shh*. The spatiotemporal dynamics of *Pax6* and *Barhl2* will be mapped throughout the early stages of diencephalic development in order to obtain evidence for any potential interactions between the two genes, in particular the existence of co-expression within the thalamus, or complementarity between the two genes' domains elsewhere. *Barhl2* expression in the *Pax6*-null mutant mouse will be observed in order to

identify any changes which may be due to the loss of *Pax6*, and its expression will be observed in the *Shh*-null mutant in order to gain further insight into its interactions with *Shh*. A *Shh* loss-of-function approach will be taken via the use of drug treatment to suppress *Shh* activity in order to observe the effects on the expression of *Pax6* and *Barhl2*. Finally, the technique of *in utero* electroporation will be used in a *Shh* gain-of-function approach in order to examine the effects of *Shh* pathway activation in different regions of the diencephalon, and the possibility that its effects on the expression of *Pax6* and *Barhl2* are context-dependent.

The findings from these investigations will be considered together in an attempt to develop models for the control of diencephalic development based upon interactions between *Pax6*, *Barhl2* and *Shh*.

2. Materials and methods

2.1 Mice

Mice were bred in accordance with the guidelines of the UK Animals (Scientific Procedures) Act 1986.

Wild type mice used were of the *Mus musculus* strain Crl:CD1(ICR), referred to here as CD-1® (Charles River Laboratories International, Inc. 2011). *Pax6 Sey* mutant mice used were of the *Sey*^{Ed} strain in which the mutant *Sey* allele encodes a non-functioning form of *Pax6* (Hill *et al* 1991). *Pax6*$^{Sey/+}$ mice were maintained on a CD-1® background. *Pax6*$^{+/Sey}$ males were crossed with *Pax6*$^{+/Sey}$ females to generate litters comprising embryos of the genotypes *Pax6*$^{+/+}$, *Pax6*$^{+/Sey}$ and *Pax6*$^{Sey/Sey}$. Crosses were set up and female mice checked by technicians for the presence of a semen plug in the cervix. The day on which the plug was found (the plug date) was taken to be the day of conception, E0.5. Pregnant mice were culled at E9.5-E13.5 and embryos harvested. Harvested embryos were staged more precisely by their external morphology according to the Theiler Staging Criteria for mouse embryo development (Richardson *et al* 2014).

Pax6$^{Sey/Sey}$ embryos harvested at E11.5 or later were identified by the absence of eyes (Hill *et al* 1991) while *Pax6*$^{Sey/Sey}$ embryos harvested at E10.5 and earlier, before the developing eye becomes a visible feature of the external anatomy (Richardson *et al* 2014), were genotyped. Tissue samples were taken from the tail tip or limb bud of the embryo and treated using a version of the HotSHOT protocol (Truett *et al* 2000) to lyse the cells and release the genomic DNA. Tissue samples were placed in 0.5ml polymerase chain reaction (PCR) tubes, and 75µl of 25mM NaOH with 0.2mM ethylenediaminetetraacetic acid (EDTA) adjusted to pH 12 was added. This mixture was then heated to 95°C for 30 minutes before 75µl of 40mM Tris-HCl (pH 7.5) (Table 2.7) was added to neutralise the mixture. PCR was then employed to amplify a 282bp region of *Pax6* containing the single base affected in the *Sey*^{Ed} mutation (forward primer: 5'-TTAGGAAGGCTTTGTGGAGGC-3', reverse primer: 5'-CTTTCTCCAGAGCCTCAATCTG-3'- Eurofins MWG Operon). (Table 2.1).

Reaction component	Volume (µl)
Genomic DNA	1.00
Forward primer 200 ng/µl (Eurofins MWG Operon)	0.25
Reverse primer 200 ng/µl (Eurofins MWG Operon)	0.25
Deoxynucleotide triphosphate (dNTP) mix (10mM) (New England Biolabs)	2.00
GoTaq® DNA polymerase (Promega)	0.20
10x GoTaq® buffer (Promega)	4.00
Double distilled water	12.30
Total volume	**20.00**

Table 2.1: Formula for the PCR reaction for the genotyping of Sey^{Ed} *embryos.*

The PCR product was then digested with the restriction enzyme *DdeI* (New England Biolabs, catalogue number R0175S) for two hours at 37°C 9 (Table 2.2).

Reaction component	Volume (µl)
PCR product	5.0
DdeI (New England Biolabs)	0.5
CutSmart® Buffer (New England Biolabs)	2.0
Double distilled water	12.5
Total volume	**20.0**

Table 2.2: Formula for the Sey^{Ed} *genotyping PCR product digest reaction.*

Digested DNA samples were analysed using agarose gel electrophoresis performed with 50ml of 4% NuSieve agarose containing 1µl GelRed™ fluorescent nucleic acid stain (Biotium) in TBE running buffer. Digestion of DNA the $Pax6^{+}$ allele resulted in bands of 199bp and 83bp while bands of 199bp, 180bp, 83bp and 19 bp were observed following digestion of the fragment from mice carrying the Sey^{Ed} allele.

Shh-null mutant embryos (Chiang *et al* 1996) and control littermates were kindly provided by Professor Robert Hill at the MRC Human Genetics Unit, University of Edinburgh, as whole embryos in methanol. *Shh*-null mutant embryos were identified as those exhibiting cyclopia (Chiang *et al* 1996, Roessler *et al* 1996).

2.2 Tissue fixation and preparation

Harvested embryonic tissue was washed in phosphate buffered saline (PBS), made by adding one PBS tablet (Oxoid) to 100ml of double distilled water. Embryonic tissue was fixed in a solution of 4% paraformaldehyde (PFA) (Fisher Scientific) in PBS with gentle rocking at 4°C overnight.

For samples to be processed as whole mounts, tissue was washed in a solution of 0.1% Tween-20 (Fisher Scientific) in PBS- a solution referred to here as PBT. The samples were then dehydrated by washing in a series of increasingly concentrated solutions of methanol diluted in PBT, at concentrations of 25%, 50% and 75% respectively. Following these washes tissue samples were stored in 100% methanol at -20°C. Prior to processing the tissue samples were rehydrated by washing in a series of increasingly dilute solutions of methanol in PBT, at concentrations of 75%, 50% and 25% respectively before being washed in PBT.

For samples which were to be sectioned prior to further processing tissue was transferred to a solution of 30% sucrose in PBS with gentle rocking at room temperature (RT) until the tissue sank to the bottom of the solution. Sucrose-sunk tissue was placed into a truncated cryostat mould (Polysciences Inc) filled with a 1:1 mixture of 30% sucrose dissolved in PBS and optimal cutting temperature (OCT) cryosectioning compound (Sakura, Fisher Scientific). Tissue was manipulated into the desired orientation before the mould was placed into a container of dry ice to freeze the OCT/30% sucrose in PBS mixture and the tissue sample within. Mounted embryos were stored at -80°C.

Tissue samples intended to be treated with *in situ* hybridization alone, and with a single riboprobe, were cryosectioned at a thickness of 10µm. Tissue samples intended to be treated with both *in situ* hybridization and immunohistochemistry, or with *in situ* hybridization using two different riboprobes, were sectioned at a greater thickness of 16µm as a compromise to allow for the lengthier and more destructive protocols.

All tissue sections were mounted on Superfrost™ Plus slides (Fisher) and air dried at room temperature (RT) for a minimum of one hour before being processed or placed

into storage at -20°C for later use. Slides kept in storage at -20° were warmed to RT and left to dry at RT for at least one hour prior to processing in order to allow condensation to evaporate.

2.3 Preparation of plasmid DNA

Plasmid DNA was amplified in *Escherichia coli* (*E.coli*) cells. 100µl of competent *E.coli* cells (Promega) were thawed on ice for 30 minutes before being transferred to a sterile 15ml tube.

The majority of the plasmid DNA to be amplified was sourced from the plasmid bank at the laboratory of the Genes and Development Group, The University of Edinburgh. The plasmid DNA stocks in this resource are dissolved in double distilled water before being stored at -20°C. For these plasmids, 1-2µl of plasmid DNA was added to the tube containing the competent cells. A small number of plasmids were received by mail in the form of DNA solution applied to sterile filter paper and allowed to dry. For these plasmids the region of filter paper marked as the site of the DNA solution was excised and placed in 500µl of double distilled water in a 1.5ml microcentrifuge tube in order to elute the DNA. 1-2µl of the elute was added to the tube containing the competent cells. Other plasmids were sourced from the plasmid bank at the Laboratory for The Mechanisms of Thalamus Development, The RIKEN Brain Science Institute. The plasmids in this resource are added to a solution of 80% glycerol in double distilled water before being stored at -80°C as glycerol stocks. For these plasmids a small sample was taken by scratching the surface of the glycerol stock with a sterile pipette tip and dropping this into the 15ml tube containing the competent cells.

The mixture of competent cells and plasmid stock DNA was mixed gently and then incubated on ice for 30 minutes before cells were transformed using the heat shock method (Froger and Hall 2007). The tube was transferred to a thermostatically controlled water bath and incubated at 42°C for 45 seconds before being placed back on ice. 450µl of Super Optimal Concentration (SOC) medium (Sigma) was added to the tube and the mixture was then incubated at 37°C with shaking at 180RPM for two hours.

For plasmids received by mail, 200µl of the SOC medium culture was plated on agar containing the antibiotic to which the plasmid was resistant. The streak plate method was used to ensure it would be possible to distinguish and pick a single colony from the bacterial lawn (Sanders 2012). Plated cells were incubated at 37°C for 18 hours. Following incubation a sterile pipette tip was used to pick a single colony and this was incubated in 450µl of SOC medium at 37°C for 2 hours to generate a starter culture. For plasmids sourced from the plasmid banks, this step was omitted and the initial culture in SOC medium was used as a starter culture.

The starter culture was then added to 200ml of Luria Bertani (LB) broth containing the appropriate antibiotic in a conical flask of a volume of at least 400ml. the mixture was incubated at 37°C in a shaking incubator, at a speed of at least 180RPM and for a time period of no longer than 16 hours.

Bacterial cells were harvested by centrifuging the mixture at 6,000RPM at a temperature of 4°C for 15 minute. The liquid fraction was discarded. A maxiprep was performed on the remaining bacterial pellet to lyse the cells, release the cell contents and purify the plasmid DNA, using maxiprep kits (Qiagen, Viogene) and following the manufacturers' protocols.

LB broth was prepared by adding two LB broth tablets (Sigma) per 100ml of double distilled water and sterilising the resulting solution in an autoclave at a temperature of at least 140°C. 1ml of 100mg/ml ampicillin solution (Sigma) or 1ml of 50mg/ml kanamycin powder (Sigma) in double distilled water was added per 1l of autoclaved solution once cooled. Transformed *E.coli* cells were cultured in LB broth containing the antibiotic to which the plasmid DNA was resistant.

Purified plasmid DNA was stored at -20°C.

2.4 Preparation of single-stranded RNA riboprobes

DNA plasmids were first linearized in order to produce a template for the RNA riboprobe. A sample of plasmid DNA solution was added to a 1.5ml microcentrifuge tube with double distilled water and the appropriate restriction enzyme (various manufacturers) and buffer (various manufacturers). The resulting solution was at

37°C for two hours (see Table 2.3 for the volumes of the reaction components). The template DNA was then purified with the use of the phenol-chloroform extraction method (Chomczynski and Sacchi 2006) or the QIAquick Gel Extraction Kit (Qiagen).

Reaction component	Volume (µl)
Plasmid DNA	10.5
Restriction endonuclease enzyme (various manufacturers)	5.0
Enzyme buffer (various manufacturers)	10.0
Double distilled water	164.5
Total volume	**190.0**

Table 2.3: Formula for the DNA plasmid linearization reaction.

To synthesise a riboprobe using the template DNA, template DNA was added to a 1.5ml centrifuge tube with the appropriate RNA polymerase enzyme (T3, T7 or SP6) (Roche) and enzyme buffer (Roche), RNA nucleotide mix labelled with digoxigenin (DIG), 2, 4-dinitrophenyl (DNP) or fluorescein (FL) (Roche) and double distilled water. The solution was incubated at 37°C for two hours. DNAseI enzyme (Roche) was the added and the mixture incubated at 37°C for 15 minutes. (Table 2.4)

Reaction component	Volume (µl)
Template DNA	10
RNA polymerase (T3, T7, SP6)	2
RNA polymerase buffer (Roche)	2
RNA nucleotide labelling mix (DIG, DNP or FL) (Roche)	2
Double distilled water	12
Total volume	**28**

Table 2.4: Formula for the reaction for the synthesis of and RNA riboprobe from a DNA template.

To precipitate the labelled riboprobe out of the aqueous solution, 2.5µl of 4M lithium chloride (LiCl) and 2µl of 0.2M EDTA were added, along with 75µl of chilled ethanol for probes labelled with DIG or DNP, or 75µl of chilled isopropanol for probes labelled with FL. The solution was then stored at -80 overnight in order to

allow a high proportion of the labelled RNA to precipitate out of the solution. The solution was then centrifuged at 13,000RPM and 4°C for 30 minutes in order to collect the labelled RNA precipitate as a pellet.

The liquid fraction was discarded and the pellet was washed to remove residual LiCl with the addition of 200µl of 70% ethanol in double distilled water followed by centrifugation at 13,000 at RT for five minutes. The washing step was repeated once before the washed RNA pellet was air dried at 37°C for 10 minutes and the RNA then resuspended in 50µl of double distilled water.

Labelled riboprobes were stored at -20°C.

2.5 *In situ* hybridization

The required concentration for each riboprobe was determined by performing the *in situ* protocols as described below with the probe at dilutions of 1:500, 1:1,000, 1:2,000, 1:5,000 and 1:10,000 in hybridization buffer (Table 2.5). The dilution which produced an acceptably strong *in situ* signal with an acceptably low level of background staining was used for all further experiments using the same probe.

Probes were diluted to the required concentration in 200µl of hybridization buffer (Table 2.5) per slide. The diluted probe was heated to 85°C for 10 minutes in order to denature any ribonuclease enzymes (RNAses) which may be present as contaminants. The diluted probe was then pipetted onto slide-mounted tissue sections and coverslips were applied. Slides were placed into an airtight box humidified with formamide wash buffer (Table 2.5) and incubated overnight at 70°C.

Following the hybridization step sections were washed in formamide wash buffer at 70°C for 15 minutes in order to dissolve the hybridization buffer and allow coverslips to be removed without causing damage to the tissue sections. Two further washes in formamide wash buffer were performed at 70°C for 30 minutes.

For chromogenic *in situ* hybridization, sections were then washed in MABT (Table 2.6) two times for 30 minutes at RT. Slides were transferred to a box humidified with PBS and sections were outlined with a hydrophobic barrier pen (Vector Laboratories)

Solution	Reagent	Quantity
5M EDTA	EDTA (Fisher)	36.53g
	Double distilled water	250ml
	Total volume	**250ml**
pH adjusted to 8.0 with NaOH to allow EDTA to dissolve. Autoclaved. Stored at RT.		
10x salt	NaCl (Fisher)	28.50g
	Tris HCl (Fisher)	3.510g
	Tris base (Fisher)	0.355g
	$NaH_2PO_4{\cdot}2H_2O$	1.950g
	$Na2HPO_4$	1.775g
	0.5M EDTA	25ml
	Double distilled water	To total volume
	Total volume	**250ml**
pH adjusted to 8.0 with NaOH. Autoclaved. Stored at RT.		
Hybridization buffer	10x salt	20ml
	Deionized formamide (Sigma- Aldrich)	5ml
	50% dextran sulphate (Fisher)	2ml
	tRNA from bakers' yeast (Roche) 10mg/ml in double distilled water	1ml
	Denhardt's Solution (Life Technologies)	100µl
	Double distilled autoclaved water	900µl
	Total volume	**10ml**
Prepared in a fume hood. tRNA first denatured by heating to 85°C for ten minutes. Stored at -20°C.		
20x SSC buffer	NaCl	175.3g
	Sodium citrate	88.2g
	Double distilled water	1,000ml
	Total volume	**1,000ml**
Autoclaved. Stored at RT.		
Formamide wash buffer	20x SSC Buffer	15ml
	Double distilled water	135ml
	Tween-20 (Fisher)	300 µl
	Formamide (Fisher)	150ml
	Total volume	**300ml**
Prepared in a fume hood. Heated to hybridization temperature before use.		

Table 2.5: Formulae for reagents used in the hybridization steps of the section in situ *hybridization protocols.*

before a blocking solution of 20% sheep serum in PBS with 0.1% blocking reagent (Roche) (Table 2.6) was pipetted onto each slide. After an hour at RT the solution was gently shaken off the slides before anti-DIG alkaline phosphatase enzyme (Roche) at a concentration of 1:1,500 in blocking solution was added. The sections were incubated in the diluted antibody at 4°C overnight. Sections were then washed in MABT for 15 minutes RT five times before being washed in pre-staining buffer (Table 2.6) twice at RT for ten minutes. The slides were returned to the box humidified with PBS and staining buffer (Table 2.6) and from this stage onwards were covered to protect them from light. Slides were incubated at until the colour reaction had proceeded to the point where an acceptably strong *in situ* signal with an acceptably low level of background could be observed with brightfield microscopy. To arrest the colour reaction slides were washed in PBS. Sections were then covered with a 1:1 solution of glycerol and PBS before coverslips were applied and the slides were sealed with nail polish. Sealed slides were covered to protect them from light and stored at 4°C.

For fluorescence *in situ* hybridization, following the two 30 minute washes with formamide wash buffer tissue sections were washed twice in TNT wash buffer (Table 2.7) at RT for 30 minutes. Slides were transferred to a box humidified with PBS. Sections were outlined with a hydrophobic barrier pen (Vector Laboratories) and 100µl of blocking solution (Table 2.7) was pipetted onto each slide. After an incubation period of one hour at room temperature the blocking solution was gently shaken off the slides before anti-DIG (Roche), anti-DNP (Roche) or anti-FL (Roche) antibodies bound to horseradish peroxidase was pipetted onto each slide at a dilution of 1:500 in blocking solution (Table 2.7). Slides were incubated in the diluted antibody at 4°C overnight. Sections were then washed four times in TNT at RT for 15 minutes. Slides were returned to the humidified box and incubated in fluorophore solution (Table 2.7) for 15 minutes at RT. From this step onwards slides were covered to protect them from light. Sections were then washed in TNT four times for 15 minutes at RT. Slides were counterstained via incubation in 4',6-diamidino-2-phenylindole (DAPI) solution (table 2.7) for 10 minutes at RT before slides were rinsed in PBS. Sections were covered with ProLong™ Gold Antifade mounting

medium (Life Technologies), coverslips were applied and slides were sealed with nail polish. Sealed slides were stored at 4°C.

For double fluorescence *in situ* hybridization, a DIG-labelled probe was used along with a second probe labelled with either DNP or FL. Probes were diluted to the required concentration in hybridization buffer and *in situ* hybridization was performed as described above using the anti-DIG antibody and cyanine-3-tyramide as the fluorophore. Following the fluorophore incubation step slides were rinsed in TNT wash buffer and then incubated in 10mM HCl at RT for 30 minutes in order to denature the horseradish peroxidase. Slides were then washed four times in TNT buffer for 15 minutes at RT before being incubated in the second antibody (anti-FL or anti-DNP as appropriate) overnight at 4°C. Following this step slides were washed in TNT 4 times at RT for 15 minutes before being incubated in a fluorophore solution containing fluorescein for 15 minutes at room temperature. Following this step further washes in TNT wash buffer followed by counterstaining with DAPI were performed as described above. Sections were covered with ProLong™ Gold Antifade mounting medium, coverslips were applied and slides were sealed with nail polish. Sealed slides were stored at 4°C.

2.6 Fluorescence immunohistochemistry

Tissue sections were cryosectioned at a thickness of 16µm. All steps were performed with the slides covered to protect them from light. Following fluorescence *in situ* hybridization as described above, with slides incubated in a fluorophore solution containing cyanine-3-tyramide, slides were washed in cold running water for 10 minutes. Antigen retrieval was then performed by placing the slides into a 10mM solution of sodium citrate and gently heating them with low power microwave radiation for twenty minutes. Slides were left to cool to room temperature before being washed in PBT. Slides were transferred to a box humidified with PBS and incubated in a blocking solution consisting of 10% donkey serum (Sigma) in PBS for one hour. Slides were then incubated in a solution of the primary antibody- either Rabbit Poly Pax-6 (Covance Research Products) or Rabbit anti-GFP (Abcam) - at a dilution of 1:400 at 4°C overnight. The slides were then washed in PBT 6 times at

Solution	Reagent	Quantity
5xMABT	Maleic acid	58.05g
	NaOH	Approximately 32.00g
	NaCl	43.08g
	Tween-20 (Fisher)	5ml
	Double distilled water	To total volume
	Total volume	**1,000ml**
Maleic acid is added to approximately 800ml water first, followed by NaOH to adjust pH to 7.5 before other components are added and more water is added to total volume. 5x MABT is a stock solution stored diluted fivefold in water to 1xMABT before use. Stored at 4°C to inhibit growth of fungal contamination.		
Blocking solution for chromogenic *in situ* hybridization	1xMABT	4ml
	Sheep serum (Sigma-Aldrich)	1ml
	Blocking reagent (Roche)	100µg
	Total volume	**5ml**
Prepared immediately prior to use. Stirred with a magnetic stirrer for at least one hour at RT in order to allow blocking reagent to dissolve.		
1M Tris HCL pH 9.5	Tris-HCl	157.56g
	Double distilled water	1,000ml
	Total volume	**1,000ml**
pH adjusted with NaOH to pH 9.5 for chromogenic *in situ* hybridization. Autoclaved. Stored at RT.		
Pre-staining buffer	5M NaCl	6ml
	1M $MgCl_2$	15ml
	1M Tris-HCl pH9.5	30ml
	Tween-20 (Fisher)	300µl
	Double distilled water	To total volume
	Total volume	**300ml**
Prepared immediately prior to use.		
Staining buffer	5M NaCl	2ml
	1M Tris-HCL pH 9.5	10ml
	Double distilled water	83ml
	Polyvinyl alcohol (PVA) powder (Sigma-Aldrich)	9g
	1M $MgCl_2$	4.5ml
	Tween-20 (Fisher)	90µl
	Nitro blue tetrazolium and 5-Bromo-4-chloro-3-indolyl phosphate (NBT/BCIP) solution (Roche)	1.8ml
Reagents added in order given. Solution is stirred with a magnetic stirrer and heated to 85°C until PVA dissolves. Solution is cooled to RT with stirring before the remaining reagents are added. Prepared immediately prior to use.		

Table 2.6: Formulae for solutions used in the chromogenic section in situ *hybridization protocol.*

Solution	Reagent	Quantity
1M Tris HCL	Tris-HCl	157.56g
	Double distilled water	1,000ml
	Total volume	**1,000ml**
pH adjusted with NaOH to 7.5 for fluorescence *in situ* hybridization. Autoclaved. Stored at RT.		
TNT wash buffer	1M Tris-HCl pH 7.5	100.00ml
	5M NaCL	30.00ml
	Tween-20	2.25ml
	Double distilled water	To total volume
	Total volume	**1,000ml**
Prepared immediately prior to use.		
Blocking solution	1M Tris HCl pH 7.5	500µl
	5M NaCl	150µl
	Double distilled water	4.35ml
	Blocking reagent (PerkinElmer)	25µg
	Total volume	**5ml**
Prepared immediately prior to use. Stirred with a magnetic stirrer for at least one hour at RT in order to allow blocking reagent to dissolve.		
Fluorophore solution	Diluent (PerkinElmer)	100µl
	Cyanine-3-tyramide (PerkinElmer) *or* Fluorescein (PerkinElmer)	2 µl
Fluorophores are used at a dilution of 1:50 in diluent. Formula given is per slide.		
Counterstain solution	4',6-diamidino-2-phenylindole (DAPI) (Sigma Aldrich)	**1µl**
	PBS	**1ml**
DAPI prepared at a dilution of 1:1000 in PBS. Prepared immediately prior to use. 100µl is used per slide.		

Table 2.7: Formulae for solutions used in the fluorescence section in situ *hybridization protocol.*

RT for 15 minutes. Slides were then incubated in a solution of the secondary antibody, goat anti-rabbit Alexa-Fluor 488® (Abcam), at a dilution of 1:400 overnight at 4°C. Slides were then washed in PBT for 15 minutes and then incubated in counterstain solution (Table 2.7) for 10 minutes. Following two five minute washes in PBS sections were mounted with ProLong™ Gold Antifade mounting medium (Life Technologies) and the edges of the coverslips were sealed with nail polish. Sealed slides were stored at 4°C.

2.7 Vismodegib drug treatment

Administration of the drug and the control solution was performed in accordance with the UK Scientific Procedures Act (1986) by the technicians at Biological Research Resources, Hugh Robson Building. The harvesting, fixation and mounting of treated embryos were carried out by Idoia Quintana-Urzainqui.

Vismodegib (GDC-0449) powder (Selleckchem) was dissolved in a methylcellulose vehicle solution prior to administration (Lipinski et al 2010). To prepare the vehicle water was first purified by reverse osmosis. 20ml of purified water was heated to 85°C. 0.25mg of methylcellulose powder (Sigma-Aldrich) was added and the water stirred to evenly disperse the powder. 20ml of chilled purified water was then added to the suspension with stirring. The solution was stored at 4°C overnight or until the solution appeared clear. The clear solution was then allowed to reach RT before 100µl of Tween-80 (Fisher) was added. Once the Tween-80 had dissolved purified water was added to adjust the total volume of the solution to 50ml. The solution was filtered with the use of a syringe to pass the solution through disposable 0.4M filter units (Whatman). The vehicle solution was stored at 4°C for up to 1 month.

To prepare the vismodegib solution, the vehicle was allowed to equilibrate to RT. Vismodegib powder was added and the solution was sonicated in a bath sonicator for 5 minutes at a temperature not exceeding 37°. The solution was stored at 4°C for up to two weeks.

Vismodegib was administered at a dose of 4mg per animal. Control animals were administered with the vehicle only. The solutions were administered to pregnant

females at E9.5 by oral gavage and treated animals were closely monitored for adverse effects. Animals were culled at E12.5 and embryos harvested.

2.8 *In utero* electroporation

All surgical procedures were performed in accordance with the UK Scientific Procedures Act (1986). The method described here is a version of the transillumination electroporation method developed by Matsui *et al* (2011) with modifications in accordance with UK Home Office guidelines.

Timed matings were set up with mice of the CD-1® strain. Surgery was performed at E12.5. Prior to surgery all tools and working surfaces were sterilised. Animals were anaesthetised with gaseous isofluorane administered with medical oxygen via an anaesthetic rig. Anaesthetised animals were then transferred to a thermostatically-controlled heatpad, at which point anaesthesia and oxygen were administered via a facemask. A bright LED light source was positioned above the animal in order to illuminate the lower abdomen.

Pain relief was administered as a subcutaneous injection of buprenorphine diluted in sterile water for injections and given at a dose of 0.1 mg/kg of bodyweight. The lower abdomen was clipped to remove fur and washed with Dermastel antiseptic detergent (Tristel). The surgeon washed their hands with Dermastel before drying them with sterilised paper towels. Sterile nitrile gloves were worn during surgery. A window was made in a sterilised paper towel and this positioned over the animal with the window above the animal's lower abdomen.

An incision was made in the skin of the lower abdomen to expose the muscle layer. A second incision was made along the non-vascularised *linea alba* of the muscle layer, a site chosen to minimise blood loss. The body cavity was flushed with sterile PBS warmed to 37°C and administered via a sterile Pasteur pipette.

The whelps of one uterine horn were gently lifted out of the body cavity and kept moist with sterile PBS. A single whelp was held in the fingers of the surgeon's non-dominant hand and was viewed under the bright LED light in order to locate the position of the dorsal midline of the telencephalon and that of the diencephalon

immediately behind it. When these structures could be clearly seen the embryo was manipulated to orient the rostral limit of the forebrain towards the surgeon's dominant hand. Gentle pressure was applied to the whelp with fingers in order in order to position the embryo close to the uterine wall without causing damage to the embryo, the amniotic sac or other tissues.

Plasmid DNA was administered via a glass micropipette with a cut tip not exceeding a diameter of 40µm (Matsui *et al* 2011). The *cShh* pXeX plasmid (Agarwala *et al* 2001) was co-electroporated with the pTP6 Tau GFP plasmid (Pratt *et al* 2000b).

Control embryos were injected with pTP6 Tau GFP alone. The micropipette was filled with plasmid DNA solution at a concentration of no less than 1µg/µl for each plasmid and Fast Green FCF (Sigma-Aldrich) at a concentration of 10% in double distilled autoclaved water. The micropipette was then fitted into the pipette holder of a pneumatic picopump (World Precision Instruments). Using the dominant hand the surgeon inserted the tip of the micropipette through the uterine wall and the rostral extent of the left-hand telencephalic vesicle (Fig. 2.1A) until the tip of the micropipette could be seen within the third ventricle (Fig. 2.1B). The picopump was operated via a footpump control to administer the plasmid DNA (Fig. 2.1C). The presence of Fast Green within the third ventricle was taken as an indication of DNA having been administered successfully (Matsui *et al* 2011).

The pipette was removed and warmed sterile PBS was applied to the whelp in order to increase electrical conductivity. Platinum paddle electrodes (Nepagene) were placed in contact with the whelp, with the anode at the left-hand side of the diencephalon and the cathode on the right-hand side, and in such a way as to avoid passing current through the placenta (Fig. 2.1D). Gentle pressure was applied to the electrodes in order to position them close to the diencephalic tissues without causing damage to the whelp. The electroporator (Nepagene) was operated with a footpump control to administer five pulses of square wave electrical current at 30V. The treated whelp was then moistened with warmed sterile PBS.

The microinjection and electroporation procedures were repeated for further embryos in the same uterine horn before the dorsal horn was replaced in the body cavity. The

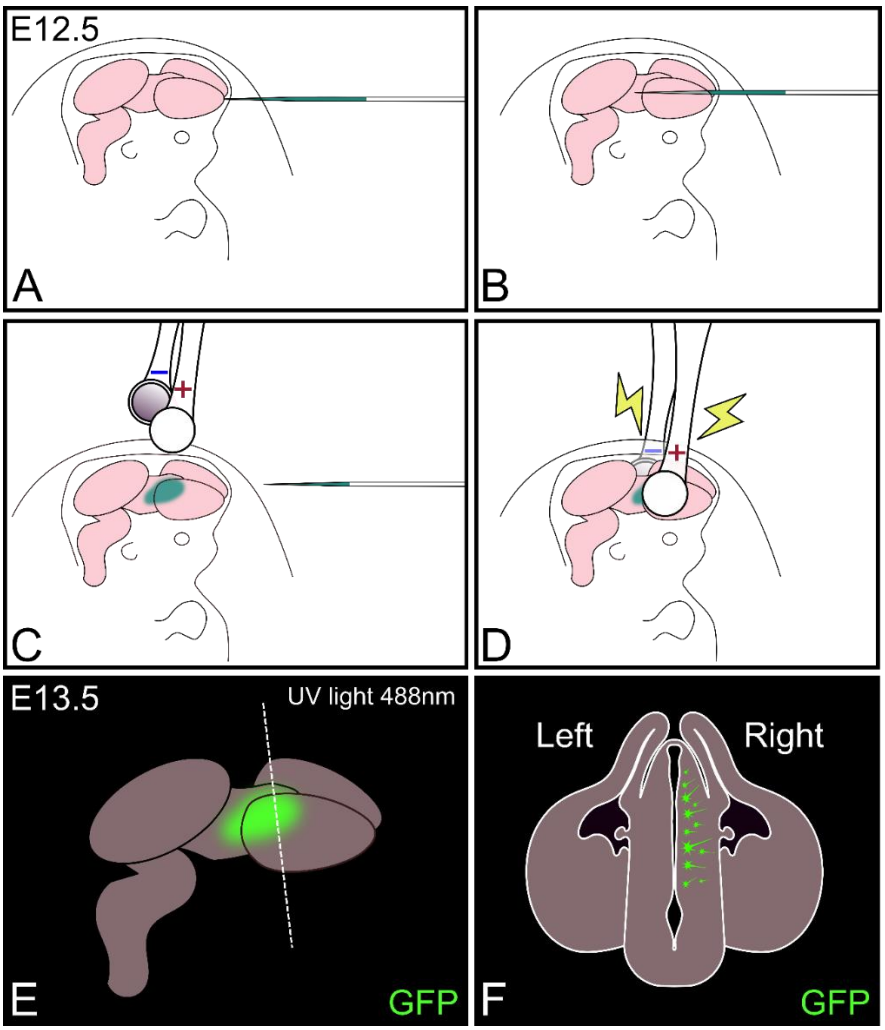

Fig. 2.1: Schematic to illustrate the positioning of the micropipette and electrodes for in utero *electroporation. A. The ventral midline of the telencephalon is located and the embryo is manipulated to ensure that the rostral extent of the brain is facing the hand the surgeon will use to inject the DNA and apply the current (in this case the right hand). B. The pipette is inserted until the tip can be seen within the third ventricle. C. The third ventricle is filled with DNA solution via a picopump and the capillary is removed before the electrodes are applied. D. The anode is placed at the left-hand side of the diencephalon while the cathode is placed at the opposite side before the current is applied. E. 24 hours after surgery animals are sacrificed, embryos are harvested and the embryonic brain tissue is isolated. Successfully electroporated embryos are identified by the use of fluorescence microscopy to detect GFP expression. F. In tissue sections the electroporated cells can then be visualised following the use of* in situ *hybridization or immunohistochemistry to detect the protein or mRNA expressed by the electroporation construct(s).*

process was then repeated for the embryos inside the whelps of the second uterine horn before this was also replaced in the body cavity. The whelps adjacent to the cervix were not treated in order to avoid tissue damage and haemorrhaging that can be caused by manipulation of the tissue at the point.

Prior to suturing approximately 1ml of sterile PBS was administered into the body cavity in order to replace fluid lost during surgery. The muscle layer was closed with Vicryl Rapide™ dissolving suture in size 5-0 (Ethicon) applied in a series of individual stitches along the length of the incision. The skin was closed with surgical clips (BD™ or Autoclip™). Administration of anaesthesia was halted and the animal transferred to a cage containing clean bedding material, fresh high-protein rodent chow and fresh water. Post-operative pain relief was administered as Buprenorphine in the form of edible jelly. The cage was placed on a thermostatically-controlled heat pad for two hours in order to optimise the animal's recovery. Cages were then transferred from the heat pad to the temperature and humidity-controlled CD-1® facility where animals were then monitored at regular intervals.

Animals were culled 24 hours after surgery, at E13.5. Embryos were harvested and dissected to isolate embryonic brain tissue. Brain tissue and this was observed under fluorescence in order to detect GFP expression as a sign of a successfully electroporated embryo and an indicator of the electroporated region (Fig. 2.1E).

2.9 Imaging

Brightfield images of tissue sections treated with chromogenic *in* situ hybridization were imaged with the Leica DMLB microscope and Leica AS Application Suite software. Tissue sections treated with fluorescence *in situ* hybridization and fluorescence immunohistochemistry were imaged with the Leica DM5500 fluorescence microscope and Leica AF6000 software. For whole embryos treated with chromogenic *in situ* hybridization, brightfield images were recorded with the Leica M165C microscope and Leica AS Application Suite software. For tissue sections treated with fluorescence techniques, widefield images were recorded with the Leica and Leica Advanced Fluorescence software. Confocal images were recorded using the Nikon A1R-FLIM confocal microscope and Nikon Elements

software. Images were recorded at a bit depth of 16 bits and a resolution of 1028x1028 pixels and were saved as stacks, with one image per channel (*Pax6* immunostaining at 488nm, *Barhl2 in situ* hybridization staining at 554nm, DAPI staining at 350nm). The "Grab large image free shape" function of Elements was used to compile a tiled image from several square images recorded at different regions of the tissue section. Confocal images were recorded at the Image Analysis, MultiPhoton, and Confocal Technologies (IMPACT) imaging facility, The University of Edinburgh.

2.10 Quantification of image data

Quantification was performed on tiled confocal images of images of medial sections of the diencephalon (Fig.1.5C). To ensure that the data from each image would be comparable images featuring comparable morphology were chosen to be analysed, with the morphology taken as a guide to the position of the section along the rostrocaudal axis of the diencephalon. In all sections chosen the prethalamus, identified by *Pax6* expression, and the ZLI and *eminentia thalami*, identified by *Barhl2* expression, were visible features.

One suitable image was selected from each of the three different embryos treated at each developmental stage from E10.5 to E13.5. Confocal images were rendered as 12 bit greyscale images in Fiji (Schindelin *et al* 2012) with pixel values ranging from 0 (black) to 4096 (white). The pixel values correlate with the intensity of the fluorescence, with an area of neuroepithelium with no signal corresponding to a pixel with a value of 0 and an area with the most intense signal possible being 4096.

For embryos harvested at E10.5-E12.5, the segmented line tool was used to draw a line of 25 pixels in width along the ventricular surface of the diencephalon, running from the dorsal midline of the diencephalon to the dorsal extent of the ZLI. The intensity plot tool was then used to record the greyscale values of the pixels along this line (Fig. 2.2A).

For embryos harvested at E13.5, the neuroepithelium of the pretectum becomes reduced in thickness while that of the remainder of the diencephalon increases in

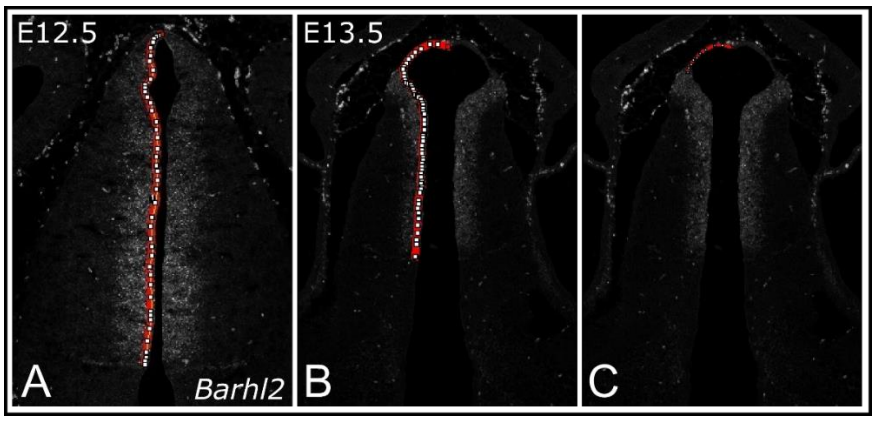

Fig. 2.2: Selection of the area of neuroepithelium along which expression gradients were quantified using Fiji. A: For sections from embryos at E10.5-E12.5 a 25 pixel line was drawn along the ventricular surface from the dorsal midline to the caudal extent of the ZLI, as marked by Barhl2 *expression. B: For embryos harvested at E13.5 a 25 pixel line was drawn along the ventricular surface from the dorsal midline to the caudal extent of the ZLI. C: A 10 pixel line was drawn along the ventricular surface from the dorsal midline to the point at which the neuroepithelium begins to thicken.*

Thickness. To account for this change in morphology, the segmented line tool was used to draw a line of 25 pixels in width as described above, and a second line of 10 pixels in width was also drawn from the dorsal midline to the point at which the diencephalic neuroepithelium begins to thicken. (Fig. 2.2B-C). Intensity plot data was recorded for both lines. The data recorded along the length of the 10 pixel line was used to quantify the gradient along with the data recorded along the length of the 25 pixel line from the point at which the 10 pixel line ended to the caudal extent of the ZLI as marked by *Barhl2* expression. Values were recorded for the *Pax6* immunostaining channel (488nm) and the *Barhl2 in situ* channel (554nm) on the left-hand side of each image. This was repeated for both channels on the right-hand side of each image.

Intensity plot data was pasted into a Microsoft Excel spreadsheet. Values were grouped into bins of five and a mean value for each bin was recorded. Using Excel, these mean values were then plotted against distance from the dorsal midline in order to produce a line graph illustrating changes in the relative intensity of the signal across the neuroepithelium. This was repeated for *Pax6* and *Barhl2*, on both the left-

hand and right-hand sides of each embryo, to take the possibility of sections being asymmetrical into account. A linear regression trend line was calculated for each plot and the gradient of this was recorded. The data from all three embryos was used to calculate the mean gradient of *Pax6* and *Barhl2* expression.

3. Expression of *Pax6* and *Barhl2* in the wild type mouse diencephalon

3.1 Introduction

Published *in situ* hybridization data for *Pax6* (Anderson *et al* 2002, Moreno *et al* 2014) and *Barhl2* (Suzuki-Hirano *et al* 2011) suggest that their expression domains may complement each other in several regions of the forebrain, with the notable exception of the thalamus and pretectum, in which both genes appear to be expressed. Within these adjacent diencephalic regions *Pax6* is expressed in a gradient running from dorsal to ventral and from caudal to rostral (Mastick *et al* 1997). Strong *Barhl2* expression has also been reported within the thalamus during some early stages of its development (Suzuki-Hirano *et al* 2011) but its expression within the developing diencephalon has yet to be described in full.

A high degree of complementarity between the two genes' expression domains would suggest the existence of a mutually repressive relationship between the two genes. The existence of a different relationship is may be suggested by their expression within the thalamic neuroepithelium.

In order to identify potential relationships between *Pax6* and *Barhl2* within the diencephalon it was first necessary to map their expression comprehensively and over a range of developmental stages. By observing changes in the expression of *Pax6* in relation to changes in the expression of *Barhl2*, and vice versa, it should be possible to gain an overview of the spatiotemporal dynamics of the two genes' expression and to then use this in order to identify any potential relationships between them.

The expression of *Pax6* and *Barhl2* was investigated at developmental stages from E8.5 to E13.5, the period of development in which the diencephalic neuroepithelium differentiates into that of the pretectum, thalamus and prethalamus and in which the majority of thalamic neurogenesis occurs. First, chromogenic *in situ* hybridization was used to comprehensively map the expression domains of *Pax6* and *Barhl2*. Fluorescence *in situ* hybridization was then employed along with fluorescence immunohistochemistry in order to investigate the complementarity of the genes' expression domains and the possibility of their co-expression within some regions of

neuroepithelium and individual cells of the diencephalon. Finally, image data obtained from the fluorescence *in situ* hybridization and fluorescence immunohistochemistry experiments were analysed quantitatively: in order to investigate the presence of expression gradient changes in the relative intensities of the *in situ* hybridization and immunohistochemistry signals were measured at points along the dorsoventral axis of the pretectum and thalamus.

Together the results from these experiments were used to predict the nature of the different relationships which may exist between *Pax6* and *Barhl2* within different regions of the diencephalic neuroepithelium.

3.2 Qualitative analysis: mapping *Pax6* and *Barhl2* in the wild-type prosencephalon

3.2.1 Introduction

OCT-mounted wild-type embryos aged between E8.5 and E13.5 were cryosectioned in the coronal plane. For each embryo alternate sections were mounted on two different sets of slides in order to collect two series of sections from the same embryo, with each individual section from the first series being adjacent to the corresponding section from the second series. Chromogenic *in situ* hybridization was carried out on both series of sections, with a digoxigenin (DIG)-labelled riboprobe for *Pax6* for the first series and DIG-labelled riboprobe for *Barhl2* for the second series. Treated sections were imaged using bright-field microscopy.

3.2.2 Results

Both *Pax6* and *Barhl2* are strongly expressed within the diencephalon during its formation and during the early stages of its development. The expression of both genes is highly dynamic, with their expression domains undergoing many spatial changes as diencephalic development progresses. The expression domains take on distinctive shapes which appear to closely correspond with the shapes and positions of particular diencephalic structures as they develop. The degree to which *Pax6* and *Barhl2* are co-expressed seems to vary greatly with the developmental stage and position, and in particular with the position in relation to that of the ZLI.

At E8.5 (Fig. 3.2.1) the neural tube is still in the process of closing, with the edges of the neural plate moving towards each other before fusing to form the roofplate. By E8.5 the neural tube has fused along the length of the developing spinal cord, mesencephalon and rhombencephalon, but remains open along the entire rostrocaudal extent of the prosencephalon (arrows, Fig. 3.2.1A).

By this point in development it appears that the prosencephalon has begun to subdivide into the more rostral telencephalon and the more caudal diencephalon and the two sub-regions appear to be morphologically distinct. At this stage the forming telencephalon begins to envelop the diencephalon (Price *et al* 2011) and in sections cut in the coronal plane this may be the structure that can be distinguished as two vesicles forming to the left and right of the third ventricle, the lumen of the developing diencephalon (Fig. 3.2.1C).

At this stage *Pax6* is already strongly expressed within the prosencephalon in a domain spanning its rostrocaudal extent, but its expression is confined to the alar plate, the anlage of the pallium (Fig. 3.2.1D).

At E8.5 the *Barhl2* domain is visible as a narrow band of expression situated within the prosencephalic *Pax6* domain, but this domain is much narrower than that of *Pax6*, with its caudal limit at the approximate location of the midbrain-hindbrain boundary (MHB) and its rostral limit at the point where the telencephalon becomes morphologically distinct from the diencephalon. Unlike *Pax6*, *Barhl2* is not confined to the dorsal neuroepithelium and its expression can be detected in ventral regions, extending as far as the floorplate (Fig. 3.2.1F-H).

By E9.5 (Fig. 3.2.2) the edges of the neural plate have fused to form the roofplate of the prosencephalon and neural tube closure is complete. The telencephalon has expanded and become morphologically distinct from the diencephalon to an even greater extent than before. The telencephalon can also be seen to be forming into two distinct hemispheres and by this stage they are visible as fully-enclosed vesicles either side of the third ventricle, though this division into two hemispheres is not apparent in more rostral sections of the telencephalon (Fig. 3.2.1E and J).

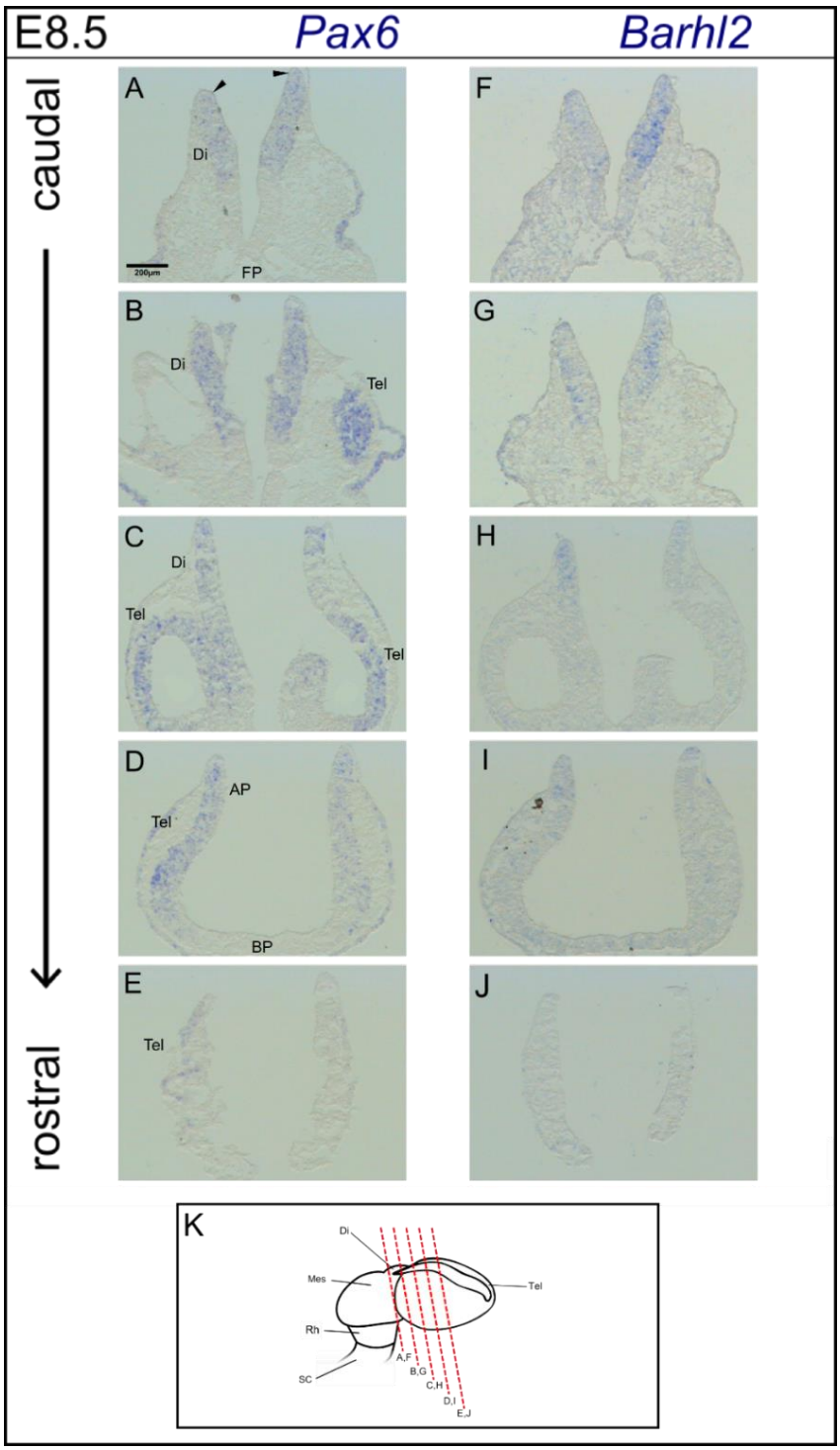

Fig. 3.2.1: The expression domains of Pax6 *and* Barhl2 *in the wild type diencephalon at E8.5 as visualised by* in situ *hybridization performed on adjacent coronal sections. The arrows in A mark the edges of the neural plate, which have yet to fuse to form the roofplate. K: Schematic illustrating the approximate plane of each section. Abbreviations: Tel- telencephalon; Di- diencephalon; Mes- mesencephalon; Rh- rhombencephalon; SC- spinal cord; FP- floorplate; AP- alar plate; BP- basal plate.*

At E9.5 *Pax6* continues to be expressed along the rostrocaudal extent of the prosencephalon while remaining absent from the basal plate. Its expression in the telencephalon now clearly corresponds with the position of the developing pallium (3.2.2D-E).

Barhl2 remains absent from the telencephalon and while it is still expressed within the diencephalon its domain appears to span a smaller proportion of the diencephalon as a whole (3.2.F-H). In more caudal sections two smaller domains of *Barhl2* can be seen either side of the third ventricle, caudal to the broader diencephalic domain of *Barhl2*, but it is not clear which diencephalic structures they correspond with, if any (arrows, Fig. 3.2.2F). These may be visible as a consequence of the plane of section in which the tissue was cut, and could possibly represent the caudal extent of the thalamic *Barhl2* domain visible in Fig. 3.2.2G.

At E10.5 (Fig. 3.2.3) the dorsal telencephalon begins to fold inwards along the dorsal midline and the two telencephalic hemispheres become distinct from each other along the entire rostrocaudal extent of the telencephalon. The lumen of the diencephalon narrows as it becomes elongated along the dorsoventral axis. Many more molecular changes become apparent at this stage, possibly as a consequence of the ZLI being established around this time (Shimamura *et al* 1995). The eyes can also be seen ventral to the diencephalic hemispheres, marked by strong *Pax6* staining in the developing retina (arrows, Fig. 3.2.3C).

In caudal and medial sections the *Barhl2* domain becomes fragmented into two separate domains separated by a narrow strip of *Barhl2*-negative neuroepithelium (arrows, Fig. 3.2.3F). The more ventral of the two domains is visible as a wedge-shaped region of expression in the centre of the diencephalon, tapering as it extends from the ventricular surface towards the lateral extent of the diencephalic neuroepithelium, and corresponding with the shape and the position of the ZLI. Dorsal to this domain and the *Barhl2*- negative region is an area of strong *Barhl2* expression corresponding with the developing thalamus and pretectum. Within this more dorsal expression domain *Barhl2* now appears to be expressed in a ventral-to-dorsal gradient, in contrast to its apparently uniform expression throughout the diencephalon in earlier developmental stages.

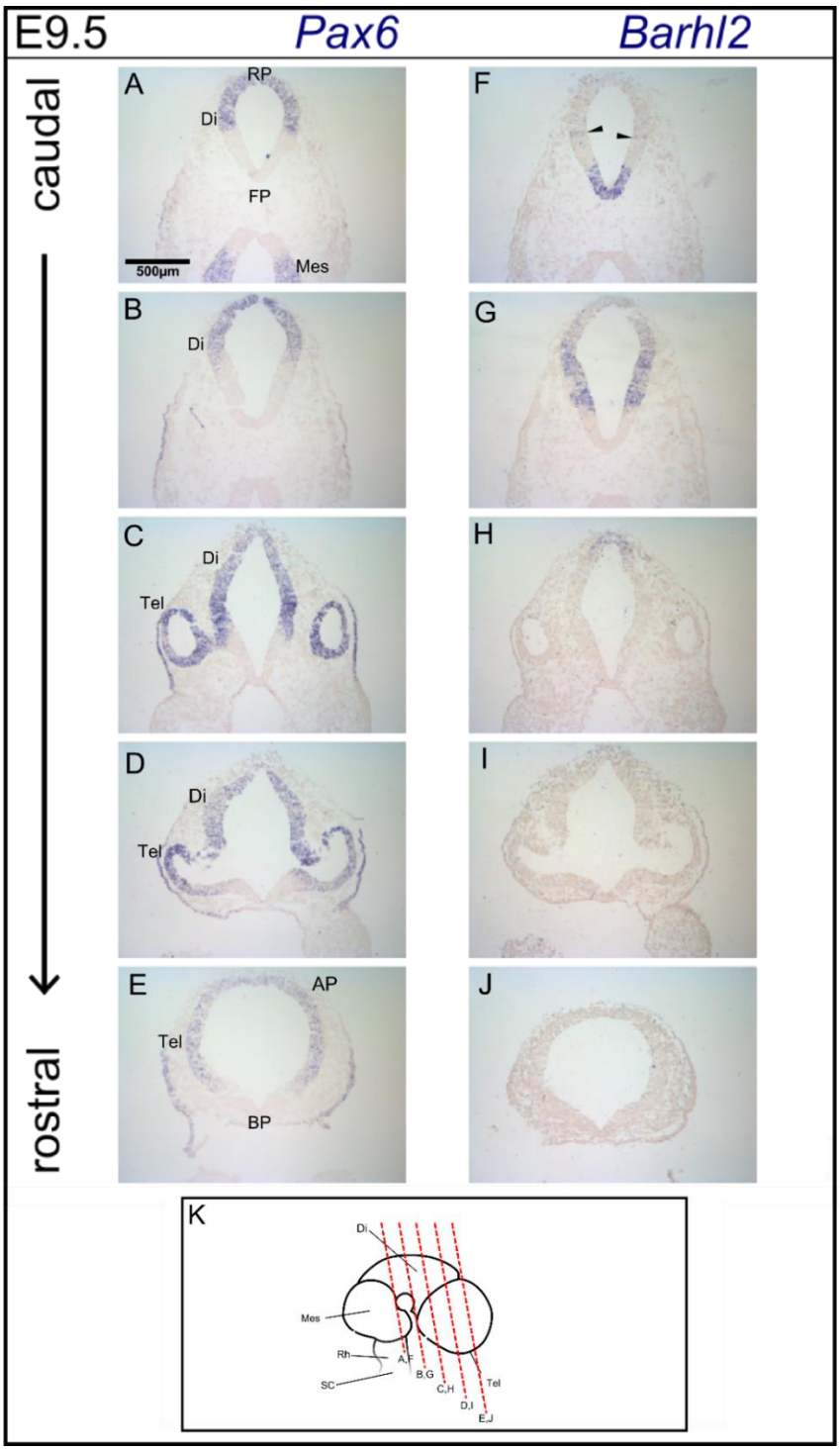

Fig. 3.2.2: The expression domains of Pax6 *and* Barhl2 *in the wild-type diencephalon at E9.5 as visualised by* in situ *hybridization performed on adjacent coronal sections. Arrows in F: Two small* Barhl2 *domains, possibly the most caudal region of the broader* Barhl2 *domain visible in G. K: Schematic illustrating the approximate plane of each section. Abbreviations: Tel- telencephalon; Di- diencephalon; Mes- mesencephalon; Rh- rhombencephalon; SC- spinal cord; RP- roofplate; FP- floorplate; AP- alar plate; BP- basal plate.*

In more rostral sections a third domain of *Barhl2* can be seen forming in a region of the diencephalon ventral to the ZLI (arrows, Fig. 3.2.3I). This domain is separated from the domain of *Barhl2* within the ZLI by a relatively broad region of *Barhl2*-free neuroepithelium. It is not clear whether this domain segregates from the solid *Barhl2* domain visible at earlier developmental stages or it arises independently of this domain with the onset of its expression in the ventral diencephalon induced by another factor.

Pax6 continues to be strongly expressed throughout the dorsal regions of the telencephalic neuroepithelium and its expression appears to be stronger in the caudal telencephalon as the caudal-to-rostral gradient of *Pax6* is established. The pallial-subpallial boundary (PSB) also becomes apparent as the ventral limit of the telencephalic *Pax6* domain (arrows, Fig. 3.2.3E).

Within the diencephalon the previously solid and continuous *Pax6* domain also begins to fragment into two discrete domains separated by a region free of *Pax6* expression (arrows, Fig. 3.2.3A). The more dorsal of these domains runs from the dorsal midline towards the ZLI and corresponds with the developing pretectum and thalamus. Within this domain *Pax6* appears to be expressed in a dorsal-to-ventral gradient, running counter to the gradient of *Barhl2* expression in the same region.

Ventral to the ZLI, *Pax6* is strongly expressed in a domain corresponding with the position of the prethalamus. There is an apparent gap in its expression corresponding with the small *Barhl2* domain in this region (arrows, Fig. 3.2.3D) and the expression of the two genes may be complementary in this region, with little to no overlap as observed in the thalamus, in which the two domains with their countergradients appear to overlap to some extent.

At E11.5 (Fig. 3.2.4) the telencephalon continues to expand rapidly and envelops the diencephalon to a greater extent, with the vesicles of the telencephalon visible on either side of the diencephalic lumen even in more caudal sections. As neurogenesis continues the wall of the diencephalon can be seen to thicken.

Pax6 continues to be strongly expressed within the dorsal telencephalon and at this stage a ventral-to-dorsal gradient becomes apparent (Fig. 3.2.3A-B). With *Pax6*

expression becoming particularly strong in the more ventral regions of the pallium the PSB becomes even more apparent as a sharp border at the rostral extent of the telencephalic *Pax6* domain (compare arrows, Fig. 3.2.4E, with arrows, Fig.3.3.4J).

Barhl2 begins to be expressed within the ventral telencephalon and its expression domains appear to complement the domains of *Pax6* within the telencephalon, ending sharply at the region where a spike of *Pax6* expression can be seen extending from the PSB towards the floorplate (arrows, Fig. 3.2.4J).

Within the dorsal diencephalon the dorsal-to-ventral gradient of *Pax6* also becomes more apparent (Fig. 3.2.4A-B). Its expression appears stronger in the pTh-C, and it appears that a caudal-to-rostral gradient of *Pax6* may also have been established within the thalamus and pretectum. *Pax6* expression also seems to be largely absent from the more lateral regions of the thalamic neuroepithelium and is now confined to the more medial regions, in a domain corresponding with the ventricular zone of the thalamus (the area marked by the dashed line on the left-hand side, Fig.3.2.4A).

Thalamic expression of *Barhl2* also appears to become confined to the ventricular zone at this stage (the area marked by the dashed line on the left-hand side, Fig.3.2.4F). The domain of *Barhl2* which corresponds with the ZLI can also be clearly distinguished (arrows, Fig. 3.2.4H). It has become even further separated from the thalamic *Barhl2* domain by the *Barhl2*-negative pTh-R, which continues to expand along the dorsoventral axis.

In regions of neuroepithelium ventral to the ZLI the expression domains of *Pax6* and *Barhl2* can be seen to be developing with a high degree of complementarity. In more rostral sections, a *Pax6*-negative region corresponding with the position of the *eminentia thalami* can be seen, and it is surrounded by a region of strong *Pax6* expression (Fig. 3.2.4D). In adjacent sections apparently complementary expression of *Barhl2* can be observed, with strong expression within the *eminentia thalami* itself (Fig. 3.2.4I) and no apparent expression in the surrounding neuroepithelium.

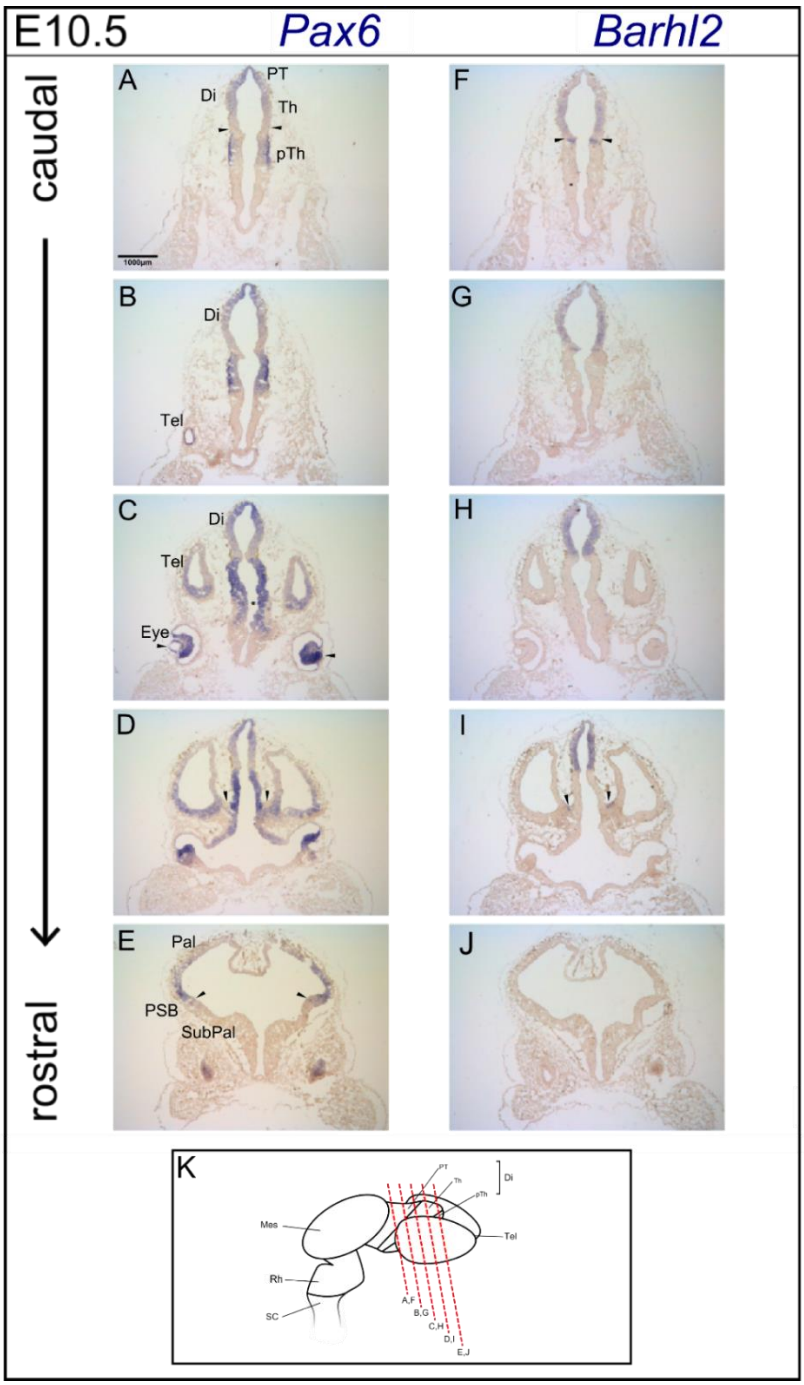

Fig. 3.2.3: The expression domains of Pax6 *and* Barhl2 *in the wild-type diencephalon at E10.5 as visualised by* in situ *hybridization performed on adjacent coronal sections. Arrows in A and B: the developing pTh-R. Arrows in C: Strong* Pax6 *expression within the eye. Arrows in E and J: Complementary expression of* Pax6 *and* Barhl2 *in and around the* eminentia thalami*. K: Schematic illustrating the approximate plane of each section. Abbreviations: Tel- telencephalon; Di- diencephalon; Mes- mesencephalon; Rh- rhombencephalon; SC- spinal cord; PT- pretectum; Th- thalamus; pTh- prethalamus; Pal- pallium; SubPal- subpallium; PSB- pallial-subpallial boundary.*

At this stage a new domain of strong *Barhl2* expression becomes visible at the ventral midline of the caudal diencephalon, corresponding with the position of the developing hypothalamus (Fig. 3.2.4F).

By E12.5 (Fig. 3.2.5) the forebrain has greatly increased in size and the neuroepithelium has thickened throughout. At this stage the pretectum, thalamus and prethalamus can be clearly visualised.

Within the thalamus the expression of *Pax6* remains confined to the ventricular zone (the area marked by the dashed line on the left-hand side, Fig. 3.2.5A) as does that of *Barhl2* (the area marked by the dashed line on the left-hand side, Fig. 3.2.5F). As neurogenesis proceeds and neurons exit the cell cycle the thalamic ventricular zone- the site of the majority of thalamic neurogenesis- occupies an increasingly smaller proportion of the diencephalon. The thalamic expression domains of both *Pax6* and *Barhl2* correspond with the position of this region and both domains also begin to extend across a smaller proportion of the diencephalic tissue along the mediolateral axis (Fig. 3.2.4A-C and F-H). This may be a consequence of neurogenesis and the reduction in size of the ventricular zone in comparison to that of the thalamus as a whole.

As with earlier developmental stages, at this stage *Pax6* expression appears to be much stronger than *Barhl2* expression within the more caudal regions of thalamic neuroepithelium and the opposite applies in more rostral regions, with thalamic *Barhl2* expression appearing to be much stronger than that of *Pax6* (Fig. 3.2.5C and H). This suggests that by this stage a gradient of *Pax6* expression may run from caudal to rostral while a countergradient of *Barhl2* expression may run from rostral to caudal.

These apparent countergradients may be present in addition to countergradients running along the dorsoventral axis of the thalamus At E12.5 *Pax6* is strongly expressed at the dorsal midline of the diencephalon and throughout the pretectum but appears to be less strongly expressed within the thalamus itself (Fig. 3.2.5C), while *Barhl2* expression remains strong in the more ventral regions of the thalamus and may be slightly weaker at the dorsal midline, although a ventral-to-dorsal gradient is

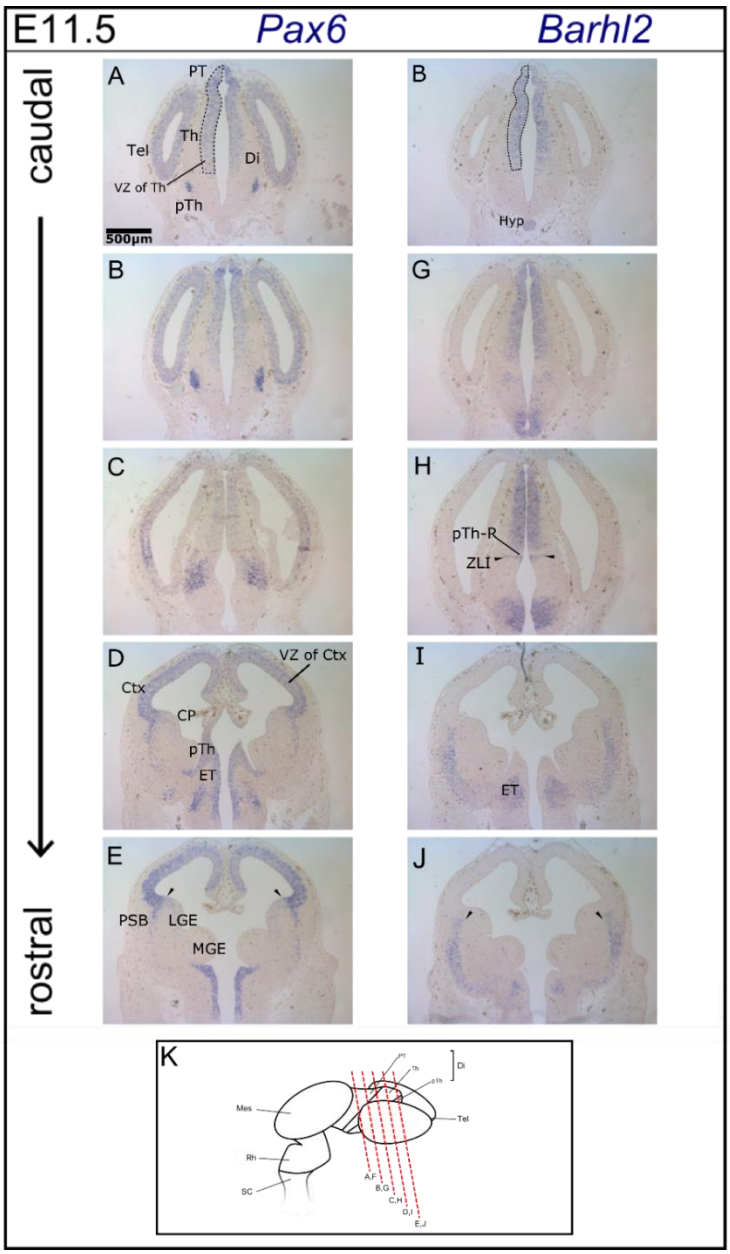

Fig. 3.2.4: The expression domains of Pax6 *and* Barhl2 *in the wild-type diencephalon at E11.5 as visualised by* in situ *hybridization performed on adjacent coronal sections. K: Schematic illustrating the approximate plane of each section. Outlined areas in A and B: The thalamic domains of* Pax6 *and* Barhl2 *are confined to the ventricular zone of the pTh-C. Arrows in H:* Barhl2 *expression within the ZLI. Arrows in E and J: the PSB, the point at which the telencephalic domains of* Pax6 *and* Barhl2 *meet. Abbreviations: Tel- telencephalon; Di- diencephalon; Mes- mesencephalon; Rh- rhombencephalon; SC- spinal cord; PT- pretectum; Th- thalamus; pTh- prethalamus; VZ- ventricular zone; Ctx- cortex; CP- choroid plexus; PSB- pallial-subpallial boundary; LGE- lateral ganglionic eminence; MGE- medial ganglionic eminence; Hyp- hypothalamus; ET-* eminentia thalami; *ZLI-* zona limitans intrathalamica*.*

not as apparent here as it is at E11.5 (Fig. 3.25H). The gradient of thalamic *Pax6* expression may therefore run from dorsal to ventral and from caudal to rostral, while the gradient of thalamic *Barhl2* may run counter to this, from ventral to dorsal and from rostral to caudal.

Within the region of neuroepithelium rostral to the ZLI, the prethalamus has increased in size and expresses *Pax6* more strongly than before (Fig. 3.2.5C). In more rostral sections the complementary expression domains of *Pax6* and *Barhl2* are apparent, with *Pax6* being absent from the *eminentia thalami* but strongly expressed in the regions surrounding it (Fig. 3.2.5D) and *Barhl2* being strongly expressed in *the Pax6*-negative region corresponding with the *eminentia thalami* Fig. 3.2.5I)

Within the telencephalon the dorsal-to-ventral gradient of *Pax6* expression can be clearly seen, along with a narrow strip of *Pax6* expression extending from the PSB into the lateral ganglionic eminence (arrows, Fig. 3.2.5E). As with the ventral telencephalon at E11.5, at this stage complementary expression domains of *Barhl2* can be seen within the regions flanked by *Pax6* expression (arrows, Fig. 3.2.5J).

Barhl2 expression within the hypothalamus remains strong (Fig. 3.2.5F and G) and it continues to be expressed within the ZLI (arrows, Fig. 3.2.5H) while being absent from the pTh-R.

Between E12.5 and E13.5 the forebrain undergoes a substantial increase in size. In order to obtain adequately detailed image data from sections of embryos treated at E13.5 these sections were imaged at a greater magnification than those treated at E10.5, E11.5 and E12.5. In order to show the expression domains of *Pax6* and *Barhl2* in adequate detail the image data are presented here across two separate figures, the first of which details the expression of *Pax6* and *Barhl2* in the dorsal diencephalon (Fig. 3.2.6) and the second of which details the gene expression data for a more ventral region of the diencephalon (Fig. 3.2.7).

At E13.5 the neuroepithelium continues to thicken and the ventricular zone continues to occupy a smaller proportion of the diencephalic neuroepithelium as neurogenesis

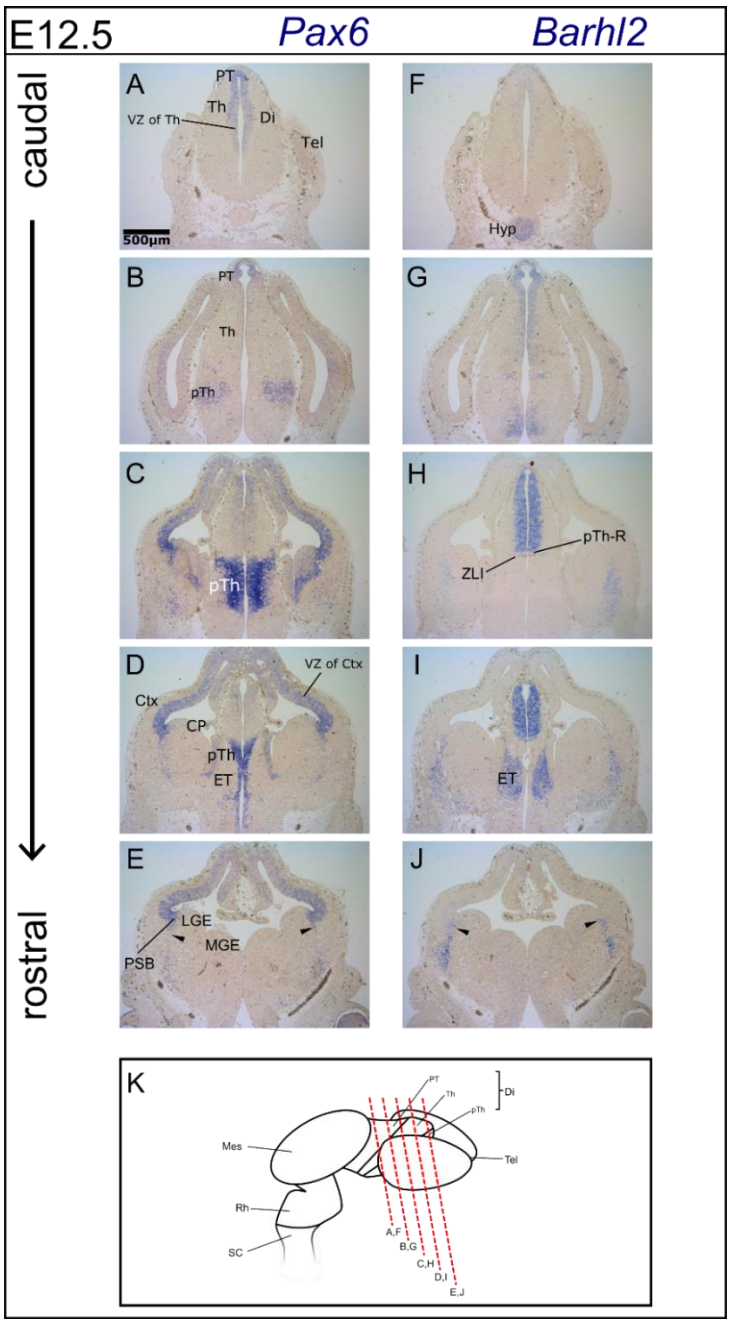

Fig. 3.2.5: The expression domains of Pax6 *and* Barhl2 *in the wild-type diencephalon at E12.5 as visualised by* in situ *hybridization performed on adjacent coronal sections. K: Schematic illustrating the approximate plane of each section. Arrows in E and J: the PSB, the point at which the telencephalic domains of* Pax6 *and* Barhl2 *meet. Abbreviations: Tel- telencephalon; Di- diencephalon; Mes- mesencephalon; Rh- rhombencephalon; SC- spinal cord; PT- pretectum; Th- thalamus; pTh- prethalamus; VZ- ventricular zone; Ctx- cortex; CP- choroid plexus; PSB- pallial-subpallial boundary; LGE- lateral ganglionic eminence; MGE- medial ganglionic eminence; Hyp- hypothalamus; ET-* eminentia thalami; *ZLI-* zona limitans intrathalamica.

proceeds. Thalamic *Pax6* expression remains confined to the ventricular zone of the thalamus (Fig. 3.2.6A-D), as does the thalamic expression of *Barhl2* (Fig 3.2.6F-I). *Pax6* expression is still at its strongest in the more rostral regions of the thalamus while the opposite is still true of *Barhl2*, suggesting that the expression countergradients are still present along the rostrocaudal axis.

The presence of *Pax6* and *Barhl2* expression countergradients along the dorsoventral axis of the thalamus is not apparent at this stage. While *Pax6* expression is still strong in the pretectum and appears to weaken towards the more ventral regions of the thalamus, expression of *Barhl2* seems to be more solid and appears to be slightly stronger in the pretectum (Fig. 3.2.6G-I).

The ZLI changes shape at this stage becomes narrower and more curved in shape prior to the stage at which it no longer appears to be maintained (Visel *et al* 2004) but it can still be seen to express *Barhl2* (arrows, Fig. 3.2.7G) and this domain remains distinct from the thalamic domain dorsal to the *Barhl2*-negative pTh-R.

Ventral to the ZLI the prethalamus continues to express *Pax6* very strongly and the prethalamic domain remains complementary to the domain of B*arhl2* in this area, though *Barhl2* expression appears to be much weaker by this stage (Fig. 3.2.7C-E and H-J).

In more dorsal sections of the ventral diencephalon *Barhl2* expression also appears weaker than before, with the exception of the hypothalamus in which it appears to be expressed more strongly than at earlier developmental stages (Fig. 3.2.7F).

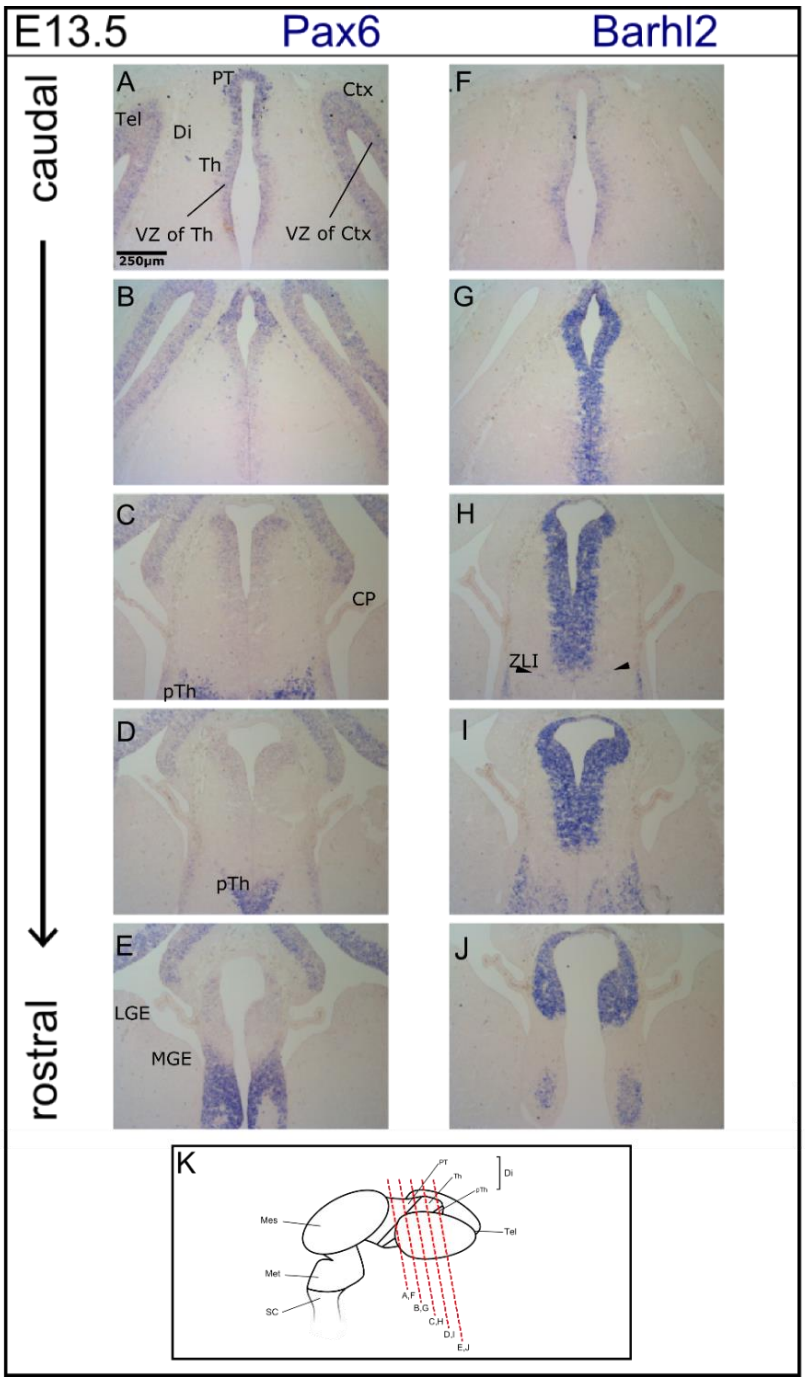

Fig. 3.2.6: The expression domains of Pax6 *and* Barhl2 *in the wild-type diencephalon at E13.5 as visualised by* in situ *hybridization performed on adjacent coronal sections- detail of the pretectum and thalamus K: Schematic illustrating the approximate plane of each section. Arrows in H:* Barhl2 *expression in the ZLI. Abbreviations: Tel- telencephalon; Di- diencephalon; Mes- mesencephalon; Rh- rhombencephalon; SC- spinal cord; PT- pretectum; Th- thalamus; pTh- prethalamus; VZ- ventricular zone; Ctx- cortex; CP- choroid plexus; LGE- lateral ganglionic eminence; MGE- medial ganglionic eminence; Hyp- hypothalamus; ET-* eminentia thalami; *ZLI-* zona limitans intrathalamica*.*

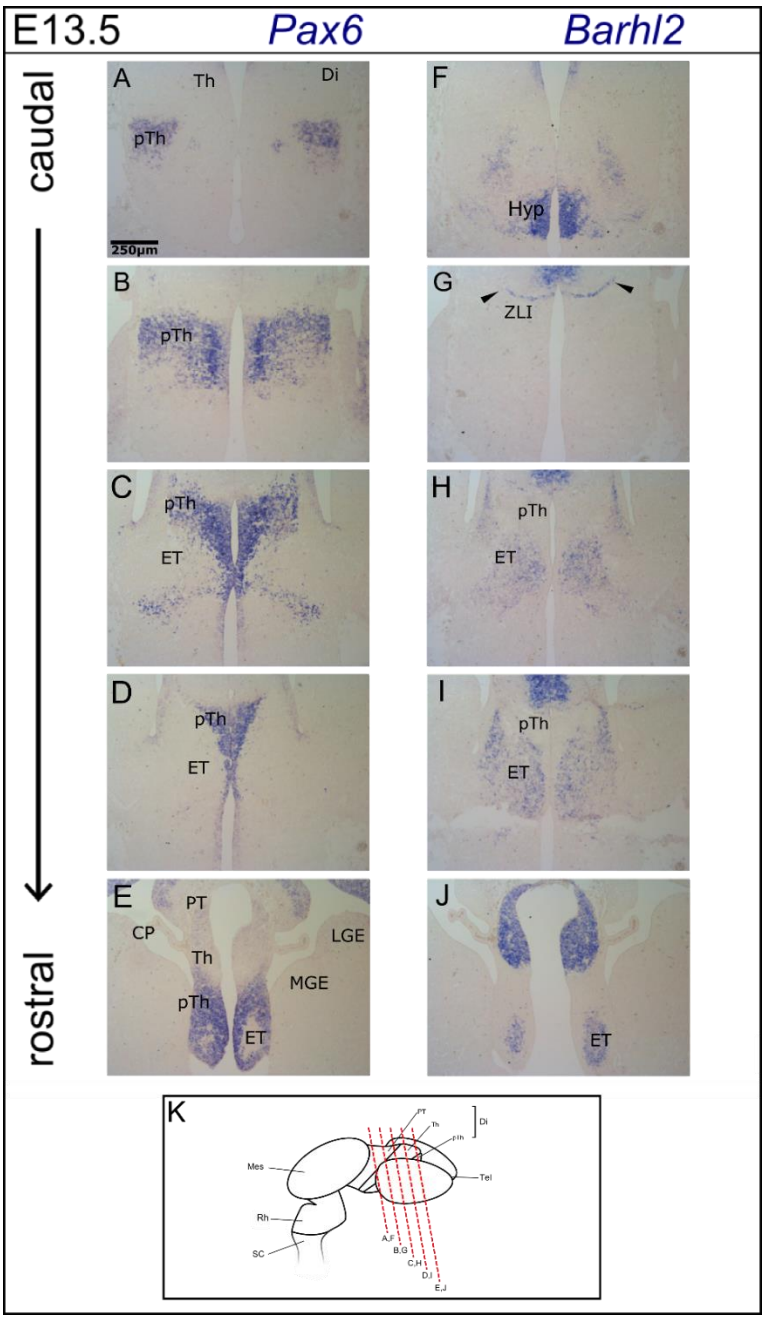

Fig. 3.2.7: The expression domains of Pax6 *and* Barhl2 *in the wild-type diencephalon at E13.5 as visualised by* in situ *hybridization performed on adjacent coronal sections- detail of the rostral thalamus, ZLI, prethalamus,* eminentia thalami *and hypothalamus. K: Schematic illustrating the approximate plane of each section. Arrows in G:* Barhl2 *expression in the ZLI. Abbreviations: Tel- telencephalon; Di- diencephalon; Mes- mesencephalon; Rh- rhombencephalon; SC- spinal cord; PT- pretectum; Th- thalamus; pTh- prethalamus; VZ- ventricular zone; CP- choroid plexus. LGE- lateral ganglionic eminence; MGE- medial ganglionic eminence; Hyp- hypothalamus; ET-* eminentia thalami; *ZLI-* zona limitans intrathalamica.

3.3 Qualitative analysis: Investigating complementarity and co-expression of *Pax6* and *Barhl2* in the wild-type diencephalon

3.3.1 Introduction

In order to confirm the complementarity of the *Pax6* and *Barhl2* domains outside the thalamus, the co-expression of the two genes within individual cells of the thalamus, and the presence of two expression gradients running counter to each other, it was necessary to employ fluorescence techniques to visualise the expression of both genes within the same tissue section.

Unfortunately it was not possible to perform double *in situ* hybridization for *Pax6* and *Barhl2* because repeated attempts to produce effective 2, 4-dinitrophenyl (DNP)-labelled probes for both genes were unsuccessful. In experiments using the DNP-labelled *Pax6* probes the signal was unacceptably weak even when the probes were diluted by a factor as low as 1:100, while use of the DNP-labelled *Barhl2* probes resulted in a very high degree of background fluorescence even at the relatively high dilution of 1:30,000. It was also not possible to perform immunohistochemistry for both genes as an effective antibody against *Barhl2* which was suited to immunohistochemical applications could not be sourced.

As a compromise, and because an effective and suitable antibody against *Pax6* was available, immunohistochemistry for *Pax6* protein was performed along with *in situ* hybridization for *Barhl2* mRNA. The protocol was performed on 16µm cryosections cut in the coronal plane and repeated for 16µm sections cut in the sagittal plane. Treated sections were imaged with confocal microscopy.

3.3.2 Results

The chromogenic *in situ* data for *Pax6* and *Barhl2* suggest that the domains of *Pax6* and *Barhl2* are complementary to each other in all forebrain regions with the exception of the thalamus (Fig. 3.2.1-Fig.3.2.7). The fluorescence *in situ* data for *Barhl2* and the fluorescence immunohistochemistry data for *Pax6* protein appear to confirm this (Fig. 3.3.1 and Fig. 3.3.2).

In a sagittal section from an embryo harvested at E9.5 a narrow spike of *Barhl2* expression can be seen within the broader domain of *Pax6*, spanning the dorsoventral extent of the diencephalon from the floorplate to the roofplate (arrow, Fig. 3.3.1B)**.** It appears that the genes are co-expressed within this area of neuroepithelium at this developmental stage.

At E10.5 a gap in the *Pax6* expression domain can be seen, apparently corresponding with the rostral extent of the thalamus and possibly with the position of the developing pTh-R (arrow, Fig. 3.3.1D). At this stage the thalamic *Barhl2* domain expands along the rostrocaudal axis, within the gap in the *Pax6* domain.

As with the chromogenic *in situ* hybridization data, a second discrete domain of *Barhl2* can be seen rostral and ventral to the thalamic domain, corresponding with the position of the developing ZLI, and separated from the thalamic domain by a narrow strip of neuroepithelium which does not express *Barhl2* (arrow, Fig. 3.3.1E). The ZLI continues to develop and express *Barhl2* at E11.5 (Fig. 3.3.1H), by E12.5 a spike-shaped domain of *Barhl2* which corresponds with the shape and position of the ZLI can be clearly discerned (arrow, Fig. 3.3.1K) and by E13.5 it can still be seen but appears to have narrowed (arrow, Fig. 3.3.1N).

The image data from the treated sagittal sections suggest that within the thalamus a gradient of *Pax6* may run from caudal to rostral and from dorsal to ventral, while a countergradient of *Barhl2* may run from rostral to caudal and from ventral to dorsal, and that these gradients may have been established by E11.5 (3.3.1G-H).

The data from the imaging of treated coronal sections also appeared to show a gap in the thalamic *Pax6* domain (arrows, 3.3.2A) developing as *Barhl2* expression becomes stronger in this region.

In the embryo treated at E10.5 and sectioned in the coronal plane, the *Barhl2* domain corresponding with the ZLI could not be clearly discerned (arrows, Fig. 3.3.2B). This could be due to the embryo appearing to be E10.5 when staged according to external morphology (Theiler 1989) while still being at a developmental stage prior to ZLI development due to the molecular changes within the neuroepithelium not corresponding exactly with the changes in external morphology.

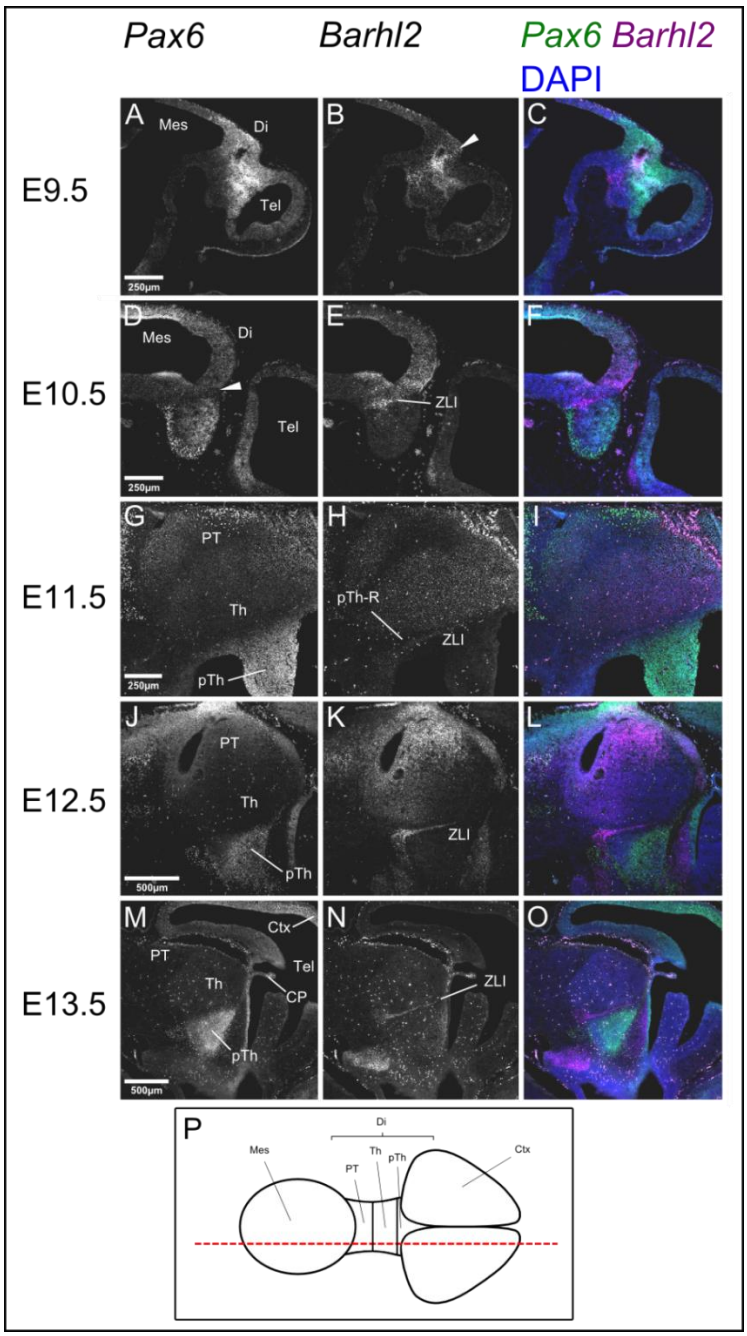

Fig.3.3.1: A-P: Sagittal sections of the wild-type diencephalon at embryonic stages from E10.5 to E13.5 (rostral to right) treated with immunohistochemistry for Pax6 protein and in situ *hybridization for* Barhl2 *mRNA. Each respective scale bar refers to the set of three images presented for each developmental stage. P. Schematic of an embryonic brain viewed from the dorsal surface to illustrate the approximate plane of each section. Arrow in B:* Barhl2 *appears to be co-expressed with Pax6 in the dorsal diencephalon at E9.5. Arrow in D: Lower levels of Pax6 expression in the presumptive ZLI and pTh-R. Abbreviations: Ctx- cortex; Di- diencephalon; PT- pretectum; Th- thalamus; pTh- prethalamus; Mes- mesencephalon; Tel- telencephalon; ZLI-* zona limitans intrathalamica*; CP- choroid plexus.*

By E11.5 the *Barhl2* domain corresponding with the ZLI can be clearly discerned (arrows, 3.3.2F) and by E13.5 the ZLI appears narrowed and in the section shown here it can only be clearly seen on the right-hand side of the diencephalon (arrow, Fig. 3.3.2L) as could be expected at a stage when the disappearance of the ZLI may be in progress (Visel *et al* 2004).

The results suggested the presence of opposing gradients of *Pax6* and *Barhl2* expression within the thalamus, but also that these gradients opposed each other more strongly at some developmental stages than they did at others. At E12.5 high magnification confocal images of the thalamus appeared to show weaker expression of *Barhl2* in regions where *Pax6* expression was strong. *Pax6* expression was strong in the pretectum and more dorsal regions of the thalamus while *Barhl2* expression in this region was relatively weak. The opposite applied in more ventral regions of the thalamus, where strong *Barhl2* expression and weak expression of *Pax6* was observed (Fig. 3.3.2H and I). Together these observations suggest the existence of an inversely proportional relationship between the two genes' expression.

The results also appeared to confirm the high complementarity of the *Pax6* and *Barhl2* domains in regions of neuroepithelium outside the thalamus. In some sections a high degree of complementarity was apparent even at low magnification (arrows, 3.3.2J) and when the boundaries between the *Pax6* and *Barhl2* domains were imaged at high magnification little to no co-expression was observed within the cells located at the borders of the *Pax6* and *Barhl2* domains (Fig. 3.3.4B).

In addition to this, a narrow and elongated region free of DAPI was observed within the *eminentia thalami*, flanked by a region of strong *Barhl2* expression (3.3.4A). This region corresponds with the axon tract along which the thalamocortical axons project from the thalamus to the cortex, and the corticothalamic axons project from the cortex to the thalamus.

When imaged at high magnification it was possible to observe the nature of *Pax6* and *Barhl2* expression within individual cells. (Fig. 3.3.5). In the majority of cells *Pax6* protein appeared to be evenly distributed throughout the nucleus and cytoplasm. In dividing cells, identified by the condensation of the chromatin which was visualised

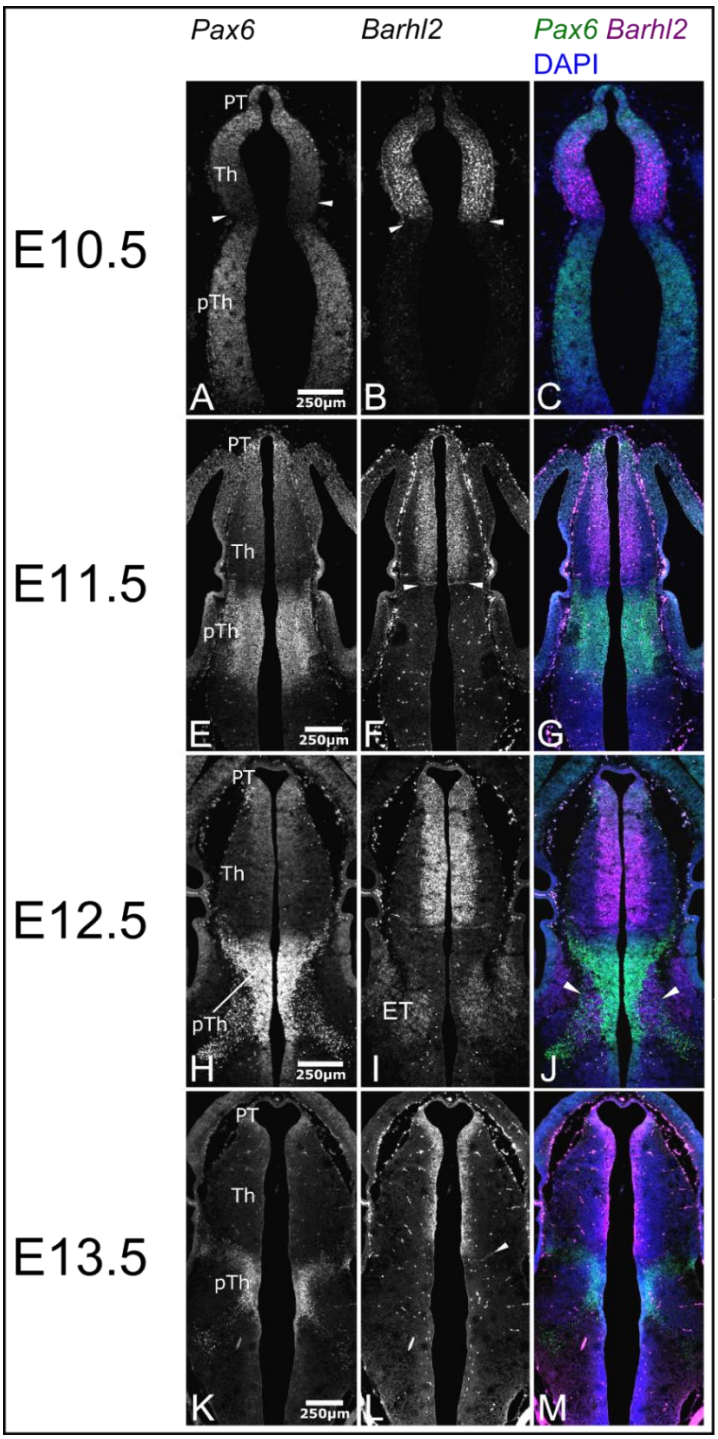

Fig. 3.3.2: Coronal sections of the wild-type diencephalon at embryonic stages from E10.5 to E13.5 treated with immunohistochemistry for Pax6 *protein and* in situ *hybridization for* Barhl2 *mRNA*. *Arrows in A and B: Levels of Pax6 protein are reduced in the presumptive ZLI at E10.5, while* Barhl2 *expression becomes stronger at this stage. Arrows in F and I:* Barhl2 *expression within the ZLI. Arrows in G: Expression of Pax6 protein and* Barhl2 *mRNA is highly complementary in regions rostral to the ZLI. Abbreviations: PT- pretectum; Th- thalamus; pTh- prethalamus; ET-* eminentia thalami*;*

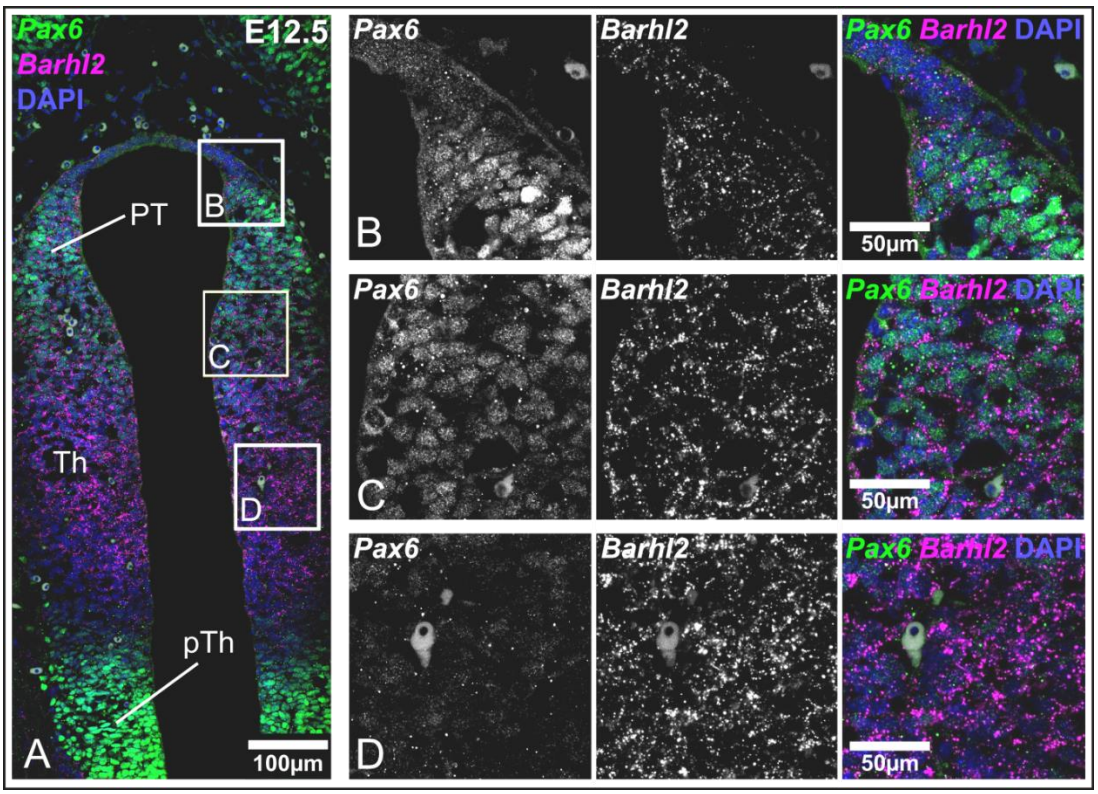

Fig. 3.3.3: A. A coronal section of the wild type diencephalon at E12.5 at high magnification, with detail of the neuroepithelium showing co-expression of Pax6 *protein and* Barhl2 *mRNA by individual cells in B: the pretectum, C: a dorsal region of the thalamus and D: a more ventral region of the thalamus. From dorsal to ventral the expression of* Pax6 *protein appears to become progressively weaker while that of* Barhl2 *mRNA appears to become stronger. Abbreviations: PT- pretectum; Th- thalamus; pTh- prethalamus.*

with DAPI staining, *Pax6* protein could not be seen within the nucleus and was seen to translocate to the cytoplasm. (Fig. 3.3.5B). In all cells *Barhl2* expression appeared to be highly punctate, and *Barhl2* mRNA was observed in discrete clusters, suggesting that *Barhl2* mRNA may become localised within the cell.

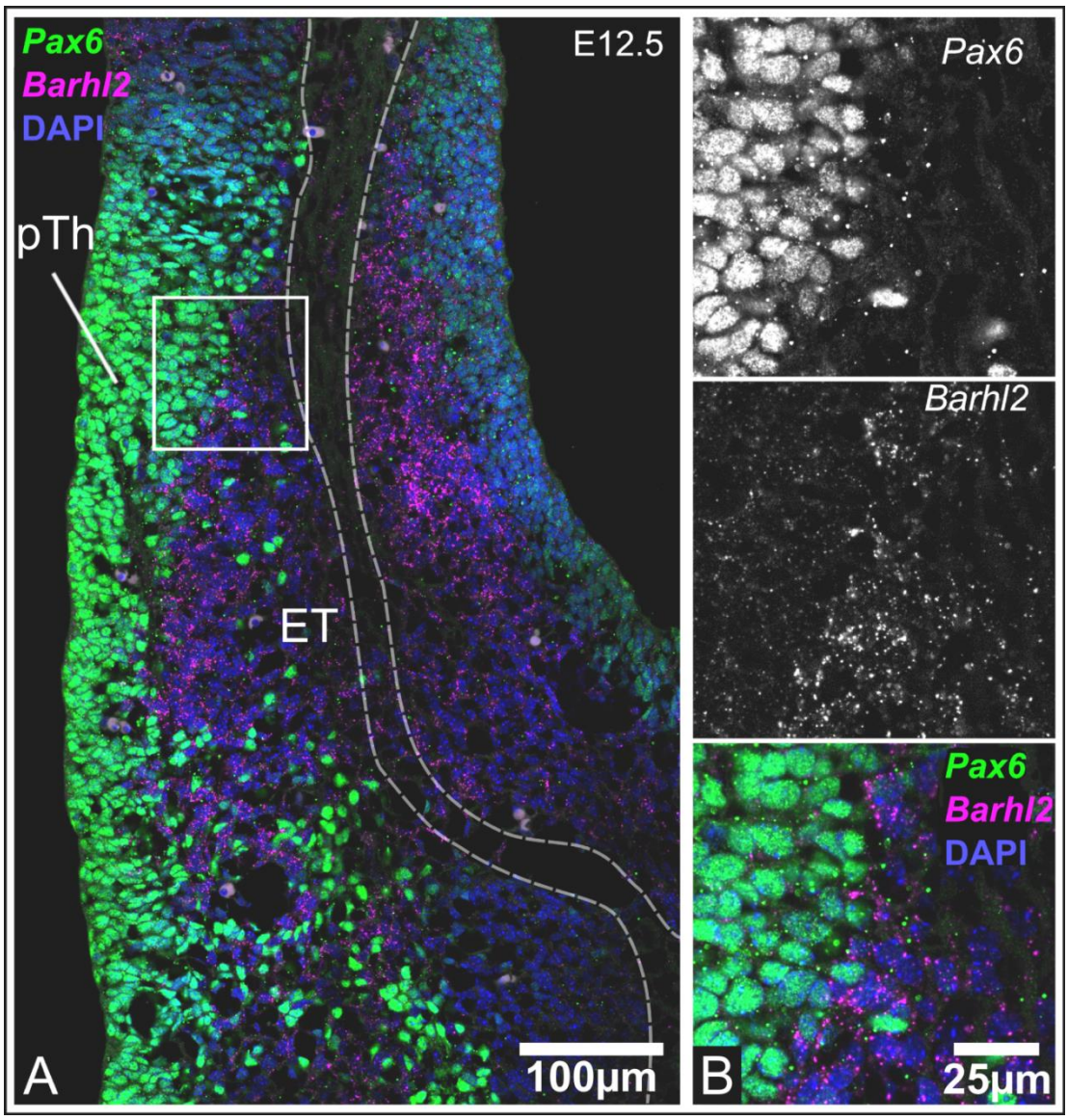

Fig. 3.3.4: Detail of the neuroepithelium at the border of the prethalamic Pax6 *domain and the* Barhl2 *domain within the eminentia thalami showing little to no co-expression of* Pax6 *protein and* Barhl2 *mRNA. B. Detail of the area outlined in A imaged at high magnification, illustrating the developing axon tracts flanked by regions of* Barhl2 *mRNA expression. Abbreviations: pTh- prethalamus; ET- eminentia thalami.*

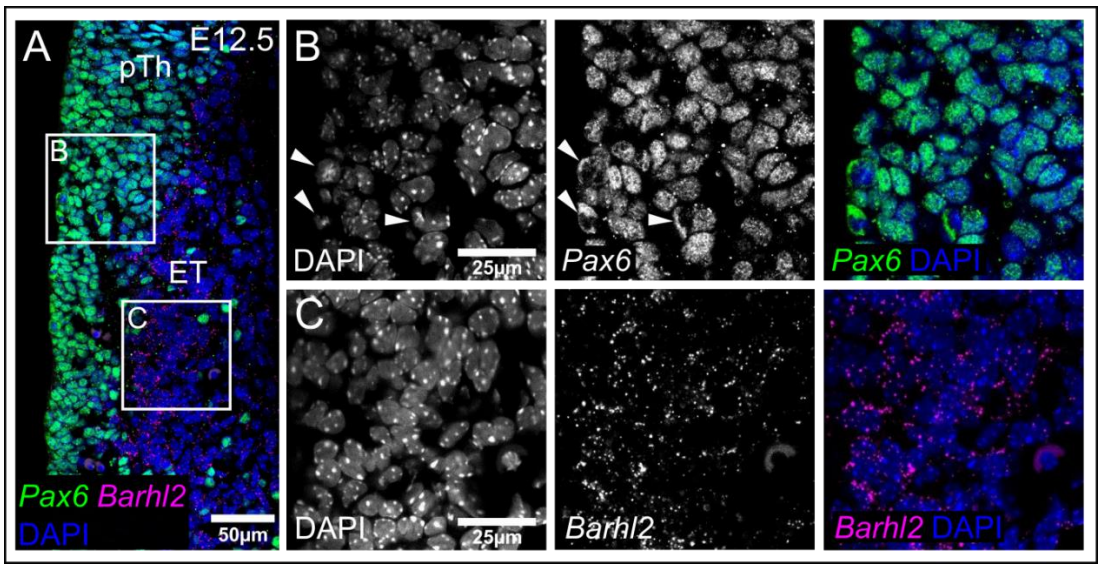

Fig. 3.3.5: A. Detail of the prethalamus and pretectum of a coronal section of the wild type diencephalon at E12.5, treated with immunohistochemistry for Pax6 *protein and* in situ *hybridization for* Barhl2 *mRNA. B. Detail of the area outlined in A imaged at high magnification, showing the translocation of* Pax6 *protein from the nucleus into the cytoplasm within dividing cells. C. Detail of the area outlined in A at high magnification showing* Barhl2 *mRNA forming clusters within the cytoplasm of individual cells. Abbreviations: pTh- prethalamus; ET- eminentia thalami.*

3.4 Quantitative analysis: spatiotemporal dynamics of *Pax6* and *Barhl2* within the thalamus

3.4.1 Introduction

In order to confirm the presence of opposing gradients of *Pax6* and *Barhl2* within the thalamus it was necessary to quantify the changes in their expression across the thalamic neuroepithelium.

The immunohistochemistry for Pax6 protein and *in situ* hybridization for *Barhl2* mRNA was repeated on tissue sections from two further embryos harvested at each developmental stage from E10.5 to E13.5. Confocal image data was recorded for a series of 16µm coronal sections from each embryo. One image of each series was chosen to be analysed, with the three images chosen for each developmental stage cut from a similar position on the rostrocaudal axis, determined by the morphological features visible, in order to ensure that the three sections were comparable.

Fiji (Schindelin *et al* 2012) was used to analyse confocal image data. The change in the intensity of the fluorescence was measured along a line drawn along the ventricular surface of the diencephalon, extending from the diencephalic midline to the dorsal extent of the ZLI. The numerical values were entered into an Excel spreadsheet and binned into groups of five. The mean values for each bin were plotted against distance from the dorsal midline to produce a line graph illustrating the changes in the relative intensity of the fluorescence signal across the neuroepithelium. A linear regression trend line was calculated for each plot and the gradient of this was taken as the steepness of the expression gradient. This was repeated for the Pax6 and *Barhl2* fluorescence signals. In order to account for the possibility of sections not being perfectly symmetrical, this was first carried out using data from the left-hand side of each embryo, then using data from the right-hand side of each embryo. In order to calculate the mean gradient of Pax6 and *Barhl2* expression at each developmental stage, binned relative intensity data from points at the same distance from the dorsal midline on the left and right-hand sides of the embryo were used. The mean for the two values recorded at each different distance from the dorsal midline was calculated. These means were then plotted against distance from the dorsal midline, a linear regression trendline was plotted and the gradient of this was recorded. This was carried out for both the Pax6 immunostaining signal and the *Barhl2 in situ* hybridization signal in each of the three embryos analysed at each developmental stage. The means of the gradients for Pax6 and *Barhl2* at each developmental stage were then recorded and these values were plotted on a bar chart.

3.4.2 Results

As with the previous *in situ* hybridization data presented here, the data from these experiments appeared to confirm the high complementarity of the Pax6 and *Barhl2* expression domains in regions of neuroepithelium outside the thalamus. Quantification of the expression gradients suggested that countergradients of Pax6 and *Barhl2* expression are present in the developing thalamus but that they are not present at every stage of development, and that they only strongly oppose each other at particular developmental stages.

At E10.5 there appeared to be a great deal of variability between the data recorded for the three different embryos analysed. Strong countergradients *of Pax6* and *Barhl2* were found to be present in the first of the three embryos analysed (Fig. 3.4.1) and the data for this embryo suggested that the relationship between Pax6 and *Barhl2* expression could be inversely proportional. Quantification of the expression gradients in the second embryo (Fig. 3.4.2) suggested that the Pax6 and *Barhl2* gradients did not run counter to each other. In the third embryo (Fig. 3.4.3) countergradients could be seen in left-hand side of the thalamus but not in the right-hand side, and on the left-hand side the relationship between Pax6 and *Barhl2* expression did not appear to be inversely proportional as it did in the first embryo.

By E11.5 countergradients of Pax6 and *Barhl2* expression were apparent on both sides of the second of the three embryos analysed (Fig. 3.4.5) but only on the left hand side of the first embryo (Fig. 3.4.4) and in the third embryo countergradients were not apparent at all. Quantification of the gradients of Pax6 and *Barhl2* in the third embryo suggested that both genes were expressed along a gradient running from dorsal to ventral, though that of *Barhl2* was much less steep than that of Pax6.

The countergradients of Pax6 and *Barhl2* were the most strongly opposed at E12.5 (Fig. 3.4.7-3.4.9) and this was observed in all three of the embryos analysed.

By E13.5 (Fig. 3.4.10-Fig. 3.4.12) the expression gradients of both Pax6 and *Barhl2* appeared to become much less steep. Analysis of the data suggested that by this stage the gradients no longer run counter to each other, and that for both genes expression is at its strongest in the dorsal diencephalon, becoming weaker along the dorsoventral axis.

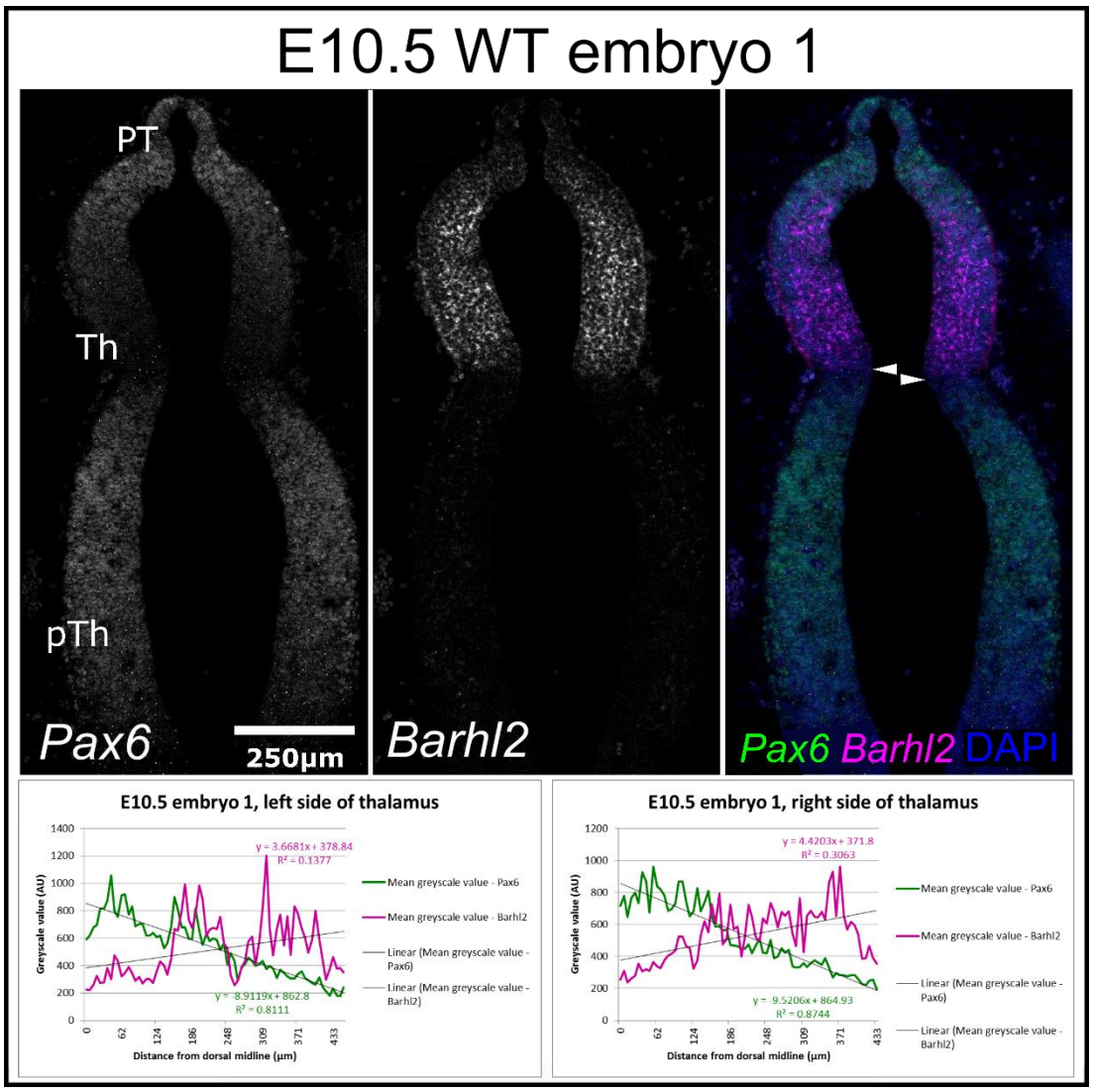

Fig. 3.4.1: Data from the analysis of the first of the three embryos harvested at E10.5. Presented here are Immunostaining data for *Pax6 protein and* in situ *hybridization data for* Barhl2 *mRNA, with line plots of relative intensity across the length of the ventricular surface. The asterisk indicates the position of the dorsal midline as the point from which data were recorded, while the arrows indicate the end of the plot for the left and right sides of the diencephalon. Abbreviations: PT- pretectum; Th- thalamus; pTh- prethalamus; AU- arbitrary units.*

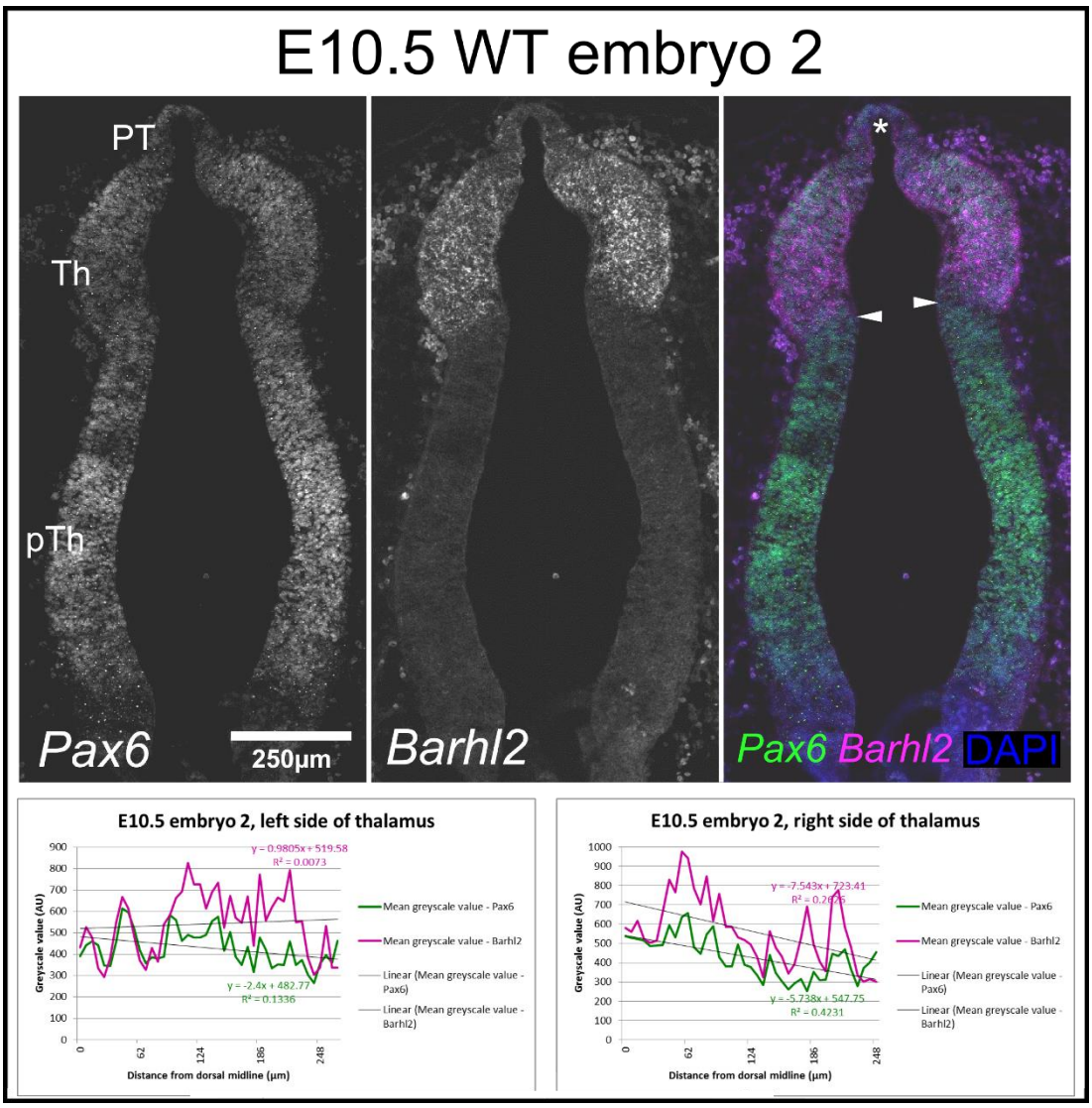

Fig. 3.4.2: Data from the analysis of the second of the three embryos harvested at E10.5. Presented here are immunostaining data for Pax6 protein and in situ *hybridization data for* Barhl2 *mRNA, with line plots of relative intensity across the length of the ventricular surface. The asterisk indicates the position of the dorsal midline as the point from which data were recorded, while the arrows indicate the end of the plot for the left and right sides of the diencephalon. Abbreviations: PT- pretectum; Th- thalamus; pTh- prethalamus; AU- arbitrary units.*

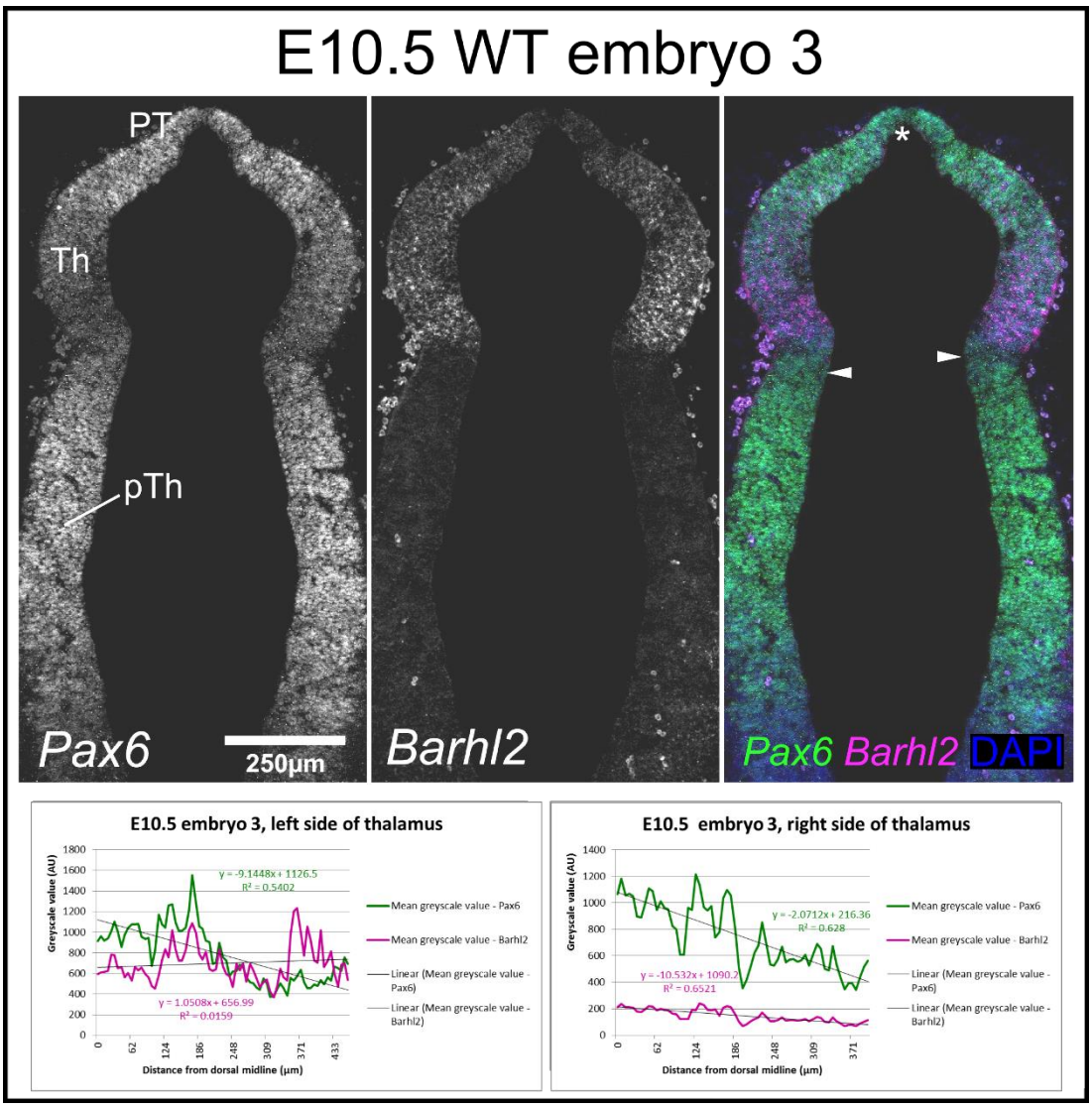

Fig. 3.4.3: Data from the analysis of the third of the three WT embryos harvested at E10.5. Presented here are immunostaining data for Pax6 protein and in situ *hybridization data for* Barhl2 *mRNA, with line plots of relative intensity across the length of the ventricular surface. The asterisk indicates the position of the dorsal midline as the point from which data were recorded, while the arrows indicate the end of the plot for the left and right sides of the diencephalon. Abbreviations: PT- pretectum; Th- thalamus; pTh- prethalamus; AU- arbitrary units.*

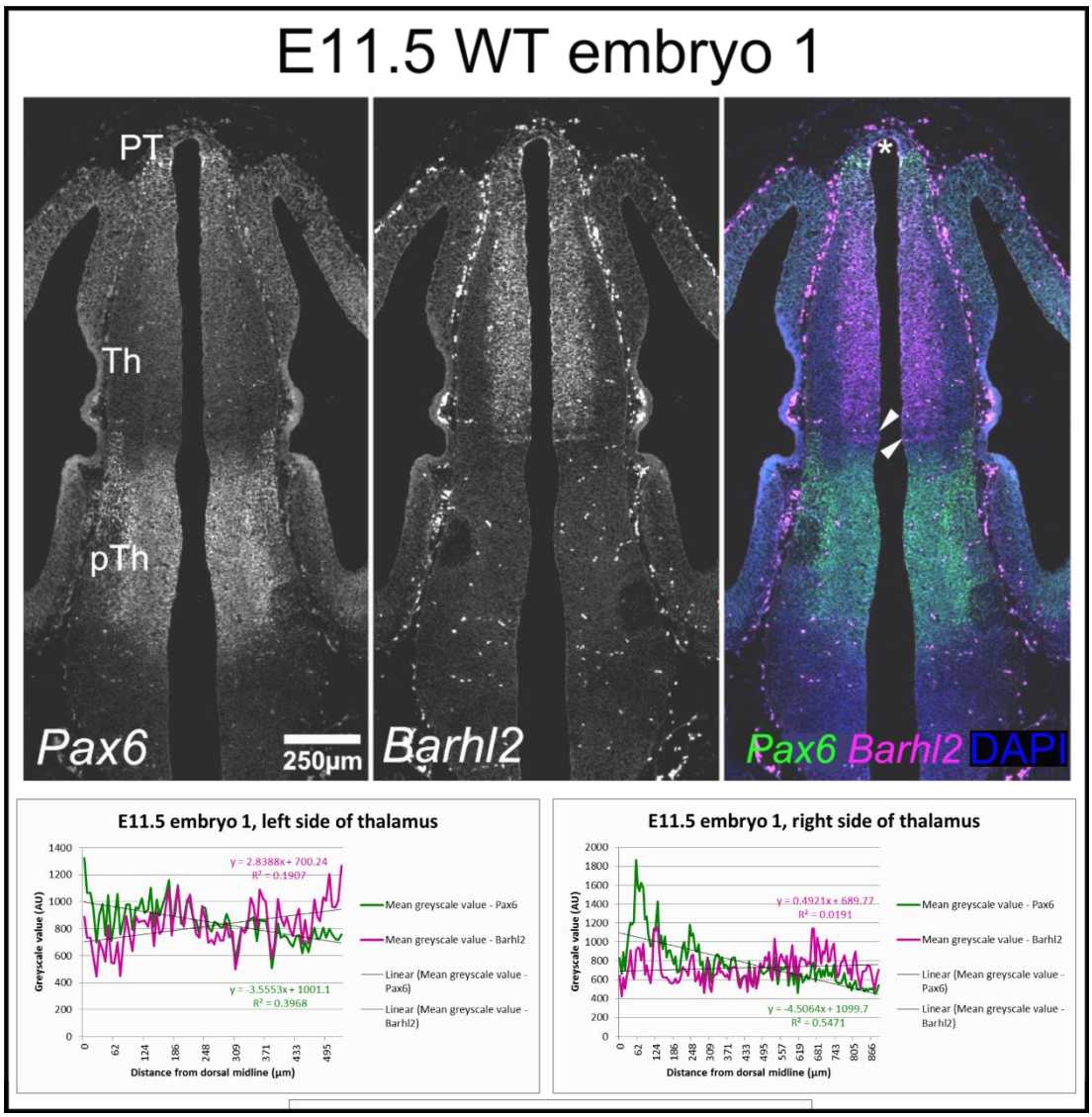

Fig. 3.4.4: Data from the analysis of the first of the three WT embryos harvested at E11.5. Presented here are immunostaining data for Pax6 protein and in situ *hybridization data for* Barhl2 *mRNA, with line plots of relative intensity across the length of the ventricular surface. The asterisk indicates the position of the dorsal midline as the point from which data were recorded, while the arrows indicate the end of the plot for the left and right sides of the diencephalon. Abbreviations: PT- pretectum; Th- thalamus; pTh- prethalamus; AU- arbitrary units.*

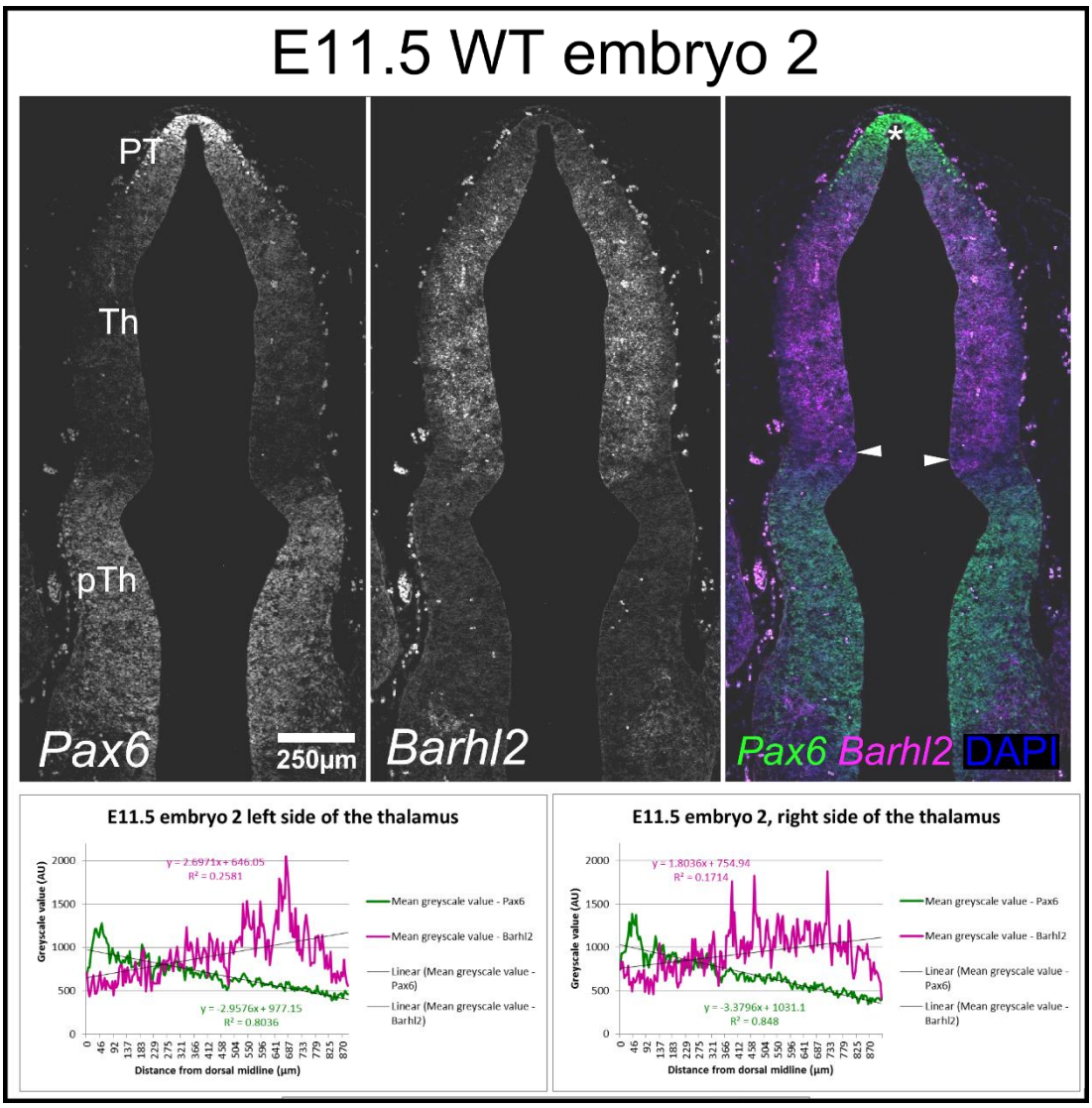

Fig. 3.4.5: Data from the analysis of the second of the three WT embryos harvested at E11.5. Presented here are immunostaining data for Pax6 protein and in situ *hybridization data for* Barhl2 *mRNA, with line plots of relative intensity across the length of the ventricular surface. The asterisk indicates the position of the dorsal midline as the point from which data were recorded, while the arrows indicate the end of the plot for the left and right sides of the diencephalon. Abbreviations: PT- pretectum; Th- thalamus; pTh- prethalamus; AU- arbitrary units.*

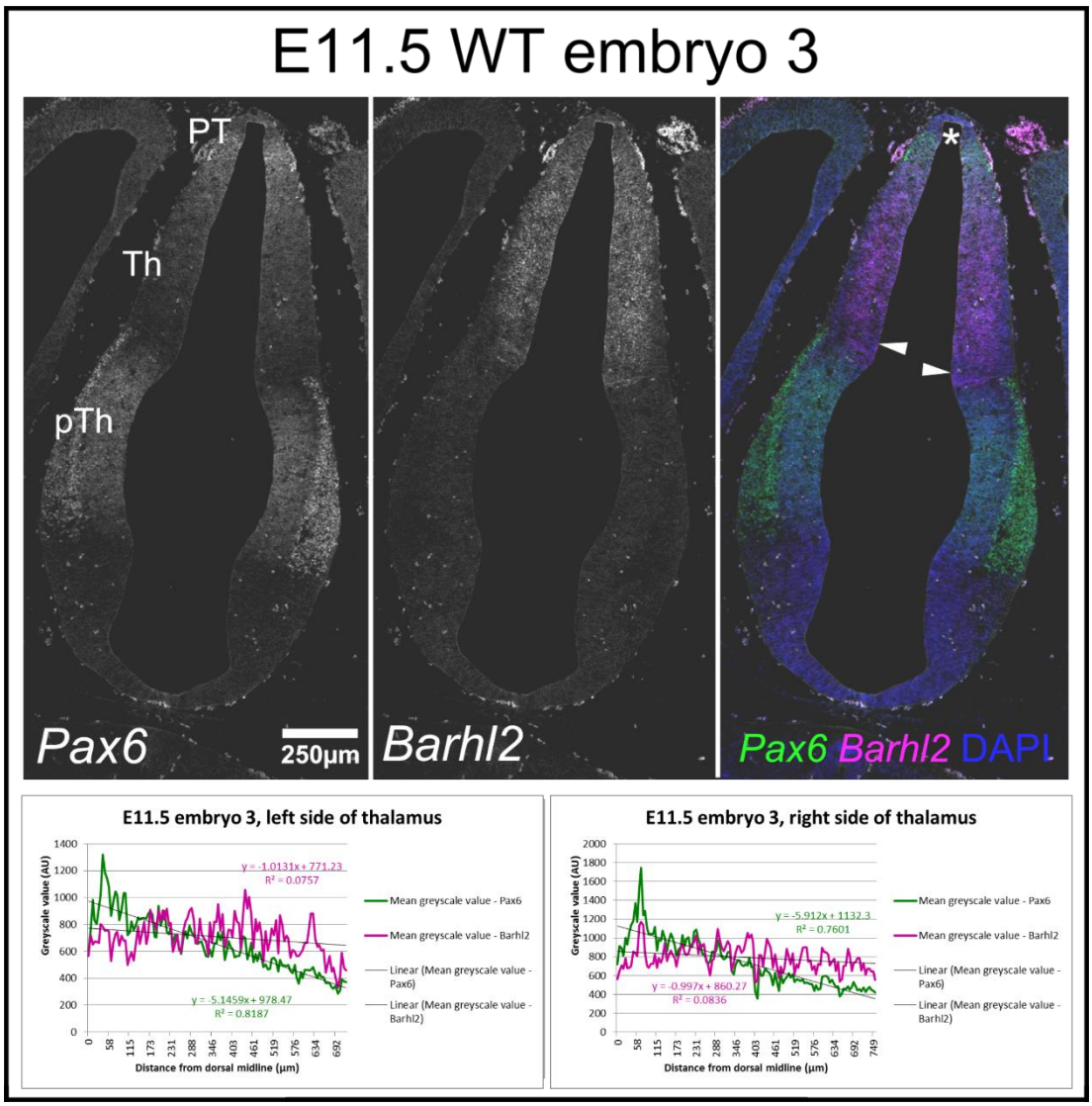

Fig. 3.4.6: Data from the analysis of the third of the three WT embryos harvested at E11.5. Presented here are immunostaining data for Pax6 protein and in situ *hybridization data for* Barhl2 *mRNA, with line plots of relative intensity across the length of the ventricular surface. The asterisk indicates the position of the dorsal midline as the point from which data were recorded, while the arrows indicate the end of the plot for the left and right sides of the diencephalon. Abbreviations: PT- pretectum; Th- thalamus; pTh- prethalamus; AU- arbitrary units.*

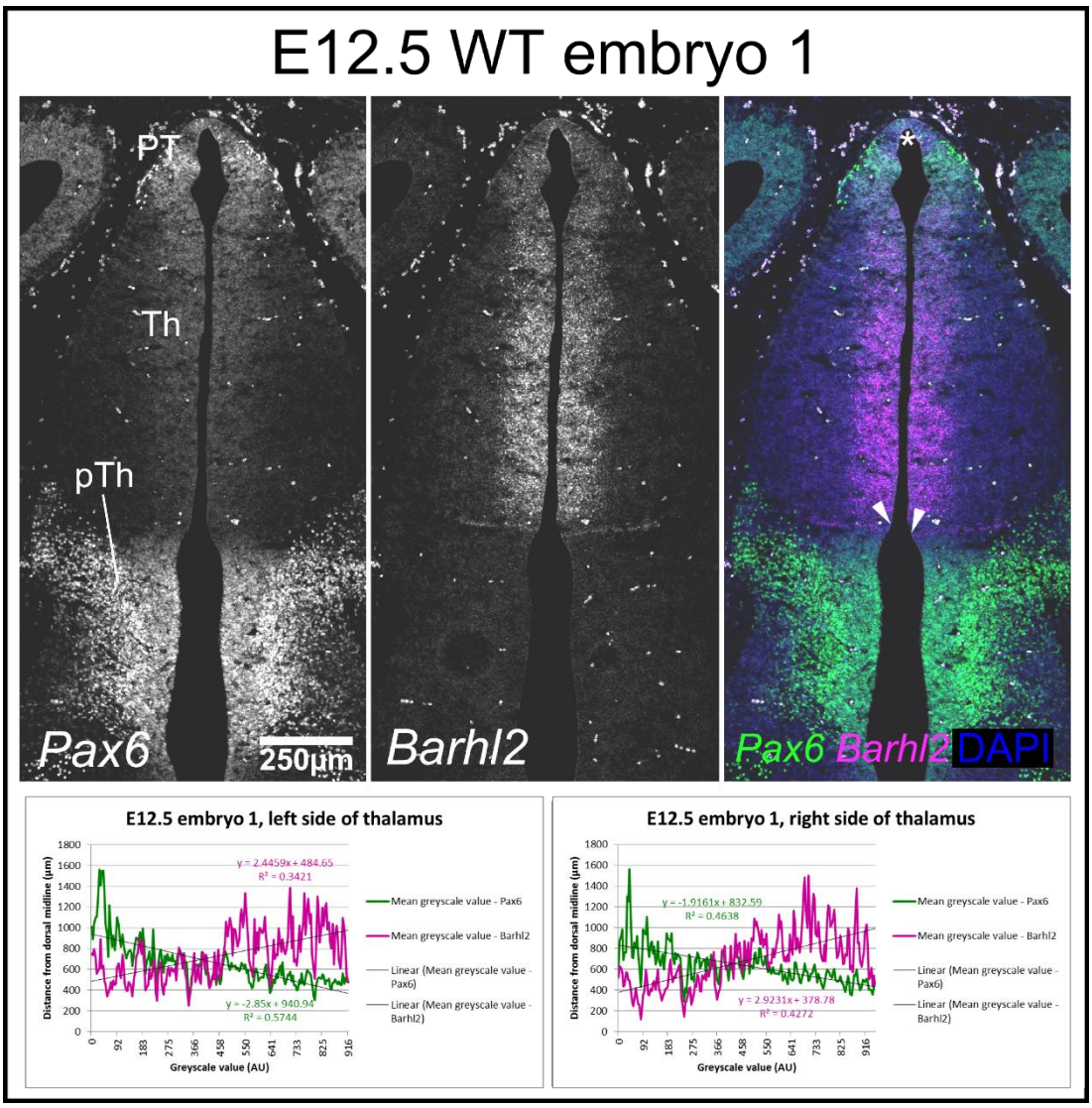

Fig. 3.4.7: Data from the analysis of the first of the three WT embryos harvested at E12.5. Presented here are immunostaining data for Pax6 protein and in situ *hybridization data for* Barhl2 *mRNA, with line plots of relative intensity across the length of the ventricular surface. The asterisk indicates the position of the dorsal midline as the point from which data were recorded, while the arrows indicate the end of the plot for the left and right sides of the diencephalon. Abbreviations: PT- pretectum; Th- thalamus; pTh- prethalamus; AU- arbitrary units.*

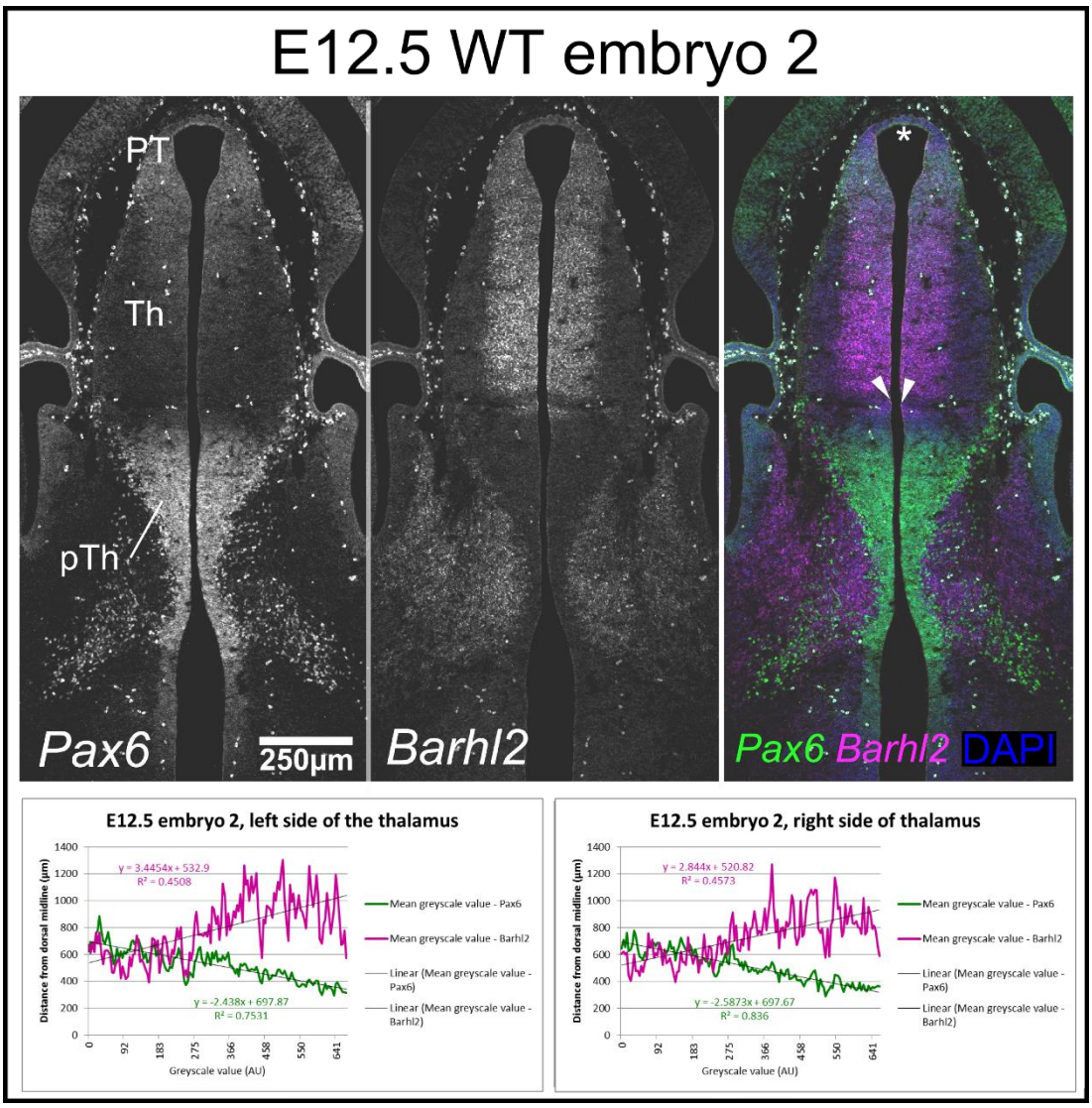

Fig. 3.4.8: Data from the analysis of the second of the three WT embryos harvested at E12.5. Presented here are immunostaining data for Pax6 protein and in situ *hybridization data for* Barhl2 *mRNA, with line plots of relative intensity across the length of the ventricular surface. The asterisk indicates the position of the dorsal midline as the point from which data were recorded, while the arrows indicate the end of the plot for the left and right sides of the diencephalon. Abbreviations: PT- pretectum; Th- thalamus; pTh- prethalamus; AU- arbitrary units.*

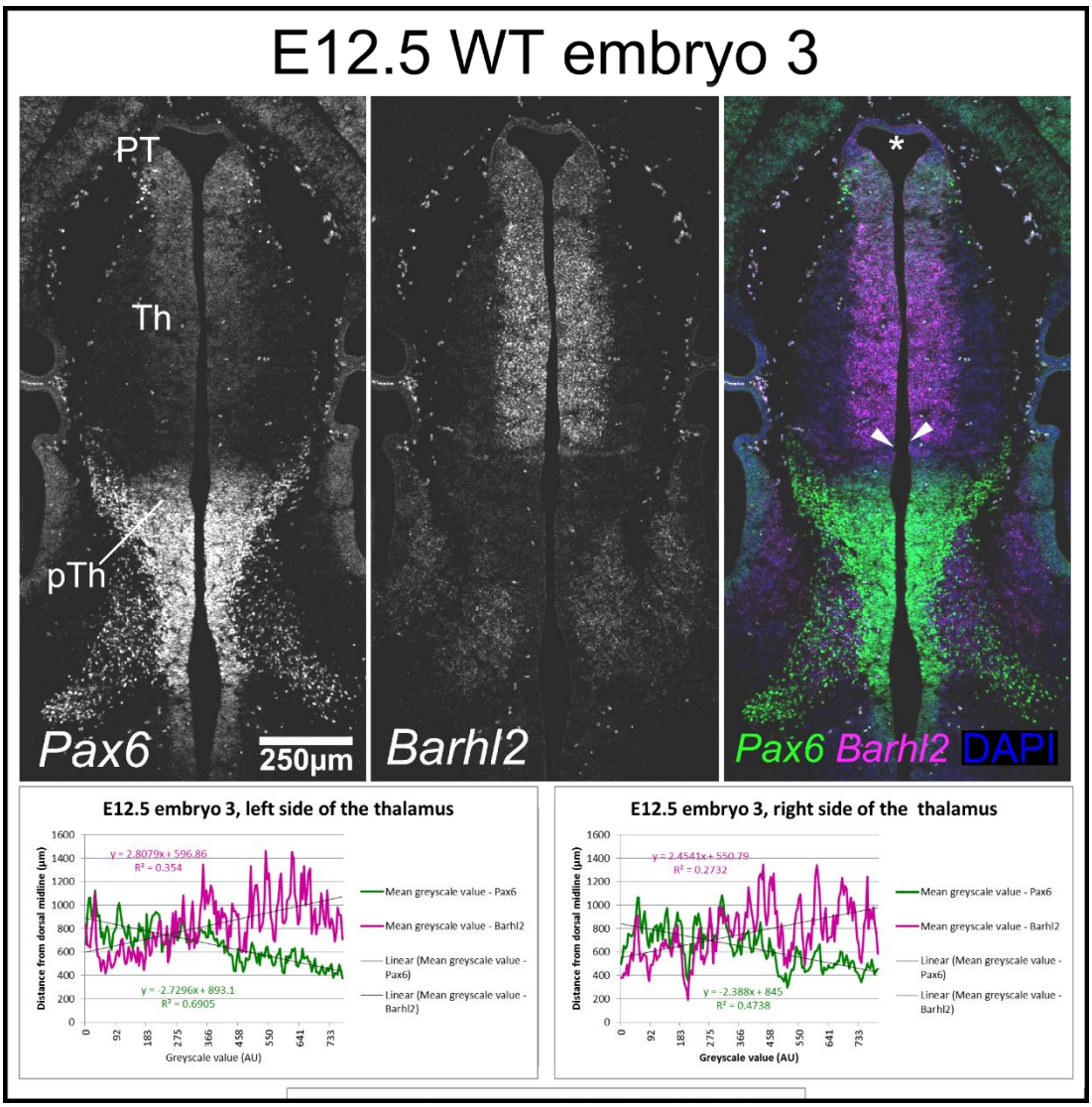

Fig. 3.4.9: Data from the analysis of the third of the three WT embryos harvested at E12.5. Presented here are immunostaining data for Pax6 protein and in situ *hybridization data for* Barhl2 *mRNA, with line plots of relative intensity across the length of the ventricular surface. The asterisk indicates the position of the dorsal midline as the point from which data were recorded, while the arrows indicate the end of the plot for the left and right sides of the diencephalon. Abbreviations: PT- pretectum; Th- thalamus; pTh- prethalamus; AU- arbitrary units.*

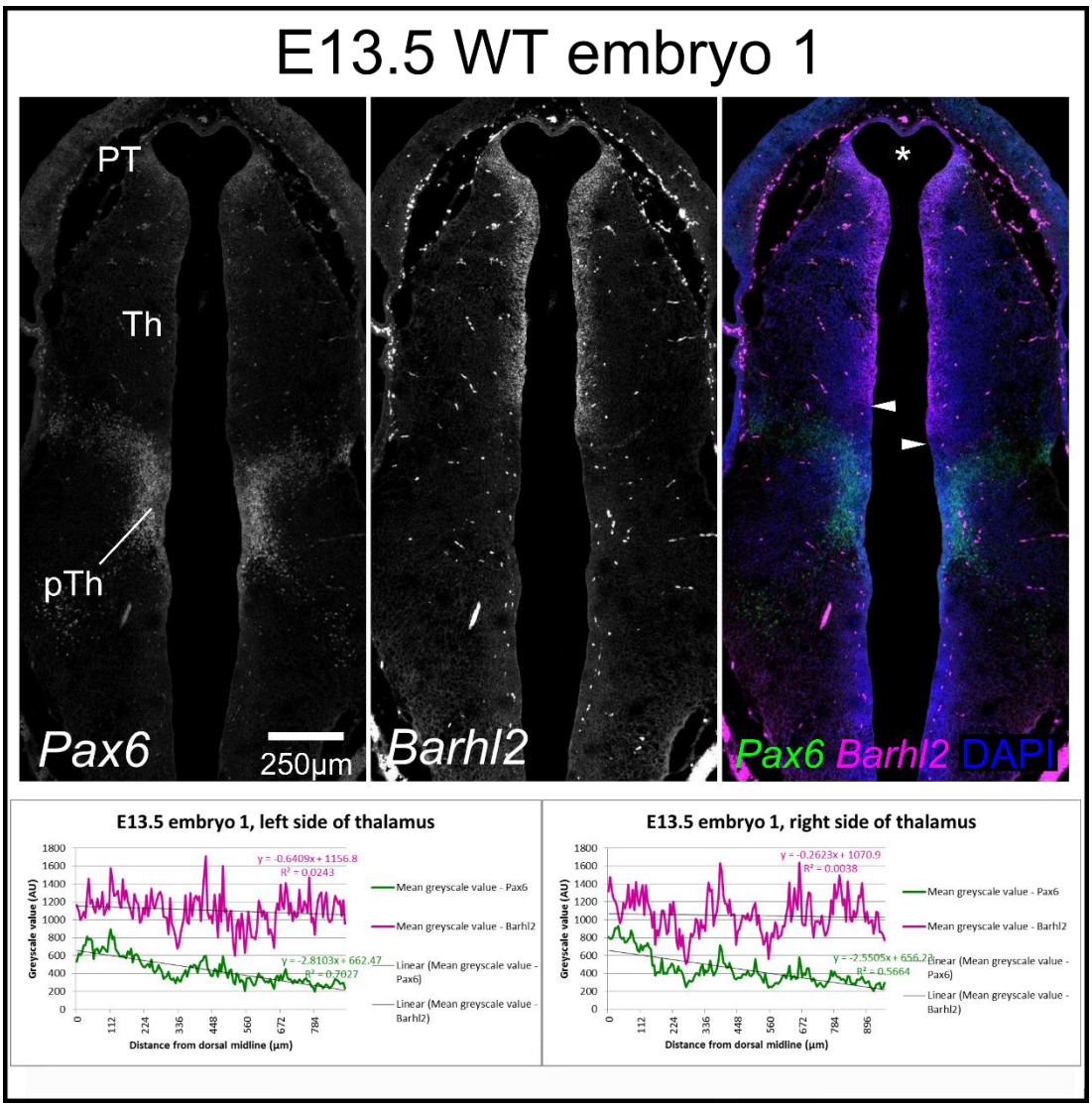

Fig. 3.4.10: Data from the analysis of the first of the three WT embryos harvested at E13.5. Presented here are immunostaining data for Pax6 protein and in situ *hybridization data for* Barhl2 *mRNA, with line plots of relative intensity across the length of the ventricular surface. The asterisk indicates the position of the dorsal midline as the point from which data were recorded, while the arrows indicate the end of the plot for the left and right sides of the diencephalon. Abbreviations: PT- pretectum; Th- thalamus; pTh- prethalamus; AU- arbitrary units.*

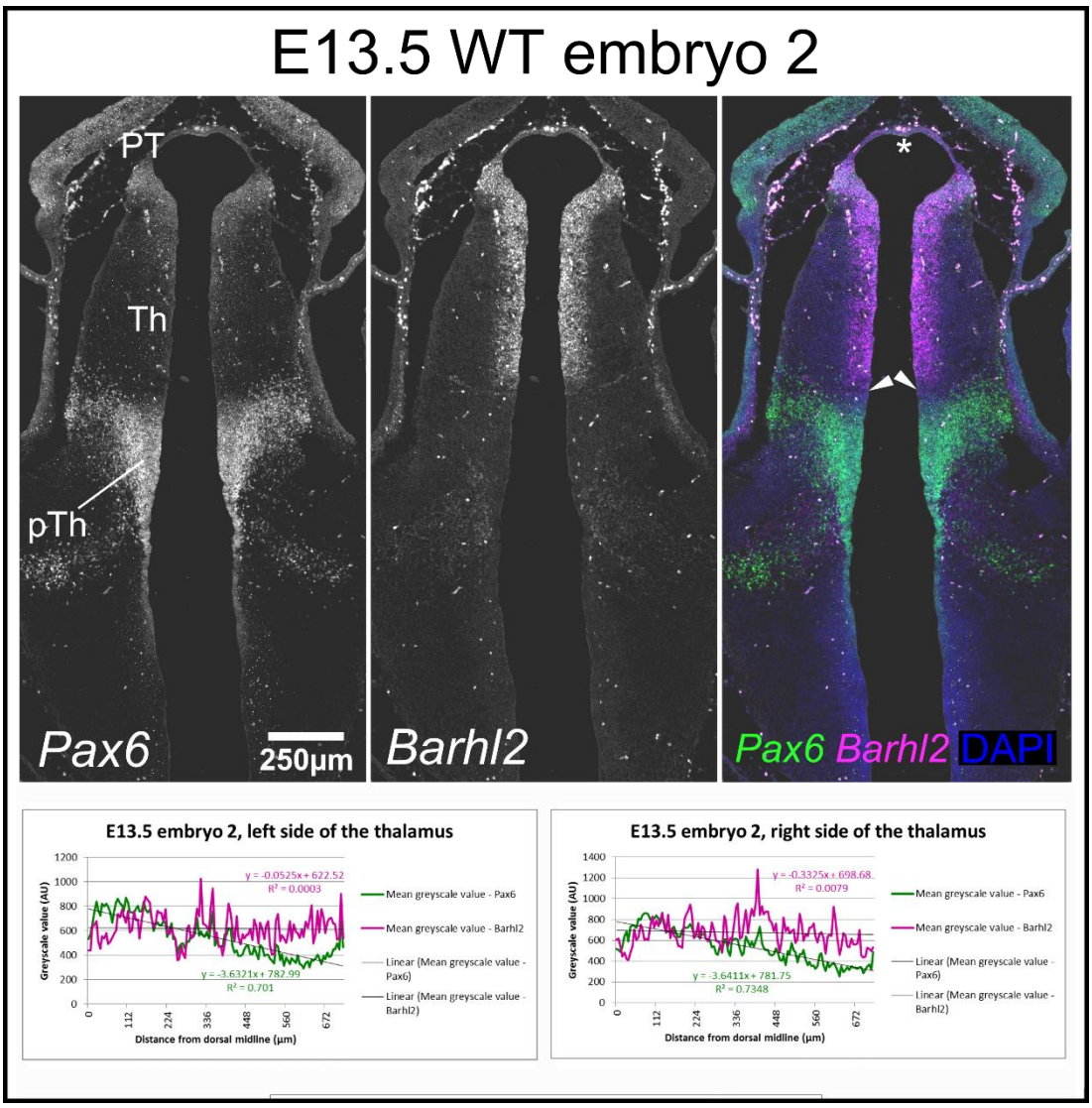

Fig. 3.4.11: Data from the analysis of the second of the three WT embryos harvested at E13.5. Presented here are immunostaining data for Pax6 protein and in situ *hybridization data for* Barhl2 *mRNA, with line plots of relative intensity across the length of the ventricular surface. The asterisk indicates the position of the dorsal midline as the point from which data were recorded, while the arrows indicate the end of the plot for the left and right sides of the diencephalon. Abbreviations: PT- pretectum; Th- thalamus; pTh- prethalamus; AU- arbitrary units.*

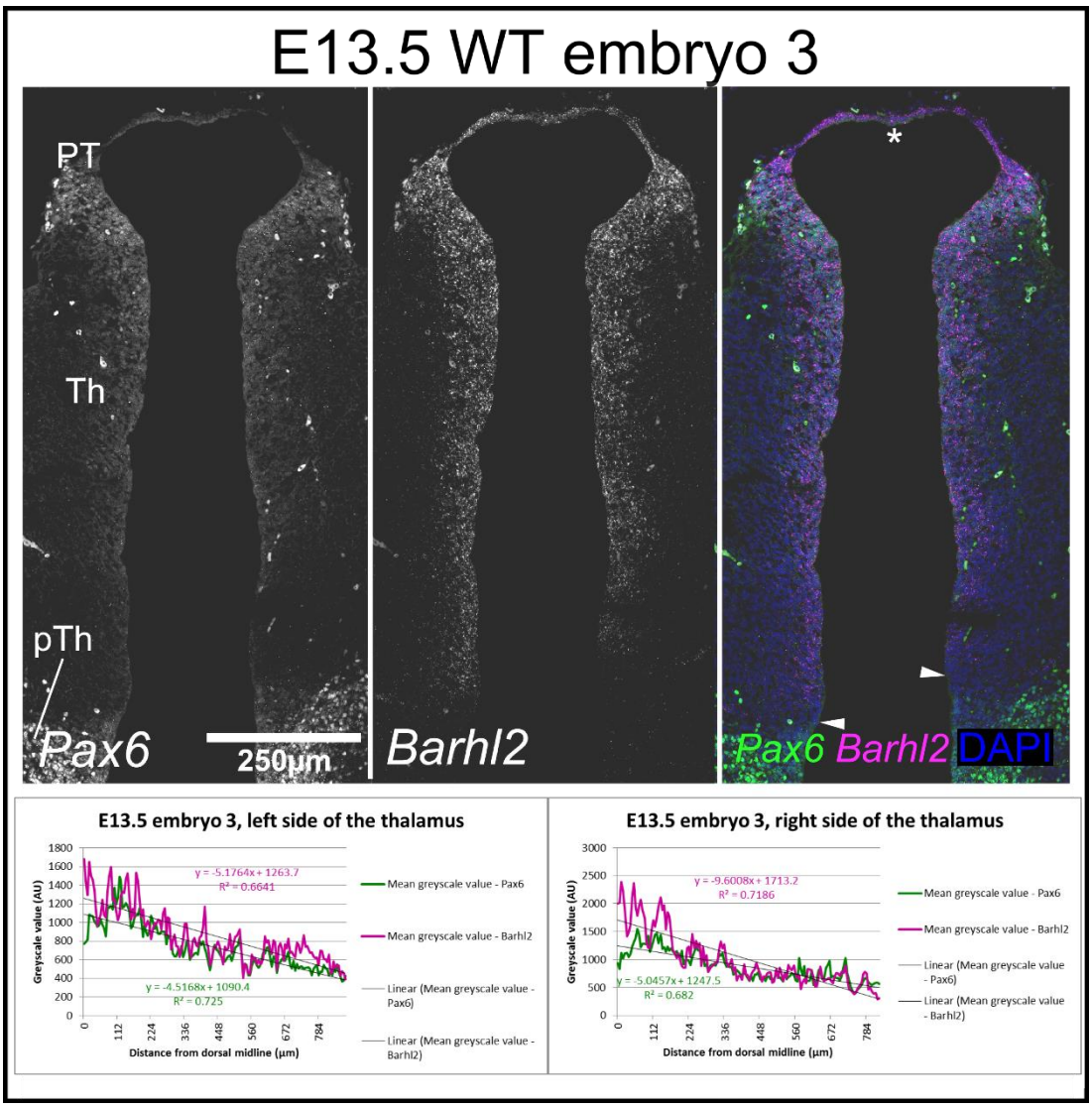

Fig. 3.4.12: Data from the analysis of the third of the three WT embryos harvested at E13.5. Presented here are immunostaining data for Pax6 protein and in situ *hybridization data for* Barhl2 *mRNA, with line plots of relative intensity across the length of the ventricular surface. The asterisk indicates the position of the dorsal midline as the point from which data were recorded, while the arrows indicate the end of the plot for the left and right sides of the diencephalon. Abbreviations: PT- pretectum; Th- thalamus; pTh- prethalamus; AU- arbitrary units.*

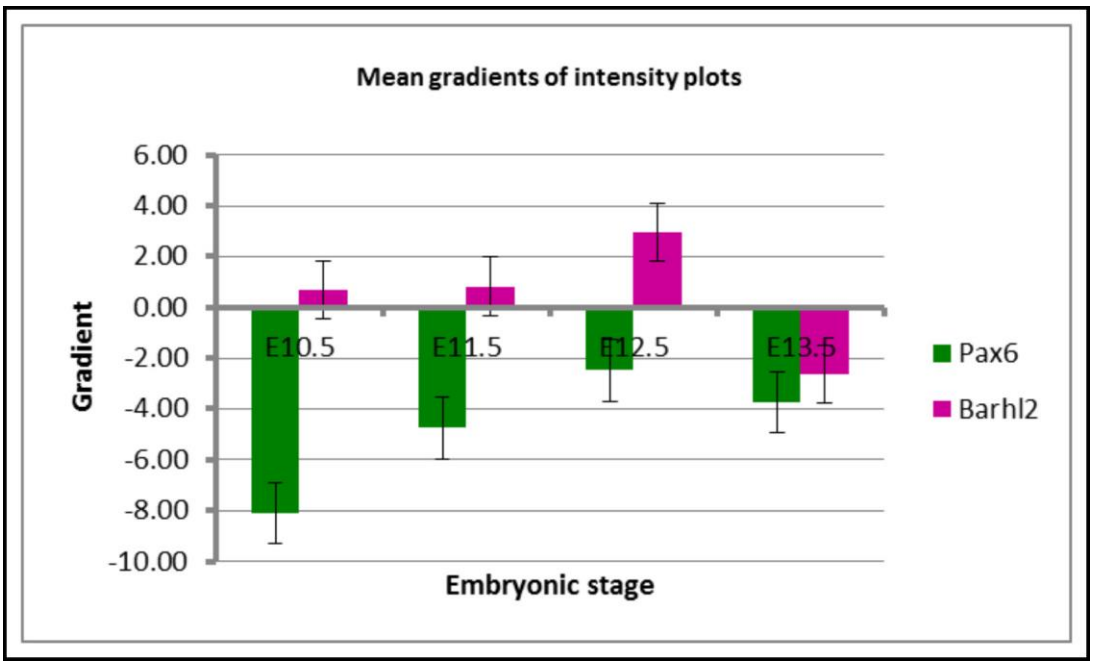

Fig. 3.4.13: The means of the slopes of the gradients for the three embryos analysed at each developmental stage, calculated by using the means of relative intensity values recorded at points the same distance from the dorsal midline on the left and right-hand sides of the embryo.

3.5 Discussion

The expression of *Pax6* within the wild type murine diencephalon has been extensive mapped and described in detail across a wide range of developmental stages (Walther and Gruss 1991, Mastick *et al* 1997, Gray et al 2004, Yokoyama 2009). While a relatively small number of previous studies have aimed to characterise the expression of *Barhl2* and its homologues in the developing CNS, these analyses have been carried out on a number of different animal models, ranging from extensive studies in *Drosophila* (Higashijima *et* al 1992, Sato *et al* 1999, Lim and Choi 2003) to a number of more recent studies in vertebrates such as *Xenopus* (Juraver-Geslin *et al* 2011, 2014), and zebrafish (Colombo *et* al 2006, Staudt and Houart 2008). The first *Barhl2*-null mutant mouse was generated relatively recently (Ding *et al* 2009) and studies of *Barhl2* expression in the mouse embryo have so far focused mainly on the retina (Ding *et al* 2009, Jin *et al* 2010) and spinal cord (Ding *et al* 2012, Duval *et al* 2014). The expression of *Barhl2* within the embryonic murine diencephalon has

not previously been described in a level of detail comparable to that with which diencephalic *Pax6* expression has been described in the mouse embryo.

The chromogenic *in situ* hybridization data for *Pax6* and *Barhl2* (Figs. 3.2.1-3.2.7) strongly suggested that the genes' respective expression domains complement each other in regions outside the thalamus and pretectum. This complementarity was confirmed with the results of the fluorescence *in situ* hybridization and fluorescence immunohistochemistry experiments (Figs. 3.3.1-3.3.3), which showed that the Pax6 and *Barhl2* expression domains meet at sharp boundaries and that little to no co-expression of Pax6 and *Barhl2* can be detected in cells located at these boundaries. The high degree of complementarity observed strongly suggests the existence of a mutually repressive relationship between Pax6 and *Barhl2*.

Mutual transcriptional repression is known to play a role in the establishment of tissue boundaries early in the formation of lineage restriction compartments (Kiecker and Lumsden 2005). In the *Drosophila* retina *BarH2* inhibits the activity of bHLH transcription factors (Lim and Choi 2003) and in the mouse spinal cord and midbrain-hindbrain boundary a comparable mechanism has been shown to induce boundary formation, involving the inhibition of the bHLH transcription factor *Ascl1* by *Hairy and enhancer of split 1* (*Hes1*) (Baek *et al* 2006). Mutual repression between *Pax6* and *Barhl2* may serve to induce the formation of boundaries, potentially via the inhibition of bHLH transcription factor activity in the diencephalon.

The relationship between *Pax6* and *Barhl2* within the thalamus and pretectum appears to be different and this may be a consequence of the different molecular character of the neuroepithelium caudal to the ZLI (Kiecker and Lumsden 2004). The chromogenic *in situ* hybridization data show that both *Pax6* and *Barhl2* are expressed within this region of the diencephalon (Figs. 3.2.1-3.2.7). The results of experiments employing fluorescence techniques on sections from E12.5 embryos confirmed that Pax6 protein and *Barhl2* RNA are co-expressed by individual cells of the thalamus and pretectum but suggested that levels of Pax6 expression may be high in regions of the neuroepithelium in which levels of *Barhl2* expression are low, and

vice versa (Fig. 3.3.3). These data suggest the possibility of incomplete mutual repression between the two genes within the thalamus and pretectum.

In the *Drosophila* retina *BarH2* exerts an antiproneural effect via the inhibition of bHLH transcription factor activity. This serves to inhibit ectopic neurogenesis and modulate the rate of neurogenic activity during the early patterning of the retina (Lim and Choi 2003). If *Barhl2* plays a comparable role in mammalian neural tissue it may be possible that *Barhl2* is required to prevent ectopic neurogenesis within regions of the mammalian diencephalon. Conversely, repression of *Barhl2* expression by Pax6 may be required in order for neurogenesis to proceed. Previous studies have shown that Pax6 induces neurogenesis (Estivill-Torrus *et al* 2002, Heins *et al* 2002) and that the level of Pax6 expression needs to be regulated in order to prevent premature neurogenesis (Sansom *et al* 2009). It may be possible that the levels of both *Pax6* and *Barhl2* need to be regulated in order for neurogenesis to process correctly, and that mutual transcriptional repression serves to modulate thalamic neurogenesis.

This possibility is supported by evidence that the ventricular zone of the thalamus strongly expresses a number of bHLH transcription factors, including *Neurogenin1* (*Ngn1*) (Vue *et al* 2007) and *Neurogenin2* (*Ngn2*) (Gradwohl *et al* 1996, Osório *et al* 2010, Suzuki-Hirano *et al* 2011) in domains of a shape comparable to that of the *Barhl2* expression domain.

Investigation of the co-expression of Pax6 protein and *Barhl2* mRNA within the thalamus and pretectum over a series of developmental stages (Fig. 3.3.1 and 3.3.2) made it possible to visualise the changing shapes of the Pax6 and *Barhl2* expression domains over time. As development proceeds the Pax6 expression domain appears to occupy an increasingly smaller area of the thalamus and pretectum, becoming increasingly restricted to the more dorsal regions of the diencephalon, and by E13.5 its expression is largely confined to the pretectum. By contrast the *Barhl2* domain expands along the dorsoventral axis, apparently at the expense of the Pax6 domain, and by E13.5 the domain of *Barhl2* spans the entire dorsoventral extent of the pretectum and thalamus, with the exception of the pTh-R.

If *Barhl2* represses the proneural activity of bHLH transcription factors in mouse, it may be necessary to suppress *Barhl2* expression in order for neurogenesis to proceed. *Pax6* may inhibit *Barhl2* expression in specific regions of neuroepithelium at specific points in development, allowing neurogenesis to proceed in a precise and controlled fashion. Likewise, *Barhl2* may be required to restrict the proneural and proliferative activity of Pax6 protein (Walcher *et al* 2013) and prevent ectopic and premature neurogenesis. Overall, mutual repression between *Pax6* and *Barhl2* could serve to control the rate of neurogenesis within the thalamus and specify the precise locations and times at which neuronal differentiation can occur.

While the *Barhl2* domain expands along the dorsoventral axis over time, it narrows along the mediolateral axis. At E8.5 its domain spans the entire thickness of the diencephalic neuroepithelium, but by E10.5 its expression begins to become restricted to the ventricular zone of the thalamus and a narrower region of the pretectum, and by E13.5 its domain in this region of the diencephalon has narrowed to an even greater extent. The narrowing of the *Barhl2* domain along the mediolateral axis could also serve to allow a wave of thalamic neurogenesis to proceed from lateral to medial. Because *Pax6* is not strongly expressed in more ventral regions of the thalamus at E13.5 this narrowing of the *Barhl2* domain is likely to be induced by a factor other than transcriptional repression by *Pax6*.

The quantification of the expression gradients of *Pax6* protein and *Barhl2* mRNA showed that strong expression countergradients were only present in the tissue sections analysed at E12.5 (Figs. 3.4.7-3.4.9), and in some of those analysed at E11.5 (Figs. 3.4.4-3.4.6). The majority of thalamic neurogenesis occurs between E10.5 and E12.5 (Bluske *et al* 2009, Suzuki-Hirano *et al* 2011) and the presence of countergradients at these stages may further support the hypothesis that incomplete mutual repression between *Pax6* and *Barhl2* serves to modulate thalamic neurogenesis. The results of the quantitative analysis strongly suggested the presence of a dorsal-to-ventral gradient of Pax6 expression at all stages analysed. While the results also suggested the presence of a ventral-to dorsal gradient of *Barhl2* at some stages, the gradient only appeared to be strong at E12.5, at stages prior to this it appeared to be much less steep, while it ran from dorsal-to-ventral at E13.5. The data

from this analysis more strongly suggest the presence of a Pax6 expression gradient, and the evidence for a countergradient of *Barhl2* expression is less convincing.

The results for the quantitative analysis were not as consistent between the different embryos analysed at E10.5 and E13.5 respectively. Strong countergradients of *Pax6* and *Barhl2* expression were only observed on both sides of the thalamus in one of the three embryos analysed at E10.5, while in the second embryo countergradients were only present on one side of the thalamus, and in the third they were not present at all. At E13.5 the gradients did not run counter to each other, and at these stages there was a high degree of variability between different embryos analysed at the same developmental stage.

This variability observed at E10.5 (Figs. 3.4.1-3.4.3) may be due to the ZLI being established at this time (Shimamura *et al* 1995). Embryos were staged according to gross external morphology and while the embryos used in these experiments all appeared to be E10.5 as defined by the Theiler staging criteria (Theiler 1989) but it is possible that changes in external morphological characteristics do not correspond exactly with changes in gene expression within the neuroepithelium. In the embryos analysed at E10.5 the ZLI could be distinguished more easily in some embryos than in others (Figs. 3.4.1-3.4.3) and it is possible that ZLI development was at a more advanced stage in the embryos in which it was easier to distinguish. In the embryos analysed at E13.5 the ZLI was more easy to distinguish in some tissue sections than in others, The variability observed at E13.5 (Figs. 3.4.10-3.4.12) may have been due to the disappearance of the ZLI possibly occurring around this time (Lim and Golden 2007, Visel *et al* 2004). ZLI development, ZLI disappearance, and the related changes in gene expression within the diencephalon occur over a relatively short period of time and this may make it more challenging to obtain sections from three different embryos at the same point in development, at least by using external morphology to stage embryos. In order to overcome this problem in future experiments it would be necessary to harvest and cryosection a greater number of embryos at E10.5 and E13.5, carry out immunohistochemistry and *in situ* hybridization as before, and compare treated tissue sections in order to identify and

collate a set of sections in which the neuroepithelium appears to be at the same developmental stage.

Barhl2 also appears to be strongly expressed within the ZLI itself. A number of bHLH transcription factors are expressed within the ZLI, including *Ngn2* and *Ascl1* (Vue *et al* 2007). It may be possible that the expression of *Barhl2* within the ZLI serves to inhibit neurogenesis and maintain the non-neural character of the ZLI for the duration of its existence, allowing it to function as organizer region.

The spatiotemporal dynamics of *Barhl2* expression exhibit a strong correlation with the developmental dynamics of the thalamus and ZLI. Fate mapping studies in zebrafish have used *Barhl2* as a marker of the presumptive thalamus (Scholpp *et al* 2007) but in mouse at least its expression does not appear to be confined to the thalamic anlage and between E8.5 and E9.5 it may also extend to the anlage of the ZLI.

In mouse the ZLI begins to develop at approximately E10.5 (Shimamura *et al* 1995). In the image data presented here the domain of *Barhl2* within the ZLI can be distinguished at E10.5, separated from the thalamic *Barhl2* domain by a *Barhl2*-negative domain corresponding with the position of the p-ThR. Experiments on embryos at the 3-5 somite stage have suggested that the ZLI may be specified much earlier than this, as early as the 3-5 somite stage (Shimamura and Rubenstein1997), or approximately E7.5-8.5 (Theiler 1989). The earliest published expression data for *Barhl2* in the mouse showed that it is expressed at E9.5 (Yokoyama *et al* 2009). The chromogenic *in situ* hybridization data presented here show that *Barhl2* is expressed in the mouse diencephalon as early as E8.5, and while further experiments would be needed to determine the onset of *Barhl2* expression, these data show that *Barhl2* is expressed in the mouse diencephalon the ZLI develops, and suggest that prior to this it may be expressed in the region fated to become the ZLI. These findings are consistent with evidence that *Barhl2* is required for ZLI specification and development in *Xenopus* (Juraver-Geslin *et al* 2014). It may also be possible that the degree to which the thalamic *Pax6* and *Barhl2* expression gradients counter each other may be directly proportional to the level of neurogenic activity occurring

within the developing thalamus, but further experiments would be needed to investigate this possibility.

The precise developmental stage at which the disappearance of the ZLI begins has yet to be determined (Lim and Golden 2007) but in mouse the ZLI can no longer be visualised with *in situ* hybridization for *Shh* mRNA at E14.5 (Visel *et al* 2004) suggesting that the disappearance of the ZLI may have occurred by this stage. The data presented here show that the domain of *Barhl2* within the ZLI becomes narrower at E13.5 and that *Barhl2* expression also becomes weaker throughout the entire diencephalon at this stage. These observations support the hypothesis that *Barhl2* is required to maintain the ZLI in its non-neural state.

In tissue sections treated using fluorescence techniques observation of the tissue at high magnification suggested that both *Pax6* protein and *Barhl2* mRNA may be able to translocate within individual cells (Fig. 3.3.5). *Pax6* protein appeared to translocate from the nucleus to the cytoplasm of dividing cells, while *Barhl2* mRNA was detected in small clusters within cells, rather than being distributed more evenly throughout the nucleus and cytoplasm. These observations suggest that the expression of both genes may be oscillatory. The possibility that *Pax6* expression may be oscillatory has been considered in one study of its expression in the mouse cerebral cortex (Sansom et al 2009) and oscillatory *Pax6* expression has also been suggested as a component of a model for the regulation of vertebrate neurogenesis, in which it interacts with the transcription factors *Oligodendrocyte transcription factor 2* (*Olig2*) and *Nkx2-2* (Panovska-Griffiths *et al* 2012).

The punctate expression of *Barhl2* has not been described previously. Further experiments would be needed in order to further investigate the possibility that *Barhl2* expression is oscillatory, or that *Barhl2* mRNA can translocate and form aggregates within individual cells.

DAPI staining of chromatin within the cells of the diencephalon at E12.5 revealed a narrow region free of cell nuclei, extending from the more ventral regions of the thalamus, through the *eminentia thalami* and into the telencephalon (Fig. 3.3.4). This region passes through the *Barhl2* domain within the *eminentia thalami* and is flanked

by two expression domains of Pax6- the domain within the prethalamus, and a second, more lateral domain within the telencephalic neuroepithelium. This area free of cell nuclei corresponds with the position of the axon tract along which the thalamocortical axons project from the thalamus to the cortex, and the corticothalamic axons project from the cortex to the thalamus (Molnár *et a*l 2012, Price *et al* 2012) and it is possible that it may serve as a physical scaffold along which axons can extend and migrate. The antiproneural action of *Barhl2* (Lim and Choi 2003) may serve to inhibit the differentiation of neurons along the presumptive axon tract, allowing the scaffold to form before the thalamocortical and corticothalamic axons begin to extend along it.

In addition to this, *Barhl2* is known to be required for the subtype specification of dl1 interneurons in the developing mouse spinal cord, and the loss of *Barhl2* causes neurons which project contralaterally to be specified at the expense of those which project ipsilaterally. (Ding *et al* 2011). This observation suggests the possibility that *Barhl2* may be indirectly involved in the control of spinal cord axon guidance. It may be possible that *Barhl2* acts upstream of genes which encode transmembrane receptors for secreted axon guidance molecules, thereby conferring them with the ability to respond to these molecular cues. The *Barhl2*-null mutant mouse exhibits an increased number of axons which cross the midline of the embryo, and this suggests that the defect may be a consequence of disruption to the *Slit*/*Roundabout* (*Robo*) cell signalling pathway, which regulates the midline crossing of axons during neurogenesis (Dickson and Gilestro 2006). In this pathway, secreted signalling proteins of the *Slit* family bind to transmembrane receptor proteins of the *Robo* family where they are expressed by target cells. In many contexts *Slits* act as repulsive guidance cues and serve to inhibit midline crossing in *Robo*-expressing axons of target neurons (Nguyen-Ba-Charvet and Alain Chédotal, 2001)

It has been suggested that *Barhl2* may modulate the expression of *Roundabout 3* (*Robo3*) in the developing mouse spinal cord, acting in a context-dependent manner (Ding *et al* 2011) but further work remains to be carried out in order to characterise the relationship between *Barhl2* and *Robo3*. Further work would also be required to confirm or refute the existence of a comparable relationship between *Barhl2* and the

expression of *Robo* family in the mammalian diencephalon, and in the guidance of thalamocortical and corticothalamic axons.

The reasons for the apparent punctate expression of *Barhl2* observed within individual cells at high magnification is not clear. The translocation of protein and mRNA within the can occur as part of the process of distributing the cell's contents prior to cell division, and the distribution of those contents then determines whether the cell's division is a symmetric, proliferative division, or an asymmetric division which leads to the differentiation of one postmitotic daughter cell (Morrison and Kimble 2006). *Bar* family genes have been shown to inhibit neuronal differentiation in the *Drosophila* retina (Lim and Choi 2003) and it may be possible that the translocation of *Barhl2* mRNA within undifferentiated cells may have an influence on whether a dividing cell undergoes symmetric or asymmetric cleavage. In order to investigate this possibility further it would be necessary to quantify and characterise the distribution of Barhl2 protein *or Barhl2* mRNA or protein within individual cells. If such an investigation suggested an asymmetric distribution of *Barhl2* within cells, the nature of the divisions those cells then undergo could then be investigated in order to determine whether or not the translocation of *Barhl2* has an influence over this process.

Analysis of the gradients on the left-hand and right-hand side of the embryos revealed some variation in the steepness of gradients between embryos and between the left and right-hand sides, in particular in younger embryos. It may be possible that not all sections were adequately close to being symmetrical, or that in smaller embryos, where sectioning of the diencephalon yielded a smaller number of sections, the variation between these sections was greater than in larger embryos, in which a larger number of sections could be cut from the medial diencephalon. The variation in the steepness of gradients may also have been due to natural variation between embryos, and the gene expression between embryos not being entirely symmetrical. Data for the left-hand side of the embryos were analysed, followed by data from the right-hand side. The data from the right-hand side was broadly comparable to that from the left-hand side. The only exception was the embryos analysed at E10.5, for which the analysis of data from the right-hand side of embryo 2 and embryo 3

suggested the presence of a dorsal-to-ventral gradient of *Barhl2* expression while the data for the left hand side suggested that the gradient ran from ventral to dorsal. Again, this variation could be due to the ZLI developing around E10.5 and a number of rapid changes in gene expression occurring around this time.

4. *Barhl2* and the ZLI

4.1 Introduction

While the relationship between *Pax6* and *Shh* in vertebrate development has been studied extensively (Ekker *et al* 1995, MacDonald *et al* 1995, Kiecker and Lumsden 2004, Vieira *et al* 2005), comparatively little is known about the relationship between *Shh* and *Barhl2* in vertebrates. It is known that during the early development of the *Drosophila* retina the morphogen *Hedgehog* (*Hh*) is required to induce expression of both *BarH1* and *BarH2* (Lim and Choi, 2004). On the basis of this finding it could be expected that vertebrate *Hh* homologues act upstream of the vertebrate homologues of the two *Drosophila Bar* genes, but in *Xenopus* it appears that *Barhl2* acts upstream of *Shh*, at least in the process of ZLI development, which has been shown to require *Barhl2*, and that it is expressed in the vertebrate diencephalon prior to the onset of *Shh* expression within the ZLI (Juraver-Geslin *et al* 2014).

Fate-mapping studies in zebrafish have used *Barhl2* as a marker of the presumptive diencephalon (Staudt and Houart 2008) but the results of the experiments described in the previous chapter suggest that it may only be a marker of regions fated to become specific diencephalic structures rather than a marker of the presumptive diencephalon as a whole. In particular it seems to be strongly expressed in the neuroepithelium of the presumptive ZLI, and then at developmental stages prior to and during its development.

The spatiotemporal dynamics of *Barhl2* expression in the mouse diencephalon as described in the previous chapter suggest roles for the gene in the specification of the ZLI. Prior to ZLI formation *Barhl2* is expressed in the region of neuroepithelium in which the ZLI later develops. Its expression domain in this region assumes a characteristic spike shape extending from the floorplate and narrowing as it approaches the roofplate. The shape of the *Barhl2* domain is therefore comparable with that of the ZLI itself, as marked by *Shh* expression.

The previous chapter described a domain of *Barhl2* expression which appears to strongly correspond with the position of the ZLI following its induction at around

E10.5. In order to confirm this it would be necessary to investigate its expression in relation to known markers of the ZLI.

In order to investigate the possibility that the onset of *Barhl2* expression in mouse does not require *Shh, in situ* hybridization was performed in order to visualise *Barhl2* expression in the *Shh*-null mutant mouse (Chiang *et al* 1996). E12.5 *Shh*-null mouse embryos and wild-type littermates which had been stored in 100% methanol at 4°C were rehydrated in a series of ascending methanol washes before being fixed in 4% PFA in PBS and then mounted in OCT. Embryos were sectioned in the sagittal plane to give 10µm cryosections which were then treated with chromogenic *in situ* hybridization for *Barhl2* mRNA. Embryos were sectioned in the sagittal plane in order to divide the embryo into a relatively small number of sections, thereby allowing *in situ* hybridization to be carried out on the entire embryo more easily. By investigating *Barhl2* expression throughout the entire embryo regions of the nervous system where *Barhl2* is expressed outside the telencephalon, such as the spinal cord, could also be analysed, and it would be possible to speculate on the possibility that any changes in *Barhl2* expression were region-specific.

In order to determine potential roles for *Barhl2* in the induction and development of the ZLI, it was necessary to visualise the diencephalic *Barhl2* expression domain in a greater level of detail than in the experiments of the previous chapter. It was decided that performing chromogenic *in situ* hybridization on whole embryos would be a suitable means of achieving this aim, and that treated embryos would then be hemisecting along the midline to make it possible to observe the shape and extent of the expression domain over the ventricular surface of the diencephalon.

Pax6$^{+/Sey}$ males were crossed with *Pax6*$^{+/Sey}$ females to generate litters consisting of embryos of the genotypes *Pax6*$^{+/+}$, *Pax6*$^{+/Sey}$ and *Pax6*$^{Sey/Sey}$. Embryos were harvested at E9.5 and genotyped by PCR. Chromogenic *in situ* hybridization for *Pax6* and *Barhl2* mRNA was performed on *Pax6*$^{+/+}$ embryos. *In situ* hybridization for *Barhl2* mRNA was also performed on *Pax6*$^{Sey/Sey}$ embryos in order to visualise any changes in its expression which may have occurred as a consequence of the loss of functional *Pax6*. Treated embryos were hemisected and the flat mounts of the dissected tissue were prepared for bright-field imaging.

Finally, the expression of *Barhl2* within the ZLI following its induction was investigated with the use of double fluorescent *in situ* hybridization to visualise the potential co-expression of *Barhl2* with known markers of the ZLI. *Shh* was chosen as a marker of the ZLI itself (Kiecker and Lumsden 2004) while *Ngn2* was chosen as a marker of the more caudal compartment of the ZLI alone (Caballero *et al* 2014). 16µm cryosections cut in the coronal plane were treated with double in *situ* hybridization for *Barhl2* and *Shh*, or for *Barhl2* and *Ngn2* and imaged using fluorescence microscopy.

4.2 Results

4.2.1 *Barhl2* in the *Shh*-null mutant mouse

Barhl2 mRNA was detected in both the *Shh*-null mutant mouse embryo and the wild type littermate. In the wild type littermate expression was detected in the midbrain, thalamus, ZLI, eminentia thalami and lateral ganglionic eminence (Fig.4.1A). It was also detected within the spinal cord (arrow, Fig. 4.1B).

The morphology of the *Shh*-null mutant mouse differs greatly from that of the wild type mouse, with features including a single eye at the ventral midline, situated beneath an abnormally elongated craniofacial structure known as the proboscis (Chiang *et al* 1996) (Fig. 4.1C). While these differences in morphology made it difficult to identify the regions in which *Barhl2* expression was observed, it was possible to identify a region of *Barhl2* expression within the head of the embryo, caudal to the proboscis (dagger, Fig. 4.1C) and in an long and narrow domain running along the dorsal midline of the trunk, corresponding with the position of the spinal cord (arrow, Fig. 4.1D). It was also detected in a region situated ventral to the proboscis, possibly corresponding with the position of the single eye (arrow, Fig. 4.1C).

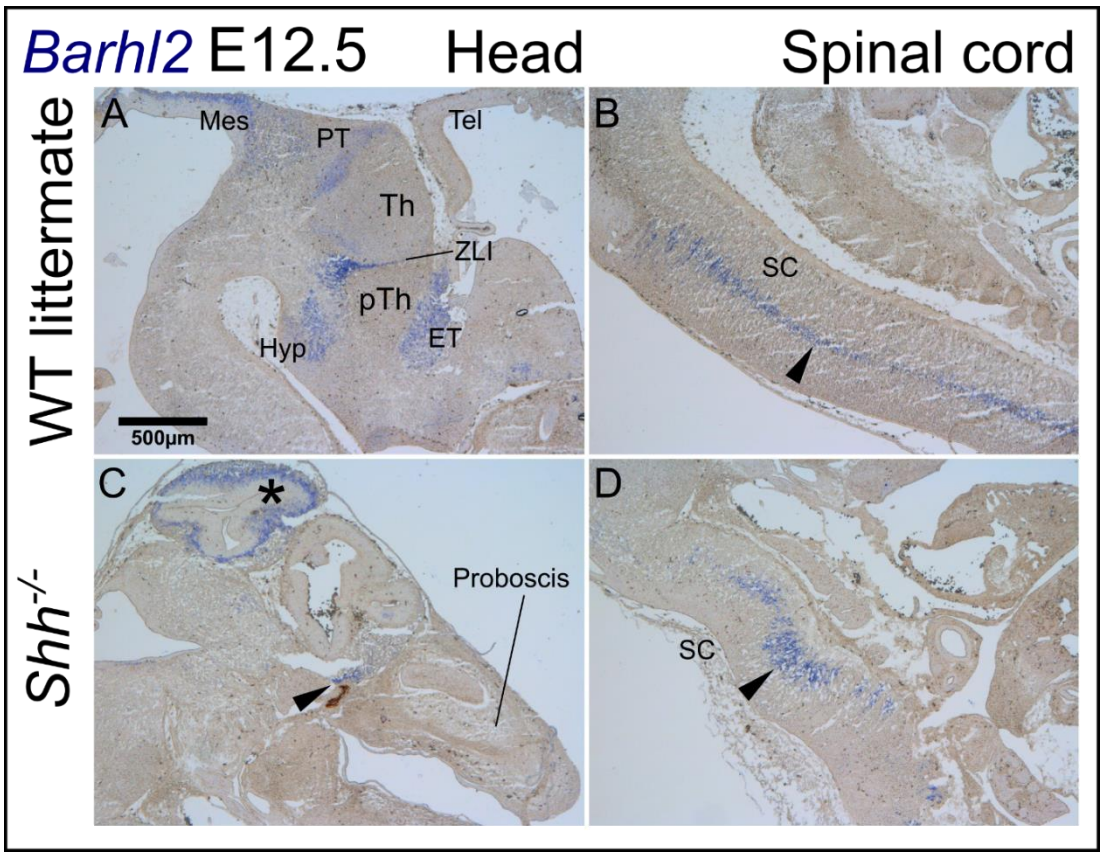

Fig.4.1: Expression of Barhl2 *in sagittal sections of a* Shh*-null mutant embryo and a wild type littermate control, rostral to the right. A:* Barhl2 *expression in the head of the wild type embryo. B:* Barhl2 *expression in the wild type spinal cord (arrow). C: Expression of* Barhl2 *in the head of a* Shh*-null mutant (asterisk), with a region which appears to correspond with the position of the single eye (arrow). D: Expression of* Barhl2 *in the Shh-null mutant spinal cord (arrow). Abbreviations: Mes- mesencephalon; PT- pretectum; Th- thalamus; ZLI-* zona limitans intrathalamica*; pTh- prethalamus; Hyp- hypothalamus; ET-* eminentia thalami*; Tel- telencephalon; SC- spinal cord*

.4.2.2 *Barhl2* expression prior to ZLI formation

Within the *Pax6*$^{+/+}$ embryo at E9.5 (Fig. 4.2) *Barhl2* was found to be expressed in an approximately oval-shaped region of the diencephalon, corresponding with the position of the developing prethalamus (Fig. 4.2B). It was also found to be expressed in a region of neuroepithelium extending from the floorplate, where

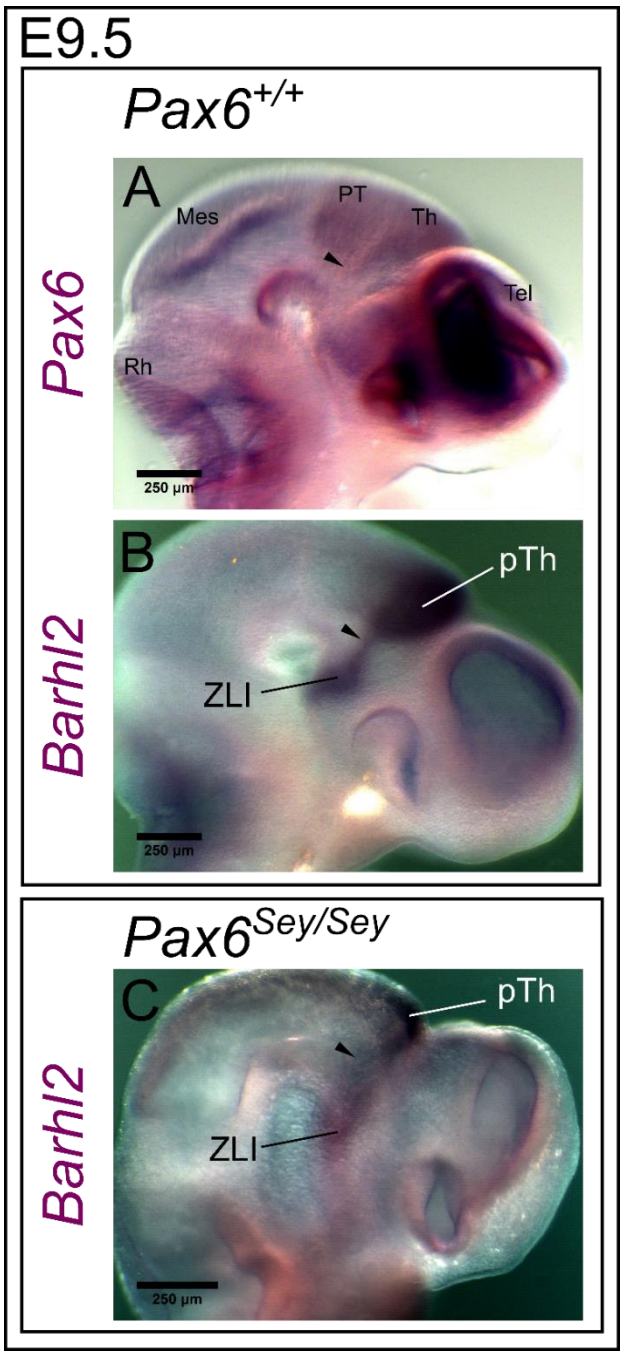

Fig. 4.2: A. Whole mount embryos at E9.5, rostral to right. A. Wild type embryo treated with in situ *hybridization for* Pax6*. A region where the expression level of Pax6 is lower can be seen at the border between the thalamus and pretectum (arrow). B. Wild type embryo treated with* in situ *hybridization for* Barhl2*. The shape of part of the expression domain resembles the shape of the ZLI (arrow). C.* Pax6*-null mutant embryo treated with* in situ *hybridization for* Barhl2*, exhibiting an apparent expansion of the ZLI (arrow). Abbreviations: Tel- telencephalon; Th- thalamus; PT- pretectum; Mes- mesencephalon; Rh- rhombencephalon.*

Barhl2 expression could be seen in a region of neuroepithelium with a broad, bulbous shape corresponding with the position of the presumptive ZLI (Fig. 4.2B), and narrowing as it approached the prethalamus, into a spike shape comparable to that of the ZLI (arrow, Fig. 4.2B). These two differently-shaped regions of expression did not appear to be two separate and discrete domains and instead appeared to make up one single domain of a complex shape. At the same developmental stage expression of *Pax6* was detected throughout the pretectum and thalamus but in a narrow region of neuroepithelium corresponding with the position of the border between these two structures its expression appeared to be weaker (arrow, Fig. 4.2A).

Within the *Pax6*$^{Sey/Sey}$ diencephalon the shape of the *Barhl2* domain also appeared to have been altered from that of the wild type embryo. While the region of strong *Barhl2* expression corresponding with the position of the prethalamus could still be seen (Fig. 4.2C) it was smaller than that observed in the wild type embryo. The more ventral region of the *Barhl2* expression domain corresponding with the position of the presumptive ZLI (, Fig. 4.2C) appeared to have broadened along the rostrocaudal axis, but the expression of *Barhl2* within it also appeared more diffuse, and this region of the expression domain did not narrow as sharply along the dorsoventral axis (arrow, Fig. 4.2C) as the corresponding region of *Barhl2* expression had in the ventral region of the wild type embryo.

4.2.3 *Barhl2* expression within the mature ZLI

Double *in situ* hybridization for *Barhl2* and *Shh* confirmed that *Barhl2* is expressed within the ZLI itself (Fig. 4.3A-D) but not throughout the entire region of neuroepithelium within the ZLI (Fig. 4.3C). Expression of *Barhl2* was confined to a narrow region of the ZLI with its caudal extent corresponding with the caudal extent of the ZLI itself, and its rostral extent located in the medial ZLI (arrow, Fig. 5.4B). A previous study has shown that the ZLI consists of two molecularly distinct subregions- a rostral region which expresses *Developing brain homeobox 1* (*Dbx1*), and a more caudal region marked by the expression of *Ngn2* (Caballero *et al* 2014). Double *in situ* hybridization for *Barhl2* and *Ngn2*

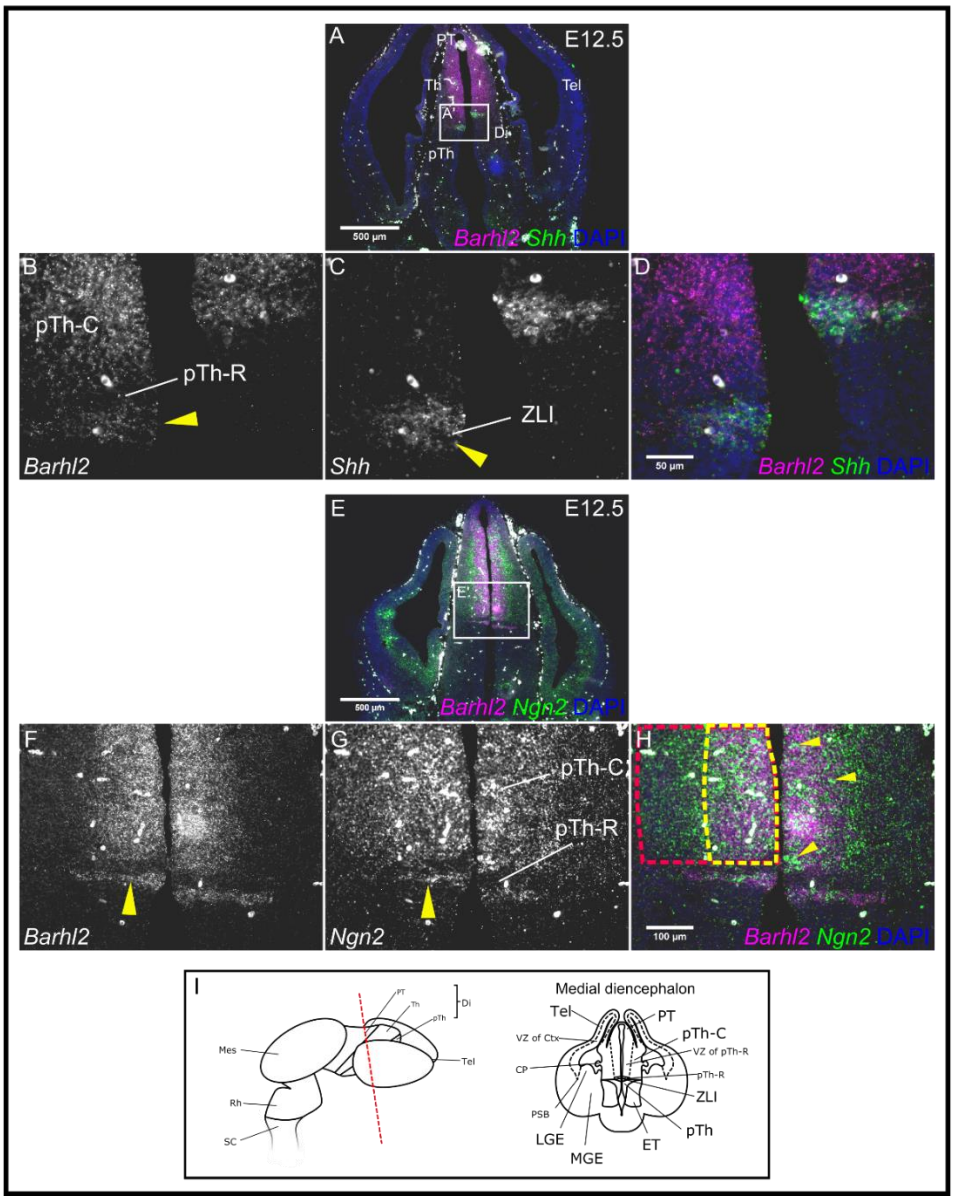

Fig. 4.3: A: Double in situ *hybridization for* Barhl2 *and* Shh*. B-C: The region of neuroepithelium in outlined area A' imaged at high magnification. E: Double* in situ *hybridization for* Barhl2 *and* Ngn2*. F-H: The region of neuroepithelium in outlined area E' imaged at high magnification. I: Schematic to illustrate the approximate plane of section and key to the anatomical features visible in this plane of section. Arrow in B:* Barhl2 *expression in only the most caudal region of the ZLI. Arrow in C:* Shh *expression throughout the entire ZLI. Yellow outlined area in H: The expression domain of* Barhl2 *situated within the broader expression domain of* Ngn2 (area outlined in pink)*. Abbreviations: PT- pretectum; Th- thalamus; pTh- prethalamus; ZLI-* zona limitans intrathalamica*; Tel- telencephalon; Di- diencephalon; Mes- mesencephalon; Rh- rhombencephalon; SC- spinal cord; ET-* eminentia thalami*; PSB- pallial-subpallial boundary; LGE- lateral ganglionic eminence; MGE- medial ganglionic eminence; VZ- ventricular zone; Ctx- cortex; CP- choroid plexus.*

was used to confirm that *Barhl2* was expressed in the more caudal of these regions (arrow, Fig. 4.3F), in a domain corresponding with that of *Ngn2* (arrow, Fig.4.3G).

It was also noted that while *Barhl2* and *Ngn2* were both expressed within the pTh-C and the caudal region of the ZLI, the domain of *Ngn2* within the pTh-C was noticeably broader than that of *Barhl2* in the same region (*Barhl2* domain marked by the outlined area, Fig. 4.2H) and that where the two domains overlapped, the expression of *Barhl2* and *Ngn2* appeared to be complementary, with *Ngn2*-positive regions of neuroepithelium within the *Barhl2* domain appearing to be *Barhl2*-negative (arrows, Fig. 4.2H). Following a repeat of the experiment, with double *in situ* hybridization for *Barhl2* and *Ngn2* being performed on sections from embryos harvested at E11.5 and E12.5, it was observed that at E11.5 the *Barhl2* and *Ngn2* domains within the pTh-C appeared to extend to approximately the same distance from the ventricular surface (arrows, Fig. 4.4A and B) and the *Ngn2* domain only appeared to be broader than that of *Barhl2* by E12.5 (arrows, Fig. 4.4D and E). In the data from this experiment, it was also possible to see a region of weaker *Ngn2* expression within the more medial regions of the pTh-C, corresponding with the domain of *Barhl2* in this area (outlined area, Fig. 4.4E).

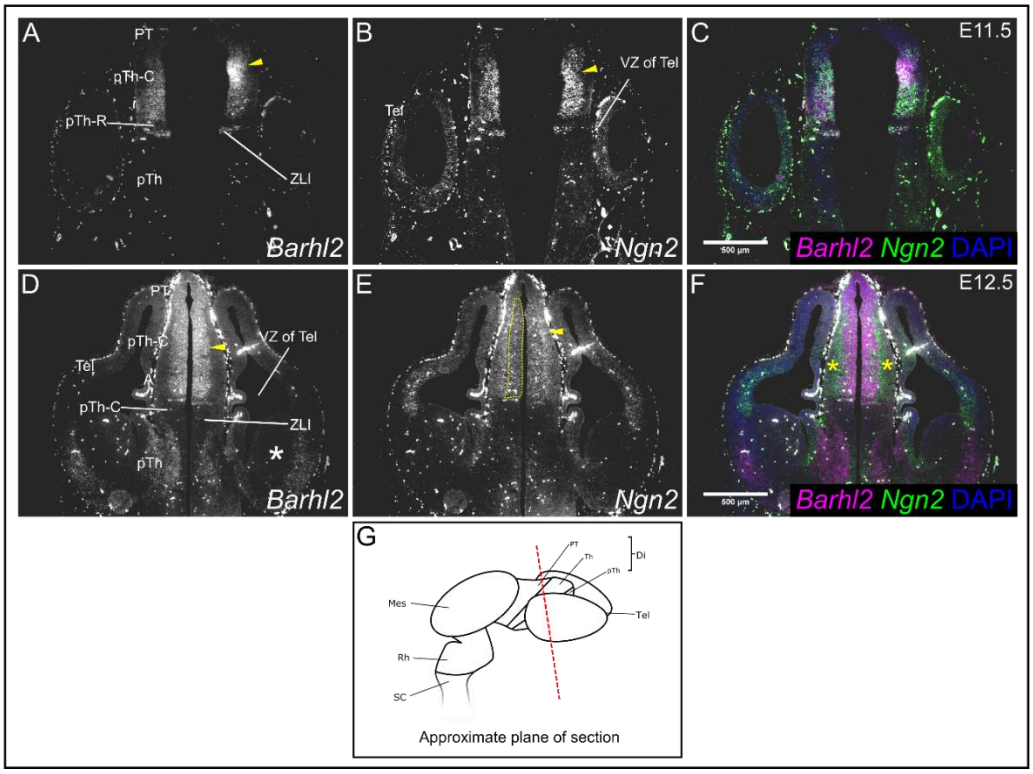

Fig. 4.4: Cryosections from wild type embryos treated with double in situ *hybridization for* Barhl2 *and* Ngn2*. A-C: Sections treated at E11.5. D-F: Sections treated at E12.5. G: Schematic to illustrate the approximate plane of section. Arrows in A and D: The lateral extent of the* Barhl2 *domain. Arrows in B and E: The lateral extent of the* Ngn2 *domain. Asterisks in F: The areas at which the domain of* Ngn2 *extends laterally, beyond the extent of the* Barhl2 *domain. Abbreviations: PT- pretectum; pTh- prethalamus; ZLI-* zona limitans intrathalamica*; ET-* eminentia thalami*; Tel- telencephalon; Di- diencephalon; VZ- ventricular zone; Th- thalamus; Mes- mesencephalon; Rh- rhombencephalon; SC- spinal cord.*

4.3 Discussion

In situ hybridization for *Barhl2* showed that it can be expressed in the complete absence of *Shh* and that *Shh* is therefore not required for the induction of *Barhl2* expression in the mouse embryo. While *Hh* is required to induce *BarH2* (Lim and Choi 2004) in *Drosophila*, this does not appear to be the case with *Shh* and *Barhl2* in mouse. The findings presented here are consistent with earlier reports that *Barhl2* acts upstream of *Shh* in the development of the ZLI in *Xenopus* (Juraver-Geslin *et al* 2014) and together these findings suggest that the relationship between vertebrate *Shh* and *Barhl2* may differ from that which exists between *Hh* and *BarH2* in the

Drosophila retina. They also suggest that in vertebrates *Barhl2* expression is induced independently of *Shh* and that another factor is required for its induction.

In situ hybridization for *Barhl2* has previously been performed on whole embryos at E10.5, and its expression in the presumptive ZLI and thalamus at this stage has been described (Suzuki-Hirano *et al* 2011). E10.5 is the stage at which development of the ZLI begins (Shimamura *et al* 1995). The data presented here show that the expression domain of *Barhl2* is of a comparable shape at E9.5, prior to ZLI development. This suggests the involvement of *Barhl2* in a prepattern which is established prior to the induction of the ZLI, rather than the expression of *Barhl2* in this region being induced by *Shh* from the newly-established ZLI. This finding is also consistent with published data showing that *Barhl2* acts upstream of *Shh* in the establishment of the ZLI (Juraver-Geslin *et al* 2014). It may also be possible that the ZLI and thalamus share a common anlage, of which *Barhl2* expression is a marker.

Double *in situ* hybridization for *Barhl2* and *Shh* confirmed that *Barhl2* continues to be expressed in the mature ZLI, but only within the caudal region marked by the expression of *Ngn2*. The antiproneural action of *Drosophila BarH2* has been documented in the *Drosophila* retina (Higashijima *et al* 1992) and potential antiproneural action of vertebrate *Barhl2* has been speculated on elsewhere on the basis of a FIL domain being present within the *Barhl2* protein (Smith and Jaynes 1996, Muhr *et al* 2001, Bae *et al* 2003). It may be possible that expression of *Barhl2* within the ZLI serves to maintain the neuroepithelium in a non-neural state for the duration of its activity as a signalling centre, but at E12.5 at least this would only be the case in the caudal region of the ZLI, and another factor- potentially *Dbx1*. Another member of the *Dbx* family, *Developing brain homeobox 2* (*Dbx2*), like *Barhl2*, may also possess the capability to repress neurogenesis (Ma *et al* 2011, Lovrics *et a*l 2014) via interactions with *Groucho* (Muhr *et al* 2001). If *Dbx1* shares this property of Dbx2 is may be possible that it could play a role in maintaining the rostral region of the ZLI. Mapping the expression of *Ngn2*, *Dbx1* and *Barhl2* by performing double *in situ* hybridization for each gene with *Shh* at developmental stages between E10.5-E13.5 may be a useful approach to investigating the development of the ZLI and its molecularly distinct subdivisions.

The potential antiproneural activity of vertebrate *Barhl2* could also be considered as a factor controlling the expression of bHLH transcription factors such as *Ngn2* (Saito *et al* 1998) in the modulation of thalamic neurogenesis. The apparent complementary expression of *Barhl2* and *Ngn2* within the developing thalamus was only investigated briefly in the experiments described here. Further investigations would be required to confirm the complementarity of the two genes' expression and could potentially provide additional evidence to suggest that *Barhl2* is an antiproneural factor which acts to suppress the transcription of proneural bHLH transcription factors in the vertebrate thalamus.

The apparent change in the degree of overlap between the *Barhl2* and *Ngn2* may suggest the possibility that a wave of thalamic neurogenesis patterns the developing thalamus, modulated by the repression of *Ngn2* expression by *Barhl2*. Such a mechanism would be comparable to that observed in *Drosophila*, in which *BarH2* serves to modulate the patterning of the retina, suppressing neurogenesis via the inhibition of *ato* expression (Lim and Choi 2003). In order to investigate this possibility further it would be necessary to map the expression of *Barhl2* in relation to that of *Ngn2* over a series of developmental stages over the course of thalamic development.

While *Shh* is the most extensively studied of all the morphogens secreted by the ZLI, the ZLI is also known to secrete the *Wnt* family morphogen *Wnt8b* (Garda *et al* 2002). *Barhl2* has been shown to indirectly inhibit the activity of β-catenin, a component of the canonical *Wnt* signalling pathway, and in turn the proliferative cell division normally induced by canonical *Wnt* signalling. This mechanism has been demonstrated in the *Xenopus* neural plate as a means of inhibiting neural plate expansion (Juraver-Geslin *et al* 2011) but it is not known if a comparable interaction exists between *Barhl2* in the diencephalon and Wnt8b protein secreted by the ZLI, or if such an interaction may play a role in diencephalic development.

5. *Barhl2* expression in the *Pax6*$^{Sey/Sey}$ and *Pax6*$^{Sey/+}$ forebrain

5.1 Introduction

In order to investigate the possibility of interactions between *Pax6* and *Barhl2*, a *Pax6* loss-of-function approach was taken. *In situ* hybridization was used to visualise the expression of *Barhl2* in the forebrain of a *Pax6-null* mouse mutant strain and the *Barhl2* expression data were compared with the data for its expression in the wild type mouse forebrain. In *situ* hybridization for *Barhl2* mRNA was also performed on cryosections from an E12.5 *Pax6*$^{+/Sey}$ forebrain. Image data for treated sections were compared with image data for the expression of *Barhl2* in the E12.5 *Pax6*$^{+/+}$ forebrain of a wild type CD-1® embryo in a qualitative analysis.

Pax6-null mice used were of a *Small-eye (Sey*) strain maintained on a CD-1® (Charles River Laboratories, Inc.2011) background. The mice carry a mutant *Pax6* allele named *Sey*^{Ed} which arose from a spontaneous mutation causing a single base pair change. The mutation led to the addition of a second stop codon at a point before the region which encodes to homeobox. This allele encodes a truncated, non-functioning form of the *Pax6* protein (Hill et al 1991). Mice carrying two wild-type *Pax6* alleles are termed *Pax6*$^{+/+}$, homozygous *Sey* mutants are referred to as *Pax6*$^{Sey/Sey}$ while heterozygous mutants are known as *Pax6*$^{+/Sey}$.

Pax6$^{+/Sey}$ males were crossed with *Pax6*$^{+/Sey}$ females in order to generate litters consisting of *Pax6*$^{+/+}$, *Pax6*$^{+/Sey}$ and *Pax6*$^{Sey/Sey}$ embryos. Litters were harvested at E8.5, E9.5, E10.5, E11.5, E12.5 and E13.5. Embryos harvested at E10.5 or earlier were genotyped by PCR while *Pax6*$^{Sey/Sey}$ embryos harvested at E11.5 and later identified by the absence of eyes. The genotype of the E12.5 *Pax6*$^{+/Sey}$ embryo was also determined via PCR. Embryos were fixed and cryosectioned in the coronal plane. Tissue sections were treated with chromogenic *in situ* hybridization with the *Barhl2* riboprobe in order to visualise *Barhl2* mRNA.

5.2 Results

5.2.1 *Barhl2* expression in the *Pax6*$^{Sey/Sey}$ forebrain

The morphology of the *Pax6*$^{Sey/Sey}$ mouse embryo is markedly different from that of the *Pax6*$^{+/+}$ mouse embryo and for this reason it can be difficult to make valid comparisons between sections from embryos of each of these genotypes. The figures in this chapter each feature an image of a section cut from a *Pax6*$^{+/+}$ embryo presented alongside an image of a section from the *Pax6*$^{Sey/Sey}$ forebrain in which comparable features can be identified. Each figure also includes a key with a schematic of the wild type embryonic forebrain on which the approximate plane of section is detailed.

Deletion of *Pax6* results in a number of changes in forebrain morphology, including a marked reduction in the size of the forebrain overall (Quinn *et al* 2007) and a reduction in the thickness of the neuroepithelium (Jones *et al* 2002, Quinn *et al* 2007). The data presented here show that these features are apparent in all developmental stages analysed and manifest as early as E8.5 (Fig. 5.1) The lumen of the diencephalon is also broader in the *Pax6*-null mouse mutant (Schmahl *et al* 1993) and in the data presented here this broadening is evident from E11.5 (Fig. 5.4F-H).

At E.8.5 (Fig. 5.1) the *Pax6*$^{Sey/Sey}$ embryo is smaller than that of the wild type embryo and the neuroepithelium is thinner but in all other respects the morphology of the *Pax6*$^{Sey/Sey}$ embryo at E8.5 broadly resembles that of the wild-type embryo at the same developmental stage. The edges of the neural plate have yet to fuse along the entire length of the neural tube and the neural tube remains open along the rostrocaudal extent of the forebrain (arrows, Fig. 5.1A). In the *Pax6*-null mutant the neural tube also appears to be open at its ventral extent (asterisk, Fig. 5.1G) but this could be a result of damage to the tissue. In coronal sections cut from the wild type embryo at this stage the telencephalon is visible as two vesicles lateral to the diencephalon (Fig. 5.1C) and this also appears to be the case with the *Pax6*$^{Sey/Sey}$ mutant embryo (Fig. 5.1H).

Barhl2 expression appeared to be absent from the telencephalon in both the wild type and the mutant (Fig. 5.1E and J) but was detected in all of the more caudal sections analysed (Fig. 5.1A-D and F-I).

At this stage *Barhl2* expression only appeared to be noticeably altered in more caudal sections of the diencephalon. In the more caudal sections from the wild type embryo *Barhl2* was found to be expressed throughout the majority of the neuroepithelium (Fig. 5.1A and B), with the exception of the floorplate in which little to no expression detected in the floorplate (Fig. 5.1A and B). In the mutant the *Barhl2* domain appeared to have narrowed along the dorsoventral axis (arrows, Fig. 5.1F and G). In more rostral sections the *Barhl2* domain appeared to extend along a similar proportion of the neuroepithelium along its dorsoventral extent in both the mutant and the wild type diencephalon (Fig. 5.1 C-D and H-I).

At E9.5 (Fig. 5.2) the reduction in forebrain size is apparent in the *Pax6*$^{Sey/Sey}$ embryo but appears as an overall narrowing of the forebrain along the mediolateral axis. Notably the lumen of the diencephalon does not appear to have undergone an expansion at this stage and the *Pax6*$^{Sey/Sey}$ diencephalon appears to be narrower than that of the wild type diencephalon (Fig. 5.2F-H). The neuroepithelium also does not appear to be noticeably thinner in the mutant at this stage. As with the wild-type embryo, neural tube closure in the mutant is complete by this stage and the edges of the neural plate have fused to form the roofplate (Fig. 5.2A and F) while in the mutant embryo the floorplate is continuous and unbroken (Fig. 5.2F). As at E8.5, *Barhl2* expression could not be detected within the telencephalon at this stage (Fig. 5.2E and I-J)

At this stage the *Barhl2* domain appears to extend along a similar proportion of the rostrocaudal axis, with *Barhl2* expression detected in more caudal sections (Fig. 5.2 A-C and F-H) but not within the telencephalon (Fig. 5.1E and J). In more caudal sections of the diencephalon *Barhl2* expression was detected in discrete domains with clearly defined borders (arrows, Fig. 5.2A-C). In the mutant *Barhl2* expression appeared to be more diffuse. In the mutant diencephalon strong expression of *Barhl2* was detected in regions of a comparable position to the *Barhl2* expression domains

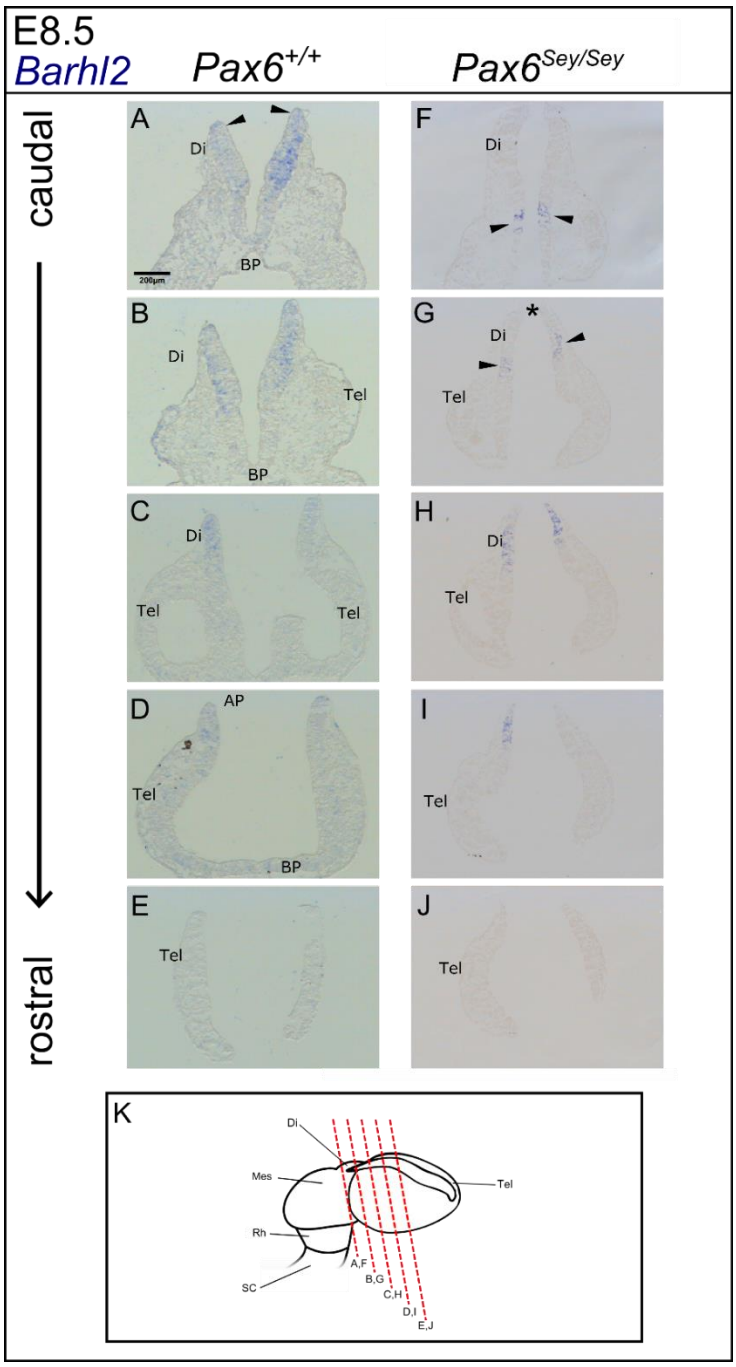

Fig. 5.1: A-J. In situ *hubridization data for* Barhl2 *mRNA in the* Pax6$^{+/+}$ *and* Pax6$^{Sey/Sey}$ *forebrain at E8.5. K. Schematic to illustrate the approximate plane of each section. Arrows in A: The edges of the neural plate, which have yet to fuse to form the roofplate. Asterisk in G: The dorsal neural tube also remains open in the* Pax6$^{Sey/Sey}$ *embryo. Arrows in F and G: The Barhl2 domain appears to have narrowed along the dorsoventral axis in the* Pax6$^{Sey/Sey}$ *diencephalon. Abbreviations: Tel- telencephalon; Di- diencephalon; Mes- mesencephalon; Rh- rhombencephalon; SC- spinal cord; FP- floorplate; AP- alar plate; BP- basal plate.*

in the the wild type diencephalon, but these regions of *Barhl2* expression appeared to span a greater proportion of the diencephalic neuroepithelium along the dorsoventral axis and their borders were not as well defined (arrows, Fig. 5.1F-H).

At E10.5 (Fig. 5.3) the neuroepithelium appeared thinner in the mutant than in the wild type and the telencephalic vesicles were greatly reduced in size (asterisks, Fig. 5.3B and G). The lumen of the diencephalon had broadened along the mediolateral axis but the morphology in this particular embryo resembled that of hydrocephalic embryos and in this case the expansion of the lumen may not have been caused by the loss of *Pax6*.

In the *Pax6*+/+ embryo at E10.5 the domains of *Barhl2* within the ZLI were apparent, separated from the domain within the pTh-C and pretectum by the *Barhl2*-negative pTh-R (arrows, Fig. 5.3A) but a comparable expression pattern could not be seen in the $Pax6^{Sey/Sey}$ embryo. In the mutant *Barhl2* was found to be expressed in a continuous domain within the neuroepithelium of the dorsal diencephalon (asterisks, Fig. 5.1G-H).

Barhl2 expression in the mutant appeared to be confined to a smaller area of neuroepithelium than in the wild-type, in a domain corresponding with the position of the pretectum and a more dorsal region of the thalamus (asterisk, Fig. 5.3G), rather than with the position of the pretectum and the entire pTh-C (asterisk, Fig. 5.3B).

In the wild type embryo *Barhl2* expression was detected in two domains rostral to the developing ZLI (arrows, Fig. 5.3D) while in the mutant *Barhl2* expression was restricted to more dorsal regions of the diencephalon and no expression was detected in rostral regions of the diencephalic neuroepithelium (Fig. 5.3A-J).

As with earlier developmental stages, no *Barhl2* expression could be detected in the telencephalon of both the wild type and the mutant (Fig. 5.3E and J).

In the $Pax6^{Sey/Sey}$ mutant at E11.5 (Fig. 5.4F-J) the neuroepithelium appeared to be reduced in thickness throughout all areas of the forebrain in comparison with that of

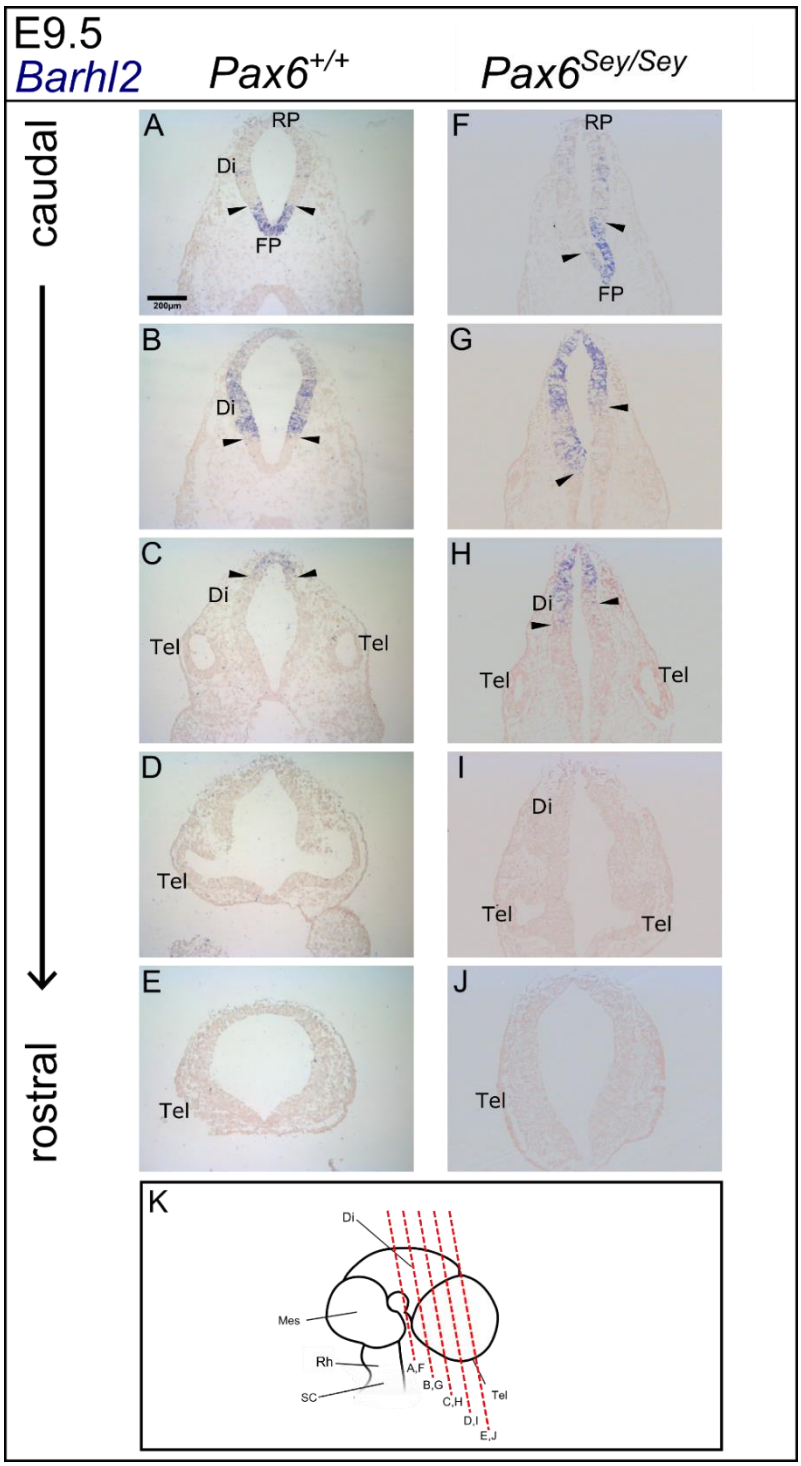

Fig. 5.2: A-J. In situ *hubridization data for* Barhl2 *mRNA in the* Pax6$^{+/+}$ *and* Pax6$^{Sey/Sey}$ *forebrain at E9.5. K. Schematic to illustrate the approximate plane of each section. Arrows in A and F: The caudal extent of the* Barhl2 *domains. Arrows in B, C, G and H: The rostral extent of the* Barhl2 *domain in these sections. Abbreviations: Tel- telencephalon; Di- diencephalon; Mes- mesencephalon; Rh- rhombencephalon; SC- spinal cord; RP- roofplate; FP- floorplate.*

the wild type forebrain (Fig. 5.4A-E). The reduction in overall forebrain size was also apparent, with the telencephalic vesicles being affected to a particularly great extent (asterisks, Fig. 5.4C and H). The lumen of the diencephalon was also noticeably broader along the mediolateral axis than that of the wild type diencephalon (asterisks, Fig. 5.4A and F). The medial ganglionic eminence (MGE) and lateral ganglionic eminence (LGE) could be seen to be developing in the wild type telencephalon (asterisks, Fig.5.4E) but could not be clearly distinguished in the mutant telencephalon (asterisks, Fig. 5.5J).

By this stage the *Barhl2*-positive region of the ZLI could be visualised in both the wild type and mutant embryos. In the wild-type it appeared as a narrow wedge-shaped region (arrows, Fig. 5.4A). An expansion of the ZLI has previously been described in the *Pax6*-null mutant (Grindley *et al* 1997, Pratt *et al* 2000a) and in the embryo analysed here a region of strong *Barhl2* expression of a shape and position comparable to that of the expanded ZLI could be visualised in more caudal sections of the diencephalon (Fig. 5.4F). This expression domain was distinct from a more dorsal domain of *Barhl2* expression which could be seen to span almost the dorsoventral extent of the thalamus, corresponding with the position of the pTh-C (Fig. 5.4F). This region appeared to occupy a smaller proportion of the diencephalic neuroepithelium in the mutant, with the pTh-C domain in the wild type embryo extending further along the dorsoventral axis (Fig. 5.4C and H). A *Barhl2*-negative region between the two domains appeared to correspond with the position of the pTh-R (arrows, Fig. 5.4F) although the borders of this *Barhl2*-negative region were irregular and not as clearly defined as the borders of the pTh-R in the wild type diencephalon (Fig. 5.4C).

In more rostral sections a region of strong *Barhl2* expression could also be seen in a region corresponding with the position of the expanded ZLI, along with a region of slightly weaker expression spanning the dorsoventral extent of the thalamus, but these regions with differing levels of *Barhl2* expression were not as distinct as they appeared in more caudal sections and were not separated from each other by a *Barhl2*-negative region of neuroepithelium corresponding with the position of the pTh-R (arrows, Fig. 5.4G and H).

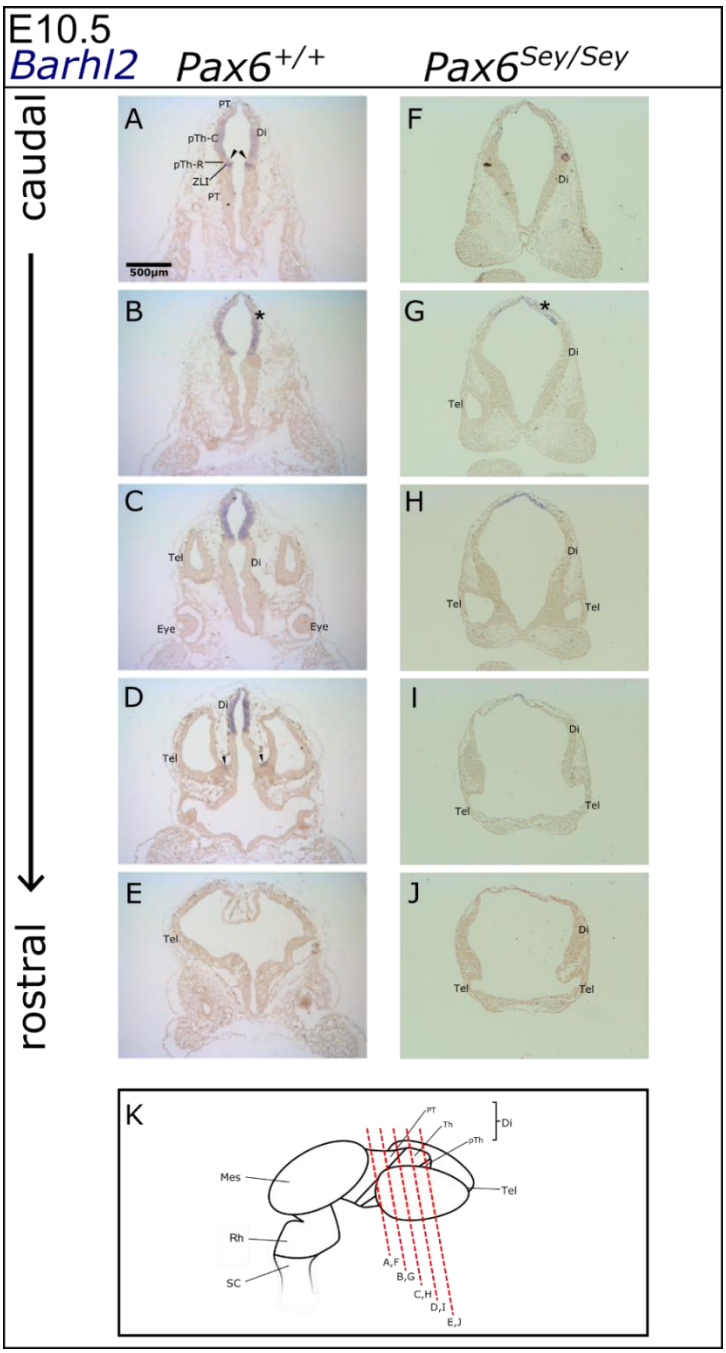

Fig. 5.3: A-J. In situ *hubridization data for* Barhl2 *mRNA in the* Pax6$^{+/+}$ *and* Pax6$^{Sey/Sey}$ *forebrain at E10.5. K. Schematic to illustrate the approximate plane of each section. Arrows in A: The* Pax6*-negative pTh-R. Asterisks in B and G: The neuroepithelium is reduced in thickness in the* Pax6$^{Sey/Sey}$ *embryo. Arrows in D: The Pax6-negative* eminentia thalami*. Asterisks in B and C: The neuroepithelium could be seen to be reduced in thickness in the mutant at this stage. Abbreviations: Tel- telencephalon; Di- diencephalon; Mes- mesencephalon; Rh- rhombencephalon; SC- spinal cord; PT- pretectum; Th- thalamus; pTh- prethalamus.*

In the *Pax6*$^{+/+}$ diencephalon the domain of *Barhl2* within the pTh-C was restricted to the ventricular zone (outlined area, Fig. 5.4C) while in the *Pax6*$^{Sey/Sey}$ mutant the thalamic *Barhl2* domain appeared to have expanded laterally and spanned the mediolateral extent of the thalamic neuroepithelium (outlined area, Fig. 5.4H).

In regions of forebrain neuroepithelium rostral to the ZLI, loss of *Pax6* appeared to have led to a downregulation of *Barhl2* expression. While *Barhl2* expression could be detected in the *eminentia thalami* of the wild type diencephalon (Fig. 5.4D), no expression of *Barhl2* could be detected rostral to the ZLI in the mutant diencephalon (asterisks, Fig. 5.4I). Within the telencephalon the *Barhl2* domain within the subpallium of the mutant appeared to be greatly reduced in size (arrows, Fig. 5.4J) compared with the subpallial *Barhl2* domain in the wild type embryo (arrows, Fig 5.4E). In the mutant this domain was also greatly altered in shape and instead of extending towards the PSB (Fig. 5.4E) the *Barhl2* domain in the mutant appeared to have adopted a narrow crescent shape at a position immediately adjacent to the pial surface of the subpallium (Fig. 5.4J).

At E12.5 (Fig. 5.5) the forebrain of the mutant appeared to be considerably smaller in size overall (Fig. 5.4 F-J) than that of the wild type (Fig. 5.4 A-E). The telencephalon of the mutant (Fig. 5.5 H) was considerably smaller than that of the wild type forebrain (Fig. 5.5C) and by this stage the subpallium appeared to be markedly underdeveloped, and while the LGE and MGE of the mutant could be distinguished as discrete structures (Fig. 5.5J) they appeared to be less distinct and smaller in size compared to the same structures in the wild type subpallium (Fig. 5.5E). The lateral expansion of the diencephalic lumen was particularly noticeable in more rostral sections (asterisk, Fig. 5.5G) while at this stage the ventricular surfaces of the wild type diencephalon were in contact at most points along their dorsoventral extents and the lumen of the diencephalon was almost completely closed (asterisk, Fig. 5.5B).

In more caudal sections of the *Pax6*-null mutant diencephalon *Barhl2* expression appeared to have been upregulated. *Barhl2* expression appeared to be relatively weak in caudal sections from the wild type diencephalon (Fig. 5.5A) while in the mutant

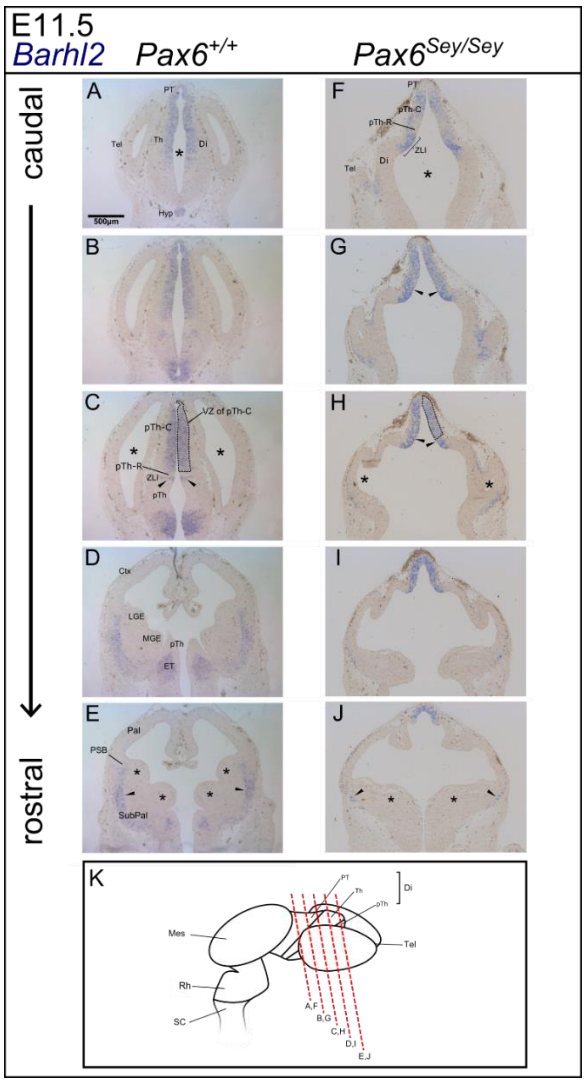

Fig. 5.4: A-J. In situ *hubridization data for* Barhl2 *mRNA in the* Pax6$^{+/+}$ *and* Pax6$^{Sey/Sey}$ *forebrain at E11.5. K. Schematic to illustrate the approximate plane of each section. Asterisks in A and B: The lumen of the diencehaphalon, which expands laterally in the* Pax6$^{Sey/Sey}$ *mutant. Asterisks in C and H: The telencephalic vesicles are greatly reduced in size in the* Pax6$^{Sey/Sey}$ *mutant. Outlined areas in C and H: The domain of* Barhl2 *expands beyond the ventricular zone of the pTh-C in the* Pax6$^{Sey/Sey}$ *mutant*. Arrows *in C and H: The domain of* Barhl2 *within the ZLi is greatly expanded in the* Pax6$^{Sey/Sey}$ *mutant. Asterisks in E and J: The ganglionic eminences are smaller and less clearly defined in the* Pax6$^{Sey/Sey}$ *mutant. Arrows in G: The pTh-R is narrower and less well defined. Abbreviations: Tel- telencephalon; Di- diencephalon; Mes- mesencephalon; Rh- rhombencephalon; SC- spinal cord; PT- pretectum; Th- thalamus; pTh- prethalamus; VZ- ventricular zone; Pal- pallium; SubPal- subpallium; PSB- pallial-subpallial boundary; LGE- lateral ganglionic eminence; MGE- medial ganglionic eminence; Hyp- hypothalamus; ET-* eminentia thalami; *ZLI-* zona limitans intrathalamica*.*

stronger expression of *Barhl2* was detected in both the thalamus and hypothalamus (Fig. 5.5F). While *Barhl2* expression was detected within the pretectum of the mutant, a small, circular *Barhl2*-negative region was also observed close to the dorsal midline (Fig. 5.5F) and this was also present in the wild-type pretectum although the weaker *Barhl2* expression in the surrounding areas of the pretectum made this more difficult to distinguish (Fig. 5.5A).

In the mutant diencephalon at E11.5 the domain of *Barhl2* within the pTh-R appeared to have expanded laterally, beyond the thalamic ventricular zone (outlined area, Fig. 5.4H). This expansion was even more pronounced in the mutant at E12.5, with the *Barhl2* domain appearing to span the entire mediolateral extent of the neuroepithelium (outlined area, Fig. 5.5G) while in the wild type diencephalon *Barhl2* expression was restricted to a narrow area immediately adjacent to the ventricular surface, with its lateral extent corresponding with the border of the ventricular zone (outlined area, Fig. 5.5B). As at earlier stages, the pTh-C of the mutant did not extend across as great a proportion of the dorsoventral axis less far as the same structure did in the wild type diencephalon (outlined areas, Fig. 5.5B and C).

As in the *Pax6*$^{Sey/Sey}$ diencephalon at E11.5, strong *Barhl2* expression was detected in a region corresponding with the position of the expanded ZLI (Fig. 5.5G). By this stage it appeared to be more distinct from the *Barhl2* domain within the pTh-C and the pTh-R was more easily distinguished as a region of *Barhl2*-negative neuroepithelium (Fig. 5.5H-I) although this was still more irregular in shape and with less clearly defined borders than that of the wild type pTh-R (Fig. 5.5C).

As at E11.5, this *Barhl2*-negative region immediately adjacent to the caudal extent of the ZLI was more easily distinguished in more rostral sections (arrows, Fig. 5.5H and I) while it could not be distinguished in more caudal sections (arrows, Fig. 5.5G) In these more caudal sections the domain of *Barhl2* within the thalamus appeared to be immediately adjacent to that within the ZLI, although the ZLI could be distinguished by its stronger expression of *Barhl2* (Fig. 5.5G).

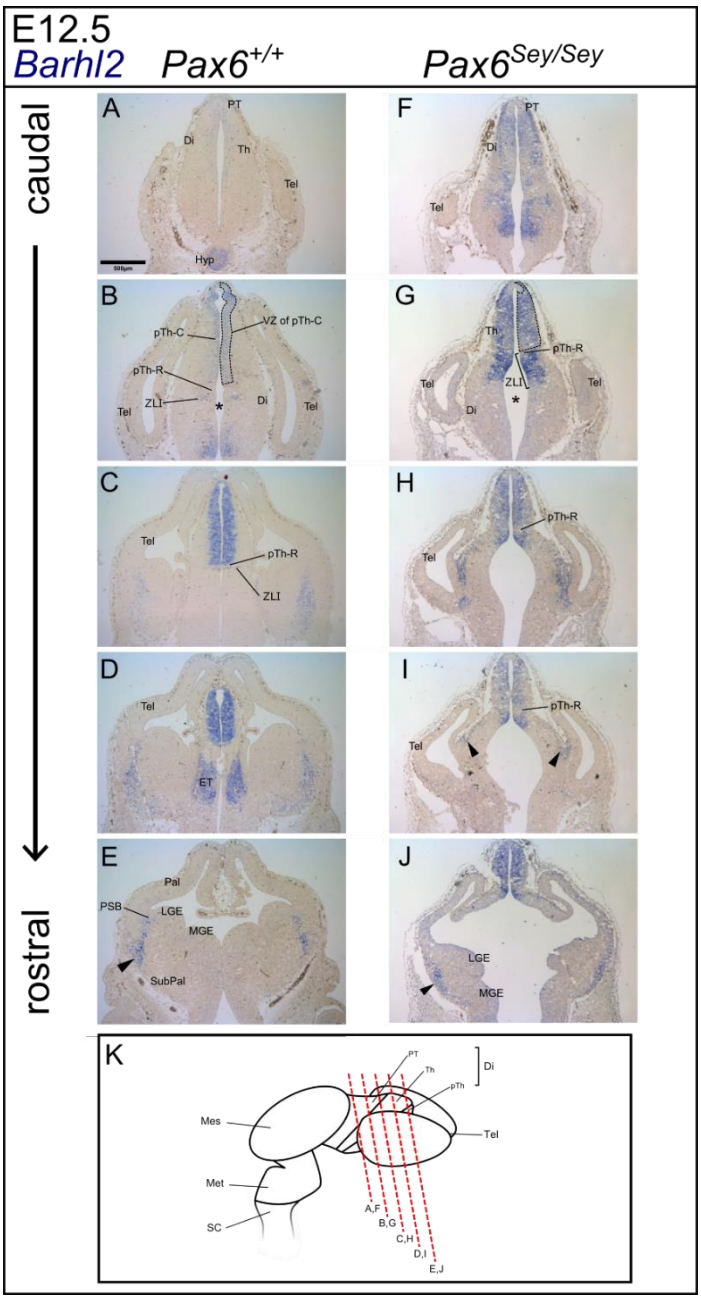

Fig. 5.5: A-J. In situ *hubridization data for* Barhl2 *mRNA in the* Pax6$^{+/+}$ *and* Pax6$^{Sey/Sey}$ *forebrain at E12.5. K. Schematic to illustrate the approximate plane of each section. Asterisks in B and G: The lumen was seen to have expanded in the mutant diencephalon. Arrows in I: Altered* Barhl2 *expression in the neuroepithelium lateral to the* eminentia thalami. Arrows in E and J: *Altered* Barhl2 *expression in the* subpallium. *Abbreviations: Tel- telencephalon; Di- diencephalon; Mes- mesencephalon; Rh- rhombencephalon; SC- spinal cord; PT- pretectum; Th- thalamus; pTh- prethalamus; VZ- ventricular zone; Pal- pallium; SubPal- subpallium; PSB- pallial-subpallial boundary; LGE- lateral ganglionic eminence; MGE- medial ganglionic eminence; Hyp- hypothalamus; ET-* eminentia thalami; *ZLI-* zona limitans intrathalamica.

Where the pTh-R could be visualised by the absence of *Barhl2* expression in the mutant, it appeared to have expanded along with the ZLI (Fig. 5.5H and I) and the pTh-R also spanned a greater proportion of the neuroepithelium than the relatively narrow pThR of the wild type diencephalon (Fig. 5.5C).

Rostral to the ZLI, the domain of *Barhl2* within the *eminentia thalami* was observed in the wild type diencephalon (Fig. 5.5D) but no *Barhl2* expression was observed in this region of the mutant diencephalon and instead a smaller domain of *Barhl2* could be seen close to the pial surface of the diencephalon, and lateral to the region where the *eminentia thalami* could be expected to be seen (arrows, Fig. 5.5I).

Within the telencephalon of the *Pax6*$^{Sey/Sey}$ mutant *Barhl2* expression was detected within the subpallium but, as in the mutant at E11.5 (arrows, Fig.5.4J) its size and shape were altered and it could be seen as a narrow crescent shape immediately adjacent to the pial surface (arrow, Fig.5.5J) rather than as a region of *Barhl2* expression located more medially and extending dorsally towards the PSB (arrow, Fig. 5.5E).

Between E12.5 and E13.5 a period of rapid growth occurs and the wild type mouse embryo greatly increases in size, and by E13.5 (Fig. 5.6) the *Pax6*$^{+/+}$ forebrain as a whole is much greater in size than that of the *Pax6*$^{Sey/Sey}$ embryo. The data for each section from the wild type embryo is presented as two images- one image detailing the pretectum and more dorsal regions of the diencephalon (Fig. 5.6A-E) and a second image detailing the more ventral regions of the diencephalon, including more ventral regions of the pTh-C, the pTh-R, the ZLI and the prethalamus (Fig. 5.6F-J). The smaller size of the mutant embryo allowed for image data to be presented as a single image for each section (Fig. 5.6K-O).

At E13.5 the lumen of the diencephalon still appeared to be broader in the mutant (asterisk, Fig. 5.6N) thank in the wild type (asterisk, Fig. 5.6N), in which the ventricular surfaces of the left and right-hand sides of the diencephalon were in contact with each other at most points along their dorsoventral extents (asterisk, Fig. 5.6I).

At E13.5 *Barhl2* continued to be expressed throughout the pTh-C of the wild type thalamus (Fig. 5.6A-E) and was restricted to an area corresponding with the thalamic ventricular zone (outlined area, Fig. 5.6A). In the mutant at E13.5 this expression domain was found to have expanded laterally and spanned the mediolateral extent of the diencephalic neuroepithelium (outlined area, Fig. 5.6K). The pTh-C of the mutant also appeared to occupy a smaller proportion of the diencephalic neuroepithelium in the mutant than it did in the wild type embryo (Fig. 5.6A and K).

Within the pretectum of both the *Pax6*$^{+/+}$ embryo and the *Pax6*$^{Sey/Sey}$ embryo a small, circular *Barhl2*-negative region was observed within the pretectum (Fig. 5.6A and K), similar in shape and position to the *Barhl2*-negative region observed in embryos of both genotypes at E12.5 (Fig. 5.5A).

While the *Barhl2* domain of the mutant pTh-C could be seen to have expanded along the mediolateral axis, expression of *Barhl2* in this region also appeared to be more diffuse and weaker than at previous stages (Fig. 5.6 M), and in comparison with the expression of *Barhl2* in the pTh-C of the wild type embryo (Fig. 5.6C).

In the wild type embryo at E13.5 the ZLI appeared narrower than it had at stages E10.5-E11.5 (Fig. 5.6G) while expression of *Barhl2* within the ZLI remained visible as a relatively broad expression domain (Fig. 5.6M) separated from the pTh-C by the *Barhl2*-negative pTh-R (Fig. 5.6M-O). In comparison with the expression of *Barhl2* in the mutant ZLI at earlier developmental stages, expression of *Barhl2* within the ZLI of the mutant at E13.5 seemed relatively weak (Fig. 5.6M).

At E13.5 low levels of *Barhl2* expression could still be detected within the *eminentia thalami* of the wild type embryo (Fig. 5.6H) but none could be visualised within the region of diencephalon rostral to the ZLI in the diencephalon of the mutant (arrows, Fig. 5.6M).

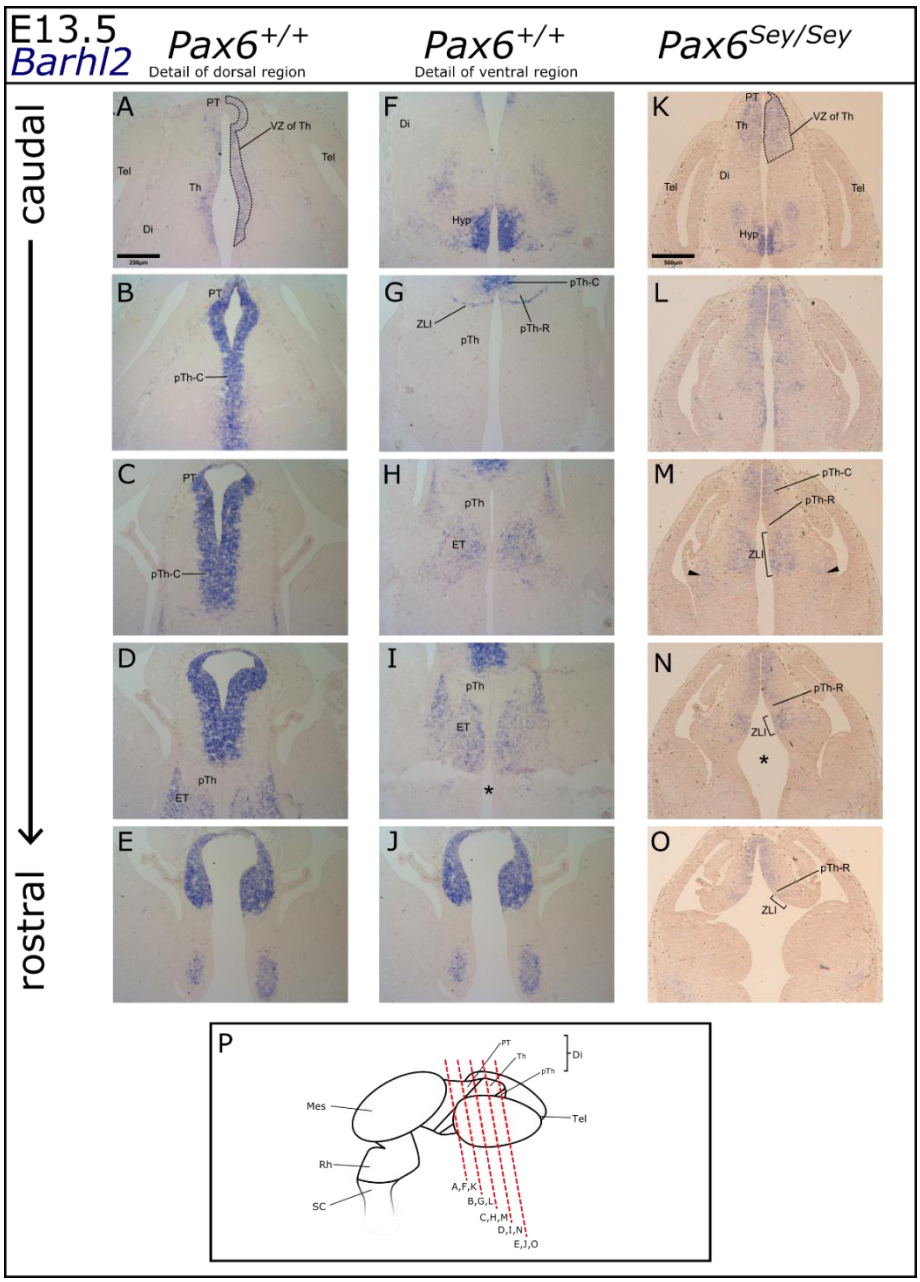

Fig. 5.6: A-O. In situ *hubridization data for* Barhl2 *mRNA in the* Pax6$^{+/+}$ *and* Pax6$^{Sey/Sey}$ *forebrain at E13.5. P. Schematic to illustrate the approximate plane of each section. Outlined areas in A and K: The* Barhl2 *domains expands laterally in the thalamus of the mutant. Asterisks in I and N: A lateral expansion of the diencephalic lumen was observed in the mutant forebrain. Arrows in M: Altered expression of* Barhl2 *in the neuroepithelium lateral to the* eminentia thalami*. Abbreviations: Tel- telencephalon; Di- diencephalon; Mes- mesencephalon; Rh- rhombencephalon; SC- spinal cord; PT- pretectum; Th- thalamus; pTh- prethalamus; VZ- ventricular zone; Pal- pallium; SubPal- subpallium; PSB- pallial-subpallial boundary; LGE- lateral ganglionic eminence; MGE- medial ganglionic eminence; Hyp- hypothalamus; ET-* eminentia thalami; *ZLI-* zona limitans intrathalamica*.*

5.2.2 *Barhl2* expression in the *Pax6*$^{+/Sey}$ forebrain

As in the E12.5 *Pax6*$^{+/+}$ forebrain (Fig. 3.2.5), expression of *Barhl2* mRNA in the E12.5 *Pax6*$^{+/Sey}$ forebrain was found to be strong in the hypothalamus (Fig. 5.7A and F), *eminentia thalami* (Fig. 5.7D and I), the ZLI (Fig. 5.7C and H) the pretectum and ventricular zone of the pTh-C (Fig. 5.7B and G) and a region of the ventral telencephalon extending ventrally from the subpallium towards to pallial-subpallial boundary (Fig. 5.7E and J). In embryos of both genotypes *Barhl2* expression could not be detected in the pTh-R (Fig. 5.7C and H), prethalamus (Fig. 5.7D and I), dorsal telencephalon (Fig. 5.7E and J), and lateral to the ventricular zone of the pTh-C (Fig. 5.7C and H).

The expression of *Barhl2* mRNA in the *Pax6*$^{+/+}$ and *Pax6*$^{+/Sey}$ forebrains appeared to be similar and no major differences were apparent.

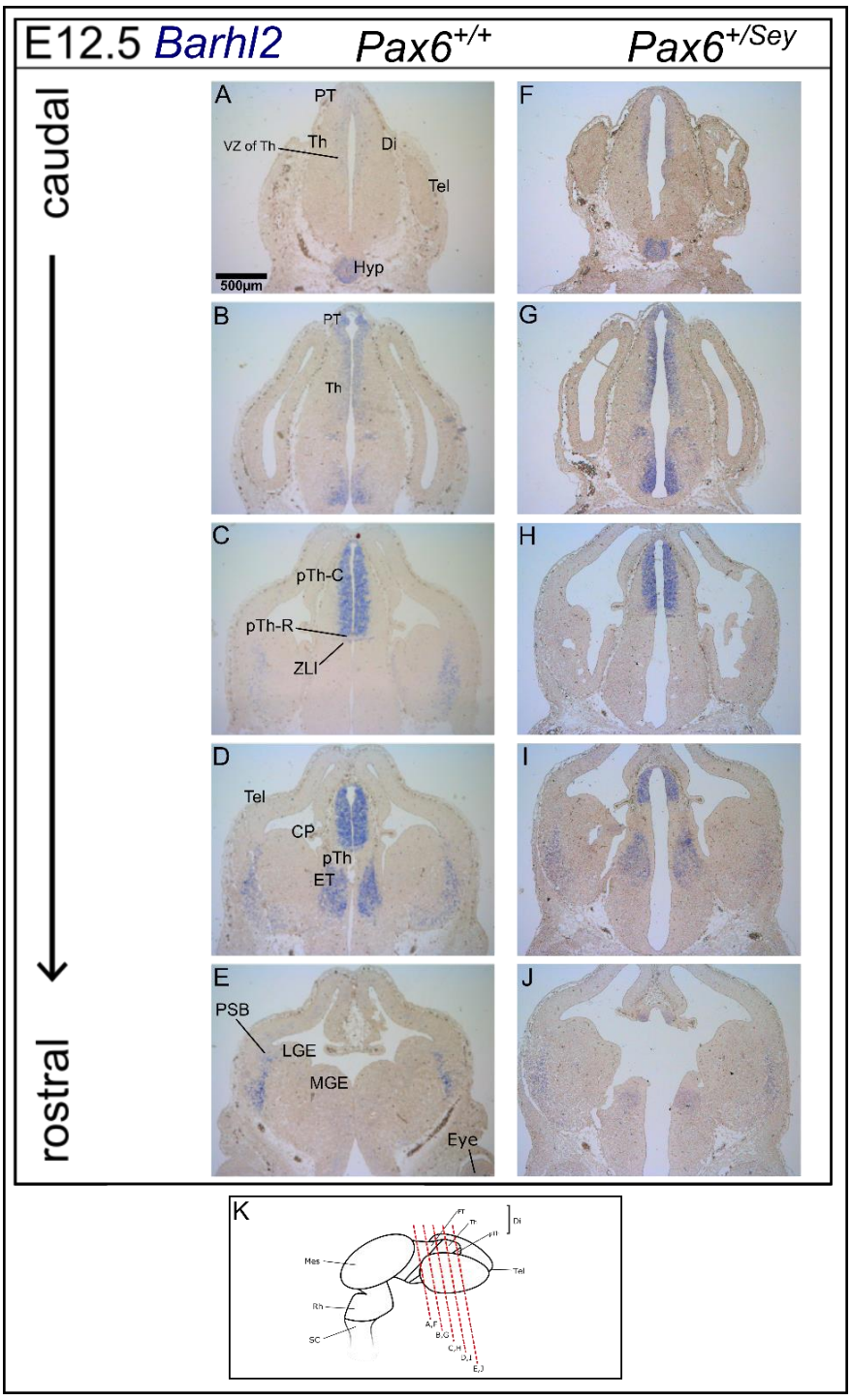

Fig. 5.7: Cryosections from Pax6$^{+/+}$ *and* Pax6$^{+/Sey}$ *embryos at E12.5 treated with* in situ *hybridization for* Barhl2*. A-E: Treated sections from a* Pax6$^{+/+}$ *embryo. F-J: Treated sections from a* Pax6$^{+/Sey}$ *embryo. K: Schematic to illustrate the approximate plane of each section. Abbreviations: Di- diencephalon; PT- pretectum; Th- thalamus; pTh- prethalamus; VZ- ventricular zone; Tel- telencephalon; Pal- pallium; SubPal- subpallium; PSB- pallial-subpallial boundary; Tel- telencephalon; Di- diencephalon; Mes- mesencephalon; Rh- rhombencephalon; SC- spinal cord.*

5.3 Discussion

While gene expression in the *Pax6*$^{Sey/Sey}$ mutant and other *Pax6*-null mutants has been studied extensively (Hill *et al* 1991, Grindley *et al* 1997, Mastick *et al* 1997, Pratt *et al* 2000a, Manuel and Price 2005, Stoykova et al 2006, Manuel *et al* 2008, Georgala *et al* 2011), the expression of *Barhl2* in the *Pax6*-null mutant forebrain has not previously been described. The data presented here suggest that interactions may exist between *Pax6* and *Barhl2*, and in particular an inhibition of *Barhl2* expression by *Pax6*.

The changes in *Barhl2* expression which were found to occur as a result of the loss of functional *Pax6* were found to be context-dependent, varying according to the position of the neuroepithelium in relation to the position of the ZLI. This observation is consistent with those described in chapter 4.

Caudal to the ZLI *Barhl2* appeared to be upregulated, while rostral to the ZLI expression of *Barhl2* appeared to be downregulated. This would be consistent with evidence that *Shh* signalling from the ZLI acts in an asymmetric manner in order to induce different patterning events in the tissues immediately rostral and caudal to its position within the diencephalon (Kiecker and Lumsden 2004).

Within the pTh-C of the mutant the *Barhl2* domain was found to have expanded along the mediolateral axis, instead of being confined to the thalamic ventricular zone as it was in the wild type diencephalon. From the data presented here it is not possible to confirm that *Barhl2* expression was upregulated in the pTh-C or if the *Barhl2* domain had merely expanded without any alteration in the overall level of *Barhl2* expression. At E13.5 in particular the expression of *Barhl2* in the thalamus of the mutant appeared to be more diffuse than it did in the thalamus of the wild-type embryo. In order to confirm or refute an upregulation of *Barhl2* it would be necessary to employ a quantitative approach such as quantitative PCR (qPCR) to determine the levels of *Barhl2* mRNA, or Western blotting to quantify the levels of *Barhl2* protein expression within the thalamus.

Suggested functions of *Barhl2* in neural development include the modulation of neuronal differentiation via the inhibition of proneural bHLH transcription factor

expression (Reig *et al* 2007). Increased expression of *Barhl2* could therefore be indicative of an increased inhibition of neuronal differentiation within the thalamus. A broadening of the *Barhl2* domain along the mediolateral axis without an increase in the overall level of *Barhl2* mRNA could indicative of ectopic inhibition of neuronal differentiation in regions of neuroepithelium outside the ventricular zone of the pTh-C.

The mediolateral expansion of the thalamic *Barhl2* domain suggests that *Pax6* may be required to restrict the thalamic expression of *Barhl2* to a region of neuroepithelium within the ventricular zone. If *Pax6* does act to inhibit the transcription of *Barhl2*, this transcriptional inhibition could serve to restrict the area of neuroepithelium in which *Barhl2* is able to inhibit neuronal differentiation, thereby ensuring that neurogenesis proceeds correctly. It is also possible that *Pax6* may act to modulate the rate of neurogenesis by controlling the levels of *Barhl2* protein expression. The changes in shape of the thalamic *Pax6* and *Barhl2* domains over time, as described in Chapter 3, could also play a role in modulating the time and place at which neuronal differentiation can occur during thalamic development.

Alternatively increased levels of *Barhl2* mRNA could be indicative of changes in neuronal subtype specification. Loss of *Barhl2* in the murine retina leads to the misspecification of amacrine interneurons, with the differentiation of cholinergic neurons occurring at the expense of GABAergic and glycinergic neurons (Ding *et al* 2009). Loss of *Barhl2* also leads to the misspecification of interneurons within the murine spinal cord and subsequent defects in axon guidance (Ding *et al* 2012). It is not yet known if *Barhl2* is required for neuronal subtype specification within the thalamus, or if the consequences of any misspecification of thalamic neurons would lead to axon guidance defects, but defects in thalamocortical and corticothalamic axon guidance have been observed in *Pax6*-null mutants. If a mutually repressive relationship exists between *Pax6* and *Barhl2* this may act to directly control neuronal subtype specification, and indirectly serve to modulate axon guidance following neuronal differentiation.

The expansion of the ZLI in the *Pax6*-null mutant has been described previously (Grindley *et al* 1997, Pratt *et al* 2000a). It is known that *Barhl2* is required for the

induction of the ZLI and that the ZLI develops within a *Barhl2*-positive region of the neural tube (Juraver-Geslin *et al* 2014). If *Pax6* exerts an inhibitory effect on the expression of *Barhl2* it may be possible that *Pax6* is required to inhibit the expansion of the *Barhl2*-positive region of neuroepithelium which is competent to develop into the ZLI. The loss of functional *Pax6* may therefore lead to an expansion of the ZLI as a result of an expansion of the *Barhl2* expression domain.

The expansion of the pTh-R in the $Pax6^{Sey/Sey}$ mouse has also been described previously, along with the possibility that this may be directly linked to the expansion of the ZLI and the resulting increase in the levels of *Shh* protein (Caballero *et al* 2014). An inhibition of *Pax6* expression by *Shh* has been shown to be required for the development of the pTh-R (Robertshaw *et al* 2013). Increased levels of *Shh* protein within the neuroepithelium of the thalamus may lead to increased inhibition of *Pax6* expression and, as a consequence, an increase in the size of the area which can then develop into the pTh-R.

Within the diencephalon of the *Pax6*-null mutant the domain of *Barhl2* within the pTh-C appeared to extend along a smaller proportion of the diencephalic neuroepithelium as a whole, with the thalamic *Barhl2* domain extending a greater distance from the dorsal midline and into more ventral regions of the neuroepithelium. It is known that part of the pTh-C is misspecified as pTh-R in *Pax6*-null mutants (Grindley *et al* 1997) and the expansion of the ZLI and pTh-R may occur at the expense of pTh-C.

Rostral to the ZLI the loss of functional *Pax6* protein appeared to cause a downregulation of *Barhl2*, and in particular the loss of its expression within the *eminentia thalami*. It may be possible that the loss of functional *Pax6* leads to a loss or misspecification of the *eminentia* thalami, or that the gene expression profile of the *eminentia thalami* is simply altered in the absence of functional *Pax6* protein. In order to investigate these possibilities further it would be necessary to investigate the expression of other known markers of the *eminentia thalami*, such as *ISL LIM homeobox 1* (*Islet1*) and the *Dlx* family of transcription factors (Fotaki *et al* 2006), within the diencephalon of the *Pax6*-null mutant.

In the *Pax6*$^{+/Sey}$ embryo no major changes in *Barhl2* mRNA expression appeared to have been induced by the loss of one copy of the functional *Pax6* allele. This may be due to the levels of *Pax6* protein not differing greatly between the *Pax6*$^{+/+}$ diencephalon and the *Pax6*$^{+/Sey}$ diencephalon (Pinson 2005), possibly as a consequence of the ability of Pax6 protein to regulate the levels of its own expression (Aota *et al* 2003, Pinson 2005, Pinson *et al* 2005, Manuel *et al* 2007).

6. The effects of the inhibition of *Shh* signalling on the expression of *Pax6* and *Barhl2* in the diencephalon

6.1 Introduction

In order to investigate the relationship between the expression of *Pax6* and *Barhl2* and signalling by the morphogen *Shh*, a *Shh* loss-of-function approach was taken via the use of drug treatment to inhibit *Shh* signalling.

In the adult brain *Shh* signalling plays roles in the regulation of stem cell maintenance and renewal (Álvarez-Buylla and Ihrie 2014). While transient *Shh* activity induces the renewal of adult stem cells, more sustained activation of *Shh* signalling has been linked to the development of malignant tumours (Taipale and Beachy 2001, Beachy *et al* 2004) and elevated levels of *Shh* have been observed in some cancers, such as basal cell carcinoma (Oro *et al* 1997), gastric cancer (Katoh and Katoh 2005) and prostate cancer (Peng and Joyner 2015). Evidence that *Shh* can induce the development of carcinomas from stem cells has led to components of the *Shh* pathway being considered as targets for chemotherapeutic agents (Bijlsma and Roelink 2010, Gupta *et al* 2010).

Elevated levels of *Shh* activity have been implicated in the development of basal cell carcinoma, a form of skin cancer (Epstein 2008, Athar *et al* 2014). One chemotherapeutic agent currently used to treat basal cell carcinoma is the relatively novel *Shh* antagonist vismodegib (Berrada *et al* 2014, Basset-Seguin *et al* 2015). Vismodegib is able to bind to the *Shh* receptor *Smo* and suppress *Shh* signalling by acting as a competitive inhibitor of endogenous *Shh* (Yauch *et al* 2008). Its action is comparable to that of the *Shh* antagonist cyclopamine (Taipale *et al* 2000), which had also been considered as a potential treatment for carcinomas in which *Shh* signalling is implicated (Miller *et al* 2002) and then used in the treatment of medulloblastoma (Yauch *et al* 2009) but the potency of vismodegib has been found to be much greater than that of cyclopamine and vismodegib has also been found to cause fewer adverse effects in humans (Yun *et al* 2012).

While cyclopamine has been used to suppress *Shh* signalling in the study of embryonic brain development in mouse (Lipinski *et al* 2010), studies in mouse have

shown that its potency is relatively low compared to that of vismodegib, and that the solubility and chemical stability of vismodegib in aqueous solution are also greater (Robarge *et al* 2009). For these reasons it was decided that vismodegib would be used in the experiments described in this chapter.

Loss of *Shh* or inhibition of *Shh* expression leads to a very severe embryonic lethal phenotype with affected embryos exhibiting morphology which is greatly altered from that of untreated wild type embryos (Chang *et al* 1996, Roessler *et al* 1996). These differences in morphology can make it difficult to make useful comparisons between the *Shh*-null embryo and the wild type embryo. For this reason it can be preferable to use drug treatment to suppress *Shh* signalling at a stage at which the structure being investigated has been established. Delaying the administration of the drug to a point at which particular structures have already been specified can ensure that the morphology of the treated embryo will not differ too greatly from that of the untreated control embryo and make it easier to interpret changes in gene expression. In the experiments described here, vismodegib was administered at E9.5, a point at which the neural tube has closed, the murine prosencephalon has differentiated into the telencephalon and the diencephalon, and the segmentation of the diencephalon is taking place.

$Pax6^{+/Sey}$ males were crossed with $Pax6^{+/Sey}$ females in order to generate litters comprising $Pax6^{+/+}$, $Pax6^{+/Sey}$ and $Pax6^{Sey/Sey}$ embryos. The effective dose of vismodegib had been determined to be 4mg previously (Caballero *et al* 2014). At E9.5 pregnant females were administered with 4mg of vismodegib in a methylcellulose vehicle solution, or the vehicle solution alone as a control, by oral gavage. Embryos were harvested at E12.5 before being fixed and cryosectioned. $Pax6^{Sey/Sey}$ embryos were identified by their lack of eyes and altered craniofacial morphology.

In situ hybridization for *Pax6* mRNA was performed on sections from control embryos of the genotypes $Pax6^{+/+}$ or $Pax6^{+/Sey}$, while *in situ* hybridization for *Barhl2* mRNA was performed on $Pax6^{+/+}$, $Pax6^{+/Sey}$ and $Pax6^{Sey/Sey}$ embryos. Each experiment was repeated three times on tissue from three different embryos.

While the expression of Pax6 protein in the *Pax6*$^{+/Sey}$ forebrain has been investigated and described previously (Pinson 2005) the expression of *Barhl2* mRNA and Barhl2 protein in the *Pax6*$^{+/Sey}$ forebrain have yet to be described. An antibody for Barhl2 protein which was suitable for immunohistochemical applications was not available, and for this reason the expression of *Barhl2* mRNA rather than that of Barhl2 protein was investigated.

For the experiments described here a limited quantity of vismodegib was available. Material from embryos treated with vismodegib was therefore scarce. For this reason it was decided that while ideally *Pax6*$^{+/+}$ embryos only would be used as controls, it would be necessary to perform some experiments using *Pax6*$^{+/Sey}$ embryos in addition to these.

The phenotype of the *Pax6*$^{Sey/+}$ mouse is less severe than of the *Pax6*$^{Sey/Sey}$ mouse. *Pax6*$^{Sey/+}$ mice exhibit gross morphology that is similar to that the wild-type mouse, with the exception of the eyes, which are reduced in size (Hill *et al* 1991), while the forebrain morphology is also similar in mice of both genotypes (Mastick *et al* 1997). Quantification of the expression levels of Pax6 protein have shown that they are broadly similar in the *Pax6*$^{+/+}$ and *Pax6*$^{+/Sey}$ mouse forebrain (Pinson 2005), possibly as a consequence of the ability of Pax6 to autoregulate its expression within the forebrain (Aota *et al* 2003, Pinson 2005, Pinson *et al* 2005, Manuel *et al* 2007). The *Pax6*$^{+/Sey}$ forebrain exhibits a mild axon pathfinding defect in the postoptic commissure but appears normal in other respects (Mastick *et al* 1997). In addition to these earlier published findings, the data presented in chapter 5 suggest that the expression pattern of *Barhl2* in the *Pax6*$^{+/Sey}$ forebrain does not differ greatly from that observed in the *Pax6*$^{+/+}$ forebrain (Fig. 5.7). For these reasons *Pax6*$^{Sey/+}$ embryos were considered acceptable to use as control embryos in this study, and were used to compensate for the scarcity of treated *Pax6*$^{+/+}$ embryos.

6.2 Results

In control embryos which had been exposed to the methylcellulose control vehicle alone (Fig. 6.1) *Pax6* appeared to be expressed in domains of a similar size and position to those observed in the untreated *Pax6*$^{+/+}$ embryo (Fig. 3.2.5A-E) and

appeared to have been unaltered by the experimental procedure. In the diencephalon strong *Pax6* expression was observed in the pretectum (asterisk, Fig. 6.1A) and prethalamus (asterisks, Fig. 6.1B) and the dorsal-to-ventral gradient of *Pax6* expression was visible within the ventricular zone of the pTh-C (Fig. 6.1F), while in the telencephalon *Pax6* expression was strong within the ventricular zone of the cortex (asterisks, Fig. 6.1D) and its expression gradient ended at a sharp border coinciding with the position of the pallial-subpallial boundary (arrows, Fig. 6.1D-E). Strong *Pax6* expression could also be seen in the retina of the eye (6.1J).

Barhl2 expression in control embryos which had been exposed to the methylcellulose control vehicle alone (Fig. 6.2) also appeared to have been unaltered by the experimental procedure and in these embryos the *Barhl2* expression domains appeared to be of a similar size and position to those observed in the untreated control embryo (Fig. 3.2.5F-J). Within the diencephalon *Barhl2* expression could be seen within the ventricular zone of the pTh-C in an expression gradient running from ventral to dorsal (Fig. 6.2F) and within the ZLI (Fig. 6.2L) in a domain distinct from the domain within the pTh-C and separated from it by a narrow *Barhl2*-negative domain corresponding with the position of the pTh-R (Fig. 6.2G). Rostral to the ZLI *Barhl2* expression could be seen within the *eminentia thalami* (asterisks, Fig. 6.2N) and within the telencephalon *Barhl2* was observed in a domain within the subpallium which extended dorsally and ended at the pallial-subpallial boundary (arrows, Fig. 6.2D).

In control embryos which had been exposed to 4mg of vismodegib the morphology was altered (Figs. 6.3 and 6.4) from that of the control embryos treated with the vehicle control alone (Figs. 6.1 and 6.2). The telencephalic vesicles were enlarged and the diencephalic neuroepithelium was seen to have thickened along the mediolateral axis.

Of the three wild type embryos which had been exposed to 4mg of vismodegib (Fig. 6.3 and 6.4) the first appeared to be slightly larger in size (Figs. 6.3A-E and 6.4A-E) than the second (Fig. 6.3F-J and Fig. 6.4F-J) and third (Figs. 6.3K-O and 6.4K-O). The first embryo may have reached a slightly later developmental stage than the

others but the morphology and expression domains appeared to be similar enough to allow useful comparisons to be made between the three embryos.

In the control embryos analysed, exposure to 4mg of vismodegib appeared to have altered the expression of *Pax6* (Fig. 6.3) and within several regions of neuroepithelium it differed from that observed in the embryos which had been treated with the control vehicle alone (Fig. 6.1). *Pax6* expression within the pretectum remained as strong as it had been in the pretectum of the control embryos exposed to the vehicle only (Fig. 6.3B) while in the thalamus *Pax6* expression it appeared to be stronger overall (Fig. 6.3H) Expression of *Pax6* in the ventricular zone of the pTh-C appeared to extend into a more ventral region of the neuroepithelium (arrows, Fig. 6.3D) than it had in the embryo treated with the methylcellulose control vehicle alone (Fig. 6.1). *Pax6* expression also appeared to be stronger within the ventricular zone of the cortex and the ventral-to-dorsal expression gradient of *Pax6* appeared to be less steep, with stronger expression of *Pax6* detected in more dorsal regions of the pallium (Fig. 6.3E). Expression of *Pax6* within the vismodegib-treated prethalamus appeared to be of a similar strength to that observed in the prethalamus of the embryo treated with the vehicle control and the prethalamic expression domain also appeared to be of a similar shape and position in both caudal sections (Fig. 6.3F) and rostral sections (Fig. 6.3C).

In control embryos which had been exposed to 4mg of vismodegib the expression of *Barhl2* did not appear to have been affected to as great an extent as the expression of *Pax6* within treated embryos (Fig. 6.4). Within the ventricular zone of the pTh-C strong *Barhl2* expression could still be observed and it still seemed to be confined to the ventricular zone (asterisks, Fig. 6.4G) but a ventral-to-dorsal gradient of expression was not apparent (Fig. 6.4L) as it had been in some sections from embryos treated with the vehicle control alone (asterisk, Fig. 6.4F).

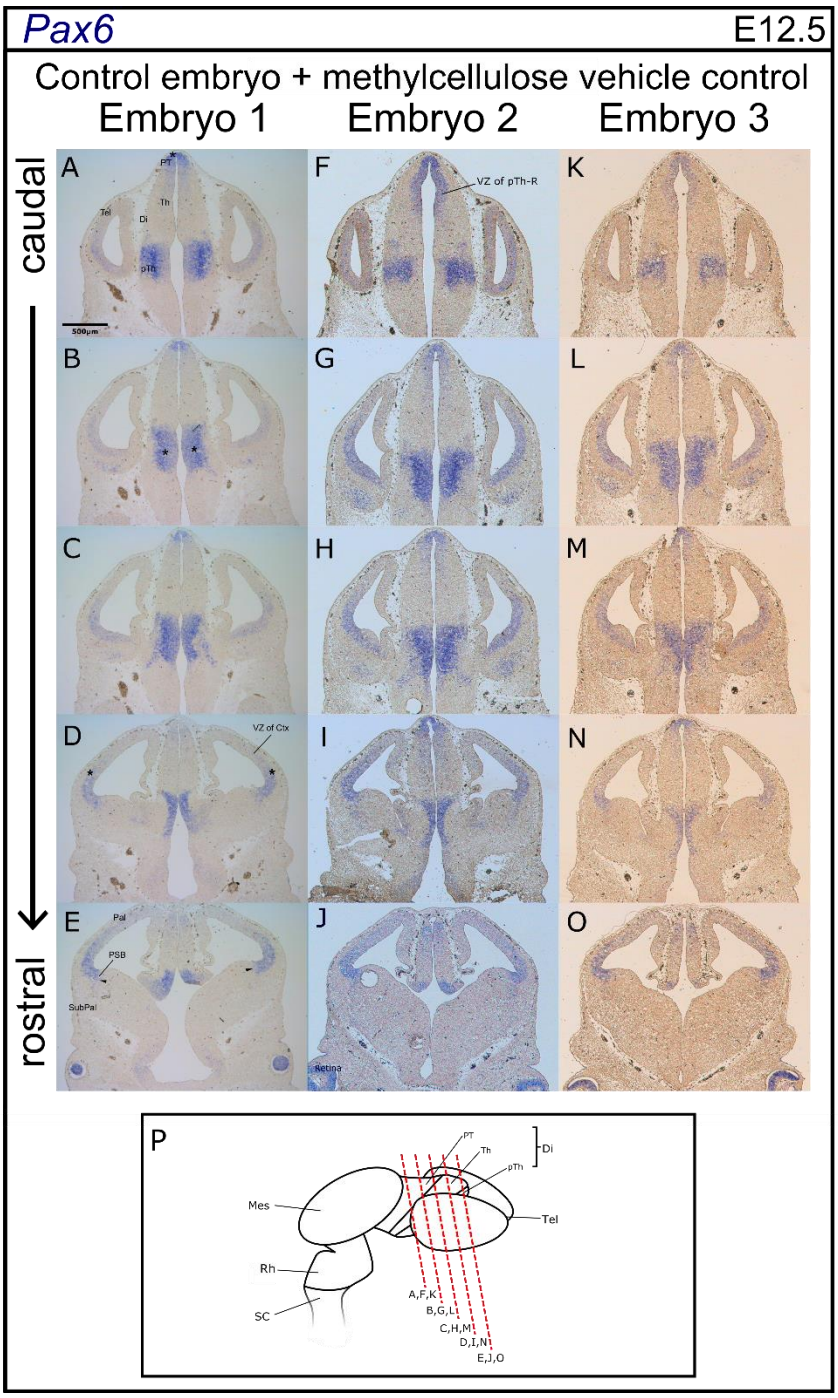

Fig. 6.1: A-O: In situ *hybridization for* Pax6 *mRNA in sections from three control embryos exposed to with the methylcellulose control vehicle alone. P: Schematic to illustrate the approximate plane of section. Asterisks: A: Strong* Pax6 *expression in the pretectum. B: Strong* Pax6 *expression in the prethalamus D: Dorsoventral gradients of Pax6 expression in the pallium. Arrows in E: The boundary of the* Pax6 *domain at the pallial-subpallial boundary. Abbreviations: Di- diencephalon; PT- pretectum; Th- thalamus; pTh- prethalamus; VZ- ventricular zone; Tel- telencephalon; Mes- mesencephalon; Rh- rhombencephalon; SC- spinal cord Pal- pallium; SubPal- subpallium; PSB- pallial-subpallial boundary; Ctx- cortex.*

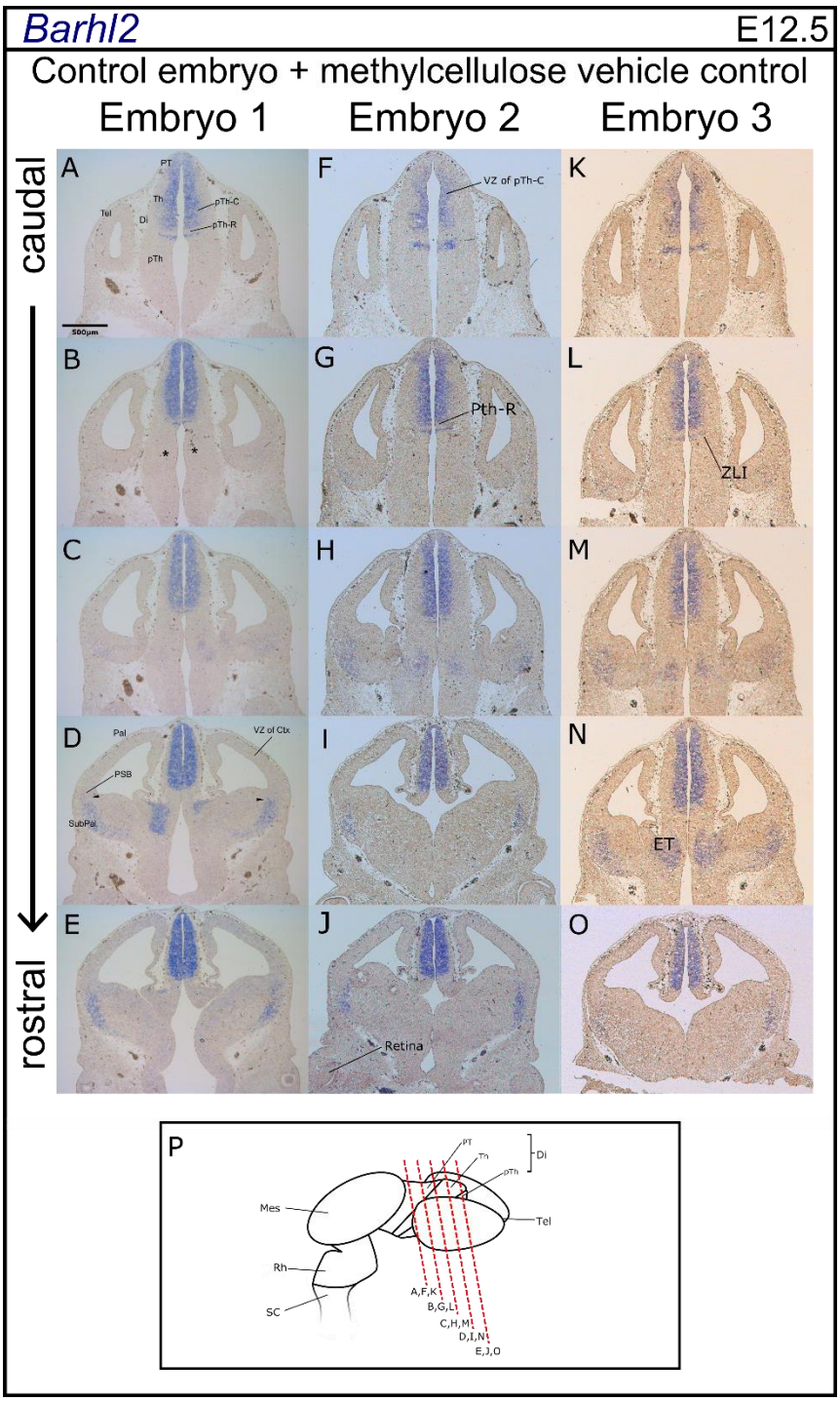

Fig. 6.2: A-O In situ *hybridization for* Barhl2 *mRNA in sections from three control embryos exposed to the methylcellulose control vehicle alone. P: Schematic to illustrate the approximate plane of section. Asterisks: B: Absence of* Barhl2 *expression in the prethalamus. Arrows in D: The PSB. Abbreviations: Di- diencephalon; PT- pretectum; Th- thalamus; pTh- prethalamus; VZ- ventricular zone; Tel- telencephalon; Mes- mesencephalon; Rh- rhombencephalon; SC- spinal cord Pal- pallium; SubPal- subpallium; PSB- pallial-subpallial boundary; Ctx- cortex.*

Barhl2 could also still be detected within the ZLI but this *Barhl2* domain appeared to have broadened slightly along the dorsoventral axis (Figs. 6.4B, H and I) and this domain was also not as sharply defined as the domain of *Barhl2* within the ZLI of the control embryo which had been exposed to the vehicle control only (Fig. 6.4L) The *Barhl2*-negative pTh-R appeared also appeared narrower and harder to distinguish (Fig. 6.4G) than the pTh-R of embryos exposed to the vehicle control alone (Fig. 6.4G).

Within more caudal sections *Barhl2* expression was detected (asterisks, Fig. 6.4F) in a domain of a shape comparable to that of the hypothalamic domain observed in untreated CD-1® embryos (Fig.3.2.5F). No expression of *Barhl2* within the ventral diencephalon had been observed in sections cut from a comparable point along the rostrocaudal axis in the embryos treated with the vehicle control alone (Fig. 6.4A, F and K).

The expression of *Barhl2* within the *eminentia thalami* (Fig. 6.4I) was of a comparable size and shape to that observed within the eminentia thalami of the embryo exposed to the vehicle control (Fig. 6.4N). Within the telencephalon the subpallial *Barhl2* domain appeared to have broadened slightly along the mediolateral axis but the overall shape did not seem to have been altered (Fig. 6.4J).

The morphology of the *Pax6*$^{Sey/Sey}$ mutant embryos exposed to the control vehicle (Fig. 6.5) was apparently unaltered from that of the untreated *Pax6*$^{Sey/Sey}$ mutant embryo (Fig. 5.5F-J). and the overall reduction in forebrain size, with the telencephalic vesicles being most severely affected (Fig. 6.5G), the reduced thickness of the neuroepithelium (asterisks, Fig. 6.5I and J) and broader diencephalic lumen (asterisk, Fig. 6.5H) as described in Chapter 3 were all apparent, and within the telencephalon the lateral ganglionice eminence and medial ganglionic eminence appeared to be underdeveloped and could not be clearly distinguished (asterisks, Fig. 6.5E).

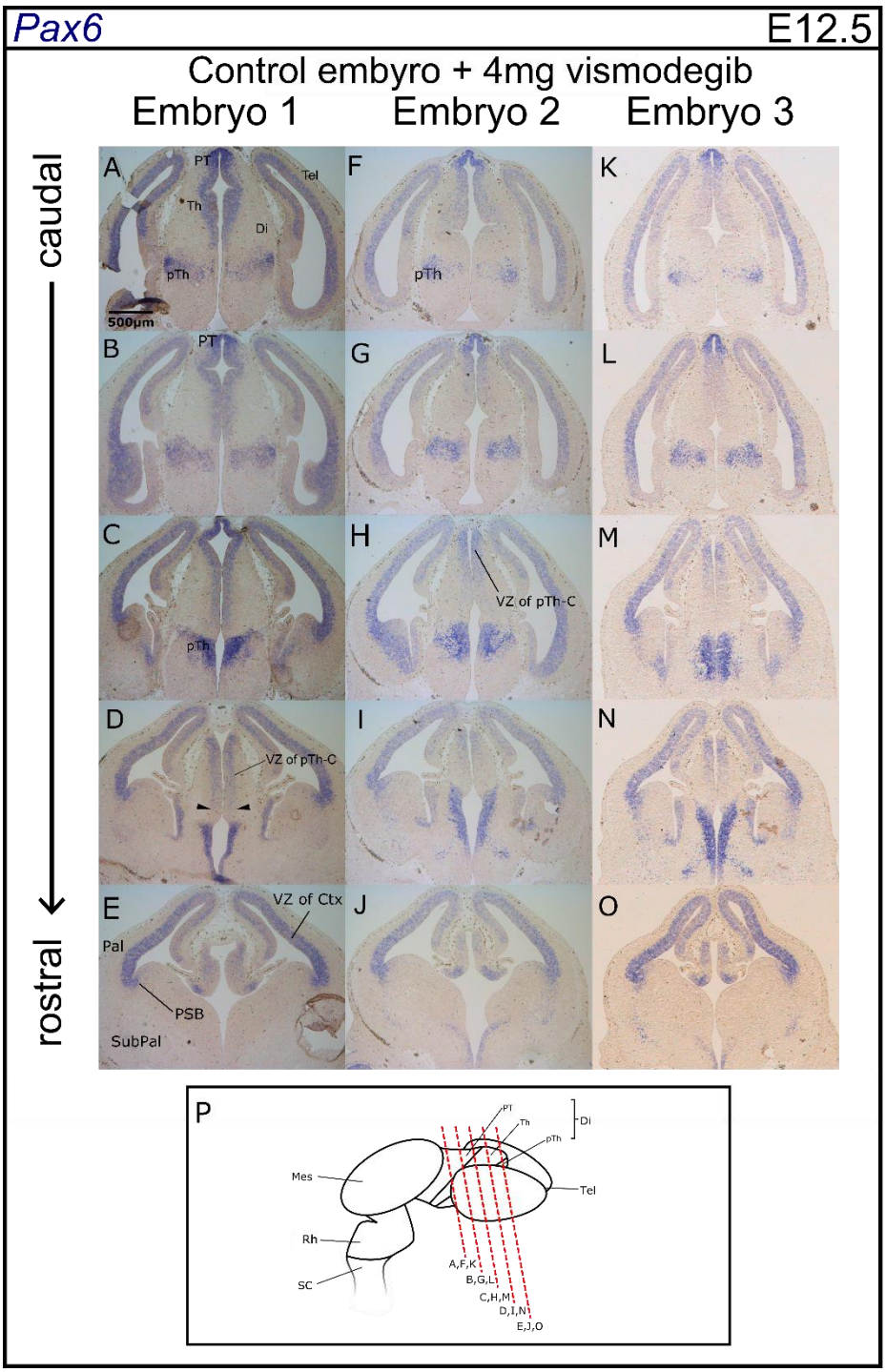

Fig. 6.3: A-O In situ *hybridization for* Pax6 *mRNA in sections from three control embryos exposed to 4mg of vismodegib. P: Schematic to illustrate the approximate plane of section. Arrows in D: Thalamic* Pax6 *extending more dorsally than in the control embryo treated with the vehicle alone. Abbreviations: Di- diencephalon; PT- pretectum; Th- thalamus; pTh- prethalamus; VZ- ventricular zone; Tel- telencephalon; Mes- mesencephalon; Rh- rhombencephalon; SC- spinal cord Pal- pallium; SubPal- subpallium; PSB- pallial-subpallial boundary; Ctx- cortex.*

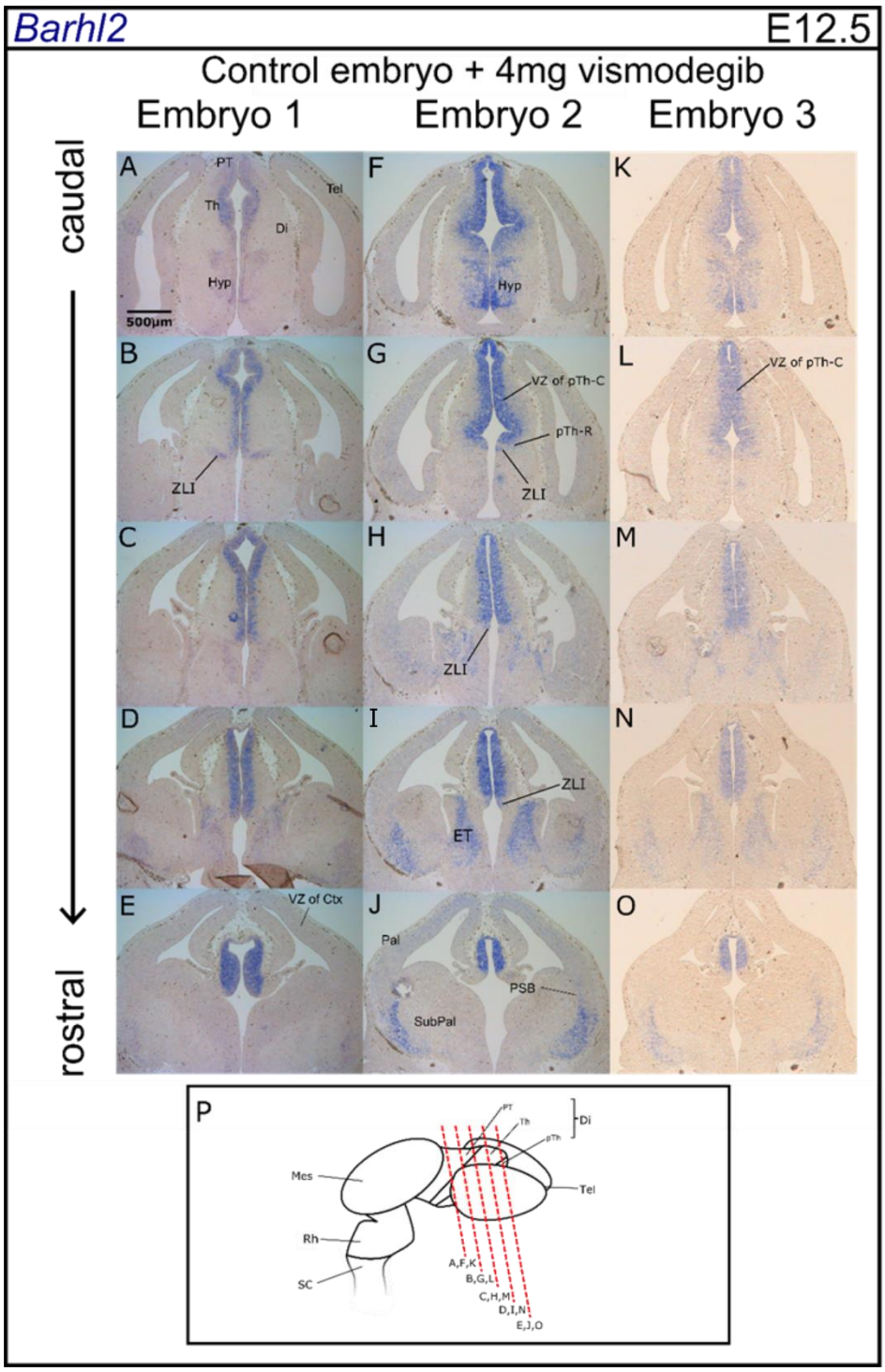

Fig. 6.4: A-O: In situ *hybridization for* Barhl2 *mRNA in sections from three control embryos exposed to 4mg of vismodegib. P: Schematic to illustrate the approximate plane of section. Abbreviations: Di- diencephalon; PT- pretectum; Th- thalamus; pTh- prethalamus; VZ- ventricular zone; Tel- telencephalon; Pal- pallium; SubPal- subpallium; PSB- pallial-subpallial boundary; Tel- telencephalon; Di- diencephalon; Mes- mesencephalon; Rh- rhombencephalon; SC- spinal cord; Ctx- cortex.*

The expression of the *Barhl2* also appeared to have been unaffected by the administration of the vehicle control. As in the untreated *Pax6*$^{Sey/Sey}$ mutant embryo at the same stage (Fig. 5.5 F-J) the *Barhl2* expression domain within the pTh-C was seen to have expanded laterally (outlined area, Fig. 6.5D) while the broadened *Barhl2* domain within the expanded ZLI (Fig. 6.5D) could be seen ventral to the pTh-C, separated from it by the *Barhl2*-negative pTh-R which was also broader than the pTh-R of the treated control embryo (Fig. 6.4G) and less sharply defined.

Within the telencephalon the *Barhl2* expression domain could be visualised within the subpallium (arrows, Fig. 6.5E), reduced in size and in a more lateral position than in the control embryo (arrows Fig. 6.4D).

In the *Pax6*$^{Sey/Sey}$ mutant embryo which had been exposed to 4mg of vismodegib (Fig. 6.6) the morphology appeared different from that of the mutant embryo which had been exposed to the control vehicle alone (Fig. 6.5). The expanded diencephalic lumen (double asterisk, Fig. 6.6I) was visible as it was in the mutant exposed to the vehicle control alone (asterisk, Fig. 6.5H) but in the mutant treated with vismodegib the overall size of the forebrain was greater and the neuroepithelium of the diencephalon was thicker (asterisk, Fig. 6.6B). While the neuroepithelium of the telencephalon did not appear to have increased in thickness to the same extent (asterisk, Fig. 6.6O) the telencephalic vesicles, while still smaller than those of the control embryo treated with the vehicle control (asterisks, Fig. 6.2D) or with 4mg of vismodegib (asterisk, Fig. 6.4E), appeared to be larger than those of the untreated mutant embryo (Fig. 6.5G). Within the diencephalon vesicle-like structures could be seen to have formed close to the lateral extent of the neuroepithelium (single asterisks, Figs. 6.6D, H and N), adjacent to the choroid plexus in more rostral sections (Fig. 6.6I and J) Within the telencephalon the lateral ganglionic eminence and medial ganglionic eminence (asterisks, Fig. 6.6J) were relatively large (asterisks, Fig. 6.6J) and more distinct from one another than the same structures in the mutant treated with the vehicle control alone (asterisks, Fig. 6.5E).

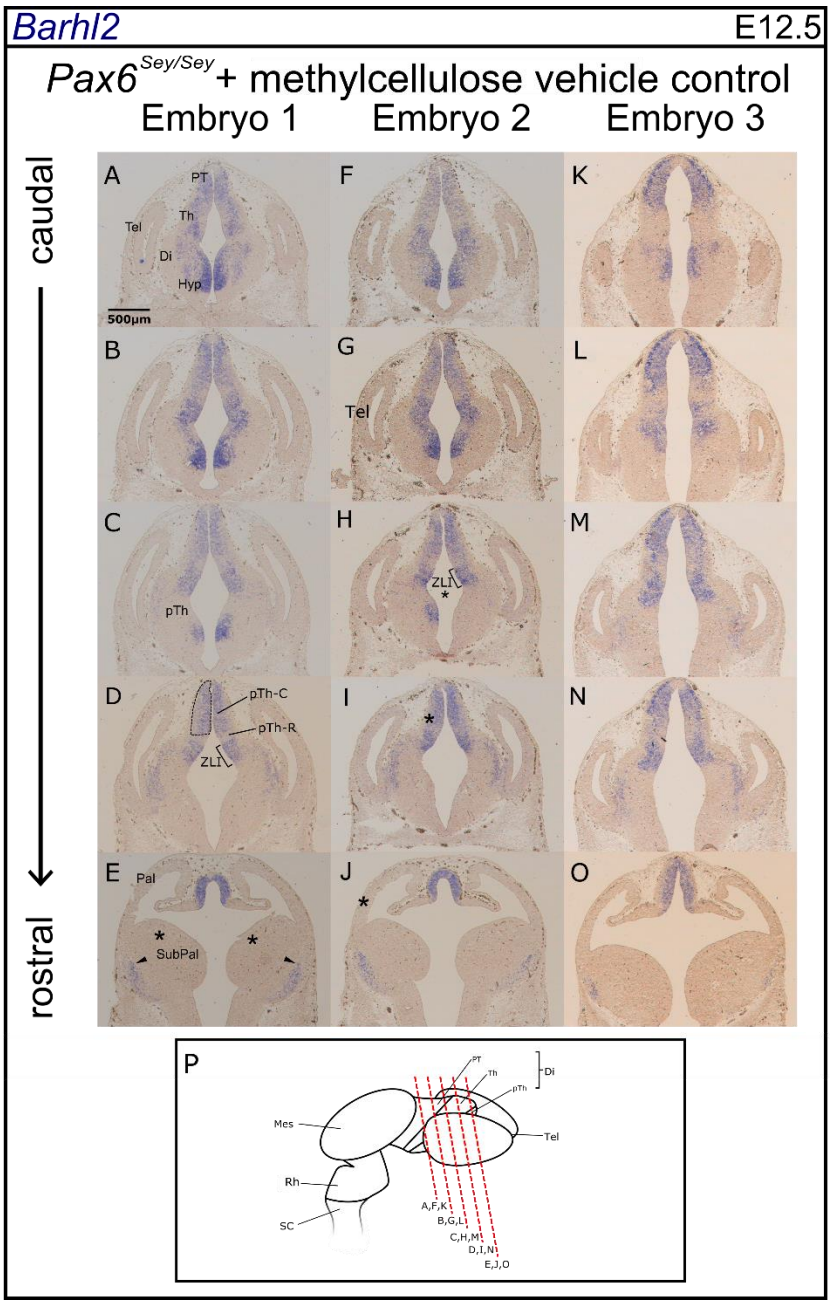

Fig. 6.5: A-O: In situ *hybridization for* Barhl2 *mRNA in sections from three* Pax6$^{Sey/Sey}$ *embryos exposed to the vehicle control only. P: Schematic to illustrate the approximate plane of section. Asterisks: E: The LGE and MGE cannot be distinguished. H: The expanded diencephalic lumen. I and J: The neuroepithelium is reduced in thickness in both the telencephalon and diencephalon. Arrows in E:* Barhl2 *expression in the subpallium is comparable to that observed in the untreated mutant subpallium. Outlined area in D: The laterally expanded thalamic* Barhl2 *domain. Abbreviations: Di- diencephalon; PT- pretectum; Th- thalamus; Mes- mesencephalon; Rh- rhombencephalon; SC- spinal cord; pTh- prethalamus; VZ- ventricular zone; Tel- telencephalon; Pal- pallium; SubPal- subpallium; PSB- pallial-subpallial boundary.*

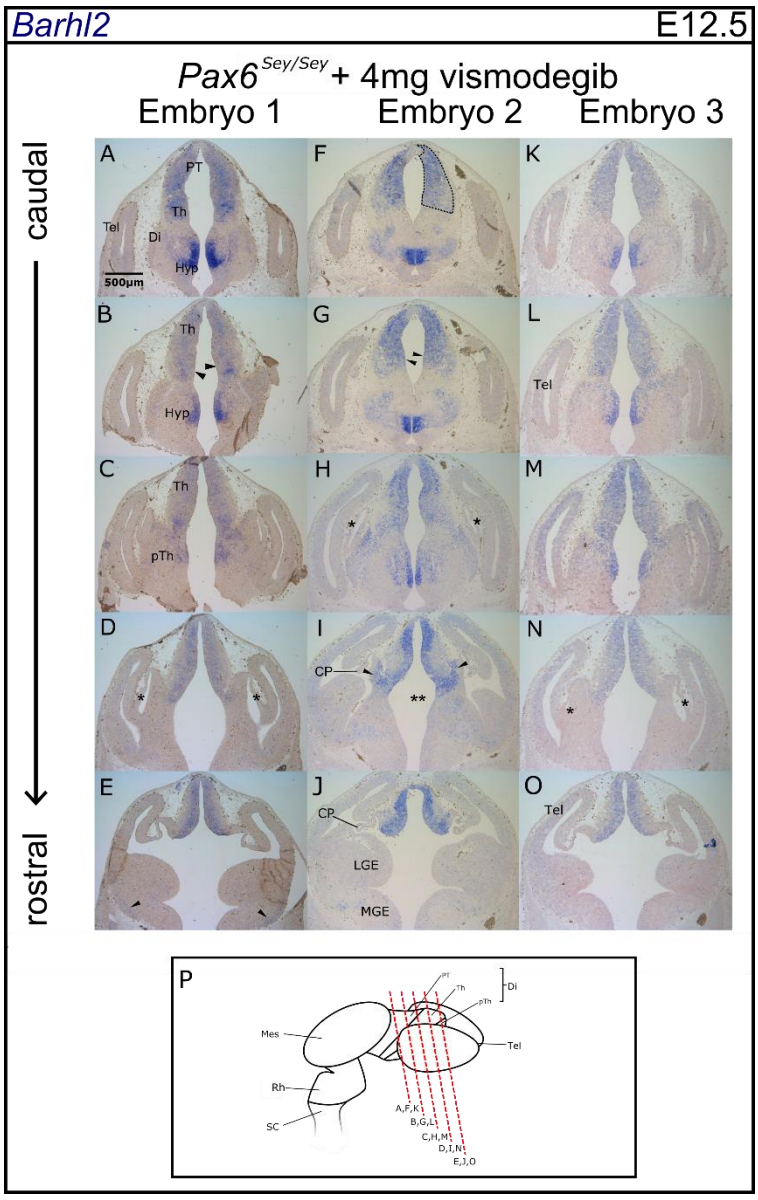

Fig. 6.6: A-O: In situ *hybridization for* Barhl2 *mRNA in sections from three* Pax6$^{Sey/Sey}$ *embryos exposed to 4mg of vismodegib. P: Schematic to illustrate the approximate plane of section. Arrows in B and G: The apparent loss of the* Barhl2*-negative pTh-R. Single asterisks: Vesicle-like structures at the position of the choroid plexus. Double asterisk in I: The expanded diencephalic lumen. Arrows in I: A lateral expansion of the* Barhl2 *domain into the telencephalic neuroepithelium. Outlined area in F: The laterally expanded thalamic* Barhl2 *domain. Arrows in E: Reduced* Barhl2 *expression in the subpallium. Abbreviations: Di- diencephalon; PT- pretectum; Th- thalamus; pTh- prethalamus; VZ- ventricular zone; Tel- telencephalon; Pal- pallium; SubPal- subpallium; PSB- pallial-subpallial boundary, LGE- lateral ganglionic eminence; MGE- medial ganglionic eminence. Mes- mesencephalon; Rh- rhombencephalon; SC- spinal cord*

The expression of *Barhl2* also appeared to have been altered by the treatment with vismodegib. Within the thalamus the *Barhl2* domain was seen to have expanded laterally (outlined area, Fig. 6.6F) as it had in the mutant embryo treated with the control vehicle (outlined area, Fig. 6.5D), but in the mutant treated with vismodegib the pTh-C, pTh-R and ZLI could not be distinguished by *Barhl2* expression. *Barhl2* appeared to be expressed in a continuous domain extending along the dorsoventral axis from the dorsal midline of the pretectum to a point corresponding with the position of the ZLI's dorsal extent (outlined area, Fig. 6.6B and F). Within this expression domain the strength of *Barhl2* expression appeared to be uniform along the dorsoventral extent, with no apparent gradient of expression. No region of stronger *Barhl2* expression corresponding with the position of the expanded ZLI was seen, as it had been in the mutant exposed to the control vehicle alone (Fig. 6.5D), and the *Barhl2*-negative region corresponding with the position of the pTh-R was also absent (arrows, Fig. 6.6B and G). In the second of the three embryos analysed the ventral *Barhl2* domain was seen to extend laterally into the telencephalic neuroepithelium (arrows, Fig. 6.6I).

Within the telencephalon a domain of *Barhl2* could be seen close to the pial surface of the subpallium (arrows, Fig. 6.6E) but this domain appeared smaller than the subpallial *Barhl2* domain observed in the mutant treated with the vehicle control (arrows, Fig. 6.5E) and the expression in the mutant subpallium was also found to be much weaker.

6.4 Discussion

The suppression of *Pax6* expression by *Shh* signalling has been described in detail in previous studies using vertebrate models (, Ericson *et* al 1997, Goulding *et al* 2003, Kiecker and Lumsden 2004, Vieira *et al* 2005, Robertshaw *et al* 2013, Caballero et al 2014) but the effects of *Shh* signalling on *Barhl2* expression has not previously been described in vertebrates. *Drosophila Hh* is known to be required to initiate the expression of *Drosophila BarH2* (Lim and Choi 2004) but the data presented here in Chapter 4 (Fig. 4.1C and D) show that in mouse *Shh* is not required for the expression of *Barhl2*. The relationship between *Shh* and *Barhl2* in mouse is clearly different from that which exists between *Hh* and *BarH2* in *Drosophila*. The

experiments described here were performed in an attempt to characterise the relationship between *Shh* signalling and *Barhl2* expression within the murine diencephalon. The observation of changes in gene expression described here build on the findings from previous investigations in mouse which focused on the effects of vismodegib on a number of other genes expressed within the murine thalamus (Caballero *et al* 2014).

In addition to this the effects of suppressing *Shh* signalling on *Barhl2* expression were studied alongside the effects on the expression of *Pax6* in an attempt to gain some insight into the potential for relationships existing between *Pax6* and *Barhl2*. If a mutually repressive relationship exists between the two genes, the suppression of one gene's expression should in theory lead to an upregulation in the expression of the other. This was not observed with *Pax6* and *Barhl2*, as the apparent upregulation of *Pax6* did not appear to correlate with a downregulation of *Barhl2*, and this finding was not consistent with the hypothesis of a mutually repressive relationship existing between the two genes.

Vismodegib is a relatively novel drug and its effects on embryonic brain development have yet to be described comprehensively. Some effects of vismodegib on the development of the rat embryo (*Rattus norvegicus*) have been characterised (Morinello *et al* 2014) and its severe effects on the gross morphology of the murine telencephalon (Heyne *et al* 2015) have been described but its more subtle effects on the morphology of the murine diencephalon have yet to be described in detail. The data presented here represent an attempt to characterise some of the morphological changes which occur as a result of exposure to vismodegib as well as the changes in gene expression induced by its effects on the *Shh* signalling pathway.

While vismodegib is more soluble and more potent than cyclopamine (Robarge *et al* 2009) it has yet to be used as widely as cyclopamine and its action and effects have yet to be characterised as comprehensively. Administration of vismodegib could prove to be preferable means of suppressing *Shh* signalling in some contexts and findings related to its effects on embryonic development may also have implications for the design of future experiments and the decision to use vismodegib rather than cyclopamine.

Within the control embryos exposed to the vehicle control alone (Figs. 6.2 and 6.3), the morphology of the forebrain and the expression of both *Pax6* and *Barhl2* did not appear to have been altered. This suggested that the vehicle control and the oral gavage method by which it was administered did not exert any biological effects on the embryo, and that any changes observed in the embryos exposed to vismodegib were therefore induced by the drug itself.

In control embryos treated with vismodegib the expression of *Pax6* appeared to be stronger in the pretectum, thalamus and pallium. It is known that *Shh* signalling can inhibit the expression of *Pax6* in some contexts (Ericson *et* al 1997, Goulding *et al* 2003, Kiecker and Lumsden 2004, Vieira *et al* 2005, Robertshaw *et al* 2013, Caballero et al 2014) and that ectopic expression of *Shh* can downregulate *Pax6* expression in the thalamus (Kiecker and Lumsden 2004; Vieira et al., 2005). It may be possible that vismodegib treatment causes an upregulation of *Pax6* expression via the suppression of *Shh* signalling and this would be consistent with these earlier published findings, but it would be necessary to quantify *Pax6* levels in order to confirm this.

In the prethalamus no upregulation of *Pax6* was apparent (asterisks, Fig. 6.4C and F). This could be because *Pax6* expression within the prethalamus is very strong within the control embryo even in the absence of vismodegib (Fig. 6.2B) and any increase in the strength of its expression may therefore be subtle and hard to confirm without the use of quantitative methods. This could also be due to the differential competence to respond to the *Shh* signal in the regions of neuroepithelium rostral and caudal to the ZLI (Bulfone *et al* 1993, Hirata *et al* 2006, Kiecker and Lumsden 2004, Robertshaw *et al* 2013). The prethalamic neuroepithelium may not be competent to respond to the *Shh* signal, or it may not respond to the signal with a downregulation of *Pax6*, and if this is the case an inhibition of the *Shh* signal would not lead to an increase in *Pax6* levels.

Drug treatment with vismodegib did not appear to have a great effect on the expression of *Barhl2* in the forebrain of the control embryo (Fig. 6.5) and the shape and position of its expression domains appeared unaltered from those of the expression domains in the untreated control embryo (Fig. 6.3). Notably the domains

of *Barhl2* within the pTh-C and ZLI remained distinct from one another and separated by a *Barhl2*-negative region corresponding with the position of the pTh-R, although the borders of the pTh-R were harder to distinguish than in the control embryo exposed to the vehicle alone. Previous studies have shown that the loss of *Shh* results in a total failure of the pTh-R to develop (Szabó et al 2009, Vue et al 2009) so the observation that the pTh-R was still present, albeit harder to distinguish, is perhaps surprising. The inhibition of *Shh* with vismodegib may therefore have exerted a minor effect on pTh-R development.

The observation of pTh-R development in vismodegib-treated embryos may also be a consequence of the inhibition of *Shh* signalling by the drug being incomplete. While vismodegib has been shown to be more a more potent inhibitor of *Shh* signalling than cyclopamine (Robarge *et al* 2009) and attempts to determine the dose of vismodegib required to inhibit *Shh* signalling in mouse have found a 4mg dose to be effective (Caballero *et al* 2014) it may still be possible that this dose is not sufficient to cause a total inhibition of *Shh* signalling, although it may be reasonable to expect this dose of vismodegib to exert a greater effect on the size of the pTh-R.

The pTh-R could also be distinguished in *Pax6*$^{Sey/Sey}$ embryos which had been exposed to the control vehicle alone and only appeared to have been lost in vismodegib-treated *Pax6*$^{Sey/Sey}$ embryos. One previous study has suggested that while the inhibition of *Pax6* by *Shh* signalling is required for the development of the pTh-R, it is not sufficient to induce pTh-R development and that another function of *Shh* may play a role in pTh-R induction (Robertshaw *et al* 2013). The observation that the pTh-R is present in the control embryo treated with vismodegib and the mutant embryo exposed to the control vehicle, but absent in the vismodegib-treated *Pax6*$^{Sey/Sey}$ mutant embryo (arrows, Fig. 6.6G), is consistent with this hypothesis.

In *Pax6*$^{Sey/Sey}$ embryos the ZLI undergoes a great expansion (Grindley *et al* 1997, Pratt *et al* 2000a), as does the domain of *Barhl2* within it as described in Chapter 3. This *Barhl2* domain can ordinarily be visualised as a region of expression stronger than that within the pTh-C and separated from it by the *Barhl2*-negative pTh-R. This domain of strong *Barhl2* expression was visible in the mutant embryo which had been exposed to the control vehicle alone, but it could not be distinguished in mutant

embryos which had been exposed to vismodegib. Within the caudal diencephalon of these embryos *Barhl2* appeared to be expressed in one continuous domain extending from the pretectum to a region corresponding with the rostral extent of the expanded ZLI. The strength of *Barhl2* expression within this domain also appeared to be uniform along its entire extent, with no regions of stronger expression corresponding with the positions of the pTh-C and expanded ZLI, and no region of weaker expression corresponding with the position of the pTh-R. This suggests that the loss of functional *Pax6* combined with the suppression of *Shh* signalling led to a disruption in the specification of these structures. Observation of vismodegib-treated control embryos showed that the inhibition of *Shh* signalling alone did not affect the development of the ZLI to as great an extent. Together these findings suggest a role for *Pax6* in the normal development of the ZLI.

A lateral expansion of the *Barhl2* domain within the pTh-C was observed in $Pax6^{Sey/Sey}$ mutants whether they had been exposed to vismodegib (outlined area, Fig. 6.6F) or to the vehicle control alone (Fig.6.5D). While *Pax6* is known to repress the expression of *Shh* (Caballero *et al* 2014), this finding suggests that the altered expression of *Barhl2* in the $Pax6^{Sey/Sey}$ mutant is independent of the interactions between *Pax6* and *Shh* signalling and is more likely to be a direct effect of the loss of functional *Pax6*. Further experiments would be required to determine whether or not there is a direct relationship between the expression of *Pax6* and that of *Barhl2*.

A number of the changes in morphology caused by the loss of functional *Pax6* were not observed in $Pax6^{Sey/Sey}$ embryos which had been exposed to vismodegib. While the mutant embryos which had been exposed to the control vehicle alone exhibited a reduction in the size of the telencephalic vesicles (asterisks, Fig. 6.5G) and an underdevelopment of the lateral and medial ganglionic eminences (asterisks, 6.5E) the telencephalic vesicles of the mutant treated with vismodegib appeared to be larger (asterisks, Fig.6.6L), and the ganglionic eminences were larger and more distinct from one another (asterisks, Fig. 6.6J). In addition to this the reduction in the thickness of the diencephalic neuroepithelium observed in the mutant exposed to the control vehicle alone (outlined area, Fig.6.5D) was not observed in the mutant treated with vismodegib (outlined area, Fig. 6.6F). Following early investigations into the

possibility of a mutually repressive relationship existing between *Pax6* and *Shh* in the CNS (Goulding *et al* 1993, Ericson *et al* 1997) it was shown that the loss of *Pax6* was sufficient to rescue the loss of ventral telencephalic structures in the *Shh*-null mutant mouse (Fuccillo *et al* 2006). The apparent rescue of defects of the *Pax6*-null mutant telencephalon by the suppression signalling of *Shh* is consistent with these findings.

Previous studies of the $Pax6^{Sey/Sey}$ diencephalon have shown that the loss of the habenula and a number of specification defects of the mutant diencephalon can be rescued via the suppression of *Shh* signalling (Chatterjee *et al* 2014). The findings described here suggest that the inhibition of *Shh* activity may also be able to rescue the reduced thickness of the diencephalic neuroepithelium in the $Pax6^{Sey/Sey}$ mutant mouse. Further experiments focused on specific defects may be able to confirm which defects are related to interactions between *Pax6* and *Shh* and the extent to which the *Pax6*-null phenotype can be rescued via the suppression of *Shh* signalling. The fact that the rescue of the $Pax6^{Sey/Sey}$ phenotype was more complete in the telencephalon than it was in the diencephalon suggests that the relationship between *Pax6* and *Shh* in the diencephalon is more complex than the apparent mutually repressive relationship which exists between them in the telencephalon. This possibility would be consistent with findings which suggest that suppression of *Shh* signalling is not sufficient to rescue some defects of the $Pax6^{Sey/Sey}$ diencephalon (Caballero *et al* 2014).

It is not clear why the development of vesicle-like structures was observed within the diencephalic neuroepithelium of the $Pax6^{Sey/Sey}$ embryos treated with vismodegib (asterisks, Fig. 6.6H, D and N). These structures developed in a region adjacent to the telencephalic choroid plexus and it is possible that they could have developed as a result of choroid plexus overgrowth. In mouse embryos in which *Shh* signalling is activated the telencephalic choroid plexus fails to develop, while in embryos in which *Shh* levels are reduced it increases in size, suggesting that the level of *Shh* signalling needs to be carefully regulated in order to ensure the correct development of the choroid plexus (Himmelstein *et al* 2010). The findings presented here also

support the hypothesis that choroid plexus growth may have a direct relationship with levels of *Shh* signalling activity.

The scarcity of material for these experiments presented a number of problems. It would have been preferable to use *Pax6*$^{+/+}$ embryos as controls rather than using both ungenotyped *Pax6*$^{+/+}$ and *Pax6*$^{+/Sey}$ embryos, because the expression of both *Pax6* and *Barhl2* in the *Pax6*$^{+/+}$ embryo was described in chapter 3 while the expression of both genes in the *Pax6*$^{+/Sey}$ embryo has not been described as comprehensively, here or in the literature. While the expression of *Barhl2* in the *Pax6*$^{+/Sey}$ forebrain does not appear to differ greatly from that in the wild type forebrain at E12.5 (Fig. 5.7), it may be possible to make more useful comparisons between the data from *Pax6*$^{+/+}$ embryos described in chapter 3, and *Pax6*$^{+/+}$ embryos exposed to vismodegib. Ideally a larger quantity of vismodegib would be used, allowing more pregnant females to be treated, and a greater number of *Pax6*$^{+/+}$ embryos to be harvested so *Pax6*$^{+/Sey}$ embryos would not have to be used.

Vismodegib has previously been shown to effectively inhibit *Shh* signalling at the dose used in this study (Caballero *et al* 2014) and in the data presented here, treated embryos exhibited altered morphology, suggesting that vismodegib was biologically active in treated mouse embryos and that it altered development at the 4mg dose which was administered. It may have been preferable to have utilised an observation of a change in molecular character rather than a change in morphology, and to have chosen a *bona fide* target of the *Shh* pathway to act as this marker. *Dbx1* is an example of a marker which could be used, as its expression has been shown to be abolished following the inhibition of *Shh* signalling by vismodegib (Caballero *et al* 2014). If the experiments described in this chapter were to be repeated with a greater quantity of material available, it would be preferable to cut a number of sections from each embryo and to perform *in situ* hybridization for *Dbx1* in order to confirm its absence from the ZLI and the inhibition of *Shh* signalling by vismodegib.

In order to make a better comparison between mRNA expression levels in treated and untreated embryos, it would have been preferable to carry out the colour reaction step of the chromogenic *in situ* hybridization protocol on all sections being treated using the same solution, and allowing the reaction to proceed for the same length of

time. If this were done, darker staining would be indicative of stronger mRNA expression and not of a longer development time or a more concentrated solution of NBT/BCIP, for example. More meaningful data could also be obtained by taking a quantitative approach and measuring mRNA or protein levels directly. In order to measure levels of *Barhl2* protein by Western blotting, for example, a suitable *Barhl2* antibody would have to be obtained.

7. The effects of *Shh* pathway activation on the expression of *Pax6* and *Barhl2* in the diencephalon

7.1 Introduction

In order to further investigate the interactions between *Barhl2*, *Pax6* and *Shh*, the technique of *in utero* electroporation was used to activate *Shh* signalling throughout the diencephalic neuroepithelium. The aim of this experiment was to investigate the effects of activating *Shh* signalling *in vivo* by analysing electroporated embryos to observe changes in the expression of *Pax6* and *Barhl2*, and to investigate the possibility of *Shh* signalling exerting context-dependent effects on the expression of both transcription factors.

The plasmids used in the following experiments were *cShh* pXeX and pTP6. *cShh* pXeX (Agarwala *et al* 2001) consists of an expression construct for chick (*Gallus gallus*) *Shh* (*cShh*) (Riddle *et al* 1993) inserted into the pXeX *Xenopus* vector (Johnson and Krieg 1994). The pTP6 plasmid encodes a tau-tagged form of green fluorescent protein (GFP) (Pratt et al 2000b).

E12.5 mouse embryos were electroporated *in utero* with an aqueous solution of the DNA plasmids *cShh* pXeX and pTP6. Control embryos were electroporated with pTP6 alone. In order to target different structures along the entire rostrocaudal extent of the diencephalon, broad paddle electrodes were used to target a broad region of neuroepithelium. Embryos were harvested a minimum of 24 hours post-electroporation, at E13.5, and dissected in order to isolate whole brains from the remaining embryonic tissue. Tissue was observed under fluorescence in order to detect GFP expression. The expression of GFP was used as an indicator that the electroporation had resulted in cells being transfected successfully and to identify the location of the electroporated area. Successfully electroporated embryos were fixed and cryosectioned before being treated with *in situ* hybridization.

In situ hybridization for *cShh* mRNA was carried out in order to confirm that the *cShh* construct was being transcribed and to determine the efficiency of the electroporation. *In situ* hybridization for *cShh* mRNA and immunostaining for GFP were carried out in order to determine the efficiency of co-electroporation. Double *in*

situ hybridization for *cShh* and endogenous mouse *Shh* (*mShh*) was carried out to determine the specificity of the *cShh* probe. The findings from these experiments were considered in the design of the experiments to investigate changes in gene expression induced by the activation of *Shh* signalling.

In addition to changes in *Pax6* and *Barhl2* expression, changes in *Ptch1* expression were also investigated. *Ptch1* is the receptor for *Shh* and a *bona fide* target gene which is known to be upregulated in response to *Shh* signalling activity (Marigo *et al* 1996) and for these reasons its expression can act as an indicator of *Shh* pathway activity.

A total of nine embryos electroporated with the *cShh* pXeX construct were analysed to detect changes in gene expression induced by the ectopic expression of *cShh*. For each of these nine embryos three series of cryosections were prepared. These series were treated with *in situ* hybridization for *Ptch1*, *Pax6* and *Barhl2* respectively, in addition to *in situ* hybridization for *cShh*. Two embryos which had been electroporated with the pTP6 construct alone served as controls. These embryos were also cryosectioned and three series of sections were prepared- these were treated with *in* situ hybridization for *Ptch1*, *Pax6* and *Barhl2* respectively, in addition to immunostaining for GFP.

7.2 Results

7.2.1 Co-electroporation efficiency

In the technique of *in utero* electroporation the embryo is often transfected with plasmids encoding a fluorescent protein. Treated embryos are then observed under fluorescence in order to detect fluorescence as a consequence of ectopic fluorescent protein expression. The observation of fluorescence within the treated embryo can then be used as confirmation that cells have been successfully transfected, and to determine the location of the electroporated area (Momose *et al* 1999).

The DNA plasmid *cShh* does not encode a fluorescent protein in addition to *cShh*. For this reason it was necessary to co-electroporate the plasmid with a second plasmid encoding a fluorescent protein. The plasmid *pTP6* expresses a tau-tagged

form of green fluorescent protein (GFP) under the control of a promoter which is active in all cells of the CNS (Pratt *et al* 2000b). The protein binds to microtubules and can be visualised throughout the cytoplasm of transfected cells, a property of the protein which allows transfected cells to be visualised with ease (Pratt et al 2000b). For these reasons *pTP6* was selected as the plasmid to be co-electroporated with *cShh* pXeX.

While the co-electroporation method can be useful as a means of identifying successfully electroporated cells, its usefulness is limited because transfected cells may not necessarily have been transfected with both plasmids. The efficiency of co-expression in this experiment was evaluated with the use of *in situ* hybridization to detect the expression of *cShh* along with immunostaining for GFP in order to identify regions of co-expression and regions in which cells had taken up just one of the two plasmids.

Within the electroporated area of neuroepithelium it was found that both *cShh* mRNA and GFP were strongly expressed 24 hours post-electroporation, but while both GFP protein and *cShh* mRNA could be detected in some regions of treated neuroepithelium (arrows. Fig. 7.1A and B), many regions were found to strongly express GFP protein with little to no *cShh* mRNA (daggers, Fig. 7.1A and B), and regions of neuroepithelium which expressed *cShh* mRNA but not GFP were also observed (asterisks, Fig. 7.1A and B). The area of ectopic *cShh* expression appeared to be broader than the region in which cells expressed GFP (Fig. 7.1C).

These observations suggested that not all cells were transfected with both plasmids during the process of electroporation and that GFP expression, while useful as an indicator of a successful electroporation and of the location of the electroporated area, may not be a reliable indicator of cells in which transfection of the *cShh* pXeX plasmid had been achieved.

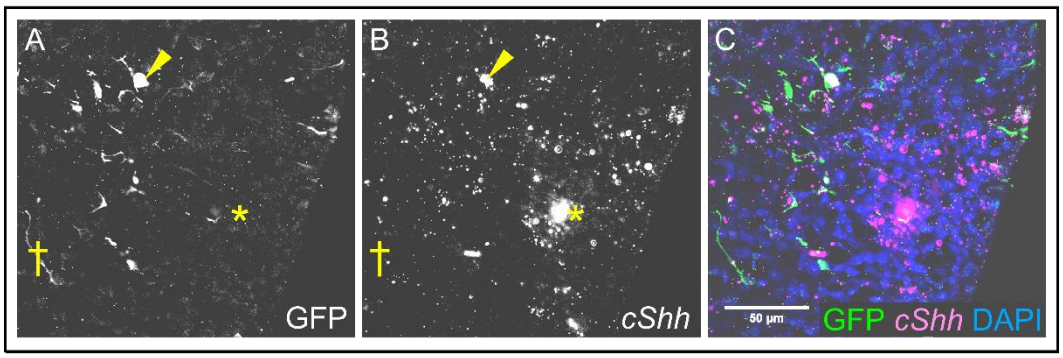

Fig.7.1: High magnification confocal image of a cryosection from an embryo electroporated with cShh *pXeX and* pTP6 *and treated with* in situ *hybridization for* cShh *and immunostaining for GFP. While some regions of neuroepithelium were successfully transfected with both GFP and* cShh *(arrow), a number of regions which expressed GFP did not express* cShh *mRNA (dagger) and* cShh *mRNA was in was detected in regions of neuroepithelium where GFP was not expressed (asterisk).*

For this reason it was decided that the detection of *cShh* mRNA via *in situ* hybridization would be a more reliable indicator that cells had been successfully transfected with the *cShh* pXeX plasmid.

For the remainder of the experiments described in this chapter, the pTP6 tau GFP plasmid was co-electroporated with *cShh* pXeX in order to allow the electroporated area to be visualised in harvested forebrain tissue, while experiments carried out to analyse electroporated tissue by *in situ* hybridization employed the *cShh* riboprobe. Electroporation with the pTP6 plasmid alone was used to generate control embryos, which were analysed with *in situ* hybridization for *Pax6*, *Barhl2* or *Ptch1* mRNA along with immunostaining for GFP to visualise the electroporated area. A total of two control embryos were produced and analysed in this manner.

7.2.2 Electroporation efficiency

Training in the thalamic transillumination electroporation method was provided by the Lab for Molecular Mechanisms of Thalamus Development at The Riken Brain Science Institute, Wako-shi, Saitama, Japan. The method was performed as described by Matsui *et al* (2011) on CD-1® embryos at E10.5-E13.5 in accordance with the Law for the Humane Treatment and Management of Animals (Japan 2009) (Hau and Schapiro 2010). In this method the embryo is illuminated with a cold light source via

a fibre optic cable, the end of which is placed in direct contact with the uterine wall, and the whelp is manipulated into the optimum position for the injection of plasmid DNA and the application of the current. In order to prevent damage to the tissue a muscle relaxant drug is administered to prevent the smooth muscle of the uterus contracting, ensuring the tissue of the uterus remains pliable and can be manipulated without causing damage. The method also involves the use of injectable anaesthesia rather than gaseous anaesthesia administered via a facemask, which allows the surgeon to change to position of the animal during surgery in order to achieve the optimum position, rather than having to manipulate the uterus itself.

For surgery performed in the UK the use of injectable anaesthesia and muscle relaxants are not permitted under the Animals (Scientific Procedures) Act 1986. For this reason it was required to develop a modified form of the method. Because of the requirement to use gaseous anaesthesia administered via a facemask the position of the animal could not be altered during surgery, and because muscle relaxant drugs could not be used, the smooth muscle of the uterine wall would contract, becoming more rigid and more difficult to manipulate into the optimum position for transillumination, the injection of plasmid DNA and the application of the current.

Attempts to perform the transillumination method at E11.5 and earlier were unsuccessful. The small size of embryos at E11.5 and earlier made it difficult to distinguish their morphological features without the use of transillumination, but attempts to manipulate embryos into the correct position in relation to the fibre optic cable, without the ability to change the position of the animal, required the tissue to be handled to an unacceptable degree, causing tissue damage and haemorrhaging.

For embryos at E12.5 and later it was found that, due to the increased size of the embryo and the morphological features being easier to distinguish, adequate illumination could be provided by a fibre optic light source placed above the embryo, rather than via a light source placed in direct contact with the tissue. Transillumination of these embryos was therefore not required, and the use of a light source placed above the embryo minimised the need to handle the uterine tissue to the degree that tissue damage and haemorrhaging could be avoided.

In situ hybridization for *cShh* mRNA was performed on sections from embryos which had been electroporated with the *cShh* pXeX plasmid via the modified method described above. These experiments employed a riboprobe for *cShh* which had been synthesised from the *cShh* pXeX plasmid itself (Agarwala *et al* 2001).

Double *in situ* hybridization for *cShh* and *mShh* was carried out on cryosections sections from an embryo electroporated with *cShh* pXeX in order to confirm that the *cShh* riboprobe did not bind to endogenous *mShh* and could therefore be used as a marker of the electroporated area, and an indicator of cells in which *cShh* was being transcribed. Expression of *cShh* mRNA within the treated embryos also confirmed that the ectopic *cShh* DNA was being transcribed 24 hours following the electroporation (Fig. 7.2).

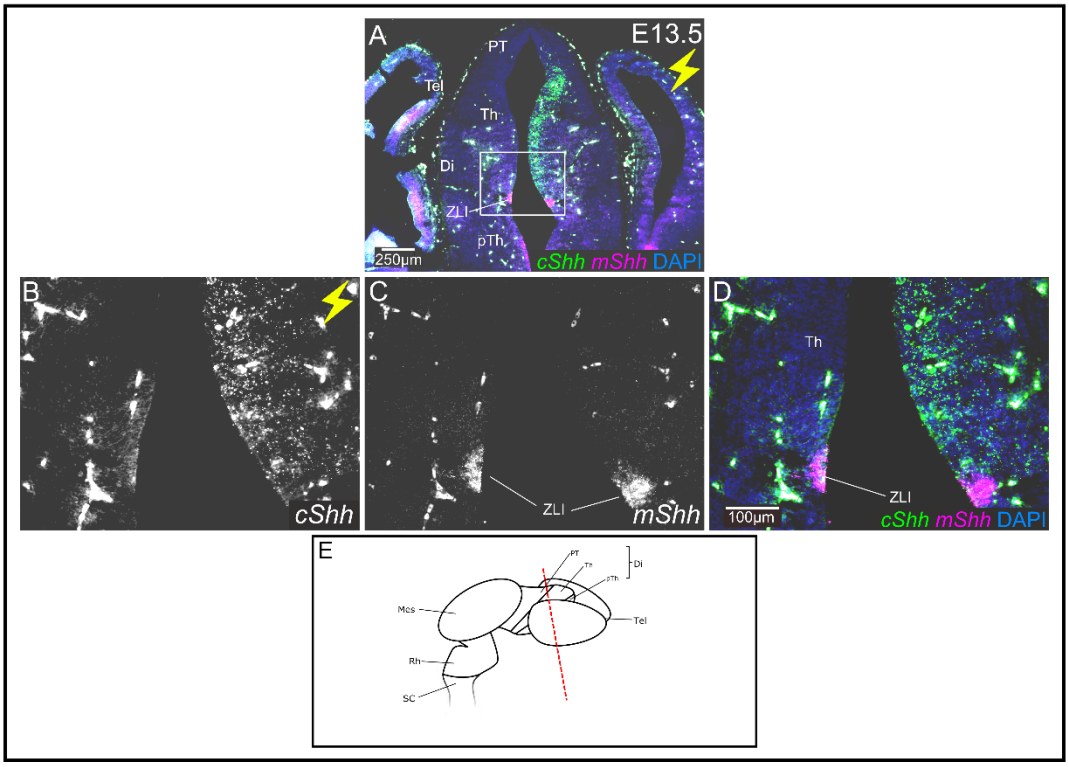

Fig. 7.2: A: A section from an embryo electroporated with cShh *pXeX and treated with double* in situ *hybridization for* cShh *mRNA and* mShh *mRNA. B-D: Detail of outlined area in A. E: Schematic to illustrate the approximate plane of section. The lightning flashes denote the electroporated side of the embryo. Abbreviations: Di- diencephalon; PT- pretectum; Th- thalamus; pTh- prethalamus; Tel- telencephalon; ZLI-* zona limitans intrathalamica*; Mes- mesencephalon; Rh- rhombencephalon; SC- spinal cord.*

Following neural tube closure at E9.5 the diencephalic lumen is relatively broad (Fig. 3.2.2) but over the course of development it becomes progressively narrower, and by E12.5 (Fig. 3.3.5) it has narrowed to such an extent that regions of the ventricular surfaces on either side of the lumen come into contact with each other at several points. When the plasmid DNA solution is injected into the lumen it does not always make direct contact with the neuroepithelium in these regions, and for this reason the electroporation of some diencephalic regions proved to be more challenging than the electroporation of others (Fig. 7.3).

Structures which are more difficult to electroporate at later developmental stages include more rostral regions of the thalamus, in which the diencephalic lumen is particularly narrow, while structures closer to broader regions of the lumen, such as the prethalamus and pretectum, can be electroporated with relative ease and transfection with DNA plasmids is more efficient (arrows, Fig. 7.3G). The limited efficiency of electroporation in the rostral thalamus made it necessary to electroporate a greater number of embryos in order to ensure that enough samples of electroporated thalamic tissue could be obtained.

For embryos electroporated with both *cShh* pXeX and pTP6 the position of the electroporated area was determined by the expression of *cShh* as detected by *in situ* hybridization. For embryos electroporated with pTP6 alone electroporated tissue was identified by the expression of GFP as detected by immunohistochemistry. The structures which were successfully electroporated in each of these embryos are summarised in Table 7.1.

Of the embryos electroporated with both *cShh* pXeX and pTP6 it was found that the pretectum had been successfully electroporated in eight embryos, with particularly strong expression of *cShh* mRNA being detected in cryosections cut from the caudal diencephalon- these were the embryos numbered 1, 2, 3, 4, 5, 7, 8 and 9 under "*cShh* pXeX" in Table 7.1. Caudal sections from these embryos were analysed for changes in expression of *Ptch1*, *Pax6* and *Barhl2* within the pretectum.

Six of the embryos electroporated with both *cShh* pXeX and pTP6 were found to have been successfully electroporated in a region of the medial diencephalon

including the ZLI and the tissues immediately adjacent to it in the thalamus and prethalamus- these were the embryos numbered 1, 3, 4, 5, 6 and 9 under "*cShh* pXeX" in Table 7.1. Medial sections from these embryos were analysed for changes in the expression of *Ptch1*, *Pax6* and *Barhl2* within the thalamus, ZLI and prethalamus.

In the figures which follow, each embryo which was analysed following electroporation with both *cShh* pXeX and pTP6 is referred to as "*cShh* pXeX" followed by the embryo number.

Of the two embryos electroporated with pTP6 alone to serve as experimental controls, described under "pTP6" in Table 7.1, only one embryo was found to have been electroporated over a region of neuroepithelium broad enough to include a substantial area of the pretectum. While the second embryo was also found to have been electroporated within the pretectum, the electroporated area was much smaller and the immunostaining for GFP performed on sections from this embryo was not strong enough to allow for the recording of high quality image data. For these reasons, changes in the expression of *Ptch1*, *Pax6* and *Barhl2* were investigated in caudal sections from the first of the two embryos electroporated with pTP6 alone.

Within the first of the two embryos electroporated with pTP6 alone, a region of the medial diencephalon including the ZLI and the regions of the prethalamus and pretectum adjacent to it was also found to have been successfully electroporated. Medial sections from this embryo were analysed for changes in the expression of *Ptch1*, *Pax6* and *Barhl2* within the thalamus, ZLI and prethalamus.

In the figures which follow, sections from the embryo electroporated with pTP6 alone are labelled "pTP6 control".

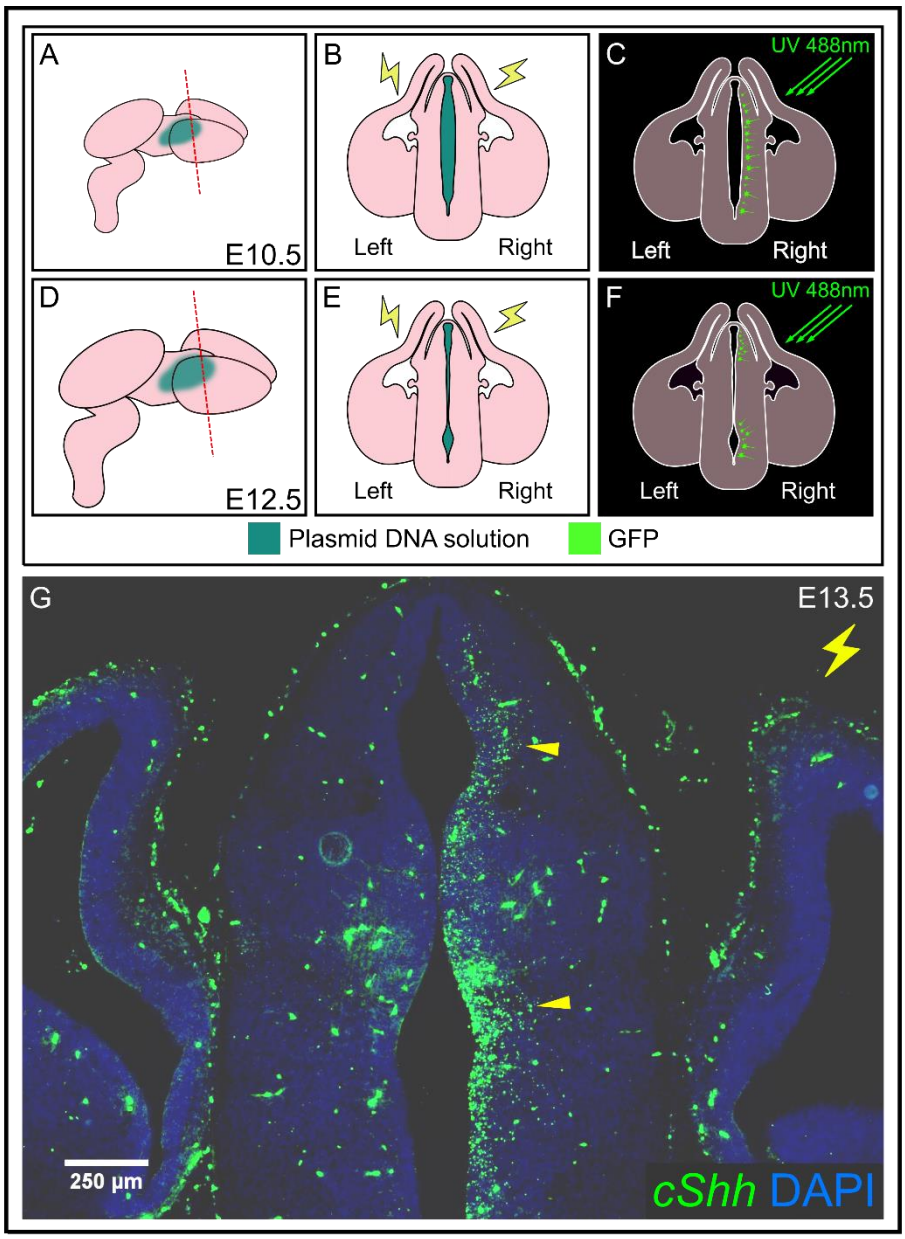

Fig. 7.3: A-C: At early developmental stages plasmid DNA solution injected into the diencephalic lumen is in contact with most of the neuroepithelium at the ventricular surface and cells can be successfully transfected with the plasmids. D-F: At later developmental stages cells which are adjacent to the lumen at points where it has narrowed are not electroporated as efficiently as those in contact with the plasmid DNA solution. G: Coronal cryosection from an embryo electroporated on the right-hand side with cShh pXeX *at E12.5 and treated with* in situ *hybridization for* cShh *mRNA at E13.5. The lightning flash denotes the electroporated side of the embryo. cShh* expression is strongest in the regions of neuroepithelium which were immediately adjacent to the open regions of the lumen at E12.5, and therefore in direct contact with the DNA solution within the lumen (arrows).

Structure electroporated		cShh pXex/pTP6									pTP6	
		1	2	3	4	5	6	7	8	9	1	2
Rostral diencephalon	Pretectum	✗	✗	✗	✗	✗	✗	✗	✗	✓	✗	✗
	pTh -C	✗	✗	✗	✗	✗	✓	✗	✗	✓	✓	✗
	pTh -R	✗	✗	✓	✓	✓	✓	✗	✗	✓	✓	✗
	ZLI	✗	✗	✓	✓	✓	✓	✗	✗	✓	✓	✗
	pTh	✗	✗	✓	✓	✓	✓	✗	✗	✗	✓	✗
Medial diencephalon	Pretectum	✗	✗	✗	✗	✗	✗	✓	✓	✓	✓	✗
	pTh -C	✓	✓	✗	✗	✓	✗	✓	✓	✓	✓	✗
	pTh -R	✓	✗	✓	✓	✓	✓	✗	✗	✓	✓	✗
	ZLI	✓	✗	✓	✓	✓	✓	✗	✗	✓	✓	✗
	pTh	✓	✗	✓	✓	✓	✓	✓	✗	✗	✓	✗
Caudal diencephalon	Pretectum	✓	✓	✓	✗	✓	✓	✓	✓	✓	✓	✓
	Thalamus	✓	✓	✓	✓	✓	✓	✓	✓	✓	✓	✓
	Hypothalamus	✗	✓	✗	✓	✗	✗	✗	✗	✗	✗	✗

Table 7.1: The regions of neuroepithelium which were successfully electroporated within the diencephalon of the nine embryos electroporated with the cShh *pXeX construct and pTP6, as determined by the expression of* cShh *mRNA detected via* in situ *hybridization, and the structures which were successfully electroporated within the diencephalon of the two control embryos electroporated with pTP6 alone, as determined by the expression of GFP detected via immunohistochemistry.*

7.2.3 Analysis of control experiments

In the pTP6 control embryo, no changes in the expression of *Ptch1*, *Pax6* or *Barhl2* appeared to have been induced.

Within the electroporated side of the pretectum in a caudal section of the pTP6 control embryo (lightning flash, Fig. 7.4B) *Ptch1* expression did not appear to have been induced and it was not detected in either the unelectroporated control side of the embryo or the electroporated side (Fig. 7.4C).

In a medial section from the pTP6 control embryo no changes in *Ptch1* expression appeared to have been induced on the electroporated side (lightning flash, Fig. 7.5B). Expression of *Ptch1* appeared to be broadly symmetrical and its expression on the electroporated side did not appear to differ from its expression on the unelectroporated control side (Fig. 7.5C), suggesting that the electroporation had not altered its expression in the thalamus, prethalamus or ZLI.

Expression of *Pax6* also appeared to have been unchanged by the electroporation. Within the electroporated side of the pretectum (lightning flash, Fig. 7.4E) no increase or decrease in the strength of *Pax6* was apparent (Fig. 7.4F). Within the electroporated side of the diencephalon in a medial section from the control embryo (lightning flash, Fig. 7.5E) expression of *Pax6* appeared broadly symmetrical and did not appear to have been altered within the thalamus, ZLI or prethalamus (Fig. 7.5F).

Within the electroporated side of the pretectum in a caudal section from the pTP6 control (lightning flash, Fig. 7.4H) *Barhl2* expression could not be detected and it did not appear to have been induced by the electroporation (Fig. 7.4I). Within the electroporated side of a medial section from the pTP6 control embryo (lightning flash, Fig. 7.5H) the expression of *Barhl2* appeared to be broadly symmetrical and no changes in its expression were noted within the thalamus, prethalamus or ZLI (Fig. 7.5I).

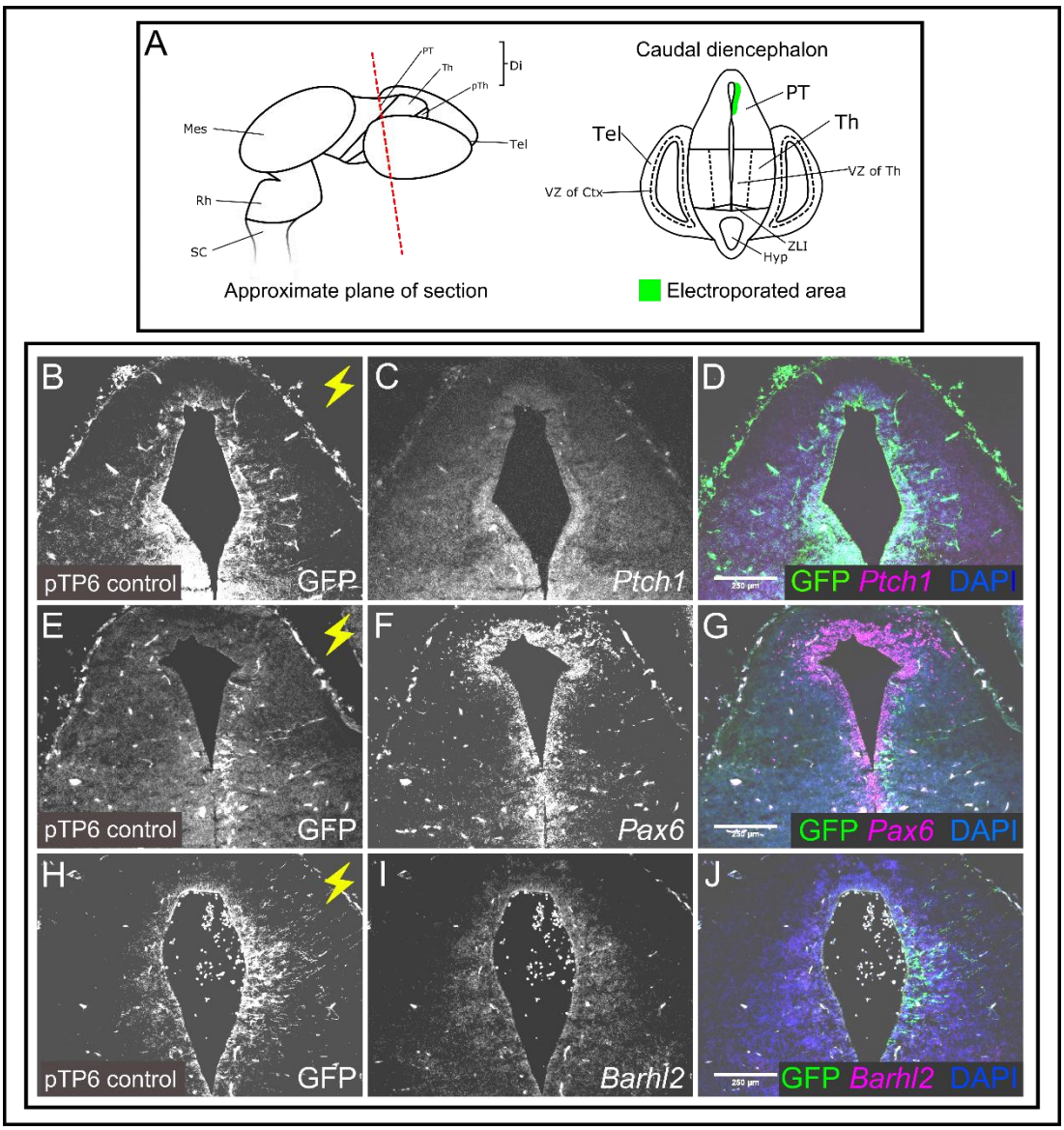

Fig. 7.4: Analysis of gene expression within the pretectum of the experimental control embryo electroporated with pTP6 alone. *A: Schematics to illustrate the approximate plane of section and the approximate position of the electroporated area. B-D: Section treated with immunohistochemistry for GFP and* in situ *hybridization for* Ptch1 *mRNA, in which no* Ptch1 *mRNA could be detected in the electroporated area or in the untreated neuroepithelium. E-G: Section treated with immunohistochemistry for GFP and* in situ *hybridization for* Pax6 *mRNA. H-J: Section treated with immunohistochemistry for GFP and* in situ *hybridization for* Barhl2 *mRNA, in which no* Barhl2 *mRNA could be detected in the electroporated area or in the untreated neuroepithelium. The lightning flashes denote the electroporated side of the embryo. Abbreviations: Tel- telencephalon; Di- diencephalon; PT- pretectum; Th- thalamus; pTh- prethalamus; Mes- mesencephalon; Rh- rhombencephalon; SC-spinal cord; VZ-ventricular zone; ZLI-* zona limitans intrathalamica*; Hyp- hypothalamus; Ctx- cortex.*

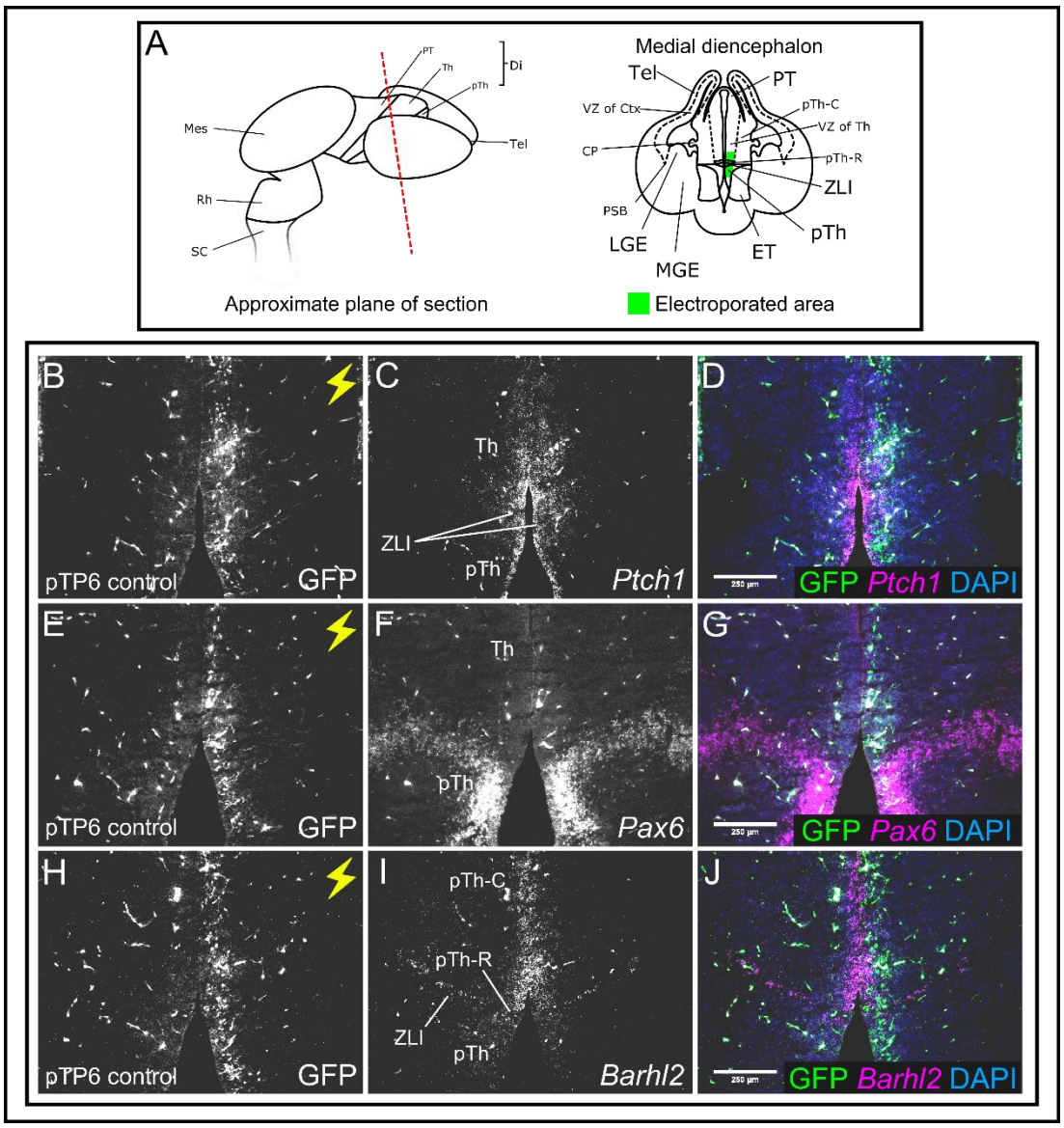

Fig. 7.5: Analysis of gene expression within the thalamus, ZLI and prethalamus of the experimental control embryo electroporated with pTP6 alone. *A: Schematics to illustrate the approximate plane of section and the approximate position of the electroporated area. B-D: Section treated with immunohistochemistry for GFP and* in situ *hybridization for* Ptch1 *mRNA. E-G: Section treated with immunohistochemistry for GFP and* in situ *hybridization for* Pax6 *mRNA*. *H-J: Section treated with immunohistochemistry for GFP and* in situ *hybridization for* Ptch1 *mRNA. The lightning flashes denote the electroporated side of the embryo. Abbreviations: Tel- telencephalon; Di- diencephalon; PT- pretectum; Th- thalamus; pTh- prethalamus; Mes- mesencephalon; Rh- rhombencephalon; SC-spinal cord; VZ- ventricular zone; ZLI-* zona limitans intrathalamica*; Hyp- hypothalamus; Ctx- cortex. LGE- lateral ganglionic eminence; MGE- medial ganglionic eminence; CP- choroid plexus; PSB- pallial-subpallial boundary.*

7.2.4 The effects of ectopic *cShh* expression on *Ptch1* expression

Following experimental confirmation that the *cShh* protein is ectopically expressed by cells which have been transfected with the *cShh* pXeX plasmid it was necessary to confirm that the translated *cShh* protein was biologically active in mouse and that any effects it exerted on the neuroepithelium of the mouse were comparable to those of endogenous murine *Shh*.

For these experiments the expression of *Ptch1* was investigated. *Ptch1* is a *bona fide* target gene of the *Shh* signalling pathway and its expression is known to be upregulated by *Shh* (Marigo *et al* 1996). Upregulation of *Ptch1* is therefore an indicator of *Shh* pathway activation and the observation of changes in its expression within the electroporated area can be used to determine whether or not the *cShh* construct is biologically active in mouse, and if it is active, the areas of neuroepithelium in which it is active, and the range of the *cShh* signal in those areas.

A series of cryosections cut from embryos which had been electroporated with *cShh* pXeX were treated with double fluorescence *in situ* hybridization for *Ptch1* and *cShh*. Sections from a total of nine different embryos were treated in this way and analysed to observe changes in *Ptch1* expression.

In embryos electroporated with the *cShh* pXeX plasmid upregulation of *Ptch1* was observed, confirming that the *cShh* protein encoded by the plasmid is able to activate the *Shh* signalling pathway in mouse, but this upregulation of *Ptch1* was only observed within particular diencephalic structures, while in others the ectopic expression of *cShh* had no noticeable effect on *Ptch1* expression.

Eight embryos were found to have been successfully electroporated in a region including the pretectum (Table 7.1). Data for changes in *Ptch1* expression was successfully obtained from seven of these embryos (Fig. 7.6 and 7.7), while the *in situ* signal in an eighth was found to be of insufficient strength to allow high quality image data to be recorded.

Within the electroporated side of the pretectum in caudal sections (lightning flashes, Fig. 7.6B, E, H and K, and Fig. 7.7B, E and H) an upregulation of *Ptch1* was

observed in all seven embryos for which *Ptch1* expression data was obtained (Fig. 7.6C, F, I and L, and Fig. 7.7C, F and I). This upregulation was observed even in the two embryos in which the ectopic expression of *cShh* was relatively weak on the electroporated side (lightning flashes, Fig. 7.6B and K).

The strength of the *Ptch1* upregulation varied greatly. On the electroporated side of embryo 8 (lightning flash, Fig. 7.7E), a relatively weak upregulation of *Ptch1* was observed (Fig. 7.7F), and this may have due to the small size of the electroporated area. On the electroporated side of embryo 3 (lightning flash, Fig. 7.6E) a weak upregulation of *Ptch1* was also observed (Fig. 7.6F) and in this case it may have been due to the ectopic expression of *cShh* being relatively weak.

On the electroporated side of embryo 1 (lightning flash, Fig. 7.6B) a slightly stronger upregulation of *Ptch1* was observed. Endogenous *Ptch1* mRNA was detected on the unelectroporated side, but its expression was noticeably stronger on the electroporated side (Fig. 7.6C). A similar increase in the strength of *Ptch1* expression was noted on the electroporated side of embryo 6 (lightening flash, Fig. 7.6K), with the expression of *Ptch1* appearing to be stronger than on the unelectroporated side (Fig. 7.6L).

On the electroporated side of embryo 5 (lightning flash, Fig. 7.6H) a strong upregulation of *Ptch1* was observed, in contrast to the unelectroporated side on which little to no *Ptch1* mRNA was detected (Fig. 7.6I). Data for this embryo are presented at a higher resolution in Fig. 7.8. On the electroporated side (lightning flash, Fig. 7.8B) strong expression of *cShh* mRNA could be detected along the majority of the ventricular surface of the pretectum, and the lateral extent of this expression was relatively far from the ventricular surface (arrows, Fig. 7.8B). A strong upregulation of *Ptch1* was observed within this *cShh*-expressing area (Fig. 7.8C), with its lateral extent closer to the ventricular surface than that of the region of ectopic *cShh* expression (Fig. 7.8D).

On the electroporated side of embryo 7 (lightning flash, Fig. 7.7B) a strong upregulation of *Ptch1* was also observed (Fig. 7.7C). Data for this embryo are presented at a higher resolution in Fig. 7.9. On the electroporated side (lightning

flash, Fig. 7.9B) expression of ectopic *cShh* was more diffuse than in embryo 5, and did not extend as far dorsally. The upregulation of *Ptch1* was confined to this area and did not extend beyond the dorsal extent of the region of *cShh* expression, and while some endogenous *Ptch1* mRNA was detected on the unelectroporated side of the embryo, in the most ventral region of the pretectum, expression of *Ptch1* was still stronger in this region of the electroporated side (Fig. 7.9C). As in embryo 5, the lateral extent of the region of ectopic *cShh* expression was slightly further away from the ventricular surface than the extent of the region of neuroepithelium in which *Ptch1* was upregulated (Fig. 7.9D).

On the electroporated side of embryo 9 (lightning flash, Fig. 7.7H) a strong upregulation of *Ptch1* was also observed (Fig. 7.7I). Data for this embryo are presented at a higher resolution in Fig. 7.10. This strong upregulation of *Ptch1* (Fig. 7.10C) was observed despite the expression of ectopic *cShh* on the electroporated side (lightning flash, Fig. 7.10B) appearing to be weaker than in embryo 5 and embryo 7. In this embryo little to no endogenous *Ptch1* mRNA was detected on the unelectoporated side (Fig. 7.10C), in contrast with the strong expression of *Ptch1* expression on the electroporated side. As with embryo 5 and embryo 7, the region in which *cShh* was expressed appeared to slightly overlap the region in which *Ptch1* upregulation was observed along the mediolateral axis (Fig. 7.10D).

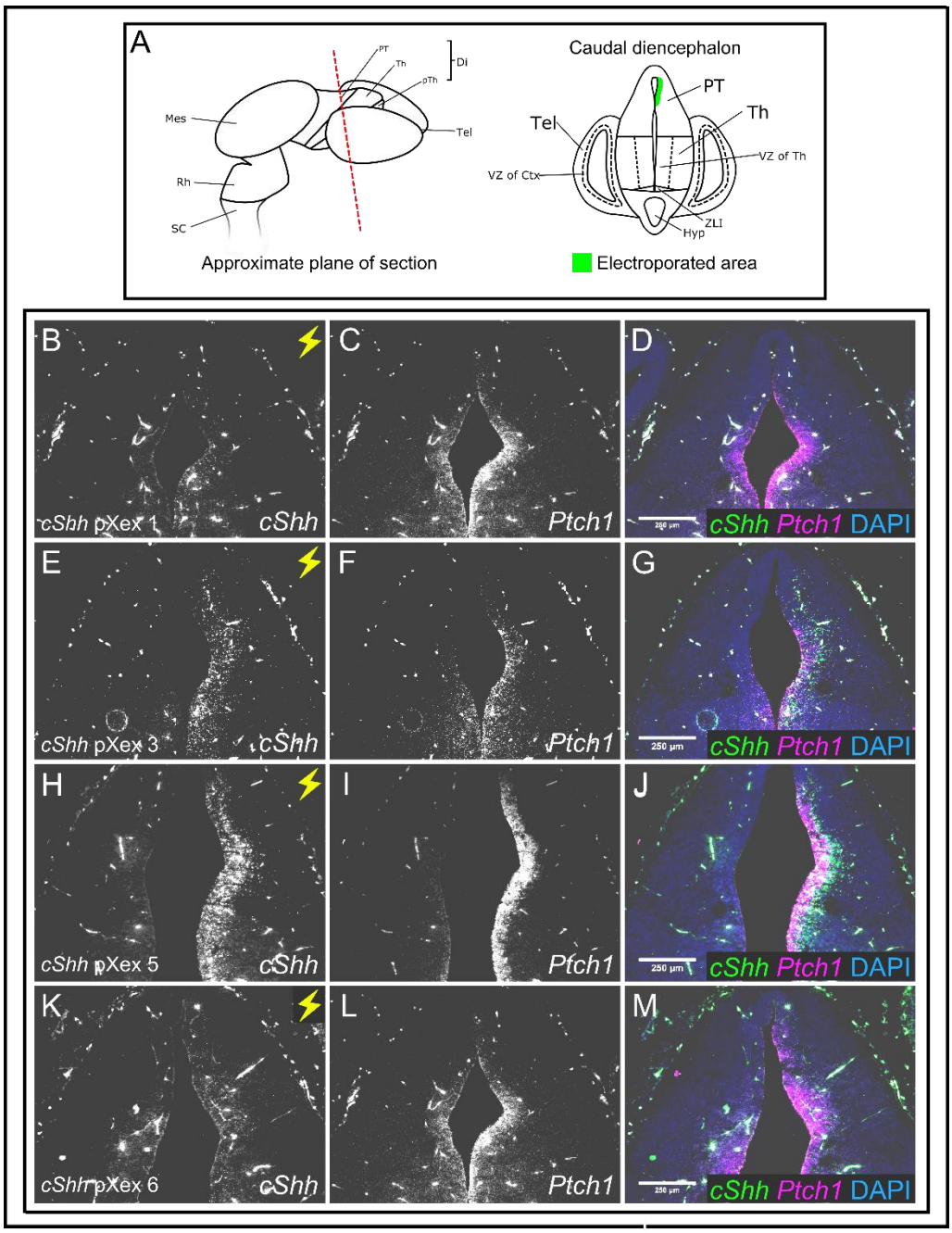

Fig. 7.6: Analysis of changes in Ptch1 *expression in the pretectum of embryos electroporated with* cShh *pXeX by double* in situ *hybridization for* Ptch1 *and* cShh mRNA. A: Schematics *to illustrate the approximate plane of section and the approximate position of the electroporated area. B-D: Data for embryo 1. E-G: Data for embryo 3. H-J: Data for embryo 5. K-M: Data for embryo 6. The lightning flashes denote the electroporated side of the embryo. Abbreviations: Tel- telencephalon; Di- diencephalon; PT- pretectum; Th- thalamus; pTh- prethalamus; Mes- mesencephalon; Rh- rhombencephalon; SC-spinal cord; VZ- ventricular zone; ZLI-* zona limitans intrathalamica*; Hyp- hypothalamus; Ctx- cortex.*

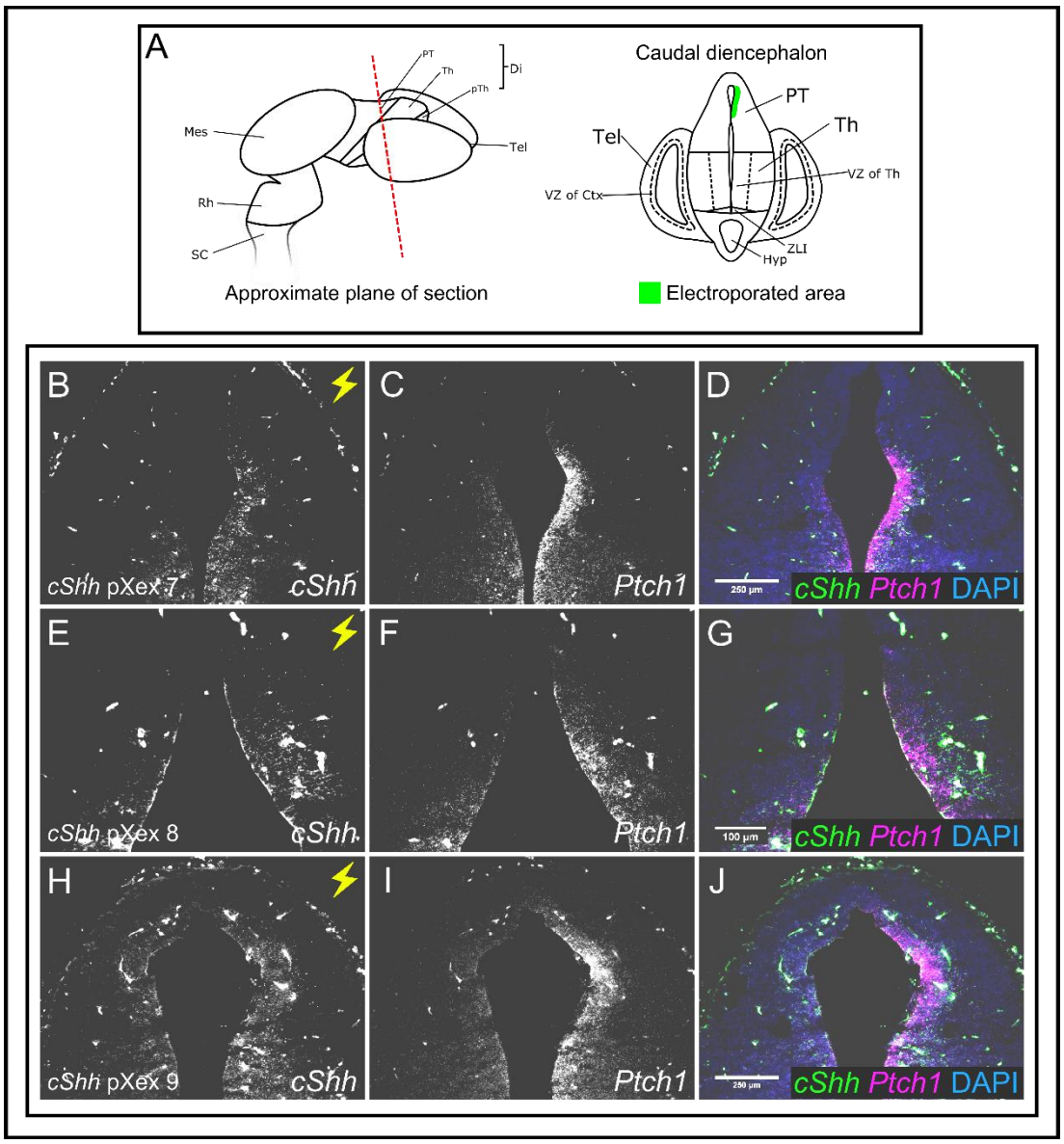

Fig. 7.7: Analysis of changes in Ptch1 *expression in the pretectum of embryos electroporated with* cShh *pXeX by double* in situ *hybridization for* Ptch1 and cShh mRNA. A: Schematics *to illustrate the approximate plane of section and the approximate position of the electroporated area. B-D: Data for embryo 7. E-G: Data for embryo 8. H-J: Data for embryo 9. The lightning flashes denote the electroporated side of the embryo. Abbreviations: Tel- telencephalon; Di- diencephalon; PT- pretectum; Th- thalamus; pTh- prethalamus; Mes- mesencephalon; Rh- rhombencephalon; SC-spinal cord; VZ- ventricular zone; ZLI-* zona limitans intrathalamica*; Hyp- hypothalamus; Ctx- cortex.*

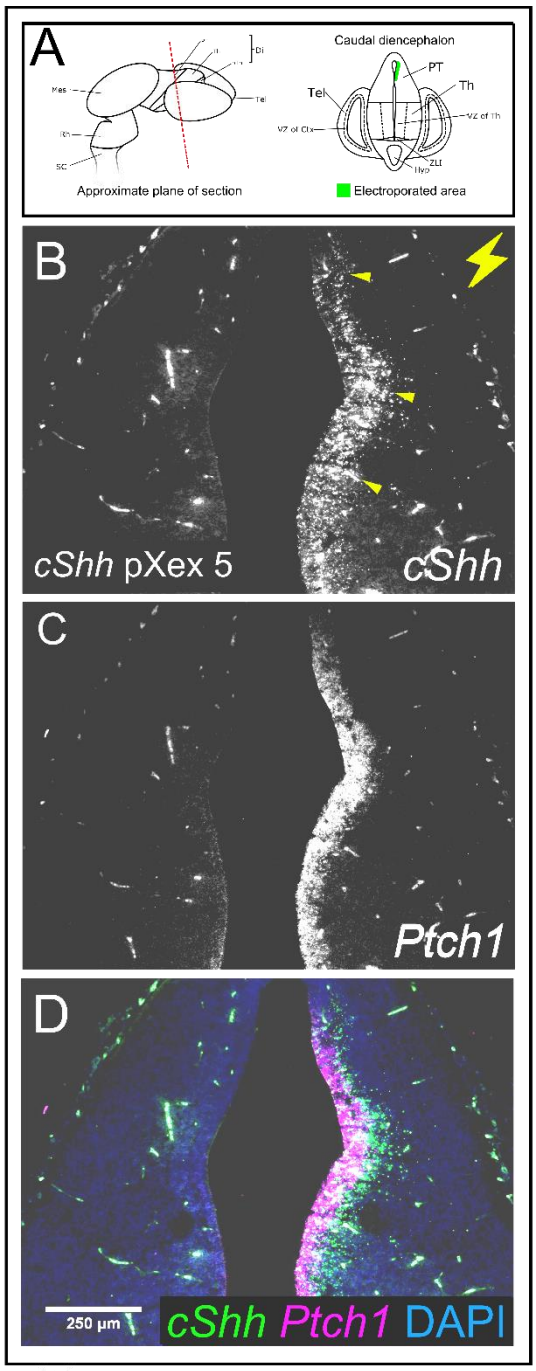

Fig. 7.8: Detail of embryo 5, caudal section. A: Schematic to illustrate the position of the electroporated area. B: In situ *hybridization data for* cShh *mRNA. The lightening flash denotes the electroporated side of the embryo. The arrows indicate areas in which cells were transfected. C:* In situ *hybridization data for* Ptch1*. D:* In situ *hybridization data for both* cShh and Ptch1*. Abbreviations: Tel- telencephalon; Di- diencephalon; PT- pretectum; Th- thalamus; pTh- prethalamus; Mes- mesencephalon; Rh- rhombencephalon; SC-spinal cord; VZ- ventricular zone; ZLI-* zona limitans intrathalamica*; Hyp- hypothalamus; Ctx- cortex.*

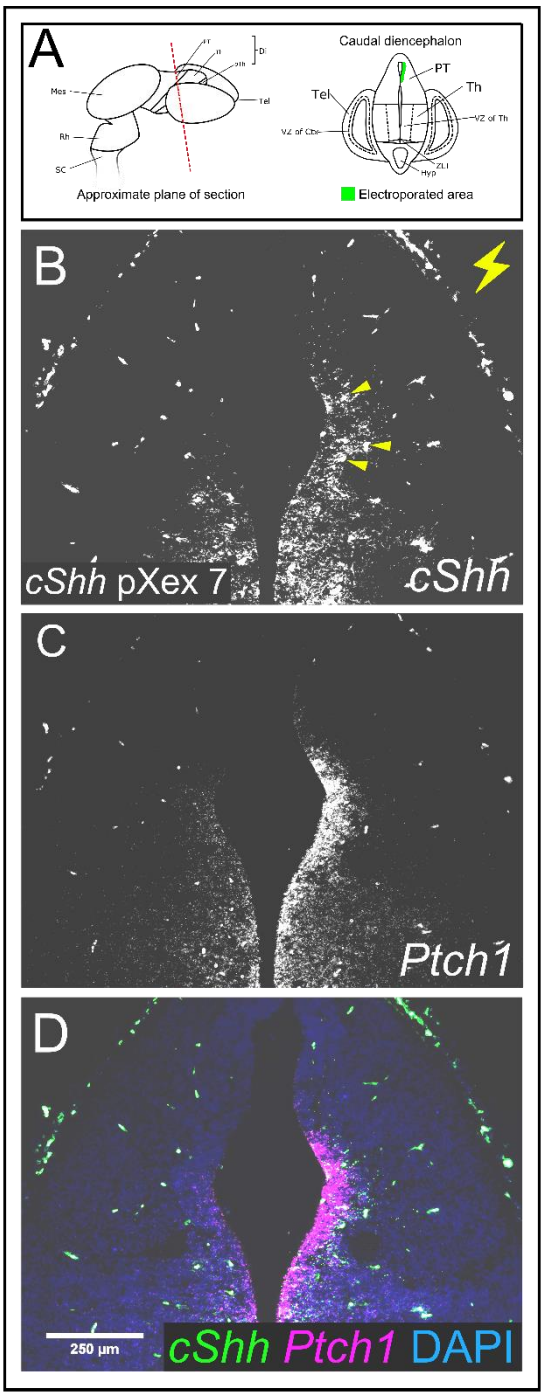

Fig. 7.9: Detail of embryo 7, caudal section. A: Schematic to illustrate the position of the electroporated area. B: In situ *hybridization data for* cShh *mRNA. The lightening flash denotes the electroporated side of the embryo. The arrows indicate areas in which cells were transfected. C:* In situ *hybridization data for* Ptch1*. D:* In situ *hybridization data for both* cShh and Ptch1*. Abbreviations: Tel- telencephalon; Di- diencephalon; PT- pretectum; Th- thalamus; pTh- prethalamus; Mes- mesencephalon; Rh- rhombencephalon; SC-spinal cord; VZ- ventricular zone; ZLI-* zona limitans intrathalamica*; Hyp- hypothalamus; Ctx- cortex.*

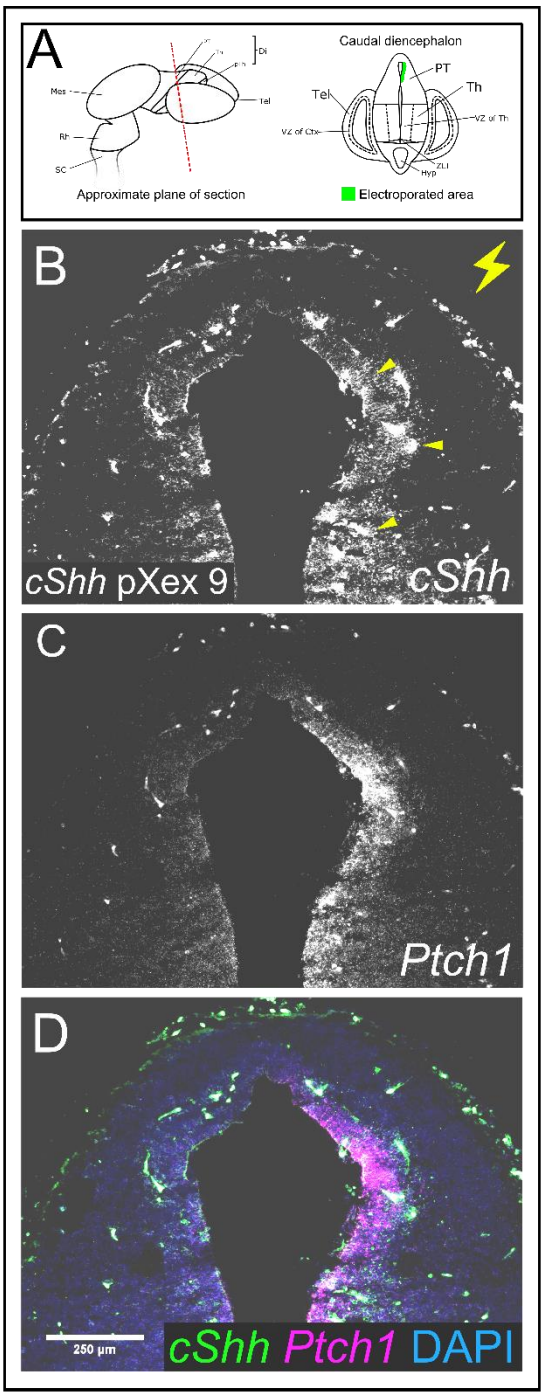

Fig. 7.10: Detail of embryo 9, caudal section. A: Schematic to illustrate the position of the electroporated area. B: In situ *hybridization data for* cShh *mRNA. The lightening flash denotes the electroporated side of the embryo. The arrows indicate areas in which cells were transfected. C:* In situ *hybridization data for* Ptch1*. D:* In situ *hybridization data for both* cShh and Ptch1*. Abbreviations: Tel- telencephalon; Di- diencephalon; PT- pretectum; Th- thalamus; pTh- prethalamus; Mes- mesencephalon; Rh- rhombencephalon; SC-spinal cord; VZ- ventricular zone; ZLI-* zona limitans intrathalamica*; Hyp- hypothalamus; Ctx- cortex.*

Data for *Ptch1* expression was obtained from all six embryos which had been successfully electroporated in a region of the medial diencephalon including the thalamus, ZLI and pretectum (Fig. 7.11 and 7.12).

As with the pretectum of treated embryos, upregulation of *Ptch1* mRNA was observed within the electroporated area of medial sections from the six embryos electroporated with *cShh* pXeX within the thalamus, ZLI and prethalamus (lightning flashes, Fig. 7.11 B, E and H, and Fig. 7.12, B, E and H), but not in all regions of the neuroepithelium within the electroporated area.

Ptch1 is not ordinarily expressed within the ZLI (Caballero *et al* 2014) and it was also found to be absent from the ZLI in all six embryos in which the neuroepithelium of the ZLI had been electroporated with *cShh* pXeX (arrows, Fig. 7.11C, F and I, and Fig. 7.12 C, F and I).

On the electroporated side of embryo 3 (lightning flash, Fig. 7.11E) no upregulation of *Ptch1* was apparent in either the thalamus or pretectum (Fig. 7.11F) and the expression domains of *Ptch1* in this embryo appeared to be broadly symmetrical. This may have been due to the relatively weak expression of ectopic *cShh* within the electroporated area.

On the electroporated side of embryo 9 (lightning flash, Fig. 7.12H) the expression domains of *Ptch1* observed in embryo 9 also appeared to be broadly similar, with no apparent change in Ptch1 expression levels on the electroporated side (Fig. 7.12I). As with embryo 3, the electroporated area of embryo 9 did not strongly express *cShh* and this may be the reason why no change in *Ptch1* expression was observed.

On the electroporated side of embryo 6 (lightning flash, Fig. 7.12E) a slight upregulation of *Ptch1* was observed in the thalamus, while no change in the level of *Ptch1* expression was apparent in the prethalamus (Fig. 7.12F), despite the expression of *cShh* being stronger than it appeared to have been in embryo 3 and embryo 9. In this embryo a region of the medial ganglionic eminence (MGE) was also electroporated and an upregulation of *Ptch1* was observed in this area (Fig. 7.12F).

On the electroporated side of embryo 4 (lightning flash, Fig. 7.11H) *cShh* expression was particularly strong within the prethalamus. A slight upregulation of *Ptch1* was observed in the thalamus, with a stronger upregulation of *Ptch1* in the prethalamus (Fig. 7.11I). The region of strong *Ptch1* upregulation in the prethalamus corresponded with the position of the neuroepithelium in which ectopic *cShh* expression was particularly strong (Fig. 7.11J).

Within the electroporated area of embryo 5 (lightning flash, Fig. 7.12B) a strong upregulation of Ptch1 was observed in the thalamus (Fig. 7.12C) Data for this embryo are presented at a higher resolution in Fig. 7.13. On the electroporated side of this embryo (lightning flash, Fig. 7.13B) *cShh* was strongly expressed over a relatively broad area of neuroepithelium were several regions where *cShh* expression was particularly strong (arrows, 7.13B), but while this electroporated region spanned the majority of the thalamic neuroepithelium, it did not extend into the prethalamus. A strong upregulation of *Ptch1* was observed within the thalamus, with no upregulation apparent in the prethalamus (Fig. 7.13C). As in the pretectum, the domain of Ptch1 did not extend as far laterally as the extent of the *cShh*-expressing electroporated area (Fig. 7.13D).

Within the electroporated side of embryo 1 (lightning flash, Fig. 7.11B) a strong upregulation of *Ptch1* was observed in both the thalamus and pretectum (Fig. 7.11C). Data for this embryo are presented at a higher resolution in Fig. 7.14. On the electroporated side of this embryo (lightning flash, Fig. 7.14B) strong *cShh* expression could be observed within several discrete regions within the electroporated area, and most of these were observed in the neuroepithelium of the ZLI and prethalamus (arrows, Fig. 7.14B). The upregulation of *Ptch1* was particularly strong in the prethalamus but *Ptch1* was also found to have been upregulated in the thalamus, despite the thalamic neuroepithelium being situated further from the electroporated area than the prethalamus (Fig. 7.14C). In this embryo some cells situated a considerable distance from the ventricular surface were found to be expressing *cShh*, but little to no upregulation of *Ptch1* was detected in or around these cells (Fig. 7.14D).

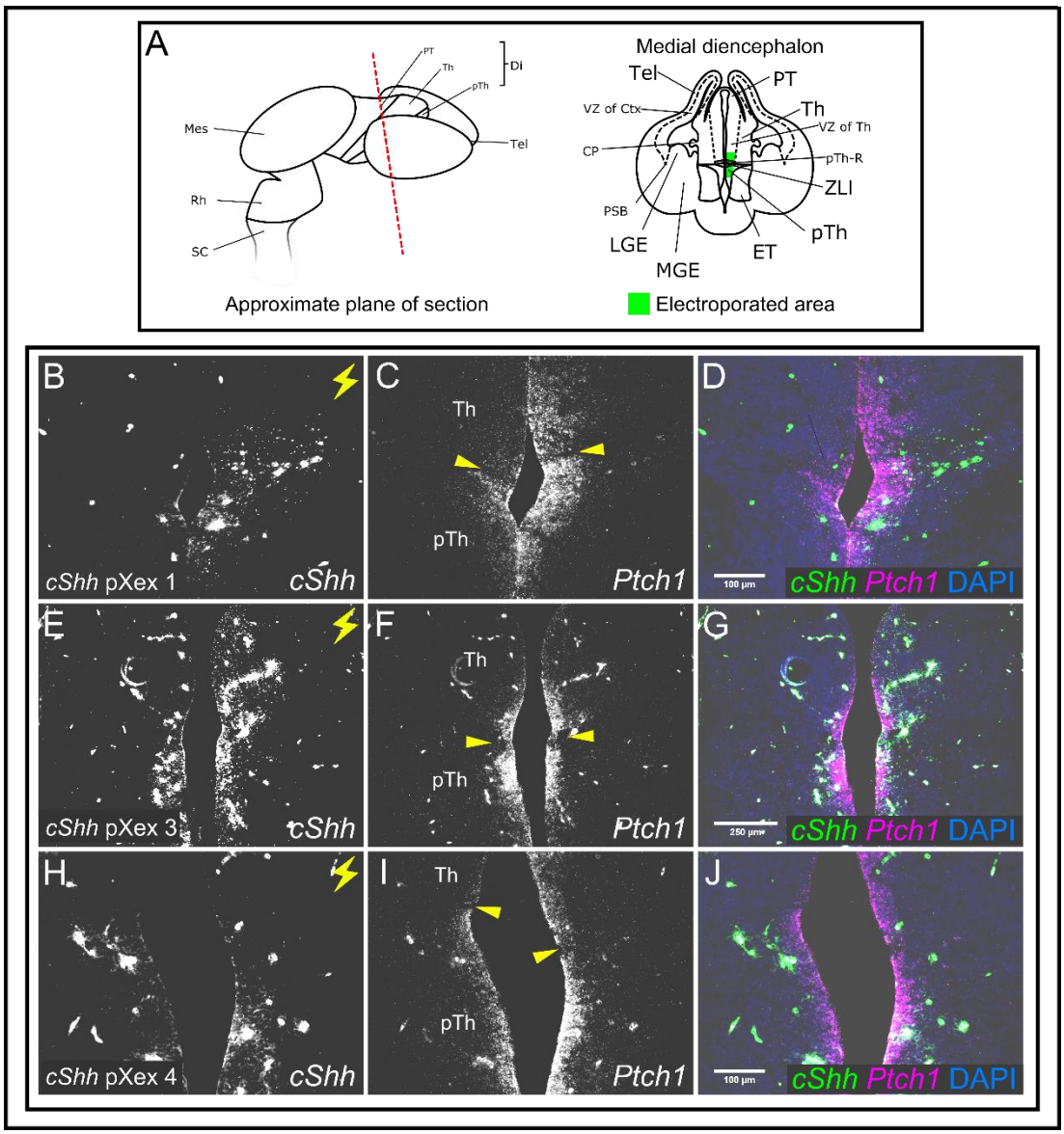

Fig. 7.11: Medial sections from embryos treated with double in situ *hybridization for* Ptch1 *and* cShh *following electroporation with* cShh *pXeX. A: Schematics to illustrate the approximate plane of section and the position of the electroporated area. B-D: Data for embryo 1. E-G: Data for embryo 3. H-J: Data for embryo 4. Lightning flashes denote the electroporated side of the embryo. Arrows indicate the approximate position of the ZLI. Abbreviations: Tel- telencephalon; Di- diencephalon; PT- pretectum; Th- thalamus; pTh- prethalamus; ZLI-* zona limitans intrathalamica*; MGE- medial ganglionic eminence; LGE- lateral ganglionic eminence; ET-* eminentia thalami*; VZ- ventricular zone; Ctx- cortex; Mes- mesencephalon; Rh- rhombencephalon; SC-spinal cord.*

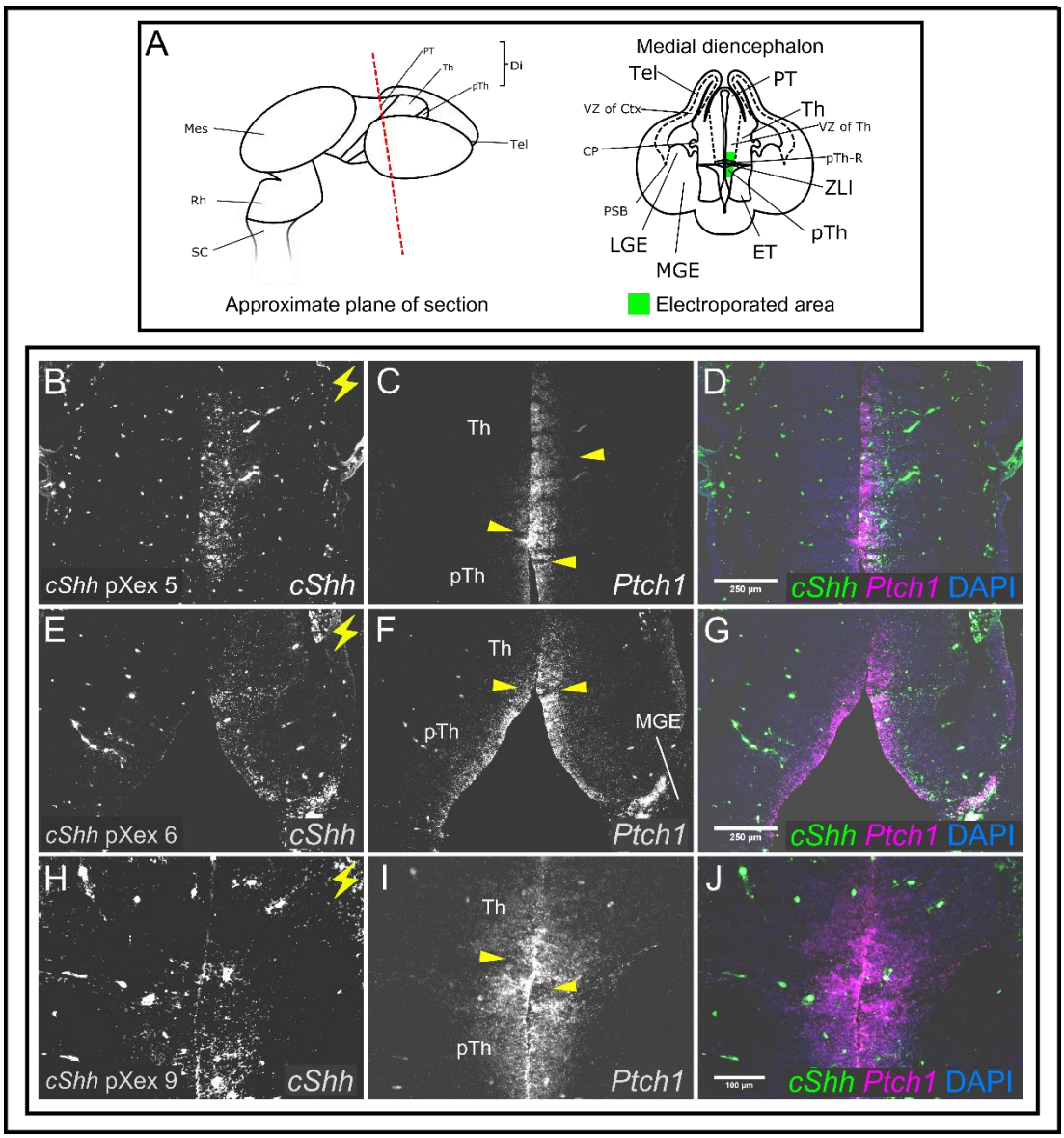

Fig. 7.12: Medial sections from embryos treated with double in situ *hybridization for* Ptch1 *and* cShh *following electroporation with* cShh *pXeX. A: Schematics to illustrate the approximate plane of section and the position of the electroporated area. B-D: Data for embryo 5. E-G: Data for embryo 6. H-J: Data for embryo 9. Lightning flashes denote the electroporated side of the embryo. Arrows indicate the approximate position of the ZLI. Abbreviations: Tel- telencephalon; Di- diencephalon; PT- pretectum; Th- thalamus; pTh- prethalamus; ZLI-* zona limitans intrathalamica*; MGE- medial ganglionic eminence; LGE- lateral ganglionic eminence; ET-* eminentia thalami*; VZ- ventricular zone; Ctx- cortex; Mes- mesencephalon; Rh- rhombencephalon; SC-spinal cord.*

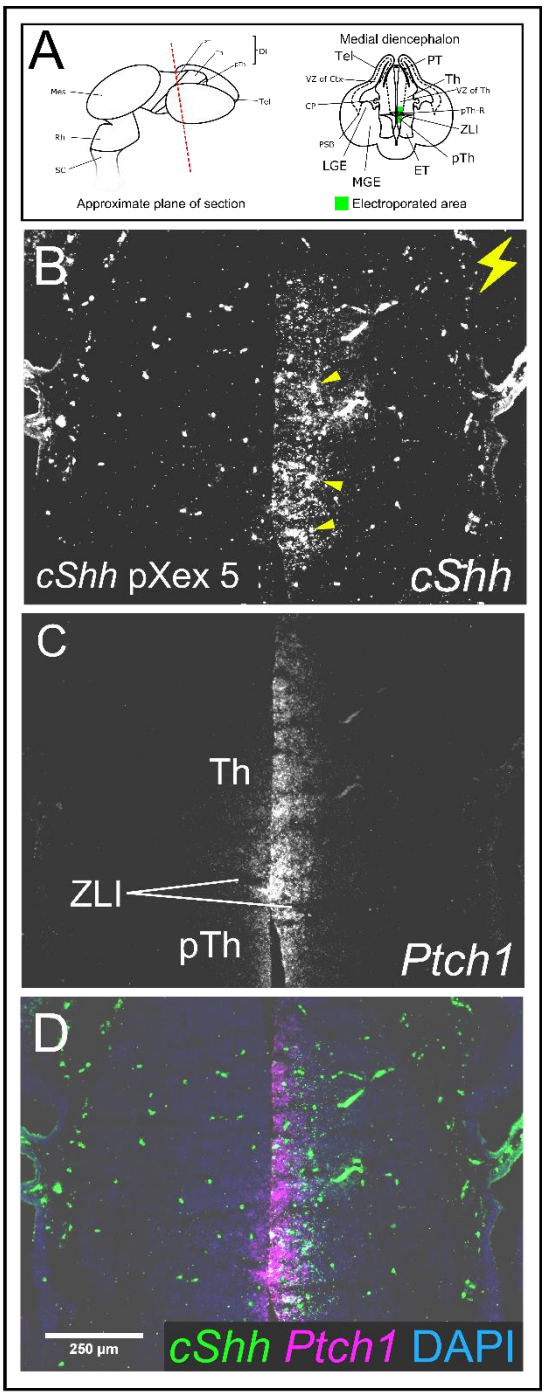

Fig. 7.13: Detail of embryo 5, medial section. A: Schematic to illustrate the position of the electroporated area. B: In situ *hybridization data for* cShh *mRNA. The lightening flash denotes the electroporated side of the embryo. The arrows indicate areas in which cells were transfected. C:* In situ *hybridization data for* Ptch1*. D:* In situ *hybridization data for both* cShh and Ptch1*. Abbreviations: Tel- telencephalon; Di- diencephalon; PT- pretectum; Th- thalamus; pTh- prethalamus; Mes- mesencephalon; Rh- rhombencephalon; SC-spinal cord; VZ- ventricular zone; ZLI-* zona limitans intrathalamica*; Hyp- hypothalamus; Ctx- cortex.*

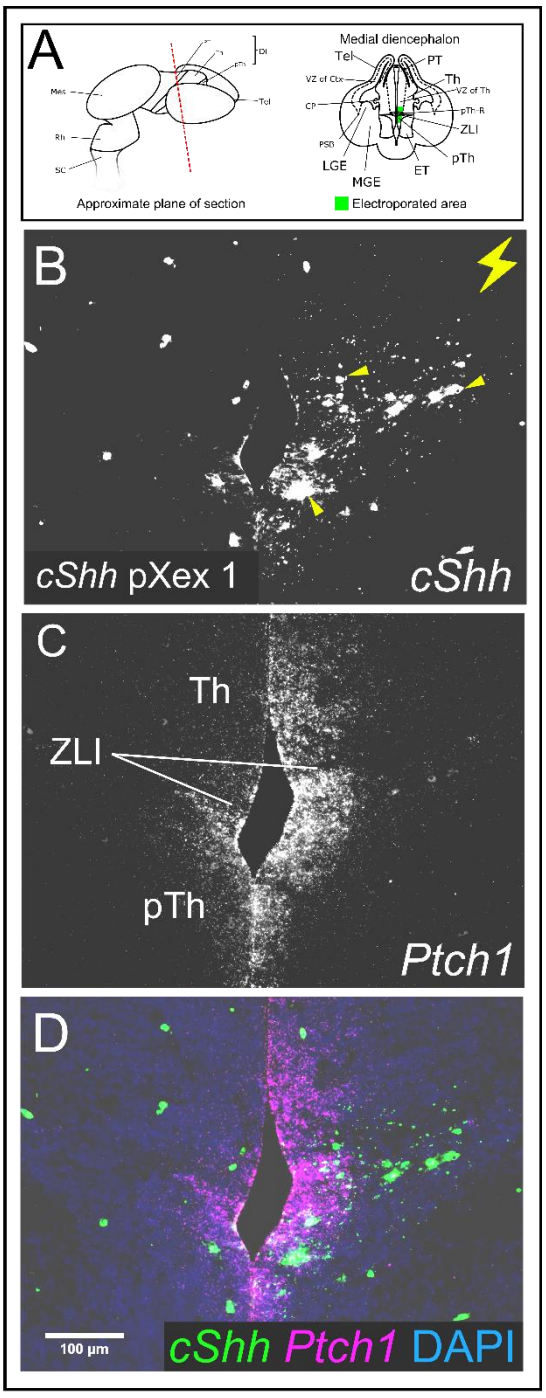

Fig. 7.14: Detail of embryo 1, medial section. A: Schematic to illustrate the position of the electroporated area. B: In situ *hybridization data for* cShh *mRNA. The lightening flash denotes the electroporated side of the embryo. The arrows indicate areas in which cells were transfected. C:* In situ *hybridization data for* Ptch1*. D:* In situ *hybridization data for both* cShh and Ptch1*. Abbreviations: Tel- telencephalon; Di- diencephalon; PT- pretectum; Th- thalamus; pTh- prethalamus; Mes- mesencephalon; Rh- rhombencephalon; SC-spinal cord; VZ- ventricular zone; ZLI-* zona limitans intrathalamica*; Hyp- hypothalamus; Ctx- cortex.*

7.2.5 The effects of ectopic *cShh* expression on *Pax6* expression

Following experimental confirmation that the *cShh* pXeX construct was biologically active in mouse and was able to activate the *Shh* pathway in some areas of neuroepithelium, experiments were performed to determine the effect of *Shh* pathway activation by ectopically expressed *cShh* on the expression of *Pax6*.

Cryosections from embryos electroporated with *cShh* pXeX were treated with double fluorescence *in situ* hybridization for *cShh* and *Pax6* in order to observe changes in *Pax6* expression induced by the activation of the *Shh* pathway. Following the treatment and analysis of cryosections cut at the level of the caudal diencephalon, data for *Pax6* expression in the pretectum was successfully obtained from all eight of the embryos in which the electroporated area included the pretectum (Figs. 7.15 and 7.16).

On the electroporated side of embryo 1 (lightning flash, Fig. 7.15B) ectopic *cShh* expression was relatively weak, no change in *Pax6* expression was observed and the expression of *Pax6* appeared to be equally strong on both the electroporated and unelectroporated sides of the embryo (Fig. 7.15C).

No change in *Pax6* expression was observed on the electroporated side of embryo 3 (lightning flash, Fig. 7.15H). *cShh* was not strongly expressed within the electroporated area and expression of *Pax6* appeared to be of equal strength on the electroporated and unelectroporated sides of the pretectum in this embryo (Fig. 7.15I).

On the electroporated side of embryo 7 (lightning flash, 7.16E) *cShh* expression was of moderate strength, with one discrete region in which it was particularly strong, but despite this no changes in *Pax6* expression were observed and expression of *Pax6* appeared to be broadly symmetrical in the pretectum of this embryo (Fig. 7.16F).

On the electroporated side of embryo 8 (lightning flash, Fig. 7.16H) the electroporated area was relatively broad, although expression of *cShh* within this area was also diffuse. No change in *Pax6* expression was observed and the strength of

Pax6 expression appeared to be equally strong on both the electroporated and unelectroporated sides of the pretectum (Fig. 7.16I).

On the electroporated side of embryo 2 (lightning flash, Fig. 7.15E) expression of *cShh* was relatively strong and extended over a relatively broad area of neuroepithelium. An apparent downregulation of *Pax6* was observed within the electroporated area of this embryo (asterisk, Fig. 7.15F). Data for this embryo are presented at a higher resolution in Fig. 7.17. On the electroporated side of this embryo (lightning flash, Fig. 7.17B) discrete regions of strong cShh expression were observed (arrows, Fig. 7.17B). While *Pax6* was strongly expressed on the unelectoporated side of the pretectum, its expression was markedly weaker within the electroporated area (asterisk, Fig. 7.17C).

On the electroporated side of embryo 6 (lightning flash, Fig. 7.16B) strong expression of *cShh* was observed within a small region of neuroepithelium and an apparent downregulation of *Pax6* was observed within this region (Fig. 7.16C). Data for this embryo are presented at a higher resolution in Fig. 7.18. On the electroporated side of this embryo (lightning flash, Fig. 7.18B) expression of *cShh* appeared to be concentrated within one small region of the pretectum (arrows, Fig. 7.18B) and in this region of the neuroepithelium *Pax6* expression appeared to be weaker than on the unelectroporated side (asterisk, Fig. 7.18C). The region of apparent downregulation corresponded with the position of the electroporated area (Fig. 7.18D).

On the electroporated side of embryo 9 (lightning flash, Fig. 7.16K) a small region of strong *cShh* expression appeared to correspond with a region of apparent *Pax6* downregulation (Fig. 7.16L). Data for this embryo are presented at a higher resolution in Fig. 7.19. On the electroporated side of this embryo (lightning flash, Fig. 7.19B) expression of *cShh* was concentrated in a small region of the ventral pretectum, close to the ventricular surface (arrows, Fig. 7.19B). An apparent downregulation of *Pax6* (asterisk, Fig. 7.19C) was also observed in the ventral pretectum, with *Pax6* expression appearing to be weaker than it appeared on the unelectroporated side. This region of apparent *Pax6* downregulation corresponded with the position of the electroporated area (Fig. 7.19D).

On the electroporated side of embryo 5 (lightning flash, Fig. 7.15K) expression of *cShh* was relatively strong and could be observed over a broad area of neuroepithelium. Data for this embryo are presented at a higher resolution in Fig. 7.20. On the electroporated side of this embryo (Fig. 7.20B) expression of *cShh* was particularly strong in the more ventral regions of the pretectum (arrows, Fig. 7.20B). Despite this a downregulation of *Pax6* expression was not observed within the electroporated region (asterisk, Fig. 7.20C).as it had been in embryo 2, embryo 6 and embryo 9. The expression domain of *Pax6* in embryo 5 appeared to be slightly broader on the electroporated side, but this may have been due to the tissue section not being entirely symmetrical. The expression of *Pax6* appeared to be of equal strength on both sides of the pretectum.

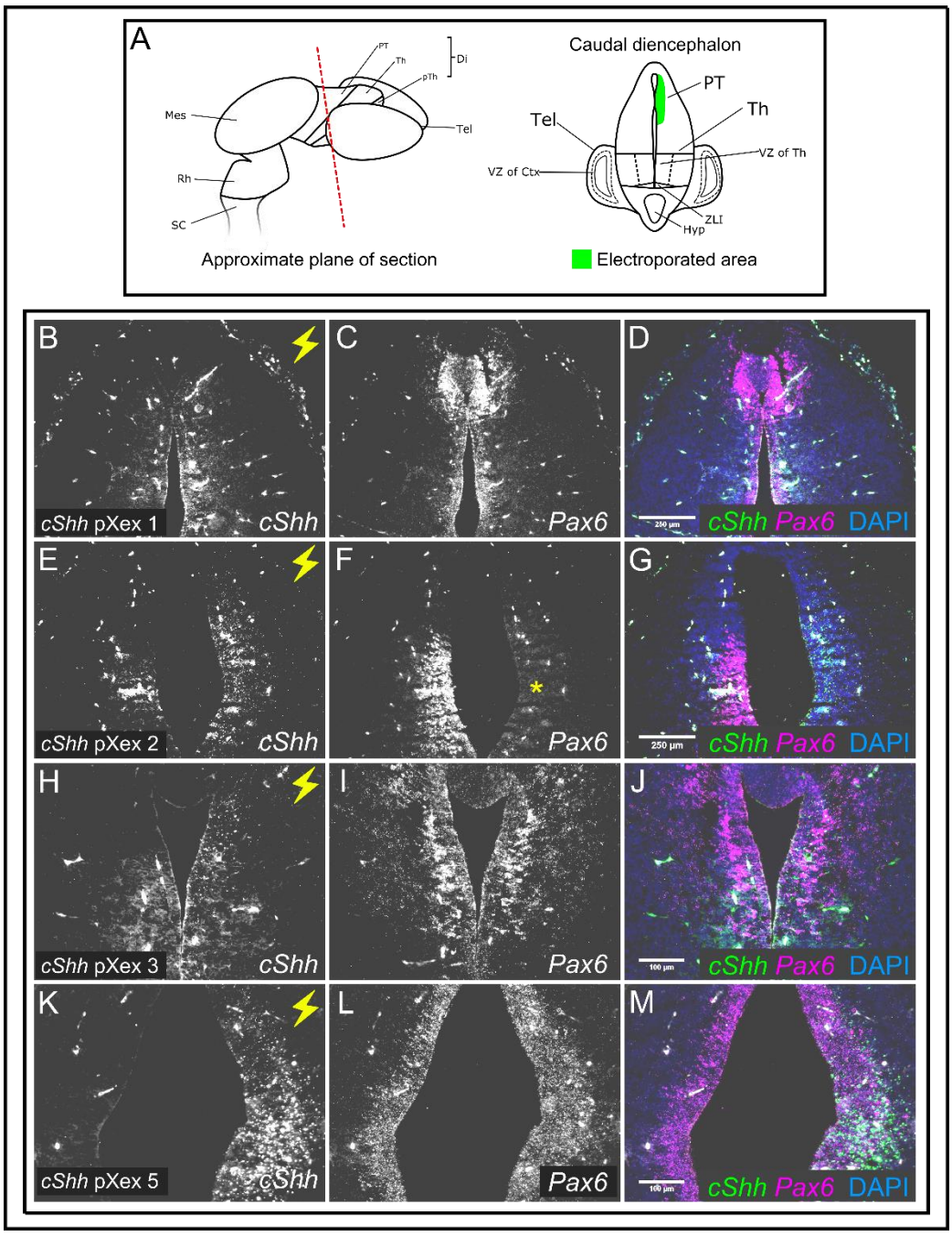

Fig. 7.15: Analysis of changes in Pax6 *expression in the pretectum of embryos electroporated with* cShh *pXeX by double* in situ *hybridization for* Pax6 *and* cShh *mRNA. A*: Schematics *to illustrate the approximate plane of section and the approximate position of the electroporated area. B-D: Data for in embryo 1. E-G: Data for embryo 2. H-J: Data for embryo 3. K-M: Data for embryo 5. The lightning flashes denote the electroporated side of the embryo. Asterisks: regions of apparent* Pax6 *downregulation. Abbreviations: Tel- telencephalon; Di- diencephalon; PT- pretectum; Th- thalamus; pTh- prethalamus; Mes- mesencephalon; Rh- rhombencephalon; SC-spinal cord; VZ- ventricular zone; ZLI-* zona limitans intrathalamica*; Hyp- hypothalamus; Ctx- cortex.*

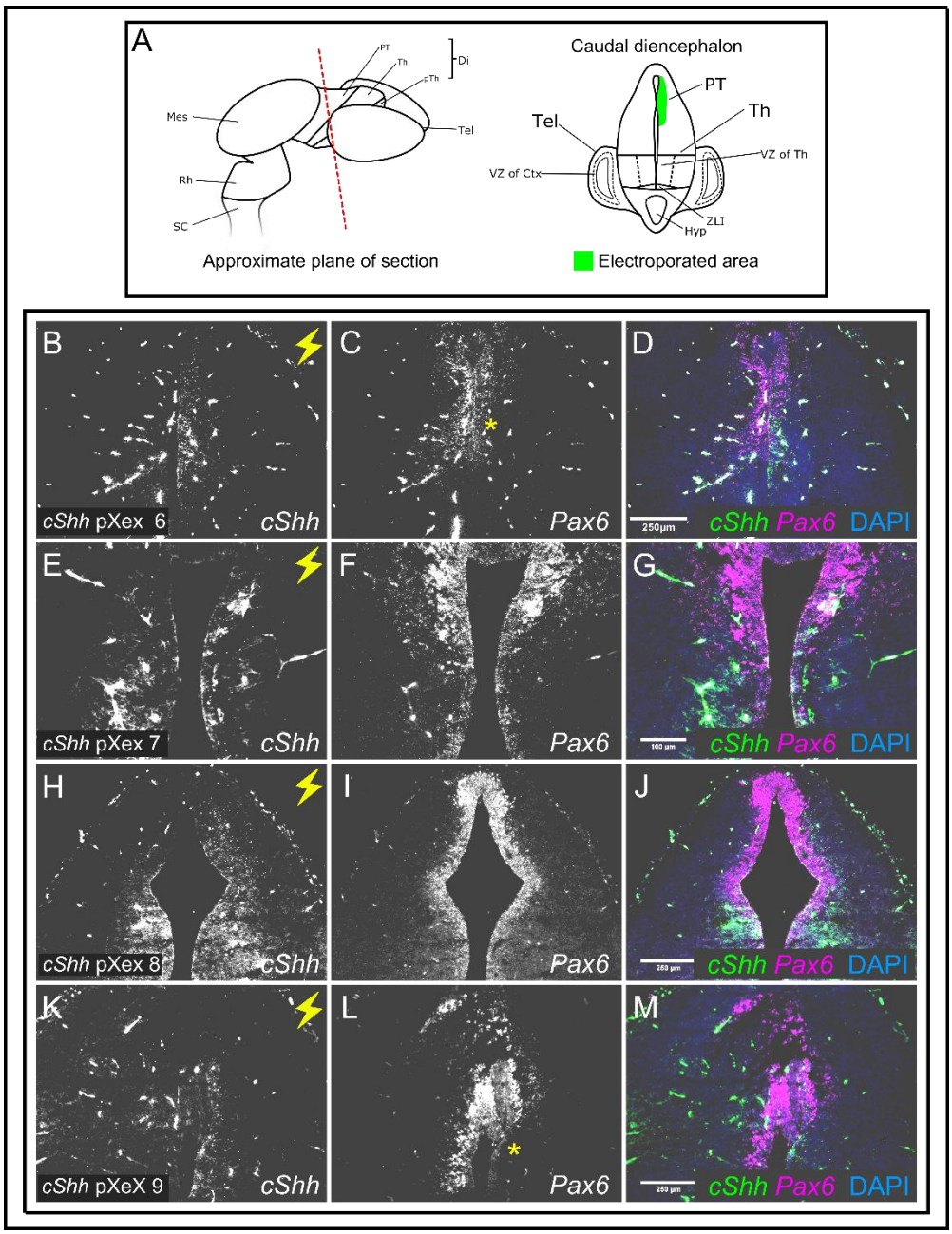

Fig. 7.16: Analysis of changes in Pax6 *expression in the pretectum of embryos electroporated with* cShh *pXeX by double* in situ *hybridization for* Pax6 *and* cShh mRNA. A: Schematics *to illustrate the approximate plane of section and the approximate position of the electroporated area. B-D: Data for embryo 6. E-G: Data for embryo 7. H-J: Data for embryo 8. K-M: Data for embryo 9. The lightning flashes denote the electroporated side of the embryo. Asterisks denote regions of apparent* Pax6 *downregulation. Abbreviations: Tel- telencephalon; Di- diencephalon; PT- pretectum; Th- thalamus; pTh- prethalamus; Mes- mesencephalon; Rh- rhombencephalon; SC-spinal cord; VZ- ventricular zone; ZLI-* zona limitans intrathalamica*; Hyp- hypothalamus; Ctx- cortex.*

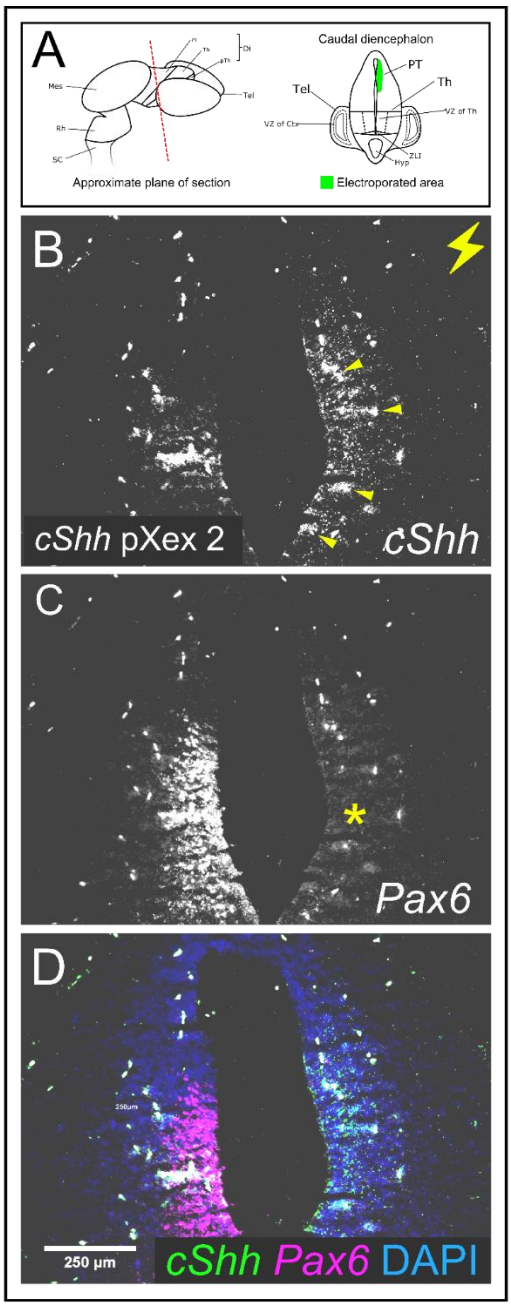

Fig. 7.17: Detail of embryo 2, caudal section. A: Schematic to illustrate the position of the electroporated area. B: In situ *hybridization data for* cShh *mRNA. The lightening flash denotes the electroporated side of the embryo. The arrows indicate areas in which cells were transfected. C:* In situ *hybridization data for* Pax6*. The asterisk denotes an apparent downregulation. D:* In situ *hybridization data for both* cShh and Pax6*. Abbreviations: Tel- telencephalon; Di- diencephalon; PT- pretectum; Th- thalamus; pTh- prethalamus; Mes- mesencephalon; Rh- rhombencephalon; SC-spinal cord; VZ- ventricular zone; ZLI-* zona limitans intrathalamica*; Hyp- hypothalamus; Ctx- cortex.*

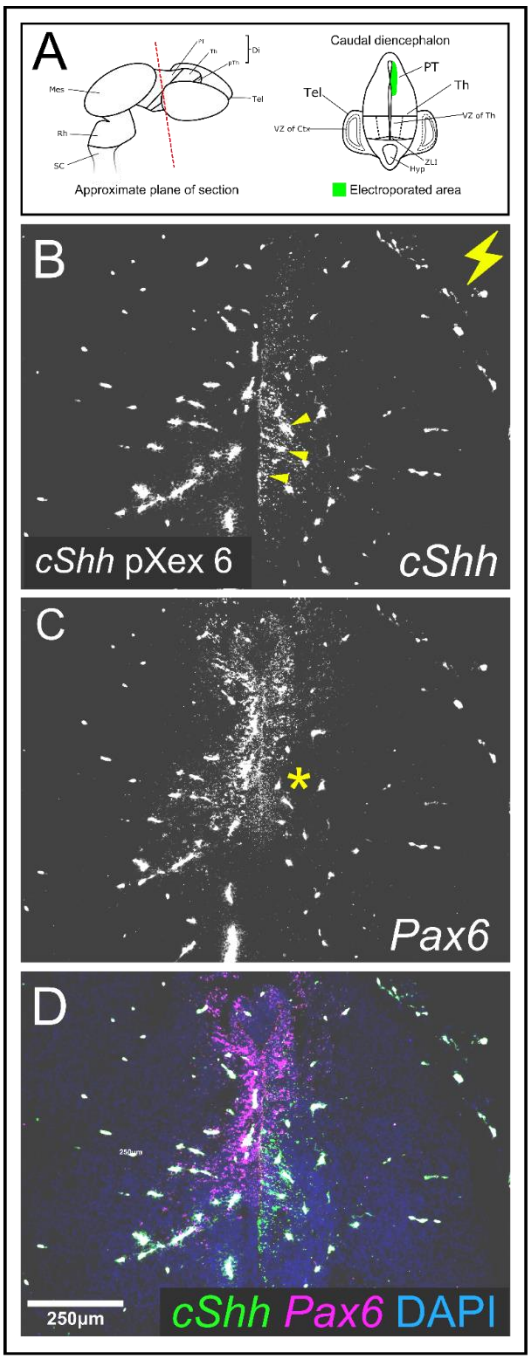

Fig. 7.18: Detail of embryo 6, caudal section. A: Schematic to illustrate the position of the electroporated area. B: In situ *hybridization data for* cShh *mRNA. The lightening flash denotes the electroporated side of the embryo. The arrows indicate areas in which cells were transfected. C:* In situ *hybridization data for* Pax6*. The asterisk denotes an apparent downregulation. D:* In situ *hybridization data for both* cShh and Pax6*. Abbreviations: Tel- telencephalon; Di- diencephalon; PT- pretectum; Th- thalamus; pTh- prethalamus; Mes- mesencephalon; Rh- rhombencephalon; SC-spinal cord; VZ- ventricular zone; ZLI-* zona limitans intrathalamica*; Hyp- hypothalamus; Ctx- cortex.*

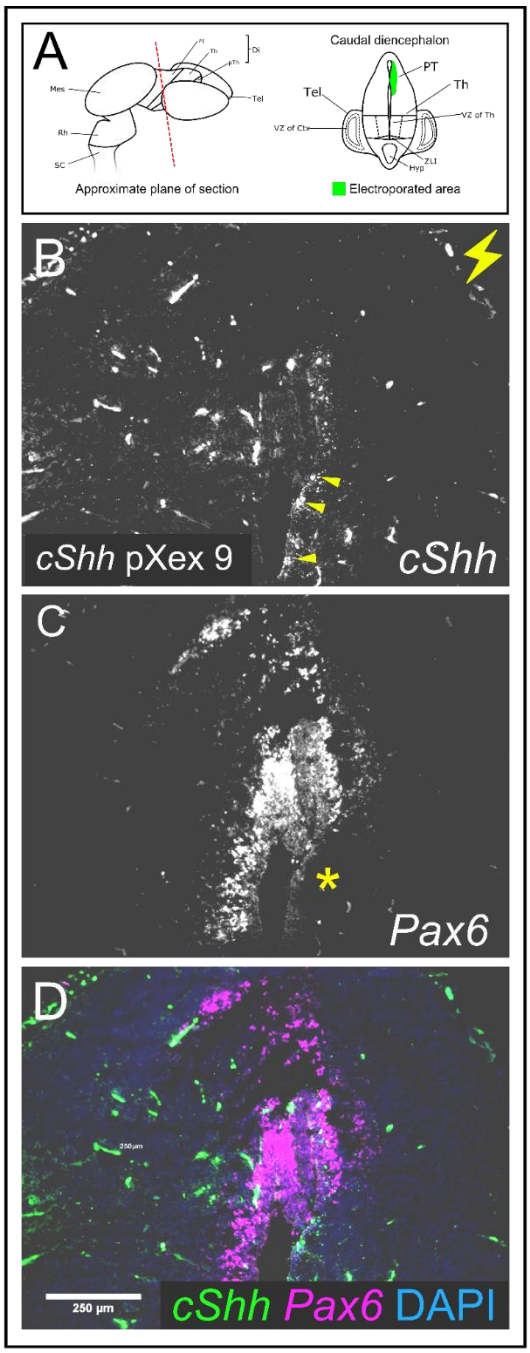

Fig. 7.19: Detail of embryo 9, caudal section. A: Schematic to illustrate the position of the electroporated area. B: In situ *hybridization data for* cShh *mRNA. The lightening flash denotes the electroporated side of the embryo. The arrows indicate areas in which cells were transfected. C:* In situ *hybridization data for* Pax6*. The asterisk denotes an apparent downregulation. D:* In situ *hybridization data for both* cShh and Pax6*. Abbreviations: Tel- telencephalon; Di- diencephalon; PT- pretectum; Th- thalamus; pTh- prethalamus; Mes- mesencephalon; Rh- rhombencephalon; SC-spinal cord; VZ- ventricular zone; ZLI-* zona limitans intrathalamica*; Hyp- hypothalamus; Ctx- cortex.*

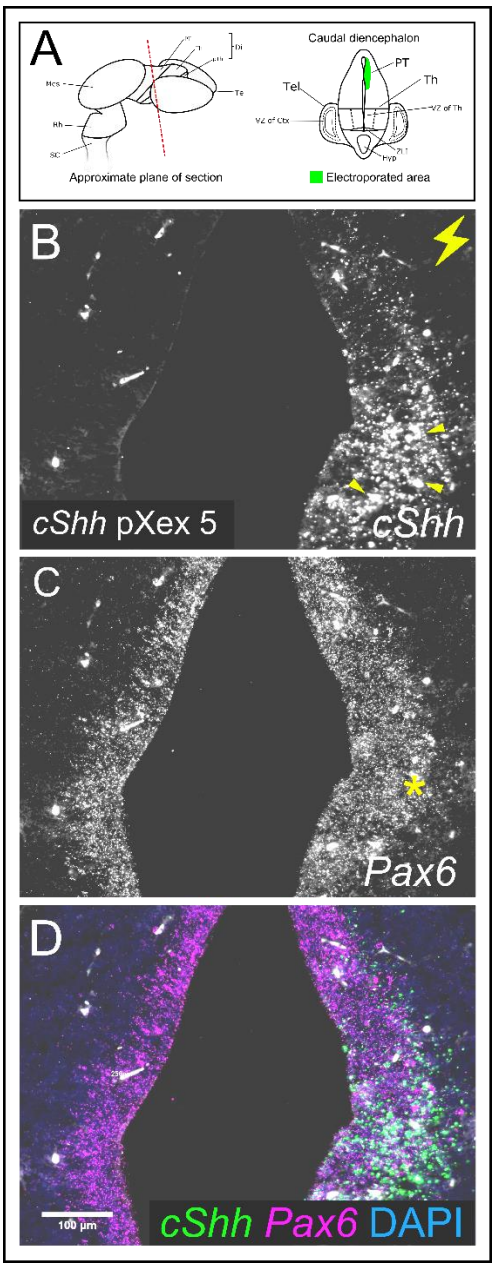

Fig. 7.20: Detail of embryo 5, caudal section. A: Schematic to illustrate the position of the electroporated area. B: In situ *hybridization data for* cShh *mRNA. The lightening flash denotes the electroporated side of the embryo. The arrows indicate areas in which cells were transfected. C:* In situ *hybridization data for* Pax6*. The asterisk denotes a region of no apparent downregulation within the electroporated area. D:* In situ *hybridization data for both* cShh and Pax6*. Abbreviations: Tel- telencephalon; Di- diencephalon; PT- pretectum; Th- thalamus; pTh- prethalamus; Mes- mesencephalon; Rh- rhombencephalon; SC-spinal cord; VZ- ventricular zone; ZLI-* zona limitans intrathalamica*; Hyp- hypothalamus; Ctx- cortex.*

Data for *Pax6* expression was obtained from five embryos which were electroporated in a medial region of the diencephalon including the thalamus, ZLI and prethalamus (Fig. 7.21, Fig. 7.22 and Fig. 7.23). On the electroporated side of embryo 1 (lightning flash, Fig. 7.21B) expression of *cShh* was relatively weak and no changes in Pax6 expression were observed within the electroporated area (Fig. 7.21C).

On the electroporated side of embryo 4 (lightning flash, Fig. 7.21E) only weak expression of *cShh* mRNA was detected. The expression domains of *Pax6* in this embryo were broadly symmetrical and no change in *Pax6* expression appeared to have been induced (Fig. 7.21F).

On the electroporated side of embryo 5 (Fig. 7.21 H) *cShh* expression was relatively weak and diffuse. The treated section cut from this embryo was not entirely symmetrical, but the strength of Pax6 expression appeared to be the same on both the electroporated and unelectoporated sides (Fig. 7.21I).

Expression of *cShh* within the electroporated area of embryo 6 was relatively strong. Data for this embryo are shown at high resolution in Fig. 7.22. On the electroporated side of this embryo (lightning flash, 7.22B) strong *cShh* expression was observed in a region spanning the ventral regions of the thalamic neuroepithelium and the ZLI (arrows, Fig. 7.22B). Expression of *Pax6* in this region of the thalamus appeared to be very slightly weaker than on the unelectroporated side (asterisk, Fig. 7.22C).

Expression of *cShh* within the electroporated area of embryo 9 was relatively strong. Data for this embryo are presented at high resolution in Fig. 7.23. The lumen of this embryo appears wider than the others described in this chapter because of damage to the roofplate during the process of tissue fixation, but the section shown here was cut at a comparable point along the rostrocaudal axis of the diencephalon. On the electroporated side of this embryo (lightning flash, Fig. 7.23B) ectopic *cShh* expression was relatively strong within the thalamus and many areas of particularly strong expression could be seen within the electroporated area (arrows, Fig. 7.23B). Despite this relatively high strength of expression, no apparent change in the expression of Pax6 was noted on the electroporated side of the embryo (Fig. 7.23C) and the domains of *Pax6* expression appeared to be broadly symmetrical.

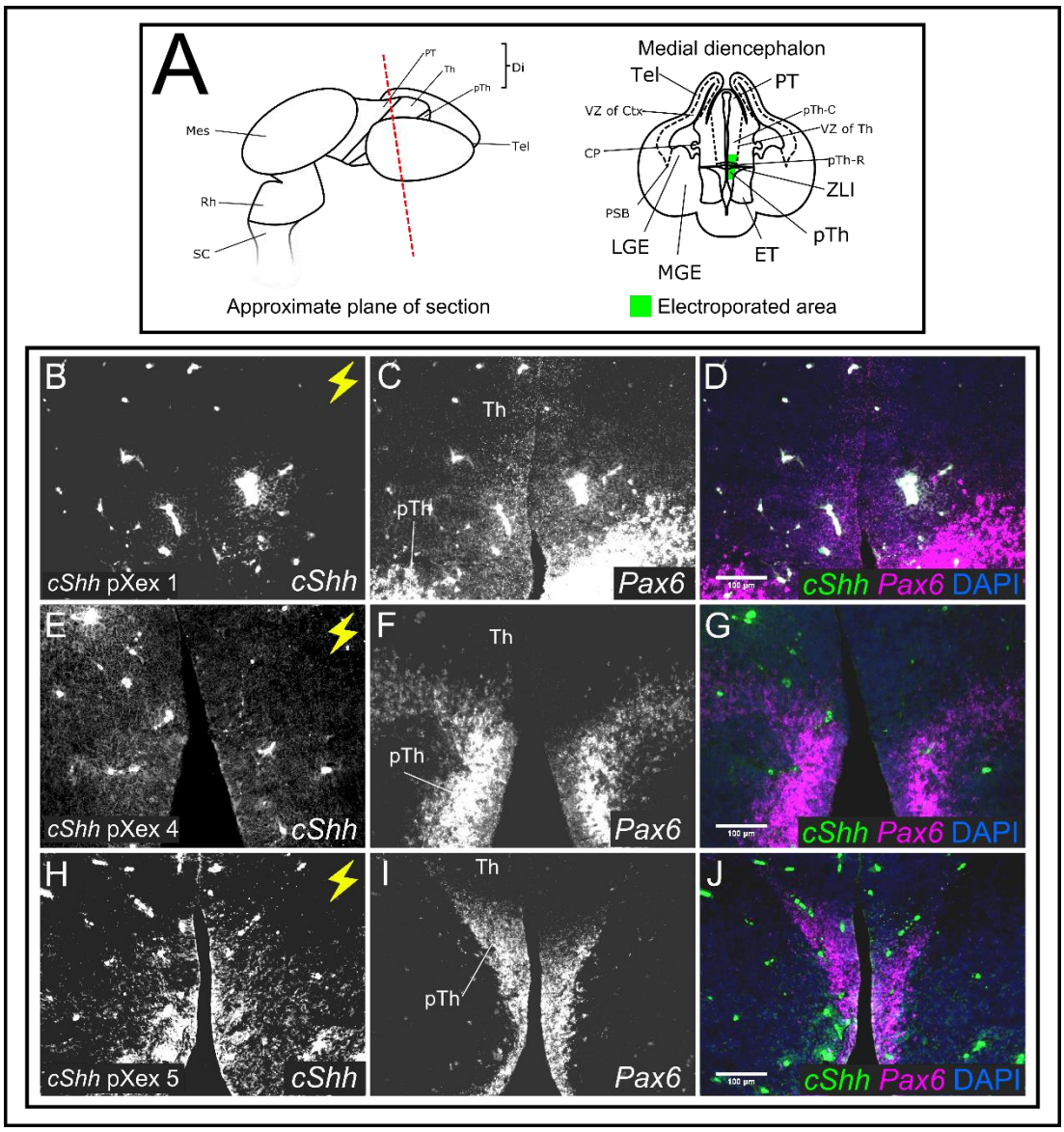

Fig. 7.21: Analysis of changes in Pax6 *expression in the thalamus, ZLI and prethalamus of embryos electroporated with* cShh *pXeX by double* in situ *hybridization for* Pax6 *and* cShh mRNA. A: Schematics *to illustrate the approximate plane of section and the approximate position of the electroporated area. B-D: Data for embryo 1. E-G: Data for embryo 4. H-J: Data for embryo 5. The lightning flashes denote the electroporated side of the embryo. Abbreviations: Tel- telencephalon; Di- diencephalon; PT- pretectum; Th- thalamus; pTh- prethalamus; ZLI-* zona limitans intrathalamica*; MGE- medial ganglionic eminence; LGE- lateral ganglionic eminence; ET-* eminentia thalami*; VZ- ventricular zone; Ctx- cortex; Mes- mesencephalon; Rh- rhombencephalon; SC-spinal cord.*

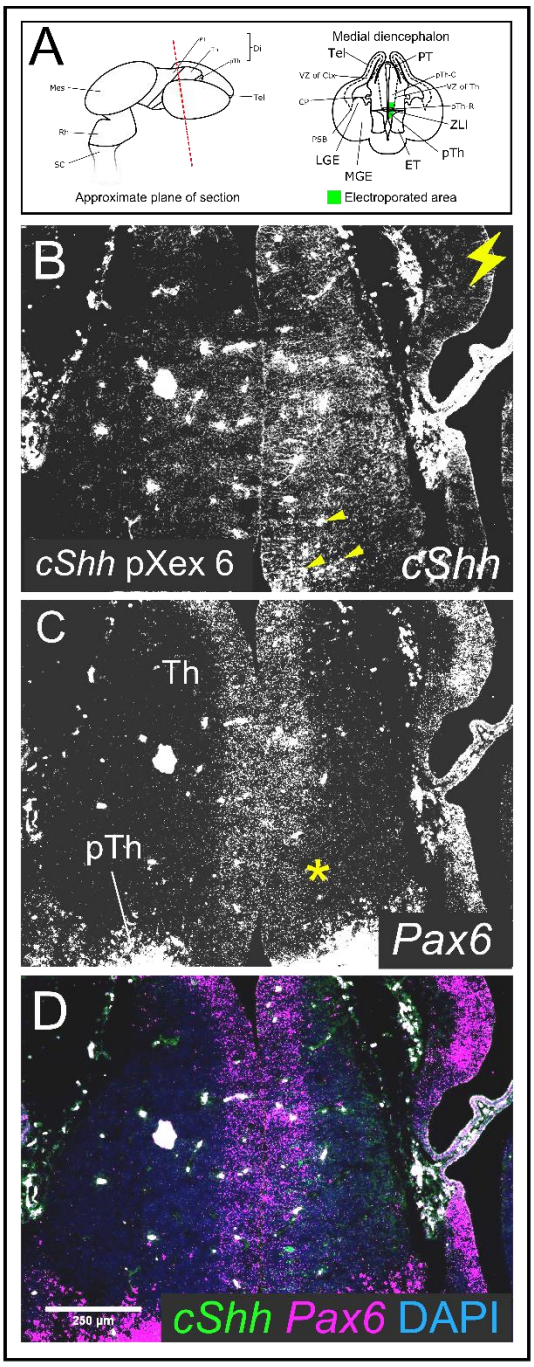

Fig. 7.22: Detail of embryo 6, medial section. A: Schematic to illustrate the position of the electroporated area. B: In situ *hybridization data for* cShh *mRNA. The lightening flash denotes the electroporated side of the embryo. The arrows indicate areas in which cells were transfected. C:* In situ *hybridization data for* Pax6*. The asterisk denotes a potential downregulation of* Pax6*. D:* In situ *hybridization data for both* cShh and Pax6*. Abbreviations: Tel- telencephalon; Di- diencephalon; PT- pretectum; Th- thalamus; pTh- prethalamus; Mes- mesencephalon; Rh- rhombencephalon; SC-spinal cord; VZ- ventricular zone; ZLI-* zona limitans intrathalamica*; Hyp- hypothalamus; Ctx- cortex.*

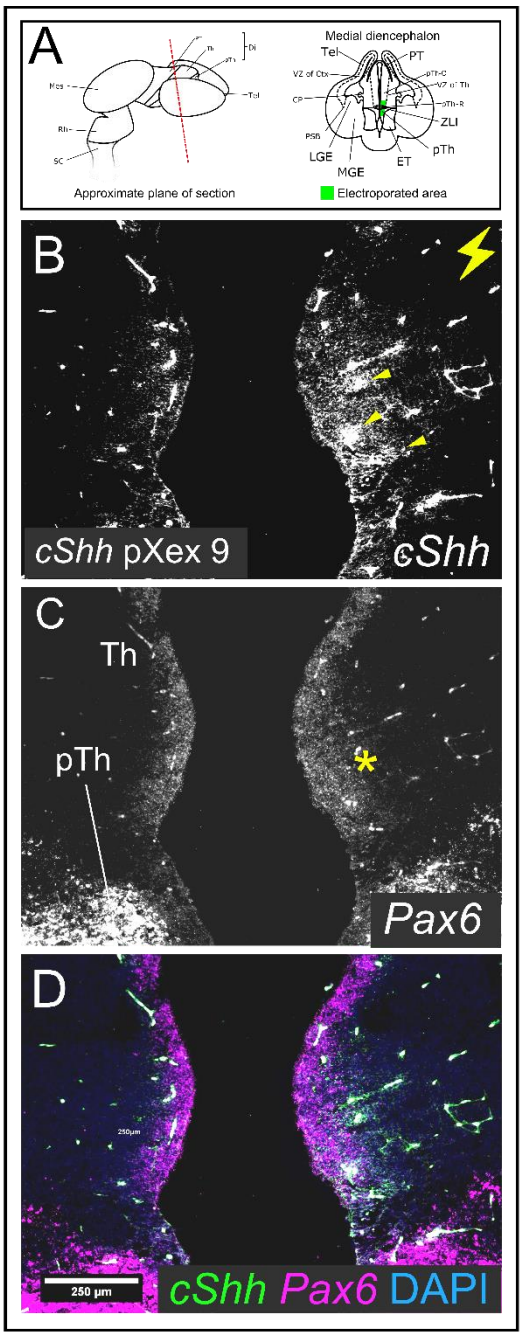

Fig. 7.23: Detail of embryo 9, medial section. A: Schematic to illustrate the position of the electroporated area. B: In situ *hybridization data for* cShh *mRNA. The lightening flash denotes the electroporated side of the embryo. The arrows indicate areas in which cells were transfected. C:* In situ *hybridization data for* Pax6*. The asterisk denotes no apparent downregulation within the electroporated area. D:* In situ *hybridization data for both* cShh and Pax6*. Abbreviations: Tel- telencephalon; Di- diencephalon; PT- pretectum; Th- thalamus; pTh- prethalamus; Mes- mesencephalon; Rh- rhombencephalon; SC-spinal cord; VZ- ventricular zone; ZLI-* zona limitans intrathalamica*; Hyp- hypothalamus; Ctx- cortex.*

7.2.6 The effects of ectopic *cShh* expression on *Barhl2* expression

Experiments were performed to determine the effect of *Shh* pathway activation by the ectopic expression of *cShh* on the expression of *Barhl2*. Cryosections from embryos electroporated with *cShh* pXeX were treated with double fluorescence *in situ* hybridization for *cShh* and *Barhl2* in order to observe changes in *Barhl2* expression induced by the activation of the *Shh* pathway.

Following the treatment and analysis of cryosections cut at the level of the caudal diencephalon, data for *Barhl2* expression in the pretectum was successfully obtained from all eight of the embryos in which the electroporated area included the pretectum (Figs. 7.24 and 7.25).

An apparent upregulation of *Barhl2* was observed in six of the eight embryos which were analysed.

On the electroporated side of embryo 1 (lightning flash, Fig. 7.24B) *cShh* was strongly expressed within a ventral region of the pretectum, close to the ventricular surface. Despite this strong expression no change in *Barhl2* expression was noted and the expression domains of *Barhl2* in this embryo appeared to be broadly symmetrical (Fig. 7.24C).

On the electroporated side of embryo 2 (lightning flash, Fig. 7.24E) *cShh* was also strongly expressed within the ventral pretectum, close to the ventricular surface. As in embryo 1, this ectopic expression of *cShh* did not appear to have induced a change in *Barhl2* expression in embryo 2, and in this embryo the expression domains of *Barhl2* were broadly symmetrical (Fig. 7.24F).

On the electroporated side of embryo 6 (lightning flash, Fig. 7.25B) *cShh* was found to be expressed in a broad region of neuroepithelium extending to a point close to the dorsal midline. In this embryo *Barhl2* expression was upregulated in the dorsal pretectum, while it was not expressed in this region on the unelectroporated side (Fig. 7.25C).

On the electroporated side of embryo 8 (lightning flash, Fig. 7.25H) *cShh* was also strongly expressed close to the dorsal midline of the embryo, and as in embryo 6,

Barhl2 was upregulated in this region, and the dorsal extent of *Barhl2* expression on the electroporated side of the embryo was closer to the dorsal midline than that of the *Barhl2* domain on the unelectroporated side of the embryo (Fig. 7.25I).

On the electroporated side of embryo 9 (lightning flash, Fig. 7.25K) *Barhl2* also appeared to have been upregulated (Fig. 7.25L). Data for this embryo are presented at higher resolution in Fig. 7.26. On the electroporated side (lightning flash, Fig. 7.26B) *cShh* expression was concentrated in a small region of the ventral pretectum close to the dorsal midline (arrows, Fig. 7.26B). A lateral expansion of the *Barhl2* domain was observed on the electroporated side (asterisk, Fig. 7.26C) and it appeared broader than the *Barhl2* domain on the unelectroporated side even in regions of neuroepithelium located relatively far from the strongest region of cShh expression (Fig. 7.26D).

On the electroporated side of embryo 7 (lightning flash, Fig. 7.25E) a lateral expansion of the *Barhl2* domain was also observed (Fig. 7.25F). Data for this embryo are presented at higher resolution in Fig. 7.27. On the electroporated side (lightning flash, Fig. 7.27B) *cShh* was strongly expressed and *cShh* mRNA could be detected at a relatively great distance from the ventricular surface (arrows, Fig. 7.27B). The *Barhl2* domain was found to have undergone an expansion around the electroporated area (asterisk, Fig. 7.27C) and appeared broader than the *Barhl2* domain on the unelectroporated side. As with embryo 9, the expanded *Barhl2* domain was broader than the region in which *cShh* was expressed (Fig. 7.27D).

On the electroporated side of embryo 3 (lightning flash, 7.24H) a lateral expansion of the *Barhl2* domain was also observed, in addition to an expansion along the dorsoventral axis (Fig. 7.24I). Data from this embryo are presented at a higher resolution in Fig. 7.28. On the electroporated side (lightning flash, Fig. 7.28B) *cShh* could be detected throughout the majority of the neuroepithelium of the pretectum, with the exception of the region closest to the dorsal midline (arrows, Fig. 7.28B). Although *cShh* expression in this embryo was relatively diffuse, it still appeared to have induced an upregulation of *Barhl2* on the electroporated side of the embryo (asterisk, Fig. 7.28C), with the *Barhl2* domain appearing to be broader along both the

dorsoventral and mediolateral axes in comparison with the *Barhl2* domain on the unelectroporated side of the embryo.

On the electroporated side of embryo 5 (lightning flash, Fig. 7.24K) an upregulation of *Barhl2* was also observed (Fig. 7.24L). Data for this embryo are presented at a higher resolution in Fig. 7.29. On the electroporated side of this embryo (lightning flash, Fig. 7.29B) *cShh* mRNA was detected throughout most regions of the pretectum, with the exception of the neuroepithelium close to the dorsal midline (arrows, Fig. 7.29B). Upregulation of *Barhl2* was observed as an expansion of the domain along to dorsoventral axis, with *Barhl2* mRNA being detected close to the dorsal midline on the electroporated side, while the domain of *Barhl2* on the unelectroporated side did not extend as far dorsally (Fig. 7.29C). A region of particularly strong *Barhl2* expression was also observed and found to coincide with the region of neuroepithelium in which *cShh* expression was at its strongest (Fig. 7.29D).

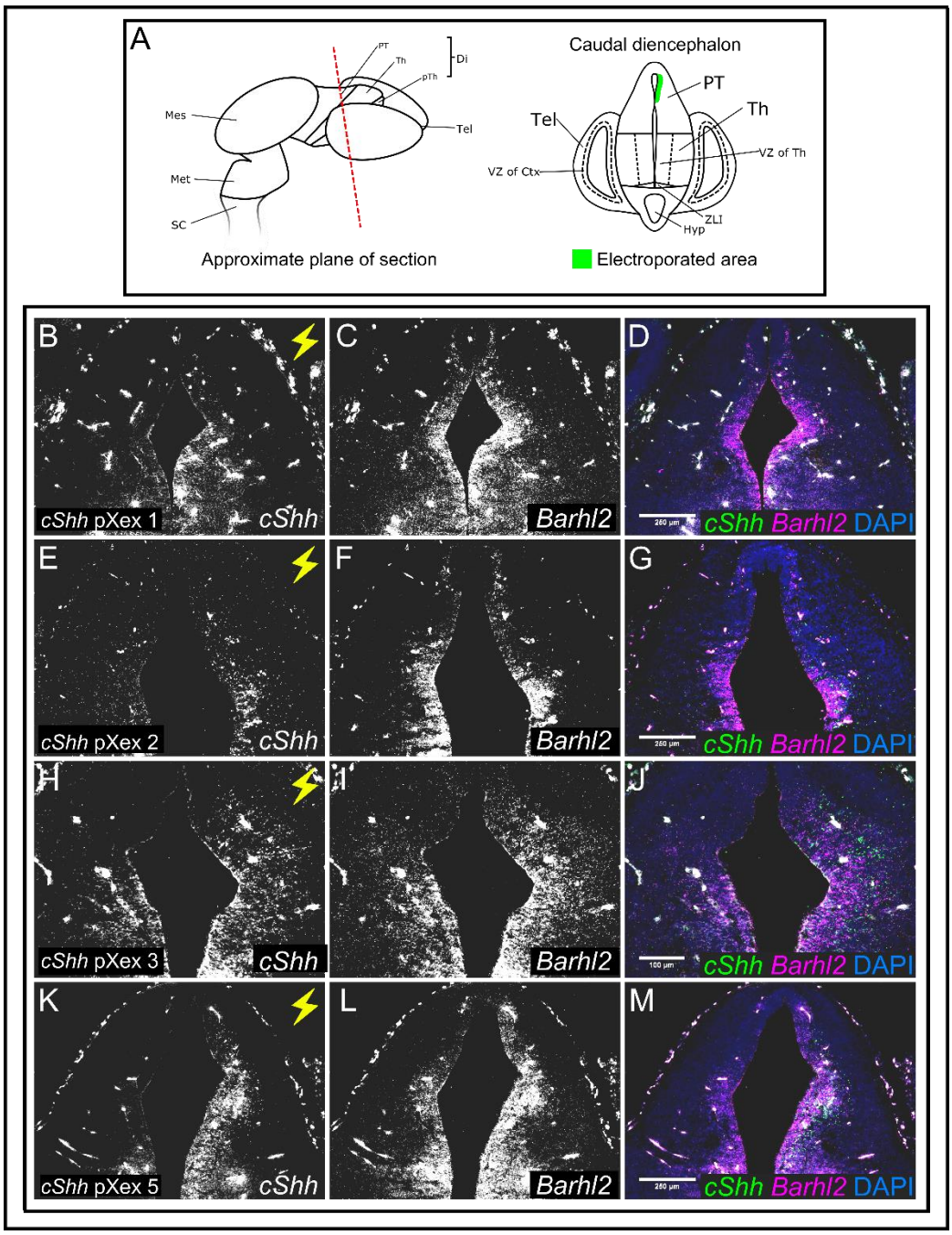

Fig. 7.24: Analysis of changes in Barhl2 *expression in the pretectum of embryos electroporated with* cShh *pXeX by double* in situ *hybridization for* Barhl2 *and* cShh *mRNA. A: Schematics to illustrate the approximate plane of section and the approximate position of the electroporated area. B-D: Data for in embryo 1. E-G: Data for embryo 2. H-J: Data for embryo 3. K-M: Data for embryo 5. The lightning flashes denote the electroporated side of the embryo. Abbreviations: Tel- telencephalon; Di- diencephalon; PT- pretectum; Th- thalamus; pTh- prethalamus; Mes- mesencephalon; Rh- rhombencephalon; SC-spinal cord; VZ- ventricular zone; ZLI-* zona limitans intrathalamica*; Hyp- hypothalamus; Ctx- cortex*.

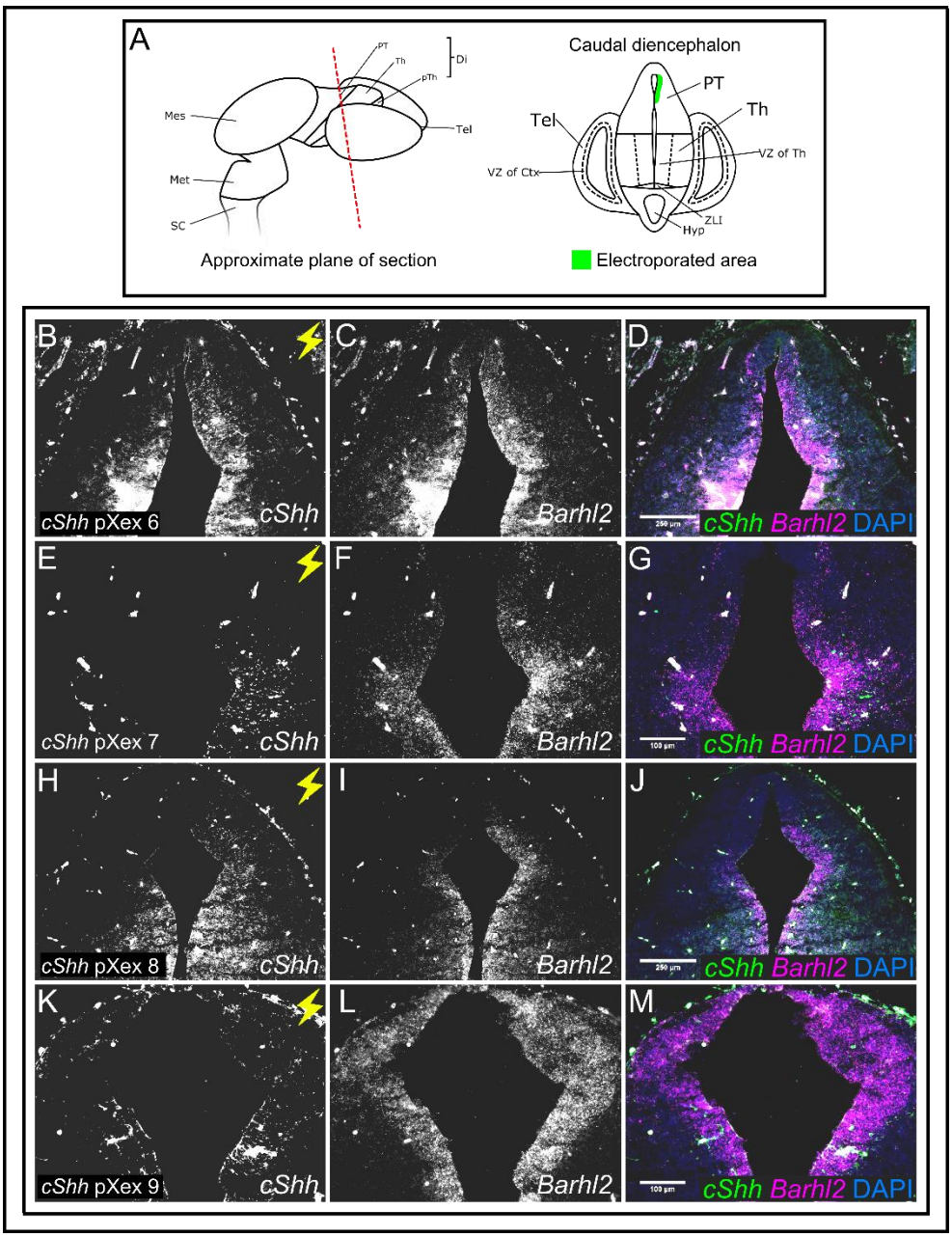

Fig. 7.25: Analysis of changes in Barhl2 *expression in the pretectum of embryos electroporated with* cShh *pXeX by double* in situ *hybridization for* Barhl2 *and* cShh mRNA. A: Schematics *to illustrate the approximate plane of section and the approximate position of the electroporated area. B-D: Data for embryo 6. E-G: Data for embryo 7. H-J: Data for embryo 8. K-M: Data for embryo 9. The lightning flashes denote the electroporated side of the embryo. Abbreviations: Tel- telencephalon; Di- diencephalon; PT- pretectum; Th- thalamus; pTh- prethalamus; Mes- mesencephalon; Rh- rhombencephalon; SC-spinal cord; VZ-ventricular zone; ZLI-* zona limitans intrathalamica*; Hyp- hypothalamus; Ctx- cortex.*

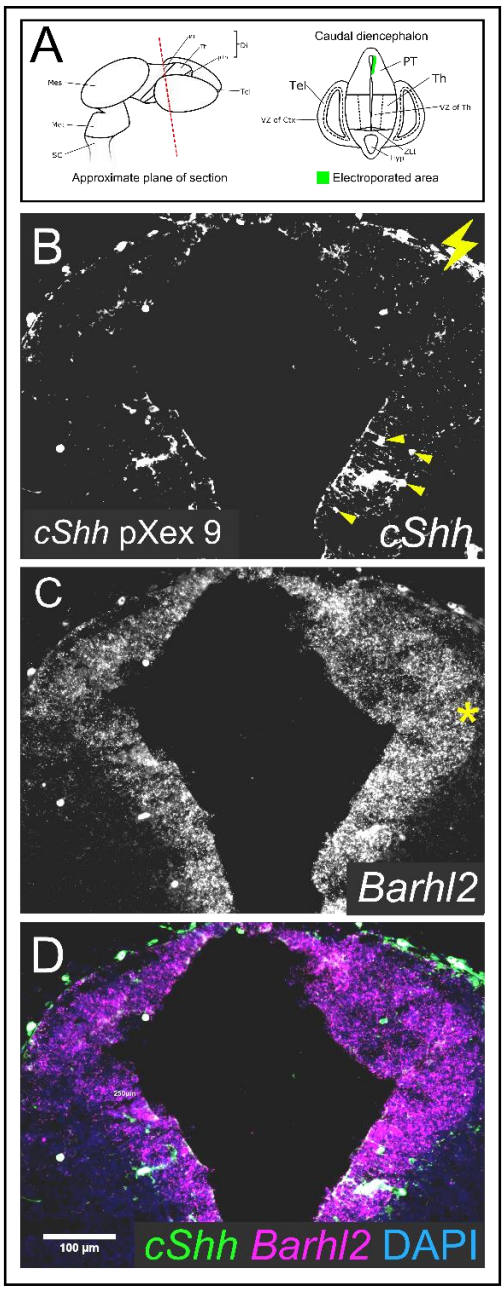

Fig. 7.26: Detail of embryo 9, caudal section. A: Schematic to illustrate the position of the electroporated area. B: In situ *hybridization data for* cShh *mRNA. The lightening flash denotes the electroporated side of the embryo. The arrows indicate areas in which cells were transfected. C:* In situ *hybridization data for* Barhl2*. The asterisk denotes an apparent upregulation of* Barhl2 *and a lateral expansion of the* Barhl2 *domain. D:* In situ *hybridization data for both* cShh and Pax6*. Abbreviations: Tel- telencephalon; Di- diencephalon; PT- pretectum; Th- thalamus; pTh- prethalamus; Mes- mesencephalon; Rh- rhombencephalon; SC-spinal cord; VZ- ventricular zone; ZLI-* zona limitans intrathalamica*; Hyp- hypothalamus; Ctx- cortex.*

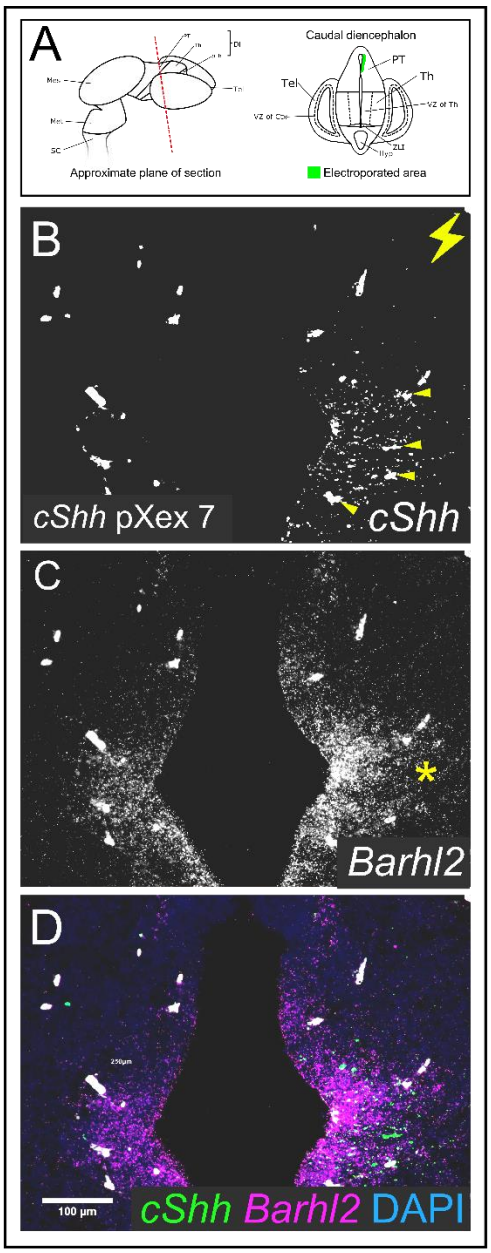

Fig. 7.27: Detail of embryo 7, caudal section. A: Schematic to illustrate the position of the electroporated area. B: In situ *hybridization data for* cShh *mRNA. The lightening flash denotes the electroporated side of the embryo. The arrows indicate areas in which cells were transfected. C:* In situ *hybridization data for* Barhl2*. The asterisk denotes an apparent upregulation of* Barhl2 *and a lateral expansion of the* Barhl2 *domain. D:* In situ *hybridization data for both* cShh and Pax6*. Abbreviations: Tel- telencephalon; Di- diencephalon; PT- pretectum; Th- thalamus; pTh- prethalamus; Mes- mesencephalon; Rh- rhombencephalon; SC-spinal cord; VZ- ventricular zone; ZLI-* zona limitans intrathalamica*; Hyp- hypothalamus; Ctx- cortex.*

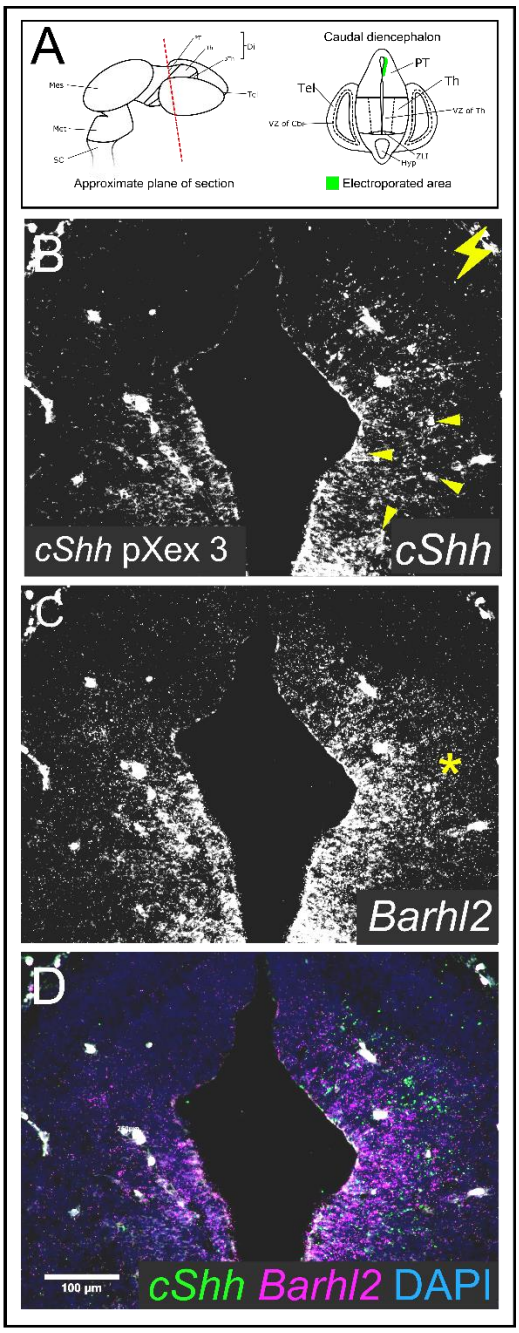

Fig. 7.28: Detail of embryo 3, caudal section. A: Schematic to illustrate the position of the electroporated area. B: In situ *hybridization data for* cShh *mRNA. The lightening flash denotes the electroporated side of the embryo. The arrows indicate areas in which cells were transfected. C:* In situ *hybridization data for* Barhl2. *The asterisk denotes an apparent upregulation of* Barhl2 *and a lateral expansion of the* Barhl2 *domain. D:* In situ *hybridization data for both* cShh and Pax6. *Abbreviations: Tel- telencephalon; Di- diencephalon; PT- pretectum; Th- thalamus; pTh- prethalamus; Mes- mesencephalon; Rh- rhombencephalon; SC-spinal cord; VZ- ventricular zone; ZLI-* zona limitans intrathalamica*; Hyp- hypothalamus; Ctx- cortex.*

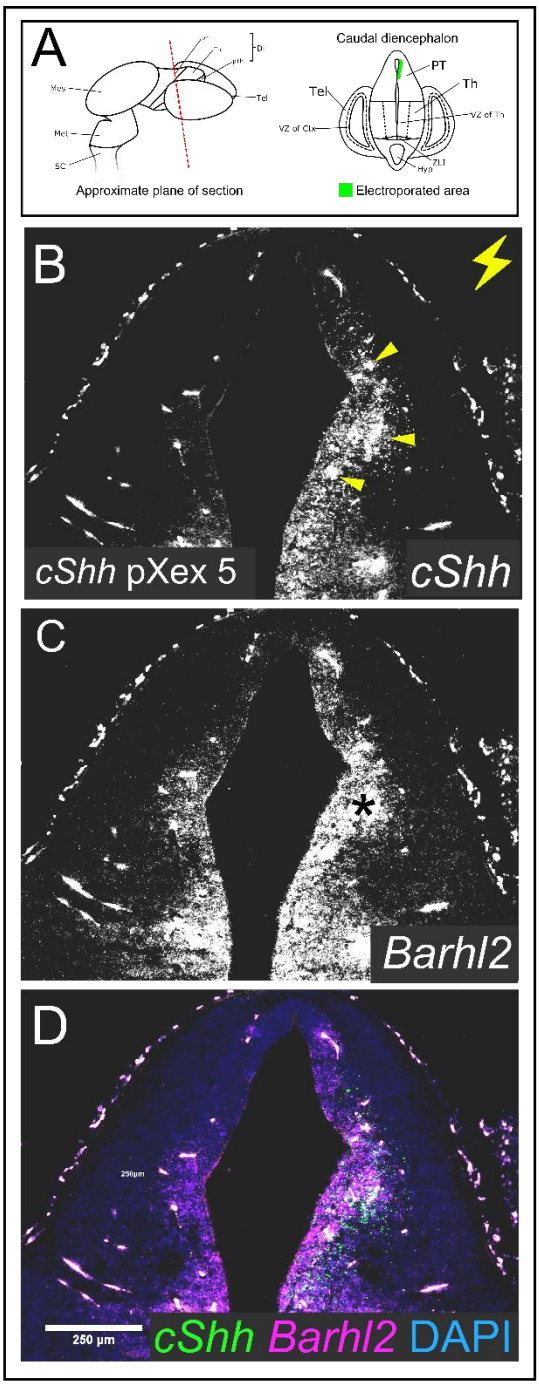

Fig. 7.29: Detail of embryo 5, caudal section. A: Schematic to illustrate the position of the electroporated area. B: In situ *hybridization data for* cShh *mRNA. The lightening flash denotes the electroporated side of the embryo. The arrows indicate areas in which cells were transfected. C:* In situ *hybridization data for* Barhl2*. The asterisk denotes a region of stronger* Barhl2 *expression within the electroporated area. D:* In situ *hybridization data for both* cShh and Pax6*. Abbreviations: Tel- telencephalon; Di- diencephalon; PT- pretectum; Th- thalamus; pTh- prethalamus; Mes- mesencephalon; Rh- rhombencephalon; SC-spinal cord; VZ- ventricular zone; ZLI-* zona limitans intrathalamica*; Hyp- hypothalamus; Ctx- cortex.*

Data for *Barhl2* expression was also obtained from two embryos which had been electroporated with cShh in the hypothalamus (Fig. 7.30). On the electroporated side of a caudal section cut from embryo 2 (lightning flash, Fig. 7.30B) *cShh* was found to be strongly expressed in a ventral region of the hypothalamus (arrows, Fig. 7.30B) and a strong downregulation of *Barhl2* was observed in this region of neuroepithelium (asterisk, Fig. 7.30C). Embryo 4 was also successfully electroporated in a region of neuroepithelium within the hypothalamus, although the expression of *cShh* was less strong than in embryo 2, and on the electroporated side of this embryo (Fig. 7.30E) *cShh* was also found to be expressed in a more ventral region of the hypothalamus (arrows, Fig. 7.30E). In this embryo no downregulation of *Barhl2* was observed within the electroporated region of neuroepithelium (asterisk, Fig. 7.30F), although this may be due to the expression of *cShh* being much weaker in the electroporated area. The hypothalamus was only successfully electroporated with *cShh* pXeX in a total of two embryos, and in neither of the two embryos electroporated with pTP6 alone (Table 7.1) so data for a control experiment for the hypothalamus was not available for comparison.

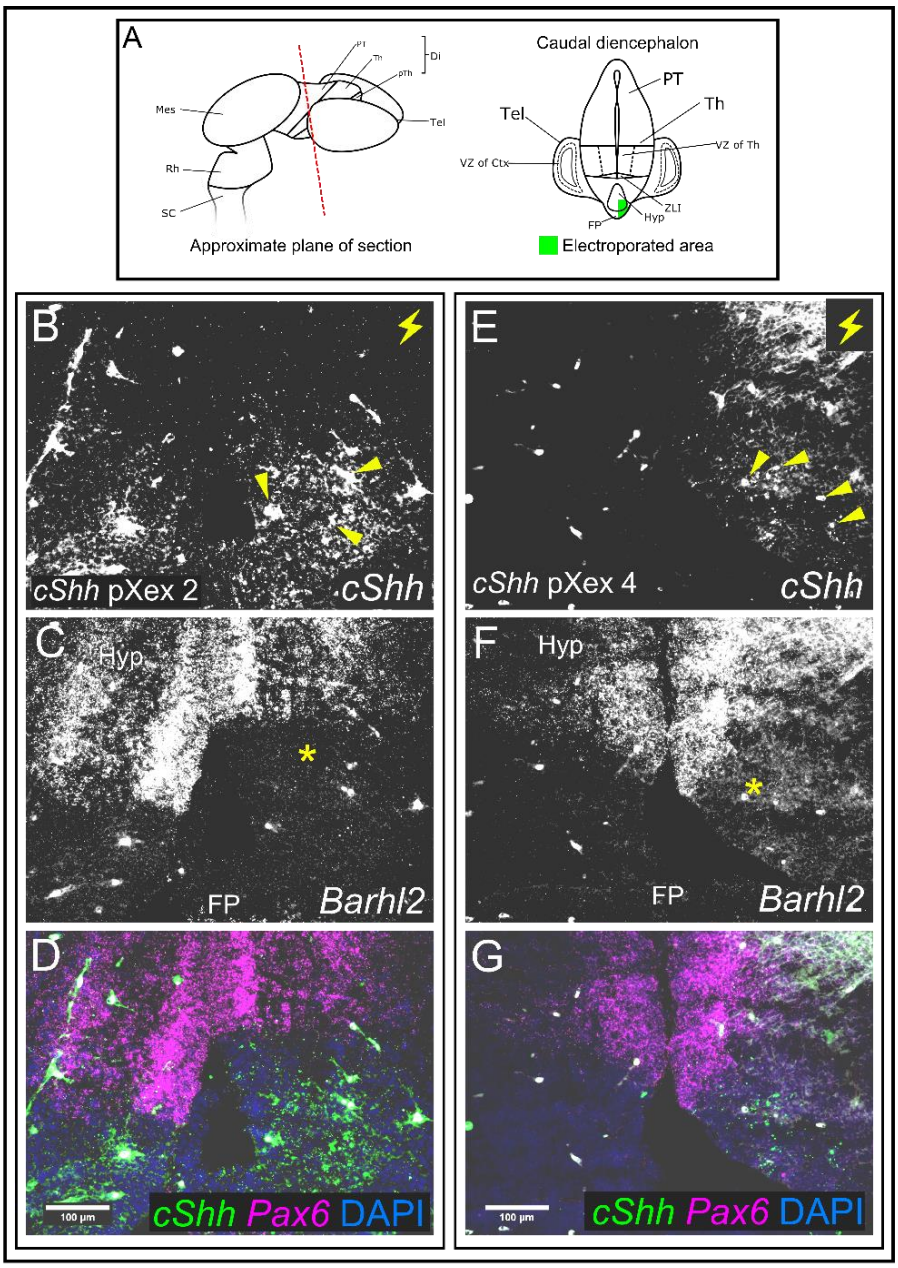

Fig. 7.30: Analysis of changes in Barhl2 *expression in the hypothalamus of embryos electroporated with* cShh *pXeX by double* in situ *hybridization for* Barhl2 *and* cShh mRNA. A: Schematics *to illustrate the approximate plane of section and the approximate position of the electroporated area. B-D: Data for embryo 2. E-G: Data for embryo 4. The lightening flashes denotes the electroporated side of the embryo. The arrows indicate areas in which cells were transfected. Asterisk in C denotes an apparent downregulation of* Barhl2*. Asterisk in F denotes no downregulation of* Barhl2 *within the electroporated area. Abbreviations: Tel- telencephalon; Di- diencephalon; PT- pretectum; Th- thalamus; pTh- prethalamus; Mes- mesencephalon; Rh- rhombencephalon; SC-spinal cord; VZ- ventricular zone; ZLI-* zona limitans intrathalamica*; Hyp- hypothalamus; Ctx- cortex.*

Data for *Barhl2* expression was successfully obtained for all six of the embryos which had been electroporated with *cShh* pXeX in a region spanning the ZLI and parts of the thalamus and prethalamus (Fig. 7.31 and Fig. 7.32).

On the electroporated side of embryo 1 (lightning flash, Fig. 7.31B) *cShh* was not strongly expressed. No changes in *Barhl2* expression were apparent (Fig. 7.31C). This was also the case with embryo 4, where little *cShh* mRNA was detected on the electroporated side (lightning flash, Fig. 7.31E) and *Barhl2* expression appeared to have been unaffected by the electroporation (Fig. 7.31F).

On the electroporated side of embryo 6 (lightning flash, Fig. 7.32B) *cShh* expression was only strong in small discrete regions within the more ventral regions of the thalamus and the ZLI. The expression domains of *Barhl2* in these regions were broadly symmetrical (Fig. 7.32C) and the expression of *Barhl2* also appeared to have been unaffected by the electroporation.

On the electroporated side of embryo 9 (lightning flash, Fig. 7.32H) *cShh* expression was strong in one small region close to the ventricular surface but was otherwise weak and diffuse. The expression domains of *Barhl2* in this embryo were broadly symmetrical (Fig. 7.32I) and no changes in the levels of *Barhl2* expression on the electroporated side appeared to have been induced by the electroporation.

On the electroporated side of embryo 5 (lightning flash, Fig. 7.31H) expression of *cShh* was relatively strong and *cShh* mRNA was detected over a broad area of neuroepithelium. Data for this embryo are presented at a higher resolution in Fig. 7.33. On the electroporated side of this embryo (lightning flash, Fig. 7.33B) expression of *cShh* was moderately strong and mostly diffuse, with a number of discrete regions of strong *cShh* expression within the electroporated area (arrows, Fig. 7.33B). *Barhl2* expression within the electroporated area (asterisk, Fig. 7.33C) did not appear to have been altered and the domains on both sides were comparable in size and the strength of *Barhl2* expression within.

On the electroporated side of embryo 7 (lightning flash, Fig. 7.32E) expression of *cShh* was relatively strong and observed across a broad region of neuroepithelium. Data for this embryo are presented at higher resolution in Fig. 7.34. On the

electroporated side of this embryo (lightning flash, Fig. 7.34B) diffuse *cShh* expression was detected over a wide area of the neuroepithelium, with small and discrete regions of strong *cShh* expression within (arrows, Fig. 7.34B). Within the electroporated area *Barhl2* expression did not appear to have been altered (asterisk, Fig. 7.34C) and the shape of the *Barhl2* domain appeared similar to that of the *Barhl2* domain on the unelectroporated side.

Data for *Barhl2* expression was successfully obtained for one embryo which had been electroporated with *cShh* pXeX in an area around the ZLI and ventral thalamus in the rostral diencephalon, and for the same region of the pTP6 control embryo (Fig. 7.35). On the electroporated side of a rostral section cut from embryo 3 (lightning flash, Fig. 7.35B) several discrete regions of strong *cShh* expression were observed over a small area of neuroepithelium spanning a ventral region of the pTh-C, the p-Th-R and the ZLI (arrows, Fig. 7.35B). Within the electroporated region an apparent downregulation of *Barhl2* was observed (asterisk, Fig. 7.35C). On the electroporated side of a rostral section cut from the pTP6 control embryo (lightning flash, 7.35E) GFP was found to be expressed in a region spanning the ventral pTh-C, the pTh-R and the ZLI (arrows, Fig. 7.35E) but no change in *Barhl2* expression was observed within the electroporated region (asterisk, Fig. 7.35F).

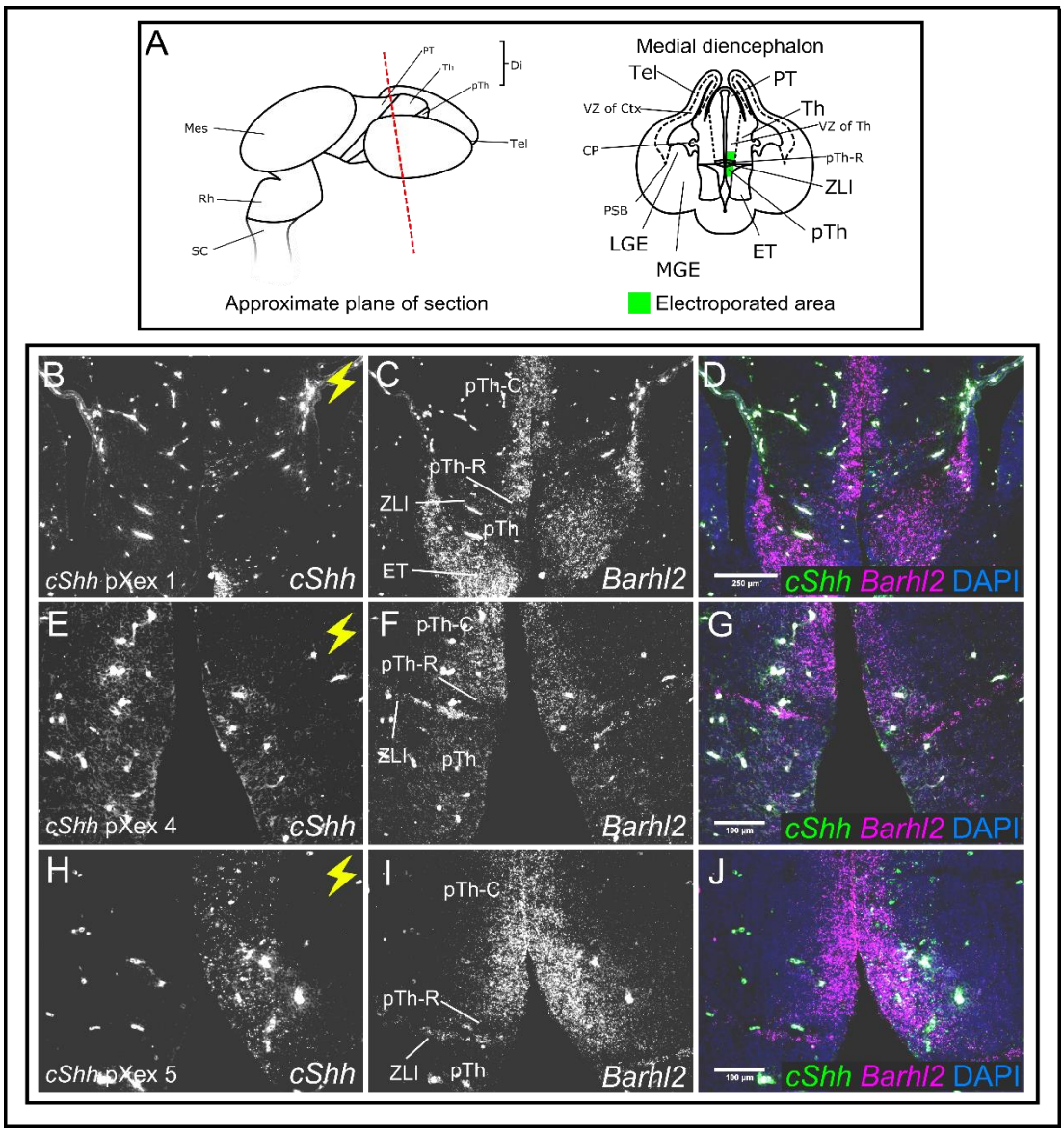

Fig. 7.31: Analysis of changes in Barhl2 *expression in the thalamus, ZLI and prethalamus of embryos electroporated with* cShh *pXeX by double* in situ *hybridization for* Barhl2 *and* cShh mRNA. A: Schematics *to illustrate the approximate plane of section and the approximate position of the electroporated area. B-D: Data for embryo 1. E-G: Data for embryo 3. H-J: Data for embryo 4. K-M: Data for embryo 5. The lightning flashes denote the electroporated side of the embryo. Single asterisks: The electroporated area of the thalamus. Double asterisks: The electroporated area of the prethalamus. Abbreviations: Tel- telencephalon; Di- diencephalon; PT- pretectum; Th- thalamus; pTh- prethalamus; ZLI-* zona limitans intrathalamica*; MGE- medial ganglionic eminence; LGE- lateral ganglionic eminence; ET-* eminentia thalami*; VZ- ventricular zone; Ctx- cortex; Mes- mesencephalon; Rh- rhombencephalon; SC-spinal cord.*

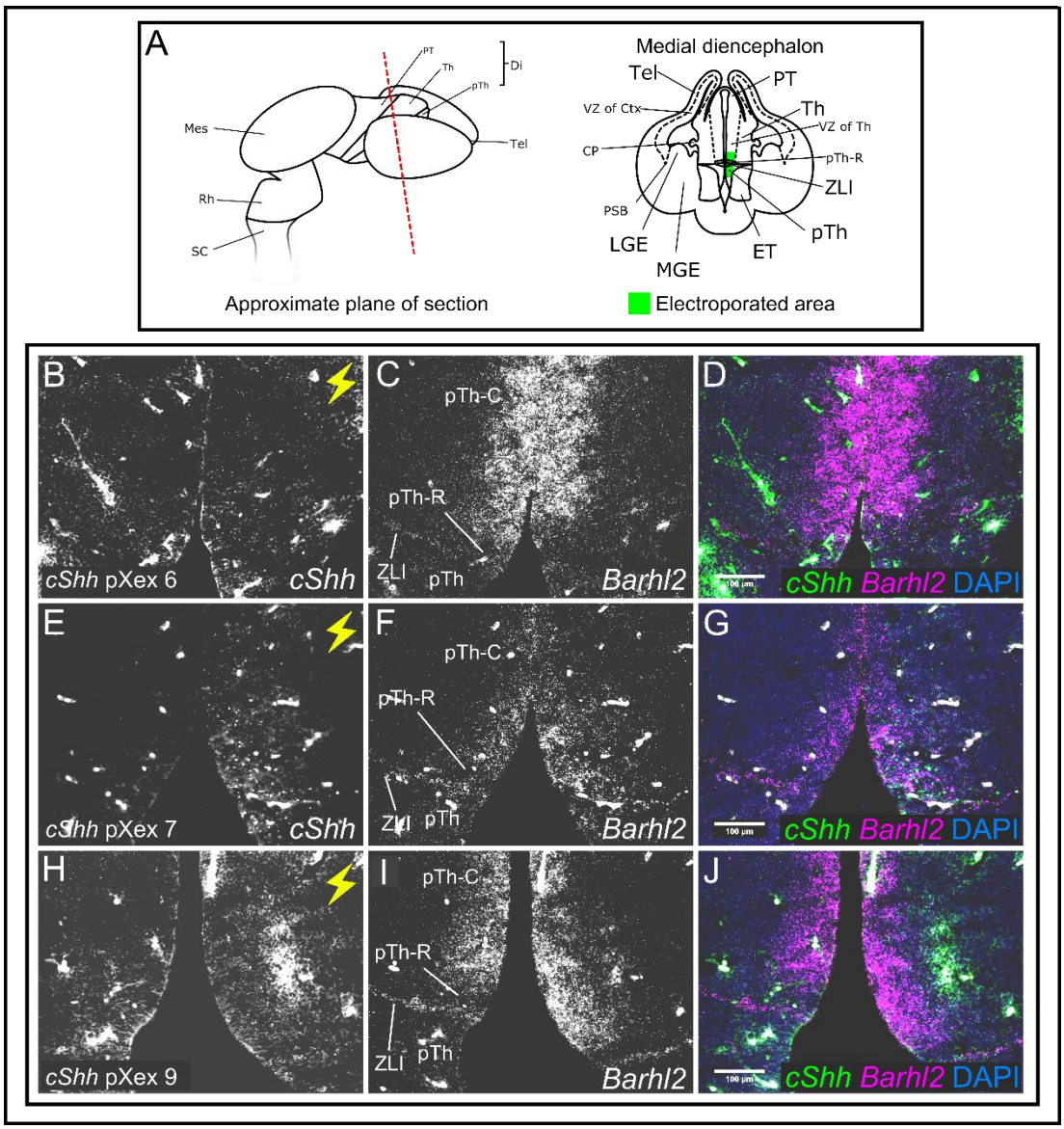

Fig. 7.32: Analysis of changes in Barhl2 *expression in the thalamus, ZLI and prethalamus of embryos electroporated with* cShh *pXeX by double* in situ *hybridization for* Barhl2 *and* cShh mRNA. A: Schematics *to illustrate the approximate plane of section and the approximate position of the electroporated area. B-D: Data for embryo 6. E-G: Data for embryo 7. H-J: Data for embryo 9. The lightning flashes denote the electroporated side of the embryo. Single asterisks: The electroporated area of the thalamus. Double asterisks: The electroporated area of the prethalamus. Abbreviations: Tel- telencephalon; Di- diencephalon; PT- pretectum; Th- thalamus; pTh- prethalamus; ZLI-* zona limitans intrathalamica*; MGE- medial ganglionic eminence; LGE- lateral ganglionic eminence; ET-* eminentia thalami*; VZ- ventricular zone; Ctx- cortex; Mes- mesencephalon; Rh- rhombencephalon; SC-spinal cord.*

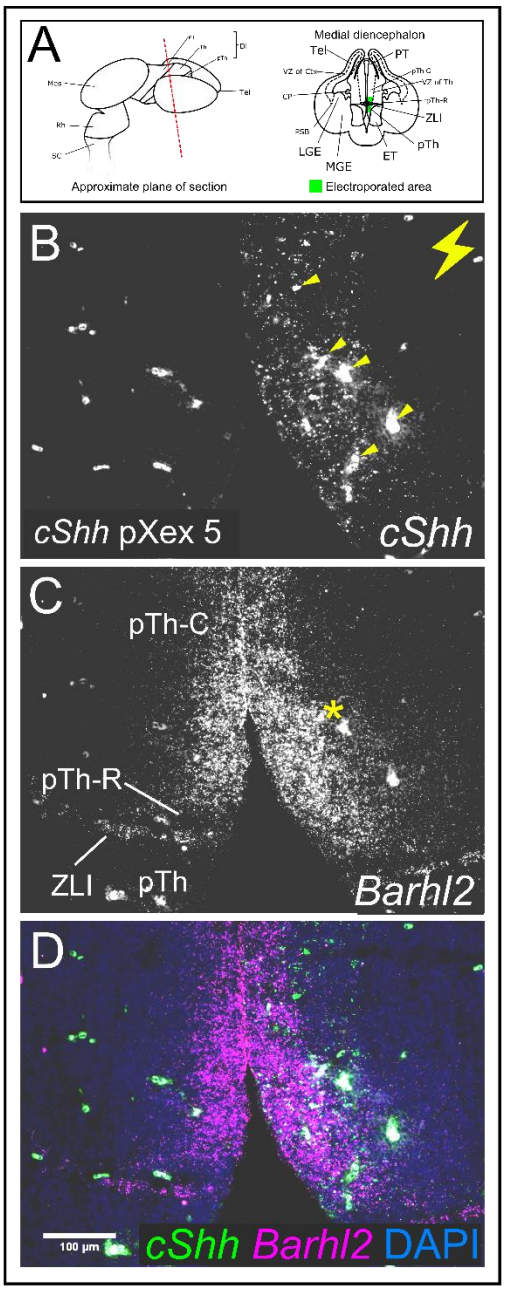

Fig. 7.33: Detail of embryo 5, medial section. A: Schematic to illustrate the position of the electroporated area. B: In situ *hybridization data for* cShh *mRNA. The lightening flash denotes the electroporated side of the embryo. The arrows indicate areas in which cells were transfected. C:* In situ *hybridization data for* Barhl2*. The asterisk denotes no apparent change in* Barhl2 *expression within the electroporated area. D:* In situ *hybridization data for both* cShh and Pax6*. Abbreviations: Tel- telencephalon; Di- diencephalon; PT- pretectum; Th- thalamus; pTh- prethalamus; Mes- mesencephalon; Rh- rhombencephalon; SC-spinal cord; VZ- ventricular zone; ZLI-* zona limitans intrathalamica*; Hyp- hypothalamus; Ctx-cortex.*

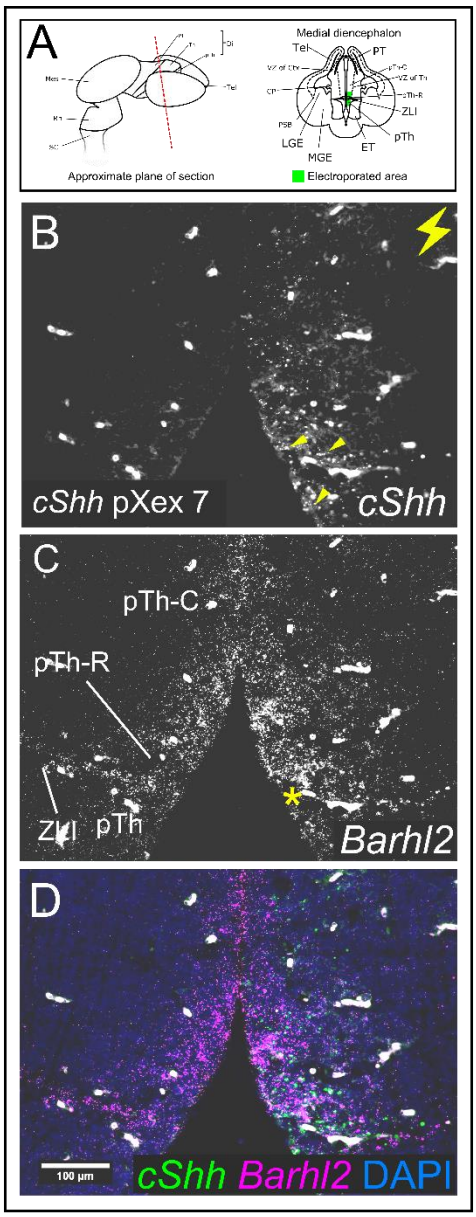

Fig. 7.34: Detail of embryo 7, medial section. A: Schematic to illustrate the position of the electroporated area. B: In situ *hybridization data for* cShh *mRNA. The lightening flash denotes the electroporated side of the embryo. The arrows indicate areas in which cells were transfected. C:* In situ *hybridization data for* Barhl2*. The asterisk denotes no apparent change in* Barhl2 *expression within the electroporated area. D:* In situ *hybridization data for both* cShh and Pax6*. Abbreviations: Tel- telencephalon; Di- diencephalon; PT- pretectum; Th- thalamus; pTh- prethalamus; Mes- mesencephalon; Rh- rhombencephalon; SC-spinal cord; VZ- ventricular zone; ZLI-* zona limitans intrathalamica*; Hyp- hypothalamus; Ctx-cortex.*

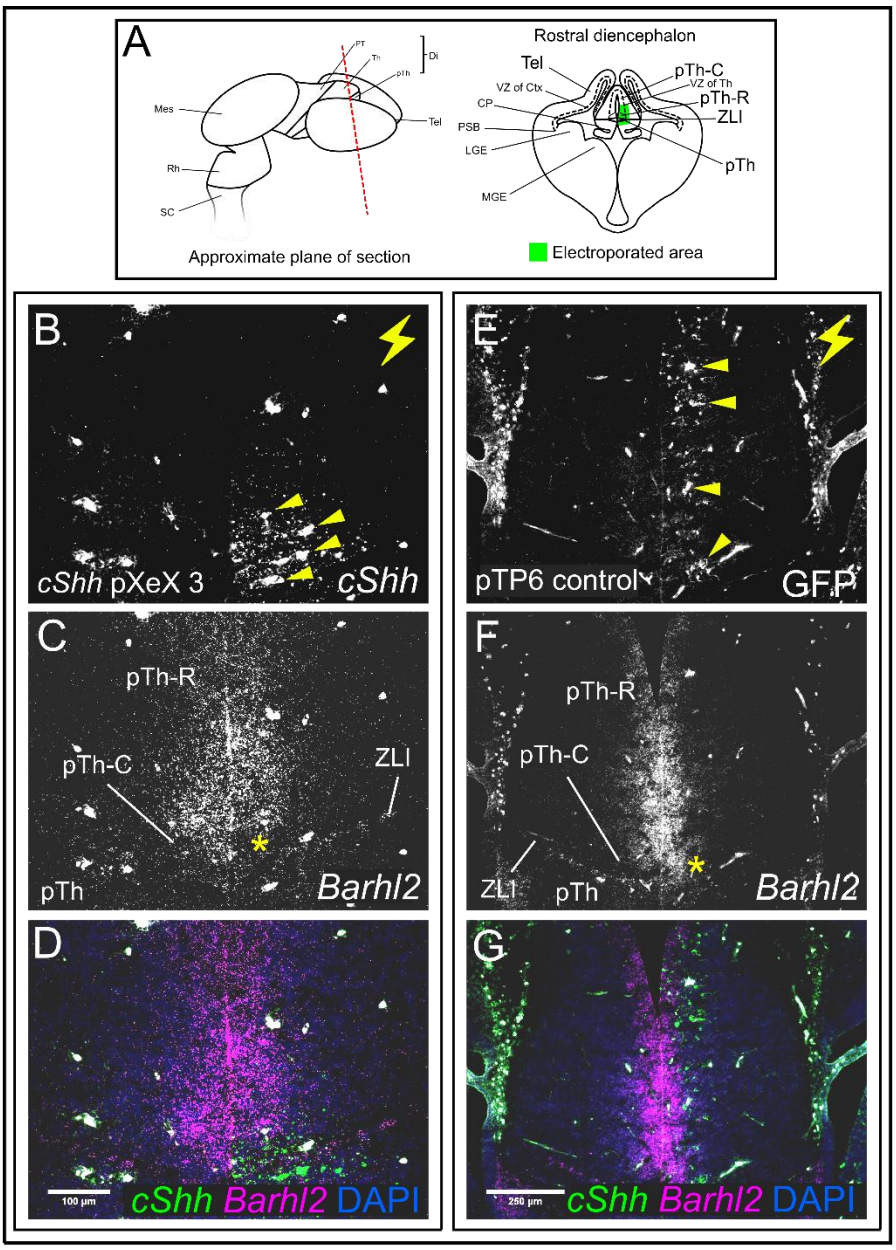

Fig. 7.35: Detail of embryo 3 and pTP6 control, rostral sections. A: Schematic to illustrate the position of the electroporated area. B: In situ *hybridization data for* cShh *mRNA. C:* In situ *hybridization data for* Barhl2*. The asterisk denotes a potential downregulation of* Barhl2 *expression within the electroporated area. D:* In situ *hybridization data for both* cShh and Pax6*. E: Immunostaining for GFP.* In situ *hybridization data for* Barhl2 *mRNA. F:* In situ *hybridization data for* Barhl2 *and immunostainign for* GFP*. The lightening flashes denote the electroporated side of the embryo. The arrows indicate areas in which cells were transfected. Abbreviations: Tel- telencephalon; Di- diencephalon; PT- pretectum; Th- thalamus; pTh- prethalamus; Mes- mesencephalon; Rh- rhombencephalon; SC-spinal cord; VZ- ventricular zone; ZLI-* zona limitans intrathalamica*; Hyp- hypothalamus; Ctx- cortex.*

7.2.7 Summary of results

A summary of the results of the experiments described in 7.2.4 - 7.2.6 is presented in Table 7.2.

Rostral diencephalon				
Gene	**pTh-C**			
Ptch1	-			
Pax6	-			
Barhl2	↓(1/1)			
Medial diencephalon				
Gene	**pTh-C**	**pTh-R**	**ZLI**	**Prethalamus**
Ptch1	↑ (4/6)	↑ (4/6)	○ (6/6)	↑ (2/6)
Pax6	↓ (1/6)	○ (6/6)	○ (6/6)	○ (6/6)
Barhl2	○ (6/6)	○ (6/6)	○ (6/6)	○ (6/6)
Caudal diencephalon				
Gene	**Pretectum**	**Hypothalamus**		
Ptch1	↑ (7/7)	-		
Pax6	↓(3/8)	-		
Barhl2	↑ (6/8)	↓(1/2)		

↑ Upregulation ↑ Downregulation

○ No change - Change not determined

Table 7.2: Summary of the changes in gene expression observed for Ptch1, Pax6, *and* Barhl2 *in the regions of the diencephalon which were electroporated with* cShh *pXeX and then analysed with* in situ *hybridization.*

7.3 Discussion

Within control embryos electroporated with pTP6 alone no apparent changes in the expression of *Ptch1*, *Pax6* and *Barhl2* were observed. This suggested that any changes in gene expression observed in the embryos electroporated with both pTP6 and *cShh* pXeX were induced as a consequence of electroporation with *cShh* pXeX and not by the electroporation technique itself, or by the ectopic expression of tau GFP encoded by the pTP6 plasmid.

Investigation of the ectopic expression of *cShh* by *in situ* hybridization confirmed that *cShh* mRNA was being expressed in electroporated cells. The upregulation of *Ptch1*, a known target of *Shh* which is upregulated by *Shh* signalling in vertebrate cells (Marigo *et al* 1996), within some areas of electroporated neuroepithelium suggests that the ectopic expression of the *cShh* protein encoded by the *cShh* pXeX plasmid was sufficient to activate the *Shh* pathway in mouse.

The upregulation of *Ptch1* apparently induced by the activation of *Shh* signalling was not observed in all the regions of diencephalic neuroepithelium which were analysed, which suggests that the activation of *Shh* signalling by the method described here is context-dependent. Upregulation of *Ptch1* was observed in the pretectum, the pTh-C and pTh-R of the thalamus, and within the MGE, but no upregulation of *Ptch1* was apparent in the electroporated neuroepithelium of the ZLI, and it was only weakly upregulated in the prethalamus in two of six embryos. *Ptch1* is the receptor to which *Shh* binds (Marigo *et al* 1996) and is normally not expressed within the ZLI (Caballero *et al* 2014) so it is perhaps to be expected that electroporation with *cShh* does not induce *Ptch1* expression within the ZLI, and that *Ptch1* is upregulated in the thalamus, where *Ptch1* is ordinarily expressed at a relatively low level (Platt *et al* 1997).

The observation that electroporation with *cShh* did not lead to a great increase in *Ptch1* mRNA levels in the prethalamus, where endogenous *Ptch1* is more strongly expressed (Platt *et al* 1997) is harder to interpret. This region of the diencephalon may be exposed to a higher concentration of endogenous *Shh* from both the ZLI and the floorplate and it may be possible that this concentration meets an upper threshold for the induction of further *Shh* activity, and that ectopic expression of *cShh* is therefore unable to activate the pathway much further. It is not clear why electroporation with *cShh* was only seen to cause a lateral expansion of the prethalamic *Ptch1* domain in one embryo while this lateral expansion was more often observed within electroporated regions of the thalamus. This observation suggests the existence of differential competence between the neuroepithelium of the thalamus and prethalamus, a possibility that would be consistent with previous published findings (Kiecker and Lumsden 2004, Robertshaw *et al* 2013).

The observed changes in the expression of *Pax6* and *Barhl2* also support the possibility that activation of *Shh* signalling via the ectopic expression of *cShh* is context-dependent. Changes in their expression induced by electroporation by *cShh* pXeX were observed in the pretectum but not within the thalamus, with the possible exception of one embryo in which a small but not entirely convincing downregulation of *Pax6* was observed, and a small region of the rostral pTh-C in which *Barhl2* expression appeared to have been more strongly downregulated.

The expression of *Barhl2* also appeared to have been downregulated in the hypothalamus in one embryo despite the fact that it seemed to have been upregulated within the pretectum of a majority of the embryos analysed. It may be possible that the effect of the *Shh* signal on *Barhl2* expression differs between different regions of neuroepithelium. In order to investigate this possibility further a greater number of embryos would need to be successfully electroporated in a region spanning the hypothalamus. The hypothalamus proved to be more difficult to electroporate than other areas of diencephalic neuroepithelium and it may be necessary to make further modifications to the electroporation technique in order to successfully electroporate a sufficient number of embryos, such as modifying the placement of the electrodes or injecting the plasmid DNA solution via a more caudal entry point, such as the midbrain. In order to further investigate the effects of *Shh* pathway activation on the expression of *Barhl2* in the most rostral region of the pTh-C it may be necessary to repeat the experiment as described, but with an alteration in the position of the electrodes during the application of the current.

The observed upregulation of *Barhl2* in response to *Shh* pathway activation in the pretectum may be consistent with findings from *Drosophila* studies, which have shown that *Hh* is required for the induction of *BarH1* and *BarH2* expression (Lim and Choi 2003). While the results of the experiment described in Chapter 4.2 showed that *Shh* is not required for the induction of *Barhl2* expression in mouse, it may still be possible that *Shh* serves to upregulate murine *Barhl2* expression.

The observed downregulation of *Pax6* within the pretectum is consistent with earlier studies showing that *Shh* is able to inhibit *Pax6* expression in some contexts (Ericson *et* al 1997, Goulding *et al* 2003, Kiecker and Lumsden 2004, Vieira *et al* 2005,

Robertshaw *et al* 2013, Caballero et al 2014) though it is not clear why this downregulation was only observed within a relatively narrow region of the pretectum, or why it was observed in a minority of the embryos analysed.

One previous study reported that the diencephalic expression domains of *Pax6* and *Irx3* overlap in a region spanning the prospective thalamus, and that their expression in this region is a requirement for the specification of the thalamus (Robertshaw *et al* 2013). It may be possible that a molecular characteristic of the thalamus, such as the co-expression of *Pax6* and *Irx3*, exerts a partial or complete "shielding" effect against the influence of *Shh* signalling on thalamic gene expression, so that while *Shh* signalling can be activated within the thalamus, it has no effect on the expression of particular genes, while the expression of these genes can be altered by elevated *Shh* activity in the pretectum.

One possible exception to the observation that *Pax6* and *Barhl2* expression was unaltered by *Shh* pathway activation in the thalamus was noted. In a region of the pTh-C in a relatively rostral section of the diencephalon *Barhl2* appeared to have been downregulated within the area electroporated with *cShh* pXeX. This effect on *Barhl2* expression was only observed in one of the eight embryos which were analysed, and only in a small number of sections from that embryo. This may suggest that only a relatively small region of thalamic neuroepithelium is competent to respond to the activation of *Shh* with the downregulation of *Barhl2* expression. Alternatively, this effect could have been caused by the ectopic expression of *cShh* being particularly strong in the sections in which *Barhl2* downregulation was observed. This possibility would suggest that thalamic *Barhl2* expression can be downregulated by high concentrations of *Shh*, and that the concentration of *Shh* may have to reach a particular threshold before downregulation of *Barhl2* can be induced. This explanation would be consistent with the fact that *Barhl2* expression is absent from the pTh-R, a region exposed to a high concentration of endogenous *cShh*, and in which further activation of the *cShh* pathway by ectopic expression of *cShh* is possible.

Pax6 expression is also normally absent from the pTh-R (Caballero *et al* 2014) and its expression within the thalamus is restricted to the pTh-C, where it induces the

differentiation of glutamatergic neurons. *Shh* signalling from the ZLI has been shown to be required for the inhibition of *Pax6* expression within the rostral extent of the thalamus, allowing the development of the GABAergic pTh-R in chick (Robertshaw *et al* 2013). It is therefore surprising that activation of *Shh* signalling via electroporation with *cShh* pXeX did not appear to be sufficient to inhibit *Pax6* expression in the experiments described here. As with *Barhl2*, this may be a consequence of the concentration of *cShh* not reaching the threshold required to inhibit *Pax6* expression. It may also be possible that the mechanism of pTh-R development in mouse differs from that in chick, although findings from studies of a mouse mutant lacking diencephalic *Shh* expression suggest that this is not the case (Szabó *et al* 2009).

Further experiments would be required to obtain more convincing evidence that *Barhl2* can be downregulated by *Shh* within the pTh-C, and to obtain evidence that thalamic *Pax6* expression can be downregulated by *Shh* pathway activation via electroporation in mouse as it can in chick. This could be achieved by injecting *cShh* pXeX plasmid DNA solution of a higher concentration, although the concentration used in the experiments described here appeared to be sufficient to activate *Ptch1* upregulation. Alternatively an electroporation construct encoding *Smo*-M2 could be used. *Smo-M2*, a construct bearing a constitutively active mutant form of *Smo*, could be used to strongly induce the effects of concentration-dependent *Shh* signalling (Hynes *et al* 2000, Ribes *et al* 2010, Vue *et al* 2009, Robertshaw *et al* 2013).

While the use of *Smo*-M2 may have been a more effective means of activating the *Shh* pathway, the electroporation of the diencephalic neuroepithelium with *cShh* pXeX, the observation of its effects, and the identification of tissues which are competent to respond to it may have provided some insights into the effects of increasing the concentration of the morphogen itself, rather than the effects of activating a process of the *Shh* pathway which is downstream of the binding of *Shh* to the receptor *Ptch1*. Further experiments using the method described here may be used to comprehensively map the regions of competence to *Shh* pathway activation and to quantify the range of the signal within different regions of the diencephalon.

The technique of *in utero* electroporation also produces variable results by its nature. Electroporation efficiency can vary greatly between treated embryos even when factors such as the voltage used and the concentration of DNA plasmid solution injected are the same for each embryo. The concentration of DNA which can be used is limited as very concentrated solutions can be too viscous to use and can block the tip of the micropipette. Administering current at a higher voltage can increase the efficiency of electroporation, but the use of too high a voltage can cause tissue damage. The solution to the problem of variability with this technique could be to treat a greater number of embryos. For this study, nine embryos were electroporated with both the *cShh* pXeX and pTP6 plasmids, and two with pTP6 alone. If this study was to be repeated, ideally a larger number of embryos would be electroporated, and only those in which the electroporated area was sufficiently broad, and the expression of the transfected genes sufficiently strong, would be used to determine whether or not the electroporation had induced changes in gene expression.

As *Ptch1* is a *bona fide* target of *Shh* signalling (Marigo *et al* 1996) the lateral extent of the *Ptch1* domain could potentially be used as an indicator of the distance *cShh* diffuses from the electroporated cells which ectopically express it, but in the experiments described here it was found that the region of *Ptch1* upregulation did not extend beyond the electroporated region, and in most cases it was confined to a smaller region within the electroporated area and overlapped by the *cShh*-expressing area, close to the ventricular surface. This suggests that *cShh* was not able to induce an upregulation of *Ptch1* throughout the whole of an electroporated region of tissue.

By contrast, in several embryos the region of *Barhl2* upregulation extended beyond the electroporated region, and in some cases *Barhl2* upregulation was observed at a considerable distance from the electroporated area.

Together these observations suggest that *cShh* was able to diffuse through the neuroepithelium and induce effects on *Barhl2* expression at a relatively long range, while it was not able to exert the same long-range effects on *Ptch1* expression.

These observations may be due to the graded nature of *Shh* signalling and the dose-dependent nature of its effects. It could be possible that *Ptch1* was only upregulated

where *cShh* expression was particularly strong and cShh protein may have been present at a high concentration, while upregulation of Barhl2 required a lower concentration of cShh protein. Alternatively, it is possible that not all neuroepithelium within the electroporated area was competent to respond to the ectopic expression of *cShh* in the same way. Cells closer to the ventricular surface may be competent to respond to respond to the *cShh* signal with an upregulation of *Ptch1* while those closer to the pial surface may not be, and it may be possible that cells of the pretectum are competent to respond to the *cShh* signal with an upregulation of *Barhl2* both in regions close to the ventricular surface and in regions close to the pial surface.

In general, the extent of the regions of gene upregulation may also be influenced by different properties of the extracellular matrix (ECM) or to differing cell densities throughout the diencephalon, both of which may affect the rate at which *cShh* protein can diffuse through the tissue, and the range of the *Shh* signal.

8. Discussion

8.1 Introduction

Barhl2 and its homologues are known to play essential roles in many processes of neural development, with findings related to its function having been obtained from studies in the *Drosophila* retina (Lim and Choi 2003), the zebrafish diencephalon (Staudt and Houart 2008), the *Xenopus* diencephalon (Juraver-Geslin et al *2014)* and the mouse spinal cord (Ding *et al* 2009) among other structures in a range of animal models. Until now the expression and functions of *Barhl2* had not been studied extensively in the murine diencephalon, where its striking expression pattern (Suzuki-Hirano *et al* 2011) is suggestive of interactions with both *Pax6* and *Shh*.

The aim of this study was to build on these earlier findings with a comprehensive analysis of *Barhl2* expression and function within a mammalian model system. It also aimed to consider the interactions between *Barhl2* and two more widely-studied genes, the transcription factor *Pax6* and the morphogen *Shh*, both of which are required for the correct development of the mammalian diencephalon.

By considering the findings from this investigation of the spatiotemporal dynamics of *Pax6* and *Barhl2*, and into the different relationships which may exist between them and *Shh*, it has been possible to speculate on the nature of these relationships, and on possible functions for the interactions between the three genes in the development of the mammalian diencephalon.

8.2 Characterisation of the relationships between *Pax6, Barhl2* and *Shh*

8.2.1 The relationship between *Pax6* and *Barhl2*

There is limited evidence from the literature to suggest the existence of a mutually repressive relationship between *Pax6* and *Barhl2*. Morpholino knockdown of *Barhl2* expression in the *Xenopus* embryo leads to an upregulation of *Pax6* (Juraver-Geslin *et al* 2011) while screening for potential binding sites of *Pax6* protein identified a total of thirteen for *Barhl2* (Coutinho *et al* 2011). A study mapping the expression of a number of novel candidates for the control of diencephalic patterning described an expression pattern of *Barhl2* (Suzuki-Hirano *et al* 2011) which appeared to be

largely complementary to that of *Pax6* (Caballero *et al* 2014), with the exception of the thalamus, in which both genes appeared to be strongly expressed.

The experiments described here built on these earlier findings by mapping the expression domains of *Pax6* and *Barhl2* in relation to one another over a series of developmental stages. These experiments confirmed that in regions outside the thalamus expression of *Pax6* and *Barhl2* is highly complementary, strongly suggesting the possibility of a mutually repressive relationship existing between the two genes. This possibility was also supported by the observation that, while *Pax6* and *Barhl2* are both expressed in the thalamus, and appear to be co-expressed within individual cells, at E12.5 they are expressed in gradients which run counter to one another, with the gradient of *Pax6* running from dorsal to ventral and from caudal to rostral, and the gradient of *Barhl2* running from ventral to dorsal and from rostral to caudal.

The existence of a different relationship between *Pax6* and *Barhl2* expression in the thalamus also suggested the possibility of mutual repression between the two genes, but also that this repression may be incomplete within the thalamus. The expression of *Pax6* and *Barhl2* in the diencephalon at E12.5 is summarised in Fig. 8.1.

Quantification of the expression gradients along the dorsoventral axis at different developmental stages then suggested that the relationship between *Pax6* and *Barhl2* within the thalamus may be more complicated than one of direct mutual repression, as a quantitative analysis of the image data showed that the expression gradients of *Pax6* and *Barhl2* only countered each other strongly at E12.5.

The possibility of a simple mutually repressive relationship existing between *Pax6* and *Barhl2* was only partially supported by the results of the investigation into *Barhl2* expression in the *Pax6 Sey*^{Ed} mutant mouse (Hill *et al* 1991). While an expansion of the *Barhl2* domain within the thalamus and pretectum was noted, *Barhl2* expression within regions of neuroepithelium rostral to the ZLI was less severely affected by the loss of functional *Pax6*.

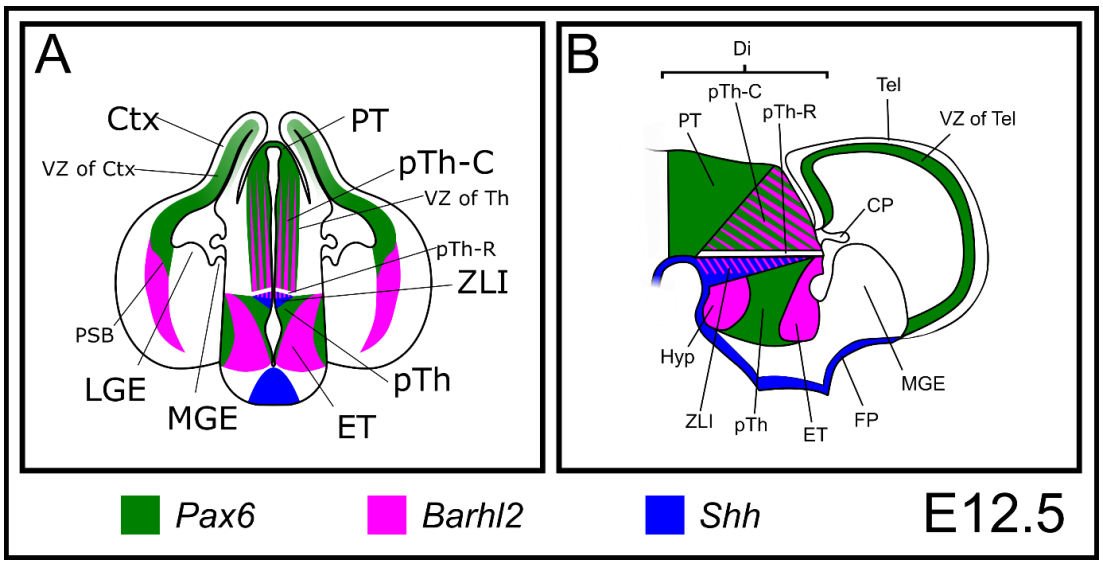

Fig. 8.1: A. Schematic to summarise expression data for Pax6, Barhl2, *and* Shh *mRNA in a coronal section cut at the level of the medial diencephalon. B: Schematic to summarise expression data for* Pax6, Barhl2, *and* Shh *mRNA in a sagittal section through the diencephalon and telencephalon, rostral to right. Abbreviations: Ctx- cortex; VZ- ventricular zone; PT- pretectum; Th- thalamus; ZLI-* zona limitans intrathalamica*; pTh- prethalamus; ET-* eminentia thalami*; MGE- medial ganglionic eminence; LGE- lateral ganglionic eminence; PSB- pallial-subpallial boundary; Di- diencephalon; Tel- telencephalon; CP- choroid plexus; Hyp- hypothalamus; FP- floorplate.*

The analysis of changes in gene expression induced by treatment with vismodegib also did not support the hypothesis that *Pax6* and *Barhl2* act to mutually repress each another's expression. The expansion in the size of the thalamic *Pax6* domain was not accompanied by a contraction of the thalamic *Barhl2* domain, suggesting that in this context *Pax6* may not act to inhibit the expression of *Barhl2*.

Activation of the *Shh* pathway by *in utero* electroporation with *cShh* pXeX was found to downregulate *Pax6* in the dorsal telencephalon while leading to an upregulation of *Barhl2*. It may be possible that an increase in the levels of *Barhl2* as a consequence of elevated *Shh* pathway activity may have led to an increased inhibition of *Pax6* expression, or vice versa, and if this is the case it would support the hypothesis of a mutually repressive relationship existing between *Pax6* and *Barhl2*. It may also be possible that the downregulation of *Pax6* and the upregulation of *Barhl2* may have been direct effects of *Shh* pathway activation and that levels of

Barhl2 may have been altered in a mechanism independent of *Pax6* levels, and vice versa.

8.2.2 The relationship between *Pax6* and *Shh*

It is known that *Shh* signalling is able to inhibit *Pax6* expression within the thalamus (Kiecker and Lumsden 2004, Vieira *et al* 2005, Caballero *et al*). The data obtained from the mapping of *Pax6* expression over several developmental stages appeared to be consistent with this, with *Pax6* expression within the region of the presumptive ZLI being downregulated at the time of ZLI induction (Shimamura *et al* 1995).

Drug treatment with vismodegib was also seen to cause an upregulation of *Pax6* within the cortex and thalamus. Some features of the $Pax6^{Sey/Sey}$ phenotype also appeared to be rescued by the administration of vismodegib, an observation consistent with that of the *Shh* mutant phenotype being rescued by the inhibition of *Pax6* expression.

The inhibition of *Shh* activity by vismodegib appeared to increase the strength of *Pax6* expression within the thalamus and the ventricular zone of the cortex, and also appeared to cause an expansion of the expression domains along the dorsoventral axis. This observation is consistent with that of *Shh* acting as a ventralising factor, and with evidence that it acts to directly inhibit the expression of *Pax6*. The observation of a partial rescue of the $Pax6^{Sey/Sey}$ mutant phenotype in response to treatment with vismodegib was consistent with the observation that inhibition of *Pax6* can rescue features of the phenotype caused by the loss of *Shh*.

Electroporation with *cShh* pXeX appeared to have no effect on *Pax6* expression within the thalamus. This was perhaps surprising given the findings from previous published studies in which a downregulation of *Pax6* expression in response to the activation of *Shh* signalling was observed (Vieira *et al* 2005, Szabó et al 2009, Vue et al 2009) but this observation may be consistent with finding that the activation of *Shh* signalling via electroporation with *Smo* M2 is only able to inhibit *Pax6* expression in more rostral regions of the pTh-C (Robertshaw *et al* 2013). It may be possible that a more focal electroporation of the rostral pTh-C, with a more

concentrated solution of *cShh* pXeX plasmid DNA, could exert a noticeable effect on *Pax6* expression.

8.2.3 The relationship between *Barhl2* and *Shh*

The spatiotemporal dynamics of *Barhl2* expression had not previously been described comprehensively within the developing mouse forebrain. Roles for *Barhl2* in the development of the mammalian forebrain had also not been studied extensively. While previous studies have attempted to characterise the relationships between *Shh* and *Pax6*, the influence of *Shh* signalling on *Barhl2* expression has not been studied as extensively or described in great detail, and not in mammalian models.

In this study the expression of *Barhl2* and *Pax6* was investigated in stages ranging from stages prior to E10.5, at which the ZLI is induced (Shimamura et al 1995) to E13.5, the stage at which the ZLI apparently begins to disappear, until *Shh* expression can no longer be detected at E14.5 (Visel *et al* 2004, Lim and Golden 2007). The spatiotemporal dynamics of *Barhl2* in particular suggested a role for the transcription factor in ZLI development, with the gene being strongly expressed in the prospective ZLI before continuing to be expressed within the ZLI itself following ZLI maturation.

A previous study has shown that *Hh* is required for the induction of *BarH2* in *Drosophila* (Lim and Choi 2003), but this finding was not consistent with a *Xenopus* study in which it was found that *Barhl2* acts upstream of *Shh* in the induction of the ZLI (Juraver-Geslin *et al* 2014). These findings suggest that the relationship between the invertebrate homologues may differ significantly from that which exists between *Barhl2* and *Shh* in vertebrates.

In the experiments described here, *in situ* hybridization for *Barhl2* mRNA in the *Shh*-null mutant mouse confirmed that *Shh* is not required for *Barhl2* expression in mouse, and suggested that *Shh* is expressed downstream of *Barhl2* in the murine ZLI as it is in the ZLI of the *Xenopus* embryo.

While *Shh* does not appear to be required for the induction of *Barhl2* in mouse, and the inhibition of *Shh* signalling via treatment with vismodegib appeared to exert little to no effect on *Barhl2* expression, *Shh* may nonetheless be able to induce an upregulation of *Barhl2* in some contexts. This effect of the *Shh* pathway was observed in a majority of embryos electroporated with *cShh* pXeX within the pretectum.

The opposite effect may have been observed in the rostral diencephalon, where a downregulation of *Barhl2* appeared to have been induced in an electroporated region of the pTh-R. This effect was only observed in one of the embryos analysed, but it was noted in a region in which the ectopic expression of *cShh* was particularly strong. Further experiments would be required to confirm the ability of the activation of *Shh* signalling to downregulate *Barhl2* in the pTh-R, possibly by the use of a more focal electroporation technique and a more concentrated solution of *cShh* pXeX plasmid DNA.

If the activation of *Shh* signalling was found to induce different effects on *Barhl2* expression in the pretectum and thalamus, this would be consistent with published evidence that the effect of *Shh* signalling on diencephalic gene expression is context-dependent (Kiecker and Lumsden 2004, Robertshaw *et al* 2013). In the case of *Barhl2* the response to *Shh* may vary between the thalamus and pretectum. *Shh* signalling may also be able to induce a downregulation of *Barhl2* expression within the hypothalamus, but in order to confirm this the electroporation of the hypothalamus would need to be repeated on a greater number of embryos.

8.3 Potential functions for the interactions between *Pax6*, *Barhl2* and *Shh*

8.3.1 The modulation of thalamic neurogenesis

The mapping of the spatiotemporal dynamics of *Pax6* and *Barhl2* expression showed that the expression of both genes is highly dynamic. The thalamic domain of *Pax6* at E9.5 is fragmented at the point at which *Barhl2* is expressed in a narrow band of neuroepithelium, and the gap in the domain widens along the dorsoventral axis over time. The expression of *Pax6* becomes increasingly confined to the more dorsal and caudal regions of the diencephalon, and by E13.5 *Pax6* expression appears to be

strong in the pretectum but greatly weakened in the remainder of the neuroepithelium caudal to the ZLI.

If *Barhl2* acts to inhibit the expression of *Pax6*, this property may serve to restrict the neurogenic activity of *Pax6* to particular regions of neuroepithelium, thereby serving to modulate thalamic neurogenesis, in particular the differentiation of GABAergic neurons. In turn, inhibition of *Barhl2* expression by *Pax6* may serve to restrict the regions of neuroepithelium in which it can inhibit neurogenesis via its potential inhibition of the expression of bHLH transcription factors.

The presence of strong countergradients of *Pax6* and *Barhl2* expression within the thalamus at E12.5 may be significant as E12.5 is a developmental stage at which a large proportion of thalamic neurogenesis occurs (Suzuki-Hirano *et al* 2011) and the thalamocortical axons begin to form (Simpson *et al* 2009). Mutual repression between *Pax6* and *Barhl2* may act to modulate thalamic neurogenesis at this stage.

This study briefly considered the relationship between *Barhl2* and one example of a *bHLH* transcription factor, *Ngn2*. At E11.5 their expression domains within the thalamus are of a comparable shape and extend laterally to approximately the same distance from the ventricular surface, but by E12.5 the thalamic domain of *Barhl2* is noticeably narrower than that of *Ngn2*. This change in the degree of overlap over time could indicate the presence of a wave of thalamic neurogenesis, with *Barhl2* acting to inhibit *Ngn2* expression in an increasingly narrow region of the pTh-R, acting to modulate neurogenesis induced by *Ngn2*. Such a model would be comparable to the mechanism by which the *Drosophila* retina is patterned by a wave of *ato* activity, and modulated by the inhibitory effect of *BarH2* (Lim and Choi 2003).

8.3.2 ZLI development and maintenance

The ZLI develops within a region of neuroepithelium expressing *Otx2*, *Irx3* and *Barhl2*, and morpholino knockdown of *Barhl2* expression results in a failure of the ZLI to develop (Juraver-Geslin *et al* 2014), while the loss of functional *Pax6* causes the ZLI to undergo an expansion along the rostrocaudal axis of the diencephalon

(Grindley *et al* 1997, Pratt *et al* 2000a). Together these findings suggest that *Barhl2* is required for ZLI initiation, while *Pax6* may play a role in the shaping of the ZLI.

This study showed that the domain of *Barhl2* within the ZLI also expands in the *Pax6*-null mutant mouse. As *Shh* expression appears to be downstream of *Barhl2* in the process of ZLI development, it may be possible that the expansion of the ZLI is a consequence of the expansion of the *Barhl2* domain in which it develops. Inhibition of *Barhl2* expression by *Pax6* may therefore serve to limit the region of *Barhl2*-positive neuroepithelium which is competent to develop into the ZLI. This could act to maintain the ZLI at a particular size, limiting the quantity of *Shh* protein it can secrete and modulating the *Shh* concentration gradients within the diencephalon to ensure that it is patterned correctly.

Further experiments would be required to investigate the expression of *Irx3* and *Otx2* in the $Pax6^{Sey/Sey}$ diencephalon, and to confirm whether or not the loss of functional *Pax6* also causes their domains to expand along with that of *Barhl2*, thereby increasing the width of the area fated to becoming ZLI and leading to the development of an expanded ZLI.

Drosophila BarH2 has been shown to act as an antiproneural transcription factor during the development of the *Drosophila* retina (Lim and Choi 2004). If mammalian *Barhl2* is also able to inhibit neurogenesis via a comparable mechanism its expression within the ZLI could serve to maintain it in a non-neural state for the duration of its activity as a signalling centre. This hypothesis is supported by the observation from this study that *Barhl2* is expressed within the mature ZLI, but not by the observation that it is only expressed within the more caudal region of the ZLI marked by Ngn2 expression (Caballero *et al* 2014).

The more ventral region of the ZLI is marked by the expression of the transcription factor *Dbx1*. A second member of the *Dbx* family, *Dbx2*, is known to act as a transcriptional repressor (Ma *et al* 2011, Lovrics *et al* 2014) via the *Groucho* repressosome (Muhr *et al* 2001, Bae *et al* 2003). The *Barhl2* protein possesses a FIL domain (Reig *et al* 2007) which may allow it to act as a transcriptional repressor (Smith and Jaynes 1996) via *Groucho* (Muhr *et al* 2001, Bae *et al* 2003). It may be

possible that *Barhl2* and *Dbx1* act together to maintain the ZLI in a non-neural state, but further experiments would be needed to confirm the antiproneural activity of *Barhl2* and *Dbx1* and their ability to act via *Groucho* before this possibility could be considered.

8.3.3 pTh-R development

The more caudal part of the thalamus, the pTh-C, is marked by the expression of *Ngn2* and *Olig3* and is gives rise to a population of glutamatergic neurons (Vue *et al* 2007, Robertshaw *et al* 2013). A narrow strip of neuroepithelium at the most rostral extent of the thalamus, the pTh-R, is marked by the expression of *Ascl1* and *Nkx2.2* and is fated to become GABAergic in character (Vue *et al* 2007, Suzuki-Hirano *et al* 2011, Robertshaw *et al* 2013).

Previous studies have shown that within the thalamus *Pax6* can induce glutamatergic neurons at the expense of GABAergic neurons (Caballero *et al* 2014) and that its expression within the rostral thalamus must be inhibited by *Shh* in order to allow the GABAergic pTh-R to develop (Szabó *et al* 2009, Vue *et al* 2009).

The results of the experiments described here showed that the pTh-R develops either at the same time as the ZLI or shortly afterwards, as both structures can be distinguished from E10.5. Prior to ZLI and pTh-R development *Barhl2* is expressed in a narrow strip of neuroepithelium within the broader *Pax6* domain. Once the ZLI has been established, the *Barhl2* domain fragments into two discrete domains, in the thalamus and ZLI respectively, which are separated by the *Barhl2*-negative pTh-R. The *Pax6* domain also becomes fragmented as its expression becomes weaker in the rostral thalamus, until its expression is completely absent from the pTh-R.

Together these observations may suggest a mechanism of pTh-R development involving *Pax6, Barhl2* and *Shh*. In this model *Barhl2* begins to be expressed in the prospective ZLI, which is shaped via mutual inhibition between *Pax6* and *Barhl2*. *Barhl2* then goes on to induce the ZLI and induce *Shh* expression. Finally, *Shh* from the ZLI diffuses into the rostral thalamus and inhibits the expression of *Pax6*, allowing development of the pTh-R and the differentiation of GABAergic neurons within it.

In this model *Barhl2* is also downregulated by *Shh* during and after pTh-R development. While the inhibition of *Pax6* by *Shh* has been shown to be required for pTh-R development (Szabó *et al* 2009, Vue *et al* 2009) one study has suggested that this inhibition may not be sufficient to induce the development of the pTh-R and that another function of *Shh* may be required (Robertshaw et al 2013). No requirement for the inhibition of *Barhl2* expression has so far been described in the literature and it may be possible that its inhibition is also required for development of the pTh-R to proceed. The results of the electroporation experiments described here suggest that ectopic activation of *Shh* signalling may be able to induce a downregulation of *Barhl2* in the pTh-C. This effect was only observed in one embryo of the eight which were electroporated in the pTh-C, but in this embryo ectopic expression of *cShh* was particularly strong, and it was also concentrated in a rostral area of the pTh-C.

It may be possible that the downregulation of *Barhl2* can be induced by *Shh* in the pTh-C, but only within the most rostral region, and with *Shh* at a particularly high concentration. This would be consistent with the published finding that ectopic *Shh* pathway activation is only able to ectopically induce pTh-R markers in more rostral regions of the pTh-R (Robertshaw et al 2013). In addition to *Pax6* and *Barhl2*, several other transcription factors are expressed in the pTh-C but not the p-Th-R, including *SRY (sex determining region Y)-box 2* (*Sox2*), *Olig2* and *Ngn2* (Caballero *et al* 2014) and the expression of these transcription factors and other may also need to be inhibited in order to allow pTh-R development to proceed.

This model for a mechanism of pTh-R development is illustrated in Fig. 8.2.

8.3.4 The modulation of *Shh* signalling within the thalamus

One previous study in chick has shown that the thalamus develops in a region of the diencephalon which expresses both *Pax6* and *Irx3*. The two transcription factors are required to confer thalamic competence on the neuroepithelium, ensuring that it responds to the *Shh* signal from the ZLI by taking on a thalamic character (Robertshaw *et al* 2013).

In the electroporation experiments described here the ectopic activation of *Shh* signalling did not appear to affect the expression of *Pax6* or *Barhl2* within the

thalamus, with the exception of one embryo in which an apparent downregulation of *Barhl2* was observed in a rostral region of the pTh-C. More noticeable effects on the expression of both transcription factors were observed within the pretectum, and in a greater proportion of the embryos which were analysed. This was despite a strong upregulation of *Ptch1* being observed in both the pTh-C and pTh-R. This suggested that the ectopic activation of *Shh* signalling had taken place, but that it had not exerted any effect on the expression of *Pax6* or *Barhl2* in the medial and caudal regions of the thalamus.

In these experiments it may have been possible that a factor within the thalamus was exerting a "shielding effect" on the thalamic neuroepithelium, acting to prevent the increase in *Shh* signalling activity inducing changes in the expression of specific transcription factors. This shielding factor may be *Irx3* or another factor expressed throughout the developing thalamus. Further experiments would be required to identify such a factor- for example, by generating mouse embryos lacking a candidate for the shielding factor and repeating the electroporation on these embryos to see if the loss of the candidate gene allows the expression of *Pax6* and *Barhl2* to be altered by activation of the *Shh* pathway.

While *Shh* the most widely-studied morphogen secreted by the ZLI, it secretes other morphogens, including *Wnt8b* (Garda *et al* 2002). *Barhl2* is known to inhibit canonical Wnt signalling by inhibiting the activity of a Wnt pathway component, β-catenin. Experiments in *Xenopus* have shown that this interacting between *Barhl2* and the canonical Wnt pathway serves to inhibit neural plate expansion (Juraver-Geslin *et al* 2011). Interactions between *Barhl2* and canonical Wnt signalling in the diencephalon have yet to be investigated. It may be possible that *Barhl2* interacts with both *Shh* and *Wnts* from the ZLI. In order to investigate this possibility, *in utero* electroporation could be used to manipulate Wnt signalling rather than *Shh* signalling, and this could be achieved by using DNA plasmid constructs encoding components of the Wnt pathway, such as activated β-catenin to activate Wnt signalling, and dominant-negative *Lymphoid enhancer binding factor 1* (*Lef1*) to inhibit Wnt signalling (Westenskow *et al* 2010).

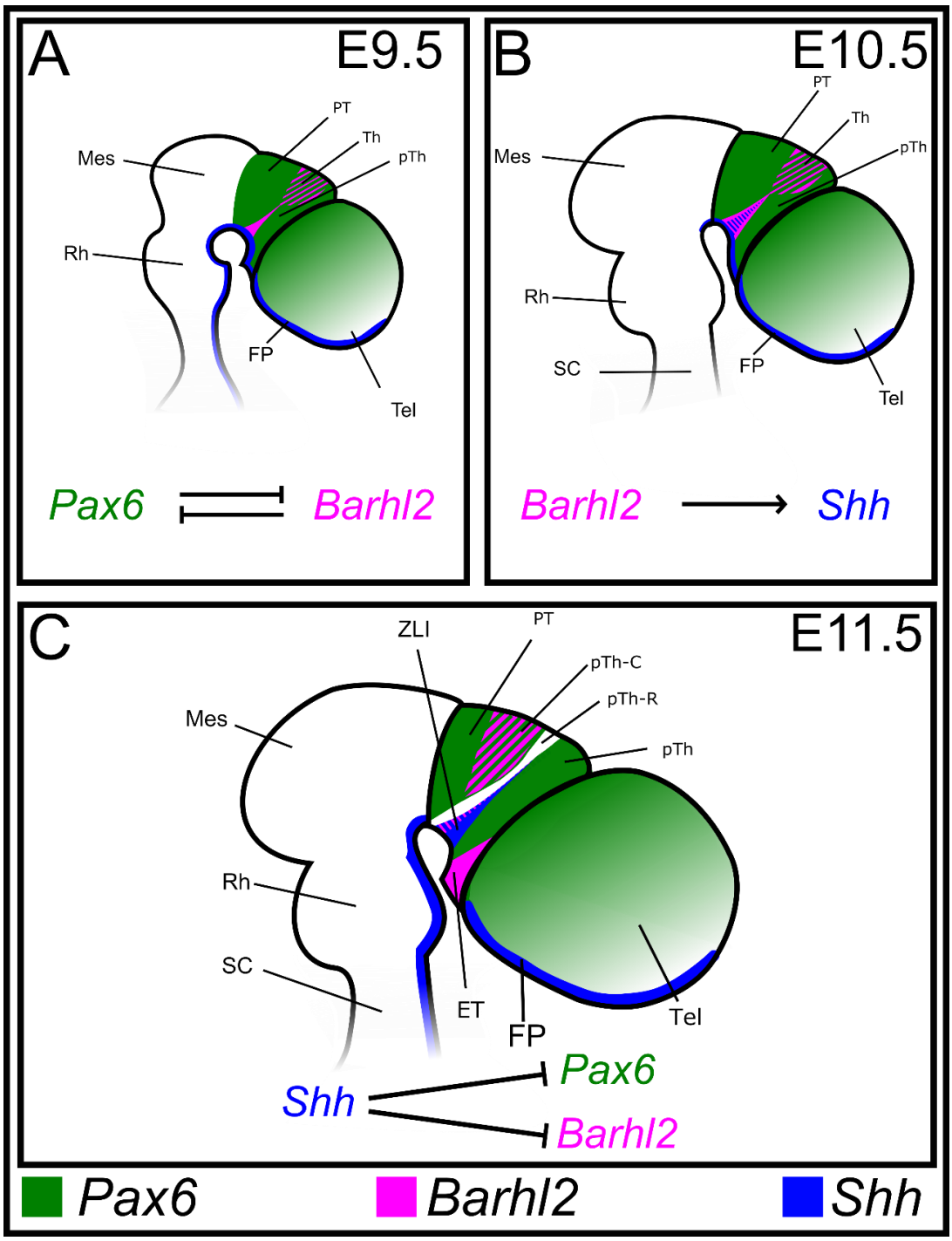

Fig.8.2: A model for the development of the pTh-R. A. Barhl2 *inhibits* Pax6 *expression within the region of neuroepithelium fated to become the ZLI.* Pax6 *inhibits* Barhl2 *expression to limit the expansion of this region. B.* Barhl2 *induces the expression of* Shh *and induces the development of the ZLI.* Shh *from the ZLI inhibits the expression of both* Pax6 *and* Barhl2 *in the rostral thalamus, allowing the pTh-R to develop. Abbreviations: Tel- telencephalon; Mes- mesencephalon; Rh- rhombencephalon; SC- spinal cord; PT- pretectum; Th- thalamus; pTh- prethalamus; ZLI-* zona limitans intrathalamica*; ET-* eminentia thalami*; FP- floorplate.*

8.4 Other factors involved in diencephalic patterning

While *Shh* is the most widely-studied morphogen in the control of diencephalic development, other less well-studied morphogens are known to be secreted by structures within the diencephalon. In addition to *Shh*, the ZLI secrets other morphogens, including Wnt3a (Shimogori *et al* 2010). *Barhl2* is known to modulate canonical Wnt signalling via interactions with Caspase3 (Juraver-Geslin *et al* 2011), preventing the nuclear accumulation of β-catenin, a component of the pathway (Rao and Kühl 2010). *Barhl2* activity can therefore modulate developmental processes in which Wnt signalling is implicated, including apoptosis and proliferative cell division (Juraver-Geslin *et al* 2011). Interactions between *Barhl2* and Wnt signalling within the developing diencephalon have yet to be investigated more extensively and it is possible that *Barhl2* may exert effects on diencephalic development via interactions with multiple signalling pathways. In addition to this, β-catenin is implicated processes unrelated to canonical Wnt signalling, such as cell adhesion (Rao and Kühl 2010) and the effects of *Barhl2* on β-catenin activity may induce effects beyond changes in the expression of Wnt target genes.

Barhl2 may play a role in limiting the expansion of the ZLI along the dorsoventral axis via interactions with *Pax6* and *Shh*, but other factors may also be involved in the shaping of the ZLI. The expansion of the ZLI along the dorsoventral axis towards the roofplate may be limited by the effects of retinoic acid (Guinazu *et al* 2007), a retinol derivative (Duester 2008) which has been shown to be synthesised by cells of the chick epithalamus during the early development of the diencephalon (Guinazu *et al* 2007). The shaping of the ZLI as a three-dimensional structure is likely to be a complex process involving a number of factors which induce different effects on its development.

8.5 Conclusion

Barhl2 is a relatively novel candidate for the control of diencephalic development. The experiments described here have provided new evidence for its involvement in a number of specific developmental processes within the embryonic diencephalon.

While the roles of *Pax6* and *Shh* in the developing diencephalon have both been investigated extensively, their interactions with *Barhl2* have not been studied as comprehensively. The findings from this study have suggested novel roles for the interactions between the three genes, and have provided scope for further investigation and the development of new models for the control of diencephalic patterning, axon guidance and neurogenesis.

References

Agarwala, S., Sanders, T.A., Ragsdale, C.W., 2001. Sonic Hedgehog Control of Size and Shape in Midbrain Pattern Formation. Science 291, 2147–2150.

Altmann, C.R., Brivanlou, A.H., 2001. Neural patterning in the vertebrate embryo. Int. Rev. Cytol. 203, 447–482.

Athar, M., Li, C., Kim, A.L., Spiegelman, V.S., Bickers, D.R., 2014. Sonic Hedgehog Signaling in Basal Cell Nevus Syndrome. Cancer Res 74, 4967–4975.

Álvarez-Buylla, A., Ihrie, R.A., 2014. Sonic hedgehog signaling in the postnatal brain. Seminars in Cell & Developmental Biology 33, 105–111.

Anderson, T.R., Hedlund, E., Carpenter, E.M., 2002. Differential Pax6 promoter activity and transcript expression during forebrain development. Mechanisms of Development 114, 171–175.

Aota, S., Nakajima, N., Sakamoto, R., Watanabe, S., Ibaraki, N., Okazaki, K., 2003. Pax6 autoregulation mediated by direct interaction of Pax6 protein with the head surface ectoderm-specific enhancer of the mouse Pax6 gene. Developmental Biology 257, 1–13.

Ashe, H.L., Briscoe, J., 2006. The interpretation of morphogen gradients. Development 133, 385–394.

Bae, Y.-K., Shimizu, T., Yabe, T., Kim, C.-H., Hirata, T., Nojima, H., Muraoka, O., Hirano, T., Hibi, M., 2003. A homeobox gene, pnx, is involved in the formation of posterior neurons in zebrafish. Development 130, 1853–1865.

Baek, J.H., Hatakeyama, J., Sakamoto, S., Ohtsuka, T., Kageyama, R., 2006. Persistent and high levels of Hes1 expression regulate boundary formation in the developing central nervous system. *Development* 133, 2467-2476.

Bai, C.B., Auerbach, W., Lee, J.S., Stephen, D., Joyner, A.L., 2002. Gli2, but not Gli1, is required for initial Shh signaling and ectopic activation of the Shh pathway. Development 129, 4753–4761.

Balaskas, N., Ribeiro, A., Panovska, J., Dessaud, E., Sasai, N., Page, K.M., Briscoe, J., Ribes, V., 2012. Gene Regulatory Logic for Reading the Sonic Hedgehog Signaling Gradient in the Vertebrate Neural Tube. Cell 148, 273–284.

Barth, K.A., Wilson, S.W., 1995. Expression of zebrafish nk2.2 is influenced by sonic hedgehog/vertebrate hedgehog-1 and demarcates a zone of neuronal differentiation in the embryonic forebrain. Development 121, 1755–1768.

Basset-Seguin, N., Sharpe, H.J., de Sauvage, F.J., 2015. Efficacy of Hedgehog pathway inhibitors in Basal cell carcinoma. Mol. Cancer Ther. 14, 633–641.

Beachy, P.A., Karhadkar, S.S., Berman, D.M., 2004. Tissue repair and stem cell renewal in carcinogenesis. Nature 432, 324–331.

Berrada, N., Lkhoyali, S., Mrabti, H., Errihani, H., 2014. Vismodegib: the proof of concept in Basal cell carcinoma. Clin Med Insights Oncol 8, 77–80.

Bijlsma, M.F., Roelink, H., 2010. Non-cell-autonomous signaling by Shh in tumors: challenges and opportunities for therapeutic targets. Expert Opin. Ther. Targets 14, 693–702.

Bluske, K.K., Kawakami, Y., Koyano-Nakagawa, N., Nakagawa, Y., 2009. Differential Activity of Wnt/β-Catenin Signaling in the Embryonic Mouse Thalamus. Dev Dyn 238, 3297–3309.

Brennan, C.A., Moses, K., 2000. Determination of Drosophila photoreceptors: timing is everything. CMLS, Cell. Mol. Life Sci. 57, 195–214.

Briscoe, J., 2009. Making a grade: Sonic Hedgehog signalling and the control of neural cell fate. EMBO J. 28, 457–465.

Briscoe, J., Thérond, P.P., 2013. The mechanisms of Hedgehog signalling and its roles in development and disease. Nat Rev Mol Cell Biol 14, 416–429.

Bulfone, A., Puelles, L., Porteus, M.H., Frohman, M.A., Martin, G.R., Rubenstein, J.L., 1993. Spatially restricted expression of Dlx-1, Dlx-2 (Tes-1), Gbx-2, and Wnt-3 in the embryonic day 12.5 mouse forebrain defines potential transverse and longitudinal segmental boundaries. J. Neurosci. 13, 3155–3172.

Bulfone, A., Menguzzato, E., Broccoli, V., Marchitiello, A., Gattuso, C., Mariani, M., Consalez, G.G., Martinez, S., Ballabio, A., Banfi, S., 2000. Barhl1, a gene belonging to a new subfamily of mammalian homeobox genes, is expressed in migrating neurons of the CNS. Hum. Mol. Genet. 9, 1443–1452.

Caballero, I. M., Manuel, M. N., Molinek, M., Quintana-Urzainqui, I., Da, M., Shimogori, T., & Price, D. J. (2014). Cell autonomous repression of Shh by transcription factor Pax6 regulates diencephalic patterning by controlling the central diencephalic organizer. Cell Reports, 8(5), 1405–1418.

Carpenter, D., Stone, D.M., Brush, J., Ryan, A., Armanini, M., Frantz, G., Rosenthal, A., Sauvage, F.J. de, 1998. Characterization of two patched receptors for the vertebrate hedgehog protein family. PNAS 95, 13630–13634.

Chang, D.T., López, A., Kessler, D.P. von, Chiang, C., Simandl, B.K., Zhao, R., Seldin, M.F., Fallon, J.F., Beachy, P.A., 1994. Products, genetic linkage and limb patterning activity of a murine hedgehog gene. Development 120, 3339–3353.

Charles River Laboratories, Inc. (2011). CD-1® IGS Mouse Model Information Sheet. Available from http://www.criver.com/files/pdfs/rms/cd1/rm_rm_d_cd1_mouse.aspx [1st October 2015]

Chatterjee, M., Guo, Q., Weber, S., Scholpp, S., Li, J.Y., 2014. Pax6 regulates the formation of the habenular nuclei by controlling the temporospatial expression of Shh in the diencephalon in vertebrates. BMC Biol 12, 13.

Chiang, C., Litingtung, Y., Lee, E., Young, K.E., Corden, J.L., Westphal, H., Beachy, P.A., 1996. Cyclopia and defective axial patterning in mice lacking Sonic hedgehog gene function. Nature 383, 407–413.

Chizhikov, V.V., Millen, K.J., 2005. Roof plate-dependent patterning of the vertebrate dorsal central nervous system. Developmental Biology 277, 287–295.

Chomczynski, P., Sacchi, N., 2006. The single-step method of RNA isolation by acid guanidinium thiocyanate-phenol-chloroform extraction: twenty-something years on. Nat Protoc 1, 581–585.

Chow, R.L., Lang, R.A., 2001. Early Eye Development in Vertebrates. Annual Review of Cell and Developmental Biology 17, 255–296.

Cohen, M., Briscoe, J., Blassberg, R., 2013. Morphogen interpretation: the transcriptional logic of neural tube patterning. Current Opinion in Genetics & Development, Developmental mechanisms, patterning and evolution 23, 423–428.

Colas, J.-F., Schoenwolf, G.C., 2001. Towards a cellular and molecular understanding of neurulation. Dev. Dyn. 221, 117–145.

Copp, A.J., Greene, N.D.E., Murdoch, J.N., 2003. The genetic basis of mammalian neurulation. Nat. Rev. Genet. 4, 784–793.

Corbit, K.C., Aanstad, P., Singla, V., Norman, A.R., Stainier, D.Y.R., Reiter, J.F., 2005. Vertebrate Smoothened functions at the primary cilium. Nature 437, 1018–1021.

Courey, A.J., Jia, S., 2001. Transcriptional repression: the long and the short of it. Genes Dev. 15, 2786–2796.

Coutinho, P., Pavlou, S., Bhatia, S., Chalmers, K.J., Kleinjan, D.A., van Heyningen, V., 2011. Discovery and assessment of conserved *Pax6* target genes and enhancers. *Genome Res* 8, 1349-59

Dickson, B.J., Gilestro, G.F., 2006. Regulation of Commissural Axon Pathfinding by Slit and its Robo Receptors. Annual Review of Cell and Developmental Biology 22, 651–675.

Ding Q, Chen H, Xie X, Libby RT, Tian N, Gan L, 2009. BARHL2 differentially regulates the development of retinal amacrine and ganglion neurons. *J Neurosci* 29 3992-4003.

Ding, Q., Joshi, P.S., Xie, Z., Xiang, M., Gan, L., 2012. BARHL2 transcription factor regulates the ipsilateral/contralateral subtype divergence in postmitotic dI1 neurons of the developing spinal cord. Proc Natl Acad Sci U S A 109, 1566–1571.

Dormoy, V., Jacqmin, D., Lang, H., Massfelder, T., 2012. From Development to Cancer: Lessons from the Kidney to Uncover New Therapeutic Targets. Anticancer Res 32, 3609–3617.

Duan, D., Fu, Y., Paxinos, G., Watson, C., 2013. Spatiotemporal expression patterns of Pax6 in the brain of embryonic, newborn, and adult mice. Brain Struct Funct 218, 353–372.

Duester, G., 2008. Retinoic Acid Synthesis and Signaling during Early Organogenesis. Cell 134, 921–931.

Duval, N., Daubas, P., Carbon, C.B. de, Clotment, C.S., Tinevez, J.-Y., Lopes, M., Ribes, V., Robert, B., 2014. Msx1 and Msx2 act as essential activators of Atoh1 expression in the murine spinal cord. Development 141, 1726–1736.

Echelard, Y., Epstein, D.J., St-Jacques, B., Shen, L., Mohler, J., McMahon, J.A., McMahon, A.P., 1993. Sonic hedgehog, a member of a family of putative signaling molecules, is implicated in the regulation of CNS polarity. Cell 75, 1417–1430.

Ekker, S.C., Ungar, A.R., Greenstein, P., Kessler, D.P. von, Porter, J.A., Moon, R.T., Beachy, P.A., 1995. Patterning activities of vertebrate hedgehog proteins in the developing eye and brain. Curr. Biol. 5, 944–955.

Epstein, E.H., 2008. Basal cell carcinomas: attack of the hedgehog. Nat Rev Cancer 8, 743–754.

Ericson, J., Rashbass, P., Schedl, A., Brenner-Morton, S., Kawakami, A., van Heyningen, V., Jessell, T.M., Briscoe, J., 1997. Pax6 controls progenitor cell identity and neuronal fate in response to graded Shh signaling. Cell 90, 169–180.

Estivill-Torrus, G., Pearson, H., van Heyningen, V., Price, D.J., Rashbass, P., 2002. Pax6 is required to regulate the cell cycle and the rate of progression from symmetrical to asymmetrical division in mammalian cortical progenitors. Development 129, 455–466.

Farhy, C., Elgart, M., Shapira, Z., Oron-Karni, V., Yaron, O., Menuchin, Y., Rechavi, G., Ashery-Padan, R., 2013. Pax6 Is Required for Normal Cell-Cycle Exit and the Differentiation Kinetics of Retinal Progenitor Cells. PLoS One 8.

Favor, J., Peters, H., Hermann, T., Schmahl, W., Chatterjee, B., Neuhäuser-Klaus, A., Sandulache, R., 2001. Molecular characterization of Pax6(2Neu) through Pax6(10Neu): an extension of the Pax6 allelic series and the identification of two possible hypomorph alleles in the mouse Mus musculus. Genetics 159, 1689–1700.

Fuccillo, M., Rutlin, M., Fishell, G., 2006. Removal of Pax6 partially rescues the loss of ventral structures in Shh null mice. Cereb. Cortex 16 Suppl 1, i96–102.

Fotaki, V., Yu, T., Zaki, P.A., Mason, J.O., Price, D.J., 2006. Abnormal Positioning of Diencephalic Cell Types in Neocortical Tissue in the Dorsal Telencephalon of Mice Lacking Functional Gli3. J Neurosci 26, 9282–9292.

Froger, A., Hall, J.E., 2007. Transformation of Plasmid DNA into E. coli Using the Heat Shock Method. J Vis Exp (6).

Fuse, N., Maiti, T., Wang, B., Porter, J.A., Hall, T.M.T., Leahy, D.J., Beachy, P.A., 1999. Sonic hedgehog protein signals not as a hydrolytic enzyme but as an apparent ligand for Patched. PNAS 96, 10992–10999.

Garda, A.L., Puelles, L., Rubenstein, J.L.R., Medina, L., 2002. Expression patterns of Wnt8b and Wnt7b in the chicken embryonic brain suggest a correlation with forebrain patterning centers and morphogenesis. Neuroscience 113, 689–698.

Garel, S., Marín, F., Mattéi, M.-G., Vesque, C., Vincent, A., Charnay, P., 1997. Family of Ebf/Olf-1-related genes potentially involved in neuronal differentiation and regional specification in the central nervous system. Dev. Dyn. 210, 191–205.

Gehring, W.J., Ikeo, K., 1999. Pax 6: mastering eye morphogenesis and eye evolution. Trends in Genetics 15, 371–377.

Georgala, P.A., Carr, C.B., Price, D.J., 2011. The role of Pax6 in forebrain development. Devel Neurobio 71, 690–709.

Goulding, M.D., Lumsden, A., Gruss, P., 1993. Signals from the notochord and floor plate regulate the region-specific expression of two Pax genes in the developing spinal cord. Development 117, 1001–1016.

Gradwohl G, Fode C, Guillemot F (1996). Restricted expression of a novel murine atonal-related bHLH protein in undifferentiated neural precursors. *Dev. Biol*. 180, 227-241.

Gray, P.A., Fu, H., Luo, P., Zhao, Q., Yu, J., Ferrari, A., Tenzen, T., Yuk, D.-I., Tsung, E.F., Cai, Z., Alberta, J.A., Cheng, L.-P., Liu, Y., Stenman, J.M., Valerius, M.T., Billings, N., Kim, H.A., Greenberg, M.E., McMahon, A.P., Rowitch, D.H., Stiles, C.D., Ma, Q., 2004. Mouse brain organization revealed through direct genome-scale TF expression analysis. Science 306, 2255–2257.

Grindley, J. C., Hargett, L., Hill, R. E., Ross, A. and Hogan, B. L. M (1997). Disruption of Pax6 function in mice homozygous for the Pax6 Sey-1NEU mutation produces abnormalities in the early development and regionalization of the diencephalon. *Mech Dev* 64, 111-126.

Guinazu, M.F., Chambers, D., Lumsden, A., Kiecker, C., 2007. Tissue interactions in the developing chick diencephalon. Neural Develop 2, 25.

Gupta, S., Takebe, N., LoRusso, P., 2010. Targeting the Hedgehog pathway in cancer. Ther Adv Med Oncol 2, 237–250.

Halder, G., Callaerts, P., Gehring, W.J., 1995. Induction of ectopic eyes by targeted expression of the eyeless gene in Drosophila. Science 267, 1788–1792.

Hau, J., Schapiro, S.J., 2010. Handbook of Laboratory Animal Science, Volume I, Essential Principles and Practices, 3rd edn, CRC Press, New York.
Heins, N., Malatesta, P., Cecconi, F., Nakafuku, M., Tucker, K.L., Hack, M.A., Chapouton, P., Barde, Y.-A., Götz, M., 2002. Glial cells generate neurons: the role of the transcription factor Pax6. Nat. Neurosci. 5, 308–315.

Heyne, G.W., Melberg, C.G., Doroodchi, P., Parins, K.F., Kietzman, H.W., Everson, J.L., Ansen-Wilson, L.J., Lipinski, R.J., 2015. Definition of Critical Periods for Hedgehog Pathway Antagonist-Induced Holoprosencephaly, Cleft Lip, and Cleft Palate. PLoS One 10.

Higashijima, S., Kojima, T., Michiue, T., Ishimaru, S., Emori, Y., Saigo, K., 1992. Dual Bar homeo box genes of Drosophila required in two photoreceptor cells, R1 and R6, and primary pigment cells for normal eye development. Genes Dev. 6, 50–60.

Hill, R.E., Favor, J., Hogan, B.L., Ton, C.C., Saunders, G.F., Hanson, I.M., Prosser, J., Jordan, T., Hastie, N.D., van Heyningen, V., 1991. Mouse small eye results from mutations in a paired-like homeobox-containing gene. Nature 354, 522–525.

Hill, R.E., 2007. How to make a zone of polarizing activity: Insights into limb development via the abnormality preaxial polydactyly. Development, Growth & Differentiation 49, 439–448.

Himmelstein, D.S., Bi, C., Clark, B.S., Bai, B., Kohtz, J.D., 2010. Balanced Shh signaling is required for proper formation and maintenance of dorsal telencephalic midline structures. BMC Dev. Biol. 10, 118.

Hirata, T., Nakazawa, M., Muraoka, O., Nakayama, R., Suda, Y., Hibi, M., 2006. Zinc-finger genes Fez and Fez-like function in the establishment of diencephalon subdivisions. Development 133, 3993–4004.

Hsieh-Li, H.M., Witte, D.P., Szucsik, J.C., Weinstein, M.B., Li, H., Potter, S.S., 1995. Gsh-2, a murine homeobox gene expressed in the developing brain. Mech Dev 50 (2-3):177-86.

Hsiung, F., Moses, K., 2002. Retinal development in Drosophila: specifying the first neuron. Hum. Mol. Genet. 11, 1207–1214.

Hui, C., Joyner, A.L., 1993. A mouse model of Greig cephalo–polysyndactyly syndrome: the extra–toes^{J} mutation contains an intragenic deletion of the Gli3 gene. Nat Genet 3, 241–246.

Hynes M, Ye W, Wang K, Stone D, Murone M, Sauvage Fd, Rosenthal A. (2004). The seven-transmembrane receptor smoothened cell-autonomously induces multiple ventral cell types. *Nat Neurosci*. 3(1):41-46.

Ingham, P.W., McMahon, A.P., 2001. Hedgehog signaling in animal development: paradigms and principles. Genes Dev. 15, 3059–3087.
Jarman, A.P., Grell, E.H., Ackerman, L., Jan, L.Y., Jan, Y.N., 1994. Atonal is the proneural gene for Drosophila photoreceptors. Nature 369, 398–400.

Jin, K., Jiang, H., Mo, Z., Xiang, M., 2010. Ebf Factors Are Required for Specifying Multiple Retinal Cell Types and Subtypes from Postmitotic Precursors. J Neurosci 30, 11902–11916.

Johnson, A.D., Krieg, P.A., 1994. pXeX, a vector for efficient expression of cloned sequences in Xenopus embryos. Gene 147, 223–226.
Jones, E.G., 2002. Thalamic circuitry and thalamocortical synchrony. Philos. Trans. R. Soc. Lond., B, Biol. Sci. 357, 1659–1673.

Jones, L., López-Bendito, G., Gruss, P., Stoykova, A., Molnár, Z., 2002. Pax6 is required for the normal development of the forebrain axonal connections. Development 129, 5041–5052.

Juraver-Geslin, H.A., Ausseil, J.J., Wassef, M., Durand, B.C., 2011. Barhl2 limits growth of the diencephalic primordium through Caspase3 inhibition of β-catenin activation. PNAS 108, 2288–2293.

Juraver-Geslin, H.A., Gómez-Skarmeta, J.L., Durand, B.C., 2014. The conserved barH-like homeobox-2 gene barhl2 acts downstream of orthodentricle-2 and together with iroquois-3 in establishment of the caudal forebrain signaling center induced by Sonic Hedgehog. Developmental Biology 396 (1) 107–120.

Jusuf, P.R., Albadri, S., Paolini, A., Currie, P.D., Argenton, F., Higashijima, S., Harris, W.A., Poggi, L., 2012. Biasing amacrine subtypes in the Atoh7 lineage through expression of Barhl2. J. Neurosci. 32, 13929–13944.

Katoh, Y., Katoh, M., 2005. Hedgehog signaling pathway and gastric cancer. Cancer Biology & Therapy 4, 1050–1054.

Kaufman, M.H., Chang, H.H., Shaw, J.P., 1995. Craniofacial abnormalities in homozygous Small eye (Sey/Sey) embryos and newborn mice. J Anat 186, 607–617.

Kawakami, A., Kimura-Kawakami, M., Nomura, T., Fujisawa, H., 1997. Distributions of PAX6 and PAX7 proteins suggest their involvement in both early and late phases of chick brain development. Mechanisms of Development 66, 119–130.

Keynes, R., Lumsden, A., 1990. Segmentation and the origin of regional diversity in the vertebrate central nervous system. Neuron 4, 1–9.

Kiecker, C., Lumsden, A., 2004. Hedgehog signaling from the ZLI regulates diencephalic regional identity. *Nat Neurosci* 7(11):1242-9.

Kiecker, C., Lumsden, A., 2005. Compartments and their boundaries in vertebrate brain development. *Nat Rev Neurosci* 6, 553-564.

Kiecker, C., Lumsden, A., 2012. The Role of Organizers in Patterning the Nervous System. Annual Review of Neuroscience 35, 347–367.

Kieran, M.W., 2014. Targeted treatment for sonic hedgehog-dependent medulloblastoma. Neuro Oncol 16, 1037–1047.

Kobayashi, D., Kobayashi, M., Matsumoto, K., Ogura, T., Nakafuku, M., Shimamura, K., 2002. Early subdivisions in the neural plate define distinct competence for inductive signals. Development 129, 83–93.

Kojima, T., Ishimaru, S., Higashijima, S., Takayama, E., Akimaru, H., Sone, M., Emori, Y., Saigo, K., 1991. Identification of a different-type homeobox gene, BarH1, possibly causing Bar (B) and Om(1D) mutations in Drosophila. Proc. Natl. Acad. Sci. U.S.A. 88, 4343–4347.

Kojima, T, Sato, M., Saigo, K. 2000. Formation and specification of distal leg segments in Drosophila by dual Bar homeobox genes, *BarH1* and *BarH2*. *Development* 127:4 769-778.

Kumar, J.P., 2011. My What Big Eyes You Have: How the Drosophila Retina Grows. Dev Neurobiol 71, 1133–1152.

Larsen, C. W., Zeltser, L. M. and Lumsden, A. (2001). Boundary formation and compartition in the avian diencephalon. J. Neurosci. 21, 4699-4711.

Li, S., Price, S.M., Cahill, H., Ryugo, D.K., Shen, M.M., Xiang, M., 2002. Hearing loss caused by progressive degeneration of cochlear hair cells in mice deficient for the Barhl1 homeobox gene. Development 129, 3523–3532.

Lim, J., Choi, K.-W., 2003. Bar homeodomain proteins are anti-proneural in the Drosophila eye: transcriptional repression of atonal by Bar prevents ectopic retinal neurogenesis. *Development* 130, 5965–5974.

Lim, J., Choi, K.-W., 2004. Induction and autoregulation of the anti-proneural gene Bar during retinal neurogenesis in Drosophila. Development 131, 5573–5580.

Lim Y, Golden JA. (2007). Patterning the developing diencephalon. *Brain Res Reviews* 53, 17–26.

Lipinski, R.J., Song, C., Sulik, K.K., Everson, J.L., Gipp, J.J., Yan, D., Bushman, W., Rowland, I.J., 2010. Cleft lip and palate results from Hedgehog signaling antagonism in the mouse: Phenotypic characterization and clinical implications. Birth Defects Research Part A: Clinical and Molecular Teratology 88, 232–240.

Lovrics, A., Gao, Y., Juhász, B., Bock, I., Byrne, H.M., Dinnyés, A., Kovács, K.A., 2014. Boolean Modelling Reveals New Regulatory Connections between Transcription Factors Orchestrating the Development of the Ventral Spinal Cord. PLoS One 9.

Ma, P., Zhao, S., Zeng, W., Yang, Q., Li, C., Lv, X., Zhou, Q., Mao, B., 2011. Xenopus Dbx2 is involved in primary neurogenesis and early neural plate patterning. Biochemical and Biophysical Research Communications 412, 170–174.

Macdonald, R., Barth, K.A., Xu, Q., Holder, N., Mikkola, I., Wilson, S.W., 1995. Midline signalling is required for Pax gene regulation and patterning of the eyes. Development 121, 3267–3278.

Manuel, M., Price, D.J., 2005. Role of Pax6 in forebrain regionalization. Brain Res. Bull. 66, 387–393.

Manuel, M., Georgala, P.A., Carr, C.B., Chanas, S., Kleinjan, D.A., Martynoga, B., Mason, J.O., Molinek, M., Pinson, J., Pratt, T., Quinn, J.C., Simpson, T.I., Tyas, D.A., Heyningen, V. van, West, J.D., Price, D.J., 2007. Controlled overexpression of Pax6 in vivo negatively autoregulates the Pax6 locus, causing cell-autonomous defects of late cortical progenitor proliferation with little effect on cortical arealization. Development 134, 545–555.

Manuel, M., Pratt, T., Liu, M., Jeffery, G., Price, D.J., 2008. Overexpression of Pax6 results in microphthalmia, retinal dysplasia and defective retinal ganglion cell axon guidance. BMC Dev. Biol. 8, 59.

Manuel, M.N., Mi, D., Mason, J.O., Price, D.J., 2015. Regulation of cerebral cortical neurogenesis by the Pax6 transcription factor. Front Cell Neurosci 9.

Marigo, V., Davey, R.A., Zuo, Y., Cunningham, J.M., Tabin, C.J., 1996. Biochemical evidence that Patched is the Hedgehog receptor. Nature 384, 176–179.

Martí, E., Bovolenta, P., 2002. Sonic hedgehog in CNS development: one signal, multiple outputs. Trends in Neurosciences 25, 89–96.

Martinez-Ferre, A., Martinez, S., 2012. Molecular regionalization of the diencephalon. Front Neurosci 6:73.

Mastick, G.S., Davis, N.M., Andrew, G.L., Easter, S.S. Jr., 1997. Pax-6 functions in boundary formation and axon guidance in the embryonic mouse forebrain. Development 124(10) 1985-97.

Matsui, A., Yoshida, A.C., Kubota, M., Ogawa, M., Shimogori, T., 2011. Mouse in utero electroporation: controlled spatiotemporal gene transfection. J Vis Exp. (54) 3024.

Maynard, T.M., Jain, M.D., Balmer, C.W., LaMantia, A.-S., 2014. High-resolution mapping of the Gli3 mutation Extra-toes^{J} reveals a 51.5-kb deletion. Mammalian Genome 13, 58–61.

McGlinn, E., Tabin, C.J., 2006. Mechanistic insight into how Shh patterns the vertebrate limb. Current Opinion in Genetics & Development, Pattern formation and developmental mechanisms 16, 426–432.

Mi, D., Carr, C.B., Georgala, P.A., Huang, Y.-T., Manuel, M.N., Jeanes, E., Niisato, E., Sansom, S.N., Livesey, F.J., Theil, T., Hasenpusch-Theil, K., Simpson, T.I.,

Mason, J.O., Price, D.J., 2013. Pax6 Exerts Regional Control of Cortical Progenitor Proliferation via Direct Repression of Cdk6 and Hypophosphorylation of pRb. Neuron 78, 269–284.

Molnár, Z., Garel, S., López-Bendito, G., Maness, P., Price, D.J., 2012. Mechanisms controlling the guidance of thalamocortical axons through the embryonic forebrain. Eur J Neurosci 35, 1573–1585.

Momose, T., Tonegawa, † Akane, Takeuchi, J., Ogawa, H., Umesono, K., Yasuda, K., 1999. Efficient targeting of gene expression in chick embryos by microelectroporation. Development, Growth & Differentiation 41, 335–344.

Motoyama, J., Takabatake, T., Takeshima, K., Hui, C., 1998. Ptch2, a second mouse Patched gene is co-expressed with Sonic hedgehog. Nat Genet 18, 104–106.

Moreno, N., Joven, A., Morona, R., Bandín, S., López, J.M., González, A., 2014. Conserved localization of Pax6 and Pax7 transcripts in the brain of representatives of sarcopterygian vertebrates during development supports homologous brain regionalization. Front. Neuroanat. 8, 75.

Morinello, E., Pignatello, M., Villabruna, L., Goelzer, P., Bürgin, H., 2014. Embryofetal development study of vismodegib, a hedgehog pathway inhibitor, in rats. Birth Defects Res. B Dev. Reprod. Toxicol. 101, 135–143.

Morrison, S.J., Kimble, J., 2006. Asymmetric and symmetric stem-cell divisions in development and cancer. Nature 441, 1068–1074.

Mouse Genome Informatics Scientific Curators, 2002. Chromosome assignment of mouse genes using the Mouse Genome Sequencing Consortium (MGSC) assembly and the ENSEMBL Database.

Mutoh, H., Hayakawa, H., Sashikawa, M., Sakamoto, H., Sugano, K., 2010. Direct repression of Sonic Hedgehog expression in the stomach by Cdx2 leads to intestinal transformation. Biochemical Journal 427, 423–434.

Nguyen-Ba-Charvet, K.T., Chédotal, A., 2002. Role of Slit proteins in the vertebrate brain. Journal of Physiology-Paris 96, 91–98.

Offner, N., Duval, N., Jamrich, M., Durand, B., 2005. The pro-apoptotic activity of a vertebrate Bar-like homeobox gene plays a key role in patterning the Xenopus neural plate by limiting the number of chordin- and shh-expressing cells. Development 132, 1807–1818.

Oro, A.E., Higgins, K.M., Hu, Z., Bonifas, J.M., Epstein, E.H., Scott, M.P., 1997. Basal Cell Carcinomas in Mice Overexpressing Sonic Hedgehog. Science 276, 817–821.

Osório, J., Mueller, T., Rétaux, S., Vernier, P., Wullimann, M.F., 2010. Phylotypic expression of the bHLH genes Neurogenin2, Neurod, and Mash1 in the mouse embryonic forebrain. J. Comp. Neurol. 518, 851-871.

Panovska-Griffiths, J., Page, K.M., Briscoe, J., 2013. A gene regulatory motif that generates oscillatory or multiway switch outputs. Journal of The Royal Society Interface 10, 20120826.

Park, H.L., Bai, C., Platt, K.A., Matise, M.P., Beeghly, A., Hui, C.C., Nakashima, M., Joyner, A.L., 2000. Mouse Gli1 mutants are viable but have defects in SHH signaling in combination with a Gli2 mutation. Development 127, 1593–1605.

Patten, I., Placzek, M., 2000. The role of Sonic hedgehog in neural tube patterning. Cell. Mol. Life Sci. 57, 1695–1708.

Patthey, C., Gunhaga, L., 2011. Specification and regionalisation of the neural plate border. European Journal of Neuroscience 34, 1516–1528.

Paxinos G, Franklin KBJ. 2001. The mouse brain in stereotaxic coordinates. San Diego, CA: Academic.

Peng, Y.-C., Joyner, A.L., 2015. Hedgehog signaling in prostate epithelial–mesenchymal growth regulation. Developmental Biology 400, 94–104.

Pinson, J., 2005. The role of Pax6 isoforms in embryonic development, The University of Edinburgh (United Kingdom).

Pinson, J., Mason, J.O., Simpson, T.I., Price, D.J., 2005. Regulation of the Pax6 : Pax6(5a) mRNA ratio in the developing mammalian brain. BMC Developmental Biology 5, 13.

Platt, K.A., Michaud, J., Joyner, A.L., 1997. Expression of the mouse Gli and Ptc genes is adjacent to embryonic sources of hedgehog signals suggesting a conservation of pathways between flies and mice. Mech. Dev. 62, 121–135.

Pratt T, Vitalis T, Warren N, Edgar JM, Mason JO, Price DJ (2000a). A role for *Pax6* in the normal development of dorsal thalamus and its cortical connections. *Development* 127(23):5167-78

Pratt, T., Sharp, L., Nichols, J., Price, D.J., Mason, J.O., 2000b. Embryonic Stem Cells and Transgenic Mice Ubiquitously Expressing a Tau-Tagged Green Fluorescent Protein. Developmental Biology 228, 19–28.

Price, D., Jarman, A.P., Mason, J.O., Kind, P.C., 2011. Building Brains: An Introduction to Neural Development. West Sussex, UK. Wiley-Blackwell.

Price, D.J., Clegg, J., Duocastella, X.O., Willshaw, D., Pratt, T., 2012. The Importance of Combinatorial Gene Expression in Early Mammalian Thalamic Patterning and Thalamocortical Axonal Guidance. Front Neurosci 6.

Puelles, L., Rubenstein, J.L.R., 2003. Forebrain gene expression domains and the evolving prosomeric model. Trends Neurosci. 26, 469–476.

Puelles, L., Harrison, M., Paxinos, G., Watson, C., 2013. A developmental ontology for the mammalian brain based on the prosomeric model. Trends in Neurosciences 36, 570–578.

Quinn, J.C., Molinek, M., Martynoga, B.S., Zaki, P.A., Faedo, A., Bulfone, A., Hevner, R.F., West, J.D., Price, D.J., 2007. Pax6 controls cerebral cortical cell number by regulating exit from the cell cycle and specifies cortical cell identity by a cell autonomous mechanism. Developmental Biology, 302(1-5), 50–65.

Quiring, R., Walldorf, U., Kloter, U., Gehring, W.J., 1994. Homology of the eyeless gene of Drosophila to the Small eye gene in mice and Aniridia in humans. Science 265, 785–789.

Rao, T.P., Kühl, M., 2010. An Updated Overview on Wnt Signaling Pathways A Prelude for More. Circ Res 106, 1798–1806.

Ready, D.F., Hanson, T.E., Benzer, S., 1976. Development of the Drosophila retina, a neurocrystalline lattice. Developmental Biology 53, 217–240.

Reifegerste, R., Moses, K., 1999. Genetics of epithelial polarity and pattern in the Drosophila retina. Bioessays 21, 275–285.

Reig, G., Cabrejos, M.E., Concha, M.L., 2007. Functions of BarH transcription factors during embryonic development. Developmental Biology 302, 367–375.

Ribes, V., Briscoe, J., 2009. Establishing and Interpreting Graded Sonic Hedgehog Signaling during Vertebrate Neural Tube Patterning: The Role of Negative Feedback. Cold Spring Harb Perspect Biol 1.

Ribes, V., Balaskas, N., Sasai N., Cruz, C., Dessaud, E., Cayuso, J., Tozer, S., Yang, L. L., Novitch, N., Marti, E., Briscoe, J., 2010. Distinct Sonic Hedgehog signaling dynamics specify floor plate and ventral neuronal progenitors in the vertebrate neural tube. *Genes Dev* 24(11):1186-1200.

Riddle, R.D., Johnson, R.L., Laufer, E., Tabin, C., 1993. Sonic hedgehog mediates the polarizing activity of the ZPA. Cell 75, 1401–1416.

Robertshaw, E., Kiecker, C., 2012. Phylogenetic Origins of Brain Organisers. Scientifica (Cairo) 2012.

Robertshaw E, Matsumoto K, Lumsden A, Kiecker C (2013). Irx3 and Pax6 establish differential competence for Shh-mediated induction of GABAergic and glutamatergic neurons of the thalamus. *Proc Natl Acad Sci U S A* 110(41):E3919-26.

Robinson, G.W., Orr, B.A., Wu, G., Gururangan, S., Lin, T., Qaddoumi, I., Packer, R.J., Goldman, S., Prados, M.D., Desjardins, A., Chintagumpala, M., Takebe, N., Kaste, S.C., Rusch, M., Allen, S.J., Onar-Thomas, A., Stewart, C.F., Fouladi, M., Boyett, J.M., Gilbertson, R.J., Curran, T., Ellison, D.W., Gajjar, A., 2015. Vismodegib Exerts Targeted Efficacy Against Recurrent Sonic Hedgehog-Subgroup Medulloblastoma: Results From Phase II Pediatric Brain Tumor Consortium Studies PBTC-025B and PBTC-032. J. Clin. Oncol. 33, 2646–2654.

Roessler, E., Belloni, E., Gaudenz, K., Jay, P., Berta, P., Scherer, S.W., Tsui, L.-C., Muenke, M., 1996. Mutations in the human Sonic Hedgehog gene cause holoprosencephaly. Nat Genet 14, 357–360.

Rogers, K.W., Schier, A.F., 2011. Morphogen Gradients: From Generation to Interpretation. Annual Review of Cell and Developmental Biology 27, 377–407.

Rubenstein, J.L.R., Shimamura, K., Martinez, S., Puelles, L., 1998. Regionalization of the Prosencephalic Neural Plate. Annual Review of Neuroscience 21, 445–477.

Ruiz-Gómez, A., Molnar, C., Holguín, H., Mayor, F., de Celis, J.F., 2007. The cell biology of Smo signalling and its relationships with GPCRs. Biochim. Biophys. Acta 1768, 901–912.

Saba, R., Nakatsuji, N., Saito, T., 2003. Mammalian BarH1 confers commissural neuron identity on dorsal cells in the spinal cord. J. Neurosci. 23, 1987–1991.

Saito, T., Sawamoto, K., Okano, H., Anderson, D.J., Mikoshiba, K., 1998. Mammalian BarH Homologue Is a Potential Regulator of Neural bHLH Genes. Developmental Biology 199, 216–225.

Sanders, E.R., 2012. Aseptic laboratory techniques: plating methods. J Vis Exp (63) e3064.
Sansom, S.N., Griffiths, D.S., Faedo, A., Kleinjan, D.-J., Ruan, Y., Smith, J., van Heyningen, V., Rubenstein, J.L., Livesey, F.J., 2009. The Level of the Transcription Factor Pax6 Is Essential for Controlling the Balance between Neural Stem Cell Self-Renewal and Neurogenesis. PLoS Genet 5.

Sato, M., Kojima, T., Michiue, T., Saigo, K., 1999. Bar homeobox genes are latitudinal prepattern genes in the developing Drosophila notum whose expression is regulated by the concerted functions of decapentaplegic and wingless. Development 126, 1457–1466.

Sato, M., Suzuki, T., Nakai, Y., 2013. Waves of differentiation in the fly visual system. Developmental Biology 380, 1–11

Schmahl, W., Knoedlseder, M., Favor, J., Davidson, D., 1993. Defects of neuronal migration and the pathogenesis of cortical malformations are associated with Small eye (Sey) in the mouse, a point mutation at the Pax-6-locus. Acta Neuropathol 86, 126–135.

Scholpp S, Foucher I, Staudt N, Peukert D, Lumsden A, Houart C (2007). Otx1l, Otx2 and Irx1b establish and position the ZLI in the diencephalon. *Development* 134(17):3167-76.

Scholpp, S., Lumsden, A., 2010. Building a bridal chamber: development of the thalamus. *Trends Neurosci* 33(8):373-80.

Schuhmacher, L.-N., Albadri, S., Ramialison, M., Poggi, L., 2011. Evolutionary relationships and diversification of barhl genes within retinal cell lineages. BMC Evol Biol 11, 340.

Schindelin, J., Arganda-Carreras, I., Frise, E., Kaynig, V., Longair, M., Pietzsch, T., Preibisch, S., Rueden, C., Saalfeld, S., Schmid, B., Tinevez, J.-Y., White, D.J., Hartenstein, V., Eliceiri, K., Tomancak, P., Cardona, A., 2012. Fiji: an open-source platform for biological-image analysis. Nat Meth 9, 676–682.

Sherman, S.M., Guillery, R.W., 2002. The role of the thalamus in the flow of information to the cortex. Philos Trans R Soc Lond B Biol Sci 357, 1695–1708.

Shimamura K, Hartigan DJ, Martinez S, Puelles L, Rubenstein JL, 1995. Longitudinal organization of the anterior neural plate and neural tube. Development 121, 3923-3933.

Shimogori, T., Lee, D.A., Miranda-Angulo, A., Yang, Y., Wang, H., Jiang, L., Yoshida, A.C., Kataoka, A., Mashiko, H., Avetisyan, M., Qi, L., Qian, J., Blackshaw, S., 2010. A genomic atlas of mouse hypothalamic development. Nat Neurosci 13, 767–775.

Simpson, T.I., Pratt, T., Mason, J.O., Price, D.J., 2009. Normal ventral telencephalic expression of Pax6 is required for normal development of thalamocortical axons in embryonic mice. Neural Development 4, 19.

Sisodiya, S.M., Free, S.L., Williamson, K.A., Mitchell, T.N., Willis, C., Stevens, J.M., Kendall, B.E., Shorvon, S.D., Hanson, I.M., Moore, A.T., van Heyningen, V., 2001. PAX6 haploinsufficiency causes cerebral malformation and olfactory dysfunction in humans. Nat Genet 28, 214–216.

Stoykova, A., Gruss, P., 1994. Roles of Pax-genes in developing and adult brain as suggested by expression patterns. *J. Neurosci*. 14, 1395-1412.

Stoykova, A., Fritsch, R., Walther, C., Gruss, P., 1996. Forebrain patterning defects in Small eye mutant mice. *Development* 122(11):3453-65.

Stoykova, A., Götz, M., Gruss, P., Price, J., 1997. Pax6-dependent regulation of adhesive patterning, R-cadherin expression and boundary formation in developing forebrain. *Development* 124(19):3765-77.

Sturtevant, A.H., 1925. The Effects of Unequal Crossing over at the Bar Locus in Drosophila. *Genetics* 10, 117–147.

Suzuki-Hirano, A., Ogawa, M., Kataoka, A., Yoshida, A.C., Itoh, D., Ueno, M., Blackshaw, S., Shimogori, T., 2011. Dynamic spatiotemporal gene expression in embryonic mouse thalamus. *J Comp Neurol* 519 528-543.

Szabó, N.-E., Zhao, T., Zhou, X., Alvarez-Bolado, G., 2009. The role of Sonic hedgehog of neural origin in thalamic differentiation in the mouse. J. Neurosci. 29, 2453–2466.

Taipale, J., Chen, J.K., Cooper, M.K., Wang, B., Mann, R.K., Milenkovic, L., Scott, M.P., Beachy, P.A., 2000. Effects of oncogenic mutations in Smoothened and Patched can be reversed by cyclopamine. Nature 406, 1005–1009.

Taipale, J., Beachy, P.A., 2001. The Hedgehog and Wnt signalling pathways in cancer. Nature 411, 349–354.

Taipale, J., Cooper, M.K., Maiti, T., Beachy, P.A., 2002. Patched acts catalytically to suppress the activity of Smoothened. Nature 418, 892–896.

Tam, P.P.L., Behringer, R.R., 1997. Mouse gastrulation: the formation of a mammalian body plan. Mechanisms of Development 68, 3–25.

Theiler, K., 1989. The House Mouse - Atlas of Embryonic Development. 2nd edn, Springer-Verlag, New York.

Tice, S.C., 1914. A New Sex-Linked Character in Drosophila. *Biol Bull* 26, 221–230.

Ton, C.C.T., Hirvonen, H., Miwa, H., Weil, M.M., Monaghan, P., Jordan, T., van Heyningen, V., Hastie, N.D., Meijers-Heijboer, H., Drechsler, M., Royer-Pokora, B., Collins, F., Swaroop, A., Strong, L.C., Saunders, G.F., 1991. Positional cloning and characterization of a paired box- and homeobox-containing gene from the aniridia region. Cell 67, 1059–1074.

Ton, C.C.T., Miwa, H., Saunders, G.F., 1992. Small eye (Sey): Cloning and characterization of the murine homolog of the human aniridia gene. Genomics 13, 251–256.

Truett, G.E., Heeger, P., Mynatt, R.L., Truett, A.A., Walker, J.A., Warman, M.L., 2000. Preparation of PCR-quality mouse genomic DNA with hot sodium hydroxide and tris (HotSHOT). BioTechniques (1): 52, 54.

Vieira, C., Garda, A.L., Shimamura, K., Martinez, S., 2005. Thalamic development induced by Shh in the chick embryo. *Dev Biol* 284(2):351-63.

Vieira, C., Pombero, A., García-Lopez, R., Gimeno, L., Echevarria, D., Martínez, S., 2010. Molecular mechanisms controlling brain development: an overview of neuroepithelial secondary organizers. Int. J. Dev. Biol. 54, 7–20.

Virolainen, S.-M., Achim, K., Peltopuro, P., Salminen, M., Partanen, J., 2012. Transcriptional regulatory mechanisms underlying the GABAergic neuron fate in different diencephalic prosomeres. Development 139, 3795–3805.

Visel, A., Thaller, C., Eichele, G., 2004. GenePaint.org: an atlas of gene expression patterns in the mouse embryo. *Nucleic Acids Res* 32, D552–556.

Vue, T.Y., Aaker, J., Taniguchi, A., Kazemzadeh, C., Skidmore, J.M., Martin, D.M., Martin, J.F., Treier, M., Nakagawa, Y., 2007. Characterization of progenitor domains in the developing mouse thalamus. J. Comp. Neurol. 505, 73–91.

Vue, T.Y., Bluske, K., Alishahi, A., Yang, L.L., Koyano-Nakagawa, N., Novitch, B., Nakagawa, Y., 2009. Sonic hedgehog signaling controls thalamic progenitor identity and nuclei specification in mice. J Neurosci 29, 4484–4497.

Walcher T, Xie Q, Sun J, Irmler M, Beckers J, Öztürk T, Niessing D, Stoykova A, Cvekl A, Ninkovic J, Götz M (March 2013). Functional dissection of the paired domain of Pax6 reveals molecular mechanisms of coordinating neurogenesis and proliferation. *Development* 140 (5): 1123-36

Walther, C., Gruss, P., 1991. Pax-6, a murine paired box gene, is expressed in the developing CNS. Development 113, 1435–1449.

Walther, C., Guenet, J.L., Simon, D., Deutsch, U., Jostes, B., Goulding, M.D., Plachov, D., Balling, R., Gruss, P., 1991. Pax: a murine multigene family of paired box-containing genes. Genomics 11, 424–434.

Warren, N., Price, D.J., 1997. Roles of Pax-6 in murine diencephalic. Development 124, 1573–1582.

Warren, N., Caric, D., Pratt, T., Clausen, J.A., Asavaritikrai, P., Mason, J.O., Hill, R.E., Price, D.J., 1999. The transcription factor, Pax6, is required for cell proliferation and differentiation in the developing cerebral cortex. *Cereb Cortex* 9(6):627-35.

Weinstein, D.C., Hemmati-Brivanlou, A., 1999. Neural induction. Annu. Rev. Cell Dev. Biol. 15, 411–433.

Westenskow, P.D., McKean, J.B., Kubo, F., Nakagawa, S., Fuhrmann, S., 2010. Ectopic Mitf in the Embryonic Chick Retina by Co-transfection of β-Catenin and Otx2. Invest Ophthalmol Vis Sci 51, 5328–5335.

White, N.M., Jarman, A.P., 2000. Drosophila Atonal controls photoreceptor R8-specific properties and modulates both Receptor Tyrosine Kinase and Hedgehog signalling. *Development* 127 1681-1689.

Wilson, S.W., Houart, C., 2004. Early Steps in the Development of the Forebrain. Dev Cell 6, 167–181.

Yauch, R.L., Gould, S.E., Scales, S.J., Tang, T., Tian, H., Ahn, C.P., Marshall, D., Fu, L., Januario, T., Kallop, D., Nannini-Pepe, M., Kotkow, K., Marsters, J.C.,

Rubin, L.L., de Sauvage, F.J., 2008. A paracrine requirement for hedgehog signalling in cancer. Nature 455, 406–410.

Yauch, R.L., Dijkgraaf, G.J.P., Alicke, B., Januario, T., Ahn, C.P., Holcomb, T., Pujara, K., Stinson, J., Callahan, C.A., Tang, T., Bazan, J.F., Kan, Z., Seshagiri, S., Hann, C.L., Gould, S.E., Low, J.A., Rudin, C.M., Sauvage, F.J. de, 2009. Smoothened Mutation Confers Resistance to a Hedgehog Pathway Inhibitor in Medulloblastoma. Science 326, 572–574.

Yokoyama, S., Ito, Y., Ueno-Kudoh, H., Shimizu, H., Uchibe, K., Albini, S., Mitsuoka, K., Miyaki, S., Kiso, M., Nagai, A., Hikata, T., Osada, T., Fukuda, N., Yamashita, S., Harada, D., Mezzano, V., Kasai, M., Puri, P.L., Hayashizaki, Y., Okado, H., Hashimoto, M., Asahara, H., 2009. A systems approach reveals that the myogenesis genome network is regulated by the transcriptional repressor RP58. *Dev. Cell* 17, 836–848

Yun, K., Potter, S., Rubenstein, J.L., 2001. Gsx2 and Pax6 play complementary roles in dorsoventral patterning of the mammalian telencephalon. *Development* 128:193–205.

Yun, J.I., Kim, H.R., Park, H., Kim, S.K., Lee, J., 2012. Small molecule inhibitors of the hedgehog signaling pathway for the treatment of cancer. Arch. Pharm. Res. 35, 1317–1333.